

Novel Approaches Targeting Phosphoinositide 3- Kinase Delta



Jonathan Andrew Spencer

University of Strathclyde

Department of Pure and Applied Chemistry

Doctor of Philosophy

2018

Declaration

This thesis is the result of the author's original research. It has been composed by the author and has not been previously submitted for examination which has led to the award of a degree.

The copyright of this thesis belongs to GSK in accordance with the author's contract of engagement with GSK under the terms of the United Kingdom Copyright Acts. Due acknowledgement must always be made of the use of any material contained in, or derived from, this thesis.

Signed:

Date:

Abstract

This thesis explores the development of inhibitors for phosphoinositide 3-kinase δ (PI3K δ), a lipid kinase implicated in COPD related inflammation.

Firstly, a macrocyclisation approach was explored (Figure 1), this involved design, synthesis and profiling of macrocyclic analogues of the ‘benzoxazine’ series of PI3K δ inhibitors. This approach showed macrocycles could provide lead-like compounds, with a number of macrocycles exhibiting potency gains, up to 200-fold, over acyclic progenitor compounds. Next, the effect of macrocyclisation on other relevant properties for drug discovery was examined. It was established that a number of these macrocycles are water soluble, permeable, low clearance compounds. Differences with acyclic compounds were observed in subsets of compounds, however broad conclusions about the effect of macrocyclisation could not be drawn.

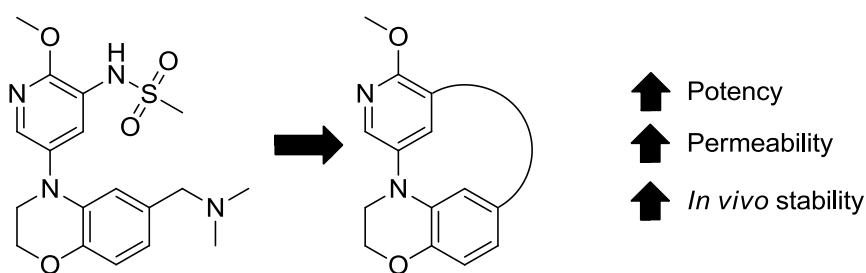


Figure 1 – A summary of the key findings from exploring macrocyclic analogues of an acyclic series of PI3K δ inhibitors.

In the second part of this study, synthetic methodology was developed for the synthesis of cyclopropyl boronic esters (Figure 2). Synthesis of compounds containing this functionality allows facile incorporation of three-dimensional character into drug-like scaffolds. A reaction manifold was developed utilising Schwartz’s Reagent for the conversion of synthetically tractable propargylic silyl ethers into complex products in a one-pot procedure, exemplified by the synthesis of aryl-, aliphatic-, quaternary- and spiro- substituted cyclopropyl boronic esters. The methodology was applied to enable a new synthesis of biologically active Sedaxane, *via* a bis-cyclopropyl boronic ester motif and to explore a growth vector from a cyclopropyl ring in an emerging series of PI3K δ inhibitors.

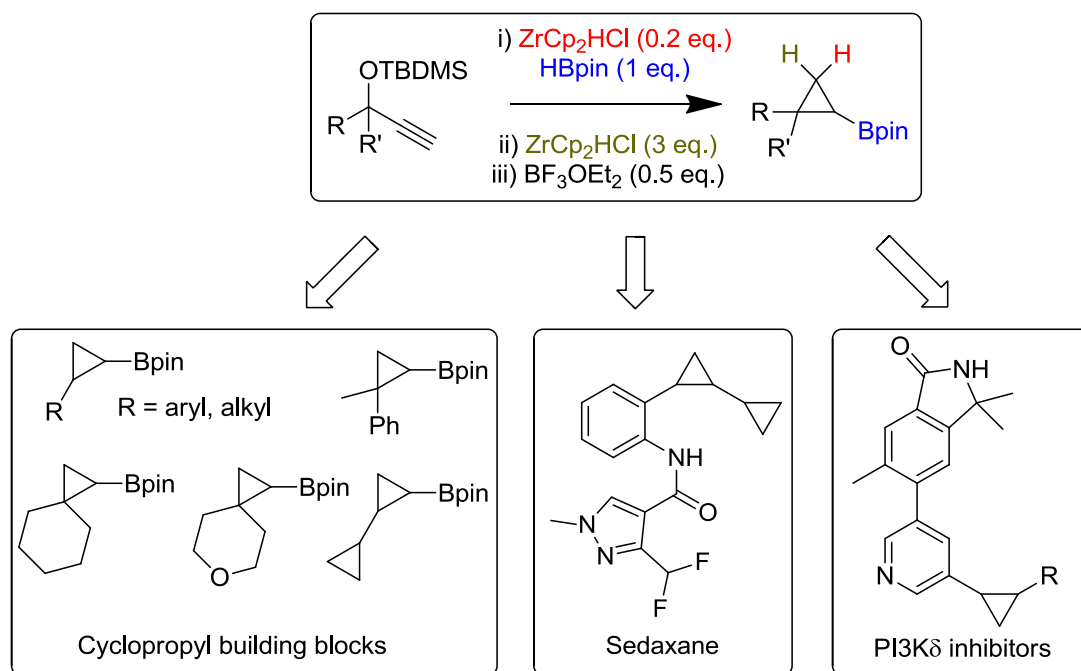


Figure 2 – Summary of methodology developed and applications of Schwartz’s Reagent mediated borylation-cyclopropanation.

Abbreviations

ADP	Adenosine Diphosphate
AGP	α -1-acid glycoprotein
ALK	Anaplastic Lymphoma Kinase
AMP	Artificial Membrane Permeability
APDS	Activated-PI3K δ -Syndrome
ATP	Adenosine Triphosphate
BACE	Beta-Secretase
BCL6	B-Cell Lymphoma 6
BINAP	2,2'-Bis(diphenylphosphino)-1,1'-binaphthyl
BINOL	1,1'-bi-2-naphthol
Boc	<i>tert</i> -Butoxycarbonyl
BOP	(Benzotriazol-1-yloxy)tris(dimethylamino)phosphonium hexafluorophosphate
BOPCI	Bis(2-oxo-3-oxazolidinyl)phosphinic chloride
CAD	Charged Aerosol Detector
Cbz	Carboxybenzyl
CDI	1,1'-Carbonyldiimidazole
CLND	Chemiluminescent Nitrogen Detection
CNS	Central Nervous System
cod	1,5-Cyclooctadiene (1-Cyano-2-ethoxy-2- oxoethylidenaminoxy)dimethylamino-morpholino- carbenium hexafluorophosphate
COMU	(1-Cyano-2-ethoxy-2-oxoethylidenaminoxy)dimethylamino-morpholino- carbenium hexafluorophosphate
COPD	Chronic Obstructive Pulmonary Disease
CPME	Cyclopentyl Methyl Ether
dba	Dibenzylideneacetone
DCE	Dichloroethane
DCM	Dichloromethane
DEPC	Diethyl cyanophosphonate
DIBAL-H	<i>Diisobutyl</i> Aluminium Hydride

CONFIDENTIAL – PROPERTY OF GSK – DO NOT COPY

DIPEA	Diisopropylethylamine
DMAP	4-(Dimethylamino)pyridine
DMF	<i>N,N</i> -Dimethylformamide
DMS	Dimethylsulfide
DMSO	Dimethylsulfoxide
DMTMM	4-(4,6-Dimethoxy-1,3,5-triazin-2-yl)-4-methylmorpholinium chloride
DPPA	Diphenylphosphoryl Azide
dppf	1,1'- bis(diphenylphosphanyl) ferrocene
EDC	3-(Ethyliminomethyleneamino)- <i>N,N</i> -dimethylpropan-1-amine
EEDQ	2-Ethoxy-2 <i>H</i> -quinoline-1-carboxylic acid ethyl ester
EHT	Extended Huckel Theory
FDA	United States Food and Drug Administration
GSK	GlaxoSmithKline
HATU	1-[Bis(dimethylamino)methylene]-1 <i>H</i> -1,2,3-triazolo[4,5- <i>b</i>]pyridinium 3-oxid hexafluorophosphate
HBTU	3-[Bis(dimethylamino)methylumyl]-3 <i>H</i> -benzotriazol-1-oxide hexafluorophosphate
HCV	Hepatitis C Virus
HEH	Hanzsch Ester Hydrate
Hep	Hepatocytes
HMBC	Heteronuclear multiple-bond correlation spectroscopy
HPLC	High Performance Liquid Chromatography
HRMS	High Resolution Mass Spectrometry
HSA	Human Serum Albumin
HSQC	Heteronuclear single quantum coherence spectroscopy
IR	Infrared
ITC	Isothermal Titration Calorimetry
JAK	Janus Kinase
LA	Lewis Acid
LABA	Long Acting Beta-2 Agonist

CONFIDENTIAL – PROPERTY OF GSK – DO NOT COPY

LAMA	Long Acting Muscarinic Receptor Antagonist
LBF	Liver Blood Flow
LCMS	Liquid Chromatography Mass Spectrometry
LE	Ligand Efficiency
LLE	Lipophilic Ligand Efficiency
L-Selectride	Lithium tri- <i>sec</i> -butyl(hydrido)borate
MCM	Mobil Composition of Matter No.
MDAP	Mass Directed Auto Preparation
MDCK	Madin-Darby Canine Kidney
MEK	Mitogen-activated Protein Kinase
mes	mesityl
Mic	Microsomes
MOE	Molecular Operating Environment 2016
M _w	Molecular Weight
NBS	<i>N</i> -Bromosuccinimide
NMR	Nuclear Magnetic Resonance
PDB	Protein Data Bank
PEI	Peroxisomal Enzyme Induction
PFI	Property Forecast Index
P-gp	P-glycoprotein
Phen	Phenanthroline
Phth	Phthalimido
PI	Phosphatidylinositol
PI3K	Phosphoinositide 3-Kinase
pin	Pinacolato
PIP	Phosphatidylinositol Phosphate
PLK4	Polo-like kinase 4
ppm	Parts Per Million
PyBOP	(Benzotriazol-1-yloxy)tripyrrolidinophosphonium hexafluorophosphate
Red-Al	Sodium bis(2-methoxyethoxy)aluminium hydride
RSV	Respiratory Syncytial Virus

CONFIDENTIAL – PROPERTY OF GSK – DO NOT COPY

Rt	Retention Time
RT	Room Temperature
RuPhos	2-Dicyclohexylphosphino-2',6'-diisopropoxybiphenyl
RuPhos-Pd G2	Chloro(2-dicyclohexylphosphino-2',6'-diisopropoxy-1,1'-biphenyl)[2-(2'-amino-1,1'-biphenyl)]palladium(II)
SAR	Structure Activity Relationship
SPR	Surface Plasmon Resonance
Suc	Succinyl
Sulfo-NHS	<i>N</i> -hydroxysulfosuccinimide
T3P	Propylphosphonic Anhydride
TBAI	Tetra- <i>n</i> -butylammonium iodide
TBDMS	<i>Tert</i> -butyldimethylsilyl
TBTU	2-(1 <i>H</i> -Benzotriazole-1-yl)-1,1,3,3-tetramethylammonium tetrafluoroborate
Tf	Triflic
TFA	Trifluoroacetic Acid
TFFH	Tetramethylfluoroformamidinium Hexafluorophosphate
THF	Tetrahydrofuran
THP	Tetrahydropyranyl
TMEDA	<i>N,N,N',N'</i> -Tetramethylethane-1,2-diamine
TMS	Trimethyl Silane
UV	Ultraviolet
Vps34	Vacuolar Protein Sorting Mutagen 34 Protein, also known as Phosphoinositide-3-kinase Class 3 (PI3KC3)

Acknowledgements

I would like to acknowledge the hard work and support of my supervisors Dr Craig Jamieson, Dr Charlotte Hardy and Dr Eric Talbot. Without their help and enthusiasm this research would not have been possible.

I would also like to acknowledge Máire Convery for protein X-ray crystallography data collection, interpretation and discussion; Chun-Wa Chung and Jingkun Zeng for designing and conducting SPR experiments; GSK PI3K δ project teams for helpful discussions and access to useful intermediates; Eric Hortense, Steve Jackson and Andy Knaggs for conducting chiral analysis and purification; GSK NMR service for running bespoke experiments and helpful discussions in structural assignment; DMPK colleagues for conducting clearance experiments; and GSK Platform, Technology and Science for running biological and physicochemical assays.

Declaration	1
Abstract	3
Abbreviations	5
Acknowledgements	9
Chapter 1. Introduction	13
1.1 Chronic Obstructive Pulmonary Disease	13
1.2 Kinases	16
1.3 Phosphoinositide 3-Kinase	18
1.4 Designing Selective PI3K δ Inhibitors	21
Chapter 2. Benzoxazine Series	27
2.1 Introduction	27
2.1.1 Development of the Benzoxazine Series.....	27
2.1.2 Macrocycles in Drug Discovery.....	30
2.1.3 Existing PI3K δ Macrocycles.....	35
2.2 Aims	36
2.3 Results and Discussion	37
2.3.1 Investigation into Potential for Macrocyclisation	37
2.3.1.1 X-Ray Crystallography.....	38
2.3.1.2 Biophysical Techniques	41
2.3.2 Initial Exploration of Ring Size	47
<i>In vitro</i> PI3K δ enzyme assay results for sulfonamide compounds	69
2.3.3 Transposition of Sulfonamide	71
<i>In vitro</i> PI3K δ enzyme assay results for reverse sulfonamide compounds	78
2.3.4 Restriction of linker.....	81
<i>In vitro</i> PI3K δ enzyme assay results for restricted linker compounds.....	89
2.3.5 Sulfonamide Replacements.....	91
<i>In vitro</i> PI3K δ enzyme assay results for sulfonamide replacement compounds	103

CONFIDENTIAL – PROPERTY OF GSK – DO NOT COPY

<i>In vitro</i> PI3K δ enzyme assay results for sulfonamide replacement macrocycles	108
2.3.6 Effect of Macrocyclisation on Drug Properties	110
2.4 Summary and Conclusions	133
2.5 Further Work	135
Chapter 3. Lactam Series	137
3.1 Introduction	137
3.1.1 Development of the Lactam Series	137
3.1.2 Cyclopropyl Rings in Drug Discovery.....	140
3.1.3 Synthesis of Cyclopropyl Rings.....	144
3.1.4 Synthetic Utility of Boronic Esters	146
3.1.5 Synthesis of Cyclopropylboronic Esters	148
3.1.6 Strategy for Novel Cyclopropylboronic Ester Synthesis	152
3.1.7 Use of Schwartz’s Reagent in Synthesis	154
3.2 Results and Discussion	156
3.2.1 Optimisation of Reaction Conditions.....	156
3.2.2 Substrate Scoping.....	177
3.2.3 Synthesis of Sedaxane.....	193
3.2.4 Synthesis of PI3K δ Inhibitors	199
<i>In vitro</i> PI3K α , PI3K β , PI3K γ and PI3K δ enzyme assay results for cyclopropyl lactam compounds.....	203
3.3 Summary and Conclusions	205
3.4 Further Work	206
Chapter 4. Conclusions	209
Chapter 5. Experimental	210
5.1 General Methods	210
5.2 Experimental procedures	214

CONFIDENTIAL – PROPERTY OF GSK – DO NOT COPY

5.2.1	Procedures for Optimisation Screens	214
	Sulfonamide Coupling Screen.....	214
	Buchwald-Hartwig Amination Screen	214
	Lactam Coupling Screen	214
	Lactam Coupling Concentration Screen	214
	Lactam Reduction Reagents Screen.....	214
	Lactam Reduction Temperature/Equivalents Screen	215
	Chloride Displacement Screen	215
	Ring Closing Metathesis Screen	215
	Cyclopropanation Optimisation Screens.....	215
5.2.2	Compound Synthesis and Characterisation – Benzoxazine Series	216
5.2.3	Compound Synthesis and Characterisation – Lactam Series	258
	General Procedure A - Synthesis of Secondary Propargylic Silyl Ethers .	258
	General Procedure B - Synthesis of Tertiary Propargylic Silyl Ethers	259
	General Procedure C - One-Pot Borylation-Cyclopropanation.....	259
	General Procedure D - One-Pot Borylation-Cyclopropanation Followed by Suzuki Coupling	260
	General Procedure E - Lactam Series Suzuki Coupling.....	260
5.2.4	Supplementary Protocols	297
	Computational modelling.....	297
	PI3K Alpha, Beta, Gamma and Delta Assays ²⁴⁶	297
	CLND and CAD Kinetic Solubility Assay ²⁶⁸	299
	ChromLogD Assay ^{44,268,271}	299
	Artificial Membrane Permeability Assay ^{268,272}	300
	pK _a determination ²⁶⁸	300
	HSA and AGP binding assay ²⁷³	301
	References	302
	Appendix	318
	Structure of amide coupling reagents.....	318
	Animal Studies Declaration	320

Chapter 1. Introduction

1.1 Chronic Obstructive Pulmonary Disease

Chronic Obstructive Pulmonary Disease (COPD) is a term used to refer to patients with chronic bronchitis, emphysema, or a combination of the two. This type of lung disease restricts the flow of air into and out of the lungs.¹ Typical symptoms include shortness of breath, cough and excess sputum production. COPD affects 11.4% of the population over the age of thirty with 384 million cases globally in 2010.² The disease is ranked as the third highest cause of death worldwide with 3.2 million deaths in 2012.³ COPD is caused by a number of factors including exposure to tobacco smoke, air pollution, and genetic factors. Around four out of every five cases of COPD are seen in smokers, as tobacco smoke causes irreversible damage to the lungs.⁴ This results in an inflammatory response from the lung cells, causing a destruction of lung tissue and difficulty in breathing.

Currently, COPD is treated with bronchodilators in conjunction with anti-inflammatory agents. An example of this combination is Trelegy Ellipta, a GSK medicine approved by the FDA in 2017. This consists of fluticasone furoate **1**, a corticosteroid, vilanterol **2**, a long acting beta-2 agonist (LABA) (Figure 3) and umeclidinium bromide **3**, a long acting muscarinic receptor antagonist (LAMA).^{5,6}

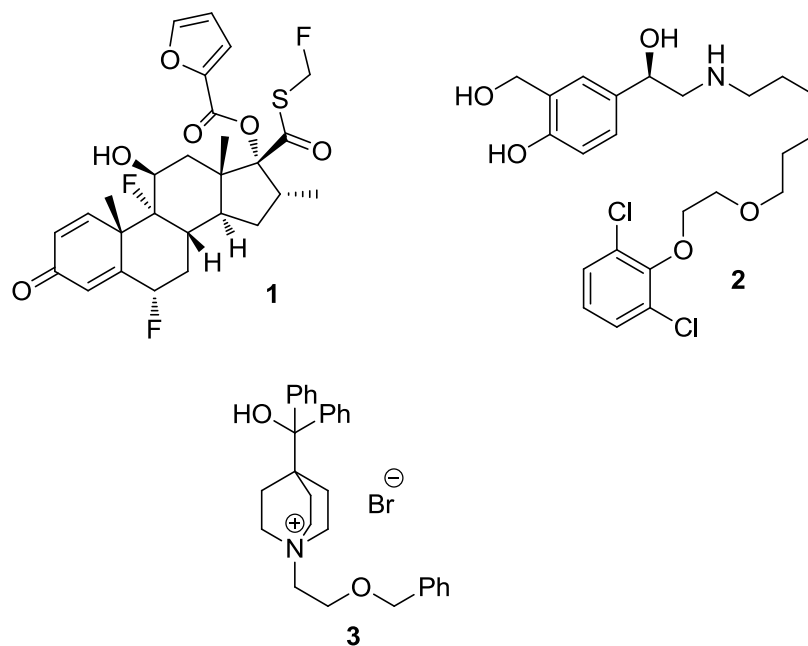


Figure 3 - Fluticasone furoate 1, vilanterol 2 and umeclidinium bromide 3 - the components of Trelegy Ellipta.

Traditionally these bronchodilators and anti-inflammatory agents would have been administered as three separate drugs, however, in this instance they are delivered in a single inhaler. The LABA results in muscle relaxation, which when inhaled is delivered to lung tissue, resulting in a widening of the airways. The LAMA inhibits muscarinic acetylcholine receptors, resulting in decreased muscle contraction leading to reduced bronchoconstriction. The corticosteroid is a glucocorticoid agonist, this affects multiple immune signalling pathways and acts as an immunosuppressant.⁷ A combination treatment, such as this, is thought to work in a synergistic manner in which the combination provides a greater degree of efficacy than either of the individual parts. This works since beta-2 agonists cause an increase in expression of glucocorticoid receptors, which allows for enhanced corticosteroid activity. The corticosteroids also increase the transcription of beta-2 receptors meaning drop off in agonism over time is reduced.⁸ Trelegy currently provides the only once daily corticosteroid/LABA/LAMA combination on the market.

However, these drugs are used only to alleviate the symptoms of COPD rather than to treat the underlying cause of the condition. There is a great demand for a disease modifying pharmacotherapy, since the only known disease modifiers are smoking

CONFIDENTIAL – PROPERTY OF GSK – DO NOT COPY

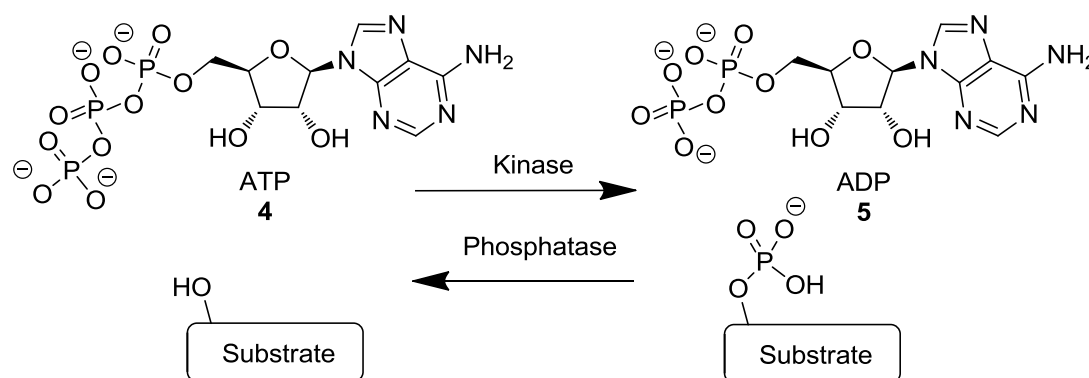
cessation and lung transplantation.^{1,4} Current COPD anti-inflammatory agents, corticosteroids and bronchodilators, are not maximally effective at reducing COPD related inflammation, and are unable to alter disease progression.⁴ These drugs also have low efficacy against COPD. Alternative therapies include oxygen administration or lung transplantation in the most severe cases. However, although these therapies have been found to extend patient life, they do not improve the overall quality of life.⁴

Another potential downside is that these drugs are administered through an inhaled route. This is not preferable since the dose through inhalation can vary between patients; however, the drug is easily delivered to the site of action in the lungs. Patient compliance is generally low through an inhaled route in comparison to oral delivery, with some devices being difficult to use, especially for the elderly.⁹ Having stated this, the Ellipta device, developed by GSK, addresses a number of these problems offering consistent dose delivery and ease of use.¹⁰ Another problem with current drugs is a lack of perceived effect of the medicines, again leading to poor compliance¹¹ due to patients expecting fast improvement in lung function. Against this background, oral drugs are preferred, since they provide a simpler route of administration for patients.

From consideration of the above, this thesis will describe attempts to identify novel therapies for COPD. Specifically, the work presented herein will focus on the design and synthesis of phosphoinositide 3-kinase (PI3K) inhibitors, suitable for oral or inhaled delivery. Strategies adopted will include a macrocyclisation approach based on an existing class of inhibitors and the development of novel methodology to access substituted cyclopropyl-derived inhibitors from a proprietary template. The basis of these approaches and relevant background are expanded upon in subsequent sections.

1.2 Kinases

Kinases are a class of proteins which catalyse the transfer of a phosphate from adenosine triphosphate **4** (ATP) to a substrate, with the reverse reaction being catalysed by phosphatases (Scheme 1). This ability to reversibly phosphorylate substrates has wide-reaching consequences in biology and medicine, and forms a key part of intracellular signalling cascades.¹² The human genome contains over 500 kinases,¹³ with substrates including proteins, lipids and nucleic acids.



Scheme 1 – General reactions catalysed by kinases and phosphatases.

Protein kinases typically selectively phosphorylate a tyrosine, serine or threonine side chain. This affects the activity of the protein towards its own substrate, due to conformational changes, and therefore can have consequences on metabolism, transcription, cell cycle progression, cell movement, apoptosis, and differentiation.¹³ Additionally, the reversibility of phosphorylation, mediated by phosphatase enzymes, allows the organism to respond to changes quickly and maintain homeostasis.

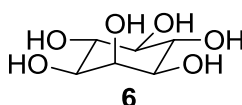


Figure 4 – Structure of inositol **6**, derivatives of which are substrates for lipid kinases.

Lipid kinases typically phosphorylate an alcohol on a derivative of inositol **6**, the products of which are ubiquitously deployed in cellular signalling. Receptor proteins interact specifically with inositol derivatives allowing for a signalling cascade to affect

CONFIDENTIAL – PROPERTY OF GSK – DO NOT COPY

cellular processes such as cell growth, proliferation, differentiation, motility, survival and intracellular trafficking.^{14,15}

Since all kinases bind ATP, their binding site is often quite similar (Figure 5). A ‘hinge’ region forms backbone hydrogen bonds to the adenine of ATP and a phosphate region forms salt bridges between the protein and the phosphate. As all kinases bind the same ATP substrate it is often difficult to achieve selectivity, however variation in protein sequence is seen in the specificity pocket and hydrophobic regions, allowing for the possibility of selective inhibition.

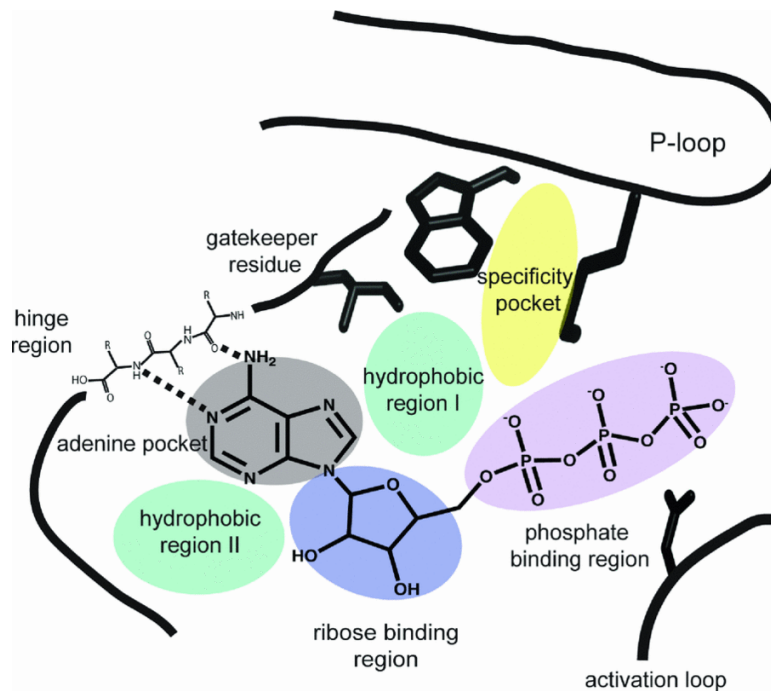


Figure 5 – Typical structure of a kinase ATP binding pocket.¹⁶

1.3 Phosphoinositide 3-Kinase

The phosphoinositide 3-kinase (PI3K) pathway offers a promising target for COPD therapies.¹⁷ PI3Ks are lipid kinases catalysing the phosphorylation of an alcohol on derivatives of the lipid, phosphatidylinositol **7** (PI) (Figure 6) to furnish phosphatidylinositol phosphates (PIPs). The products of these enzymes have wide reaching signalling consequences influencing cell growth, cell proliferation, cell survival and cell migration.¹⁸

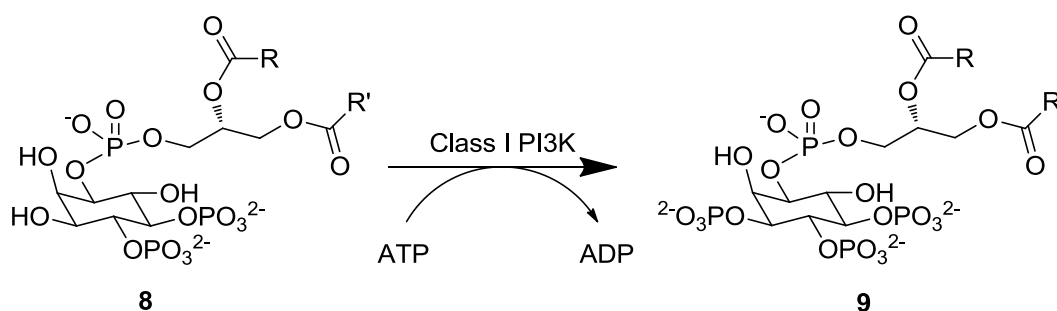


Figure 6 - The structure of phosphatidylinositol **7**.

There are four known classes of PI3K enzymes separated by their substrate, structure and site of expression (Table 1).¹⁹

	Kinase	Substrate	Product	Regulation	Site of Expression
Class IA	PI3K α	PIP ₂ 8	PIP ₃ 9	Growth factor receptor	Ubiquitous
	PI3K β				Ubiquitous
	PI3K δ				Leukocytes
Class IB	PI3K γ	PIP ₂ 8	PIP ₃ 9	G-protein coupled receptor	Neutrophils Macrophages
Class II	PI3KC2 α	PIP ₁	PIP ₂		Ubiquitous
	PI3KC2 β				Ubiquitous
	PI3KC2 γ				Liver
Class III	Vps34	PI	PIP ₁		Ubiquitous

Table 1 - Classes of PI3K enzymes and the differences between them.¹⁹



Scheme 2 - The conversion of PIP₂ **8** to PIP₃ **9** catalysed by class I PI3K enzymes including PI3K δ .

Although the class I PI3K enzymes all catalyse the same general reaction (Scheme 2), their products have differing biological functions, due to the site of expression and mechanism of activation of the respective proteins. These enzymes have been studied by genetically modified mouse experiments in which mice are specifically bred with the class I enzymes knocked out. This is lethal for both PI3K α and PI3K β , removing the possibility of chronic dosing and limiting the application for small molecule inhibitors to cancer studies. However, knock out of PI3K γ or PI3K δ leads to a viable mouse with reduced immune function, suggesting chronic dosing may be possible.^{20,21}

CONFIDENTIAL – PROPERTY OF GSK – DO NOT COPY

Since COPD is known to be caused by an over active immune response, the genetic data above suggests these targets should be of interest to this therapy area.

A number of studies have been conducted which directly link PI3K δ inhibition with treatment for COPD. It has been shown that in the presence of a PI3K δ inhibitor there is a reduced immune response in allergic airway inflammation in mouse models.²² It has also been shown that treatment of corticosteroid insensitive cigarette-smoke-exposed mice with a PI3K δ inhibitor reverses insensitivity.²³ Studies using an inactivating point mutation in the PI3K δ active site have shown that PI3K δ plays an essential role in mast cell allergic response; reducing histamine release in response to allergens and therefore inflammation.²⁴ Inhibition of PI3K δ has also been shown to reduce neutrophil influx into inflamed tissue.²⁵ In COPD, neutrophil accumulation is thought to be a major source of airway wall inflammation,^{26,27} hence prevention of this could provide benefit for COPD patients.

In 2013, a genetic study of patients with recurrent respiratory infections, a phenotype similar to COPD, found a mutation in PI3K δ (glutamic acid-1021 to lysine) in a number of patients.²⁸ Further studies on this mutation showed that this is not present in any healthy individuals and that the mutation causes enhanced kinase activity of PI3K δ .²⁸ This genetic disorder has become known as Activated PI3K δ Syndrome (APDS) and the mutation has been found in around fifty patients worldwide.²⁹ PI3K δ inhibition is therefore a viable treatment option for these patients and could provide an additional disease area of interest. Also, the fact that activating PI3K δ causes recurrent infections and inflammatory disease suggests that inhibition of PI3K δ could be used to treat diseases such as COPD in which this phenotype is common.

Based on all of the above, the role of PI3K δ in multiple relevant cell types and in a human genetic disease make the development of selective small molecule inhibitors an attractive treatment proposition for COPD.

1.4 Designing Selective PI3K δ Inhibitors

This project will focus on PI3K δ which, like the other PI3K class I enzymes, is composed of a p110 catalytic subunit and a p85 regulatory subunit. These subunits are largely conserved; however, there are non-conserved regions in the protein structure, hence allowing for selective inhibition. An X-ray structure showing the endogenous ligand, ATP **4**, bound to PI3K δ is presented in Figure 7, with the key binding regions highlighted. The key interactions are also shown, namely a backbone hydrogen-bond between valine-828 and adenosine nitrogen and hydrogen-bond from adenosine amine to backbone glutamine-826. This is known as the hinge binding interaction. Hydrogen-bonds from lysine-779 and serine-754 to the phosphate group and ionic interactions with two Mg²⁺ ions form the back-pocket interaction.

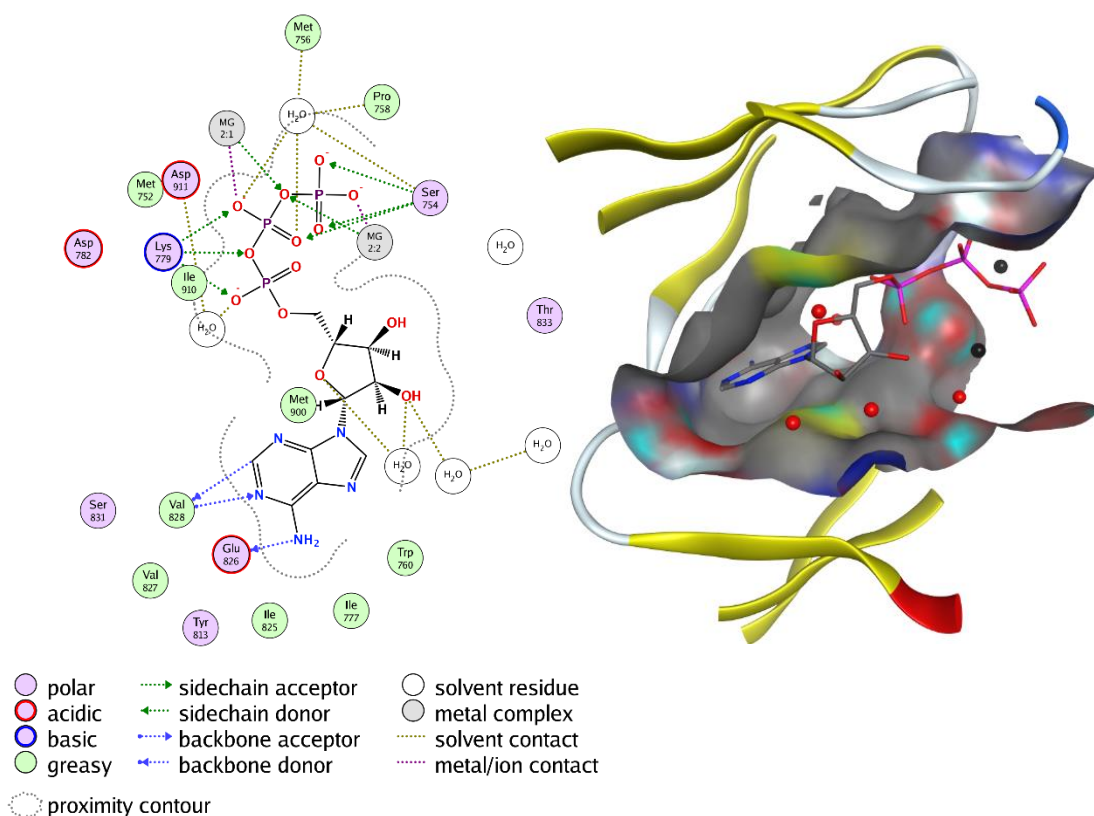
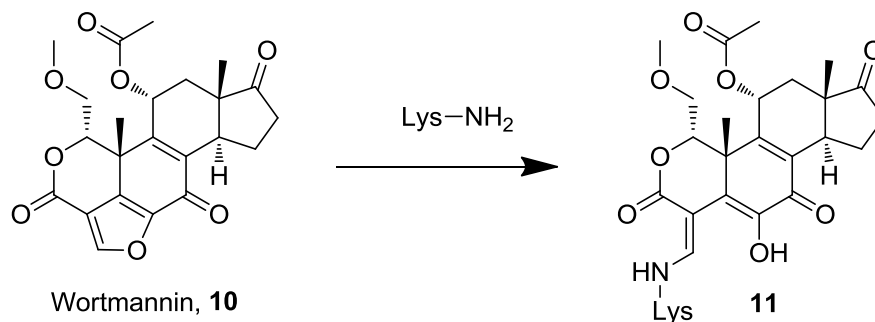


Figure 7 - X-ray crystal structure showing the natural ligand, ATP, bound within PI3K δ and interactions made by ATP, in PI3K δ . PDB ID = 2IMFR (2.23 Å). The following features are shown, as calculated by MOE: Hydrogen bond strengths >1.0 kcal mol⁻¹, ionic bond strengths >1.5 kcal mol⁻¹, residues within 4.0 Å.

CONFIDENTIAL – PROPERTY OF GSK – DO NOT COPY

The first PI3K inhibitor to be discovered as the natural product Wortmannin **10**.³⁰⁻³² This is an irreversible pan-PI3K inhibitor, which covalently binds *via* the conserved lysine-779 residue (Scheme 3). However, the lack of selectivity over other PI3K isoforms leads to high toxicity and renders the compounds unsuitable as a therapeutic.



Scheme 3 – Structure and mechanism of action of pan-PI3K inhibitor, Wortmannin **10**.

However, it has been possible to develop selective PI3K δ inhibitors. IC87114, **12**, was discovered by Icos Corporation from elaboration of a screening library hit.³³ This compound exhibits moderate selectivity and potency, however shows that selective inhibition of PI3K δ over other class I isoforms is possible.

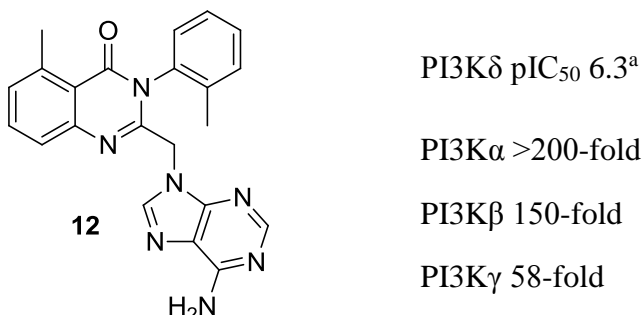
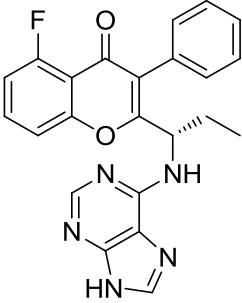
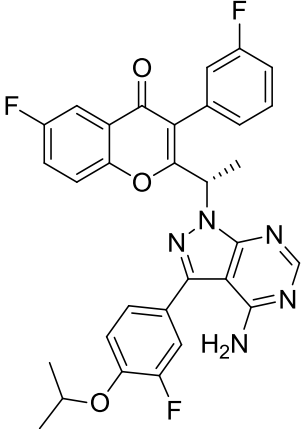
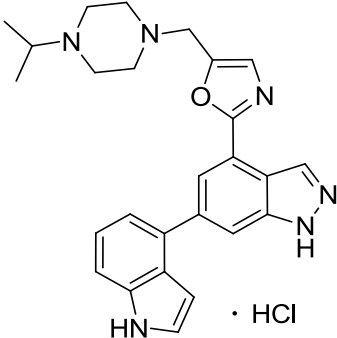


Figure 8 – The structure, potency and selectivity of IC87144, **12**. ^aData is taken from original publication.³³

A number of selective PI3K δ inhibitors have now been developed and progressed into clinical trials, and these are summarised in Table 2.

Name / Company	Structure	Indication / Status	Potency ^a / Selectivity ^a
Idelalisib ^{34,35} 13 Gilead Sciences		Oncology Oral Approved	PI3K δ pIC ₅₀ 7.7 PI3K α 453-fold PI3K β 210-fold PI3K γ 110-fold
Umbralisib ^{36,37} 14 TG Therapeutics		Oncology Once daily oral Phase II	PI3K δ pIC ₅₀ 7.7 PI3K α >10000-fold PI3K β >50-fold PI3K γ >48-fold
Nemiralisib ³⁸ 15 GSK		COPD Inhaled Phase II	PI3K δ pK _i 9.9 PI3K α >1000-fold PI3K β >1000-fold PI3K γ >1000-fold

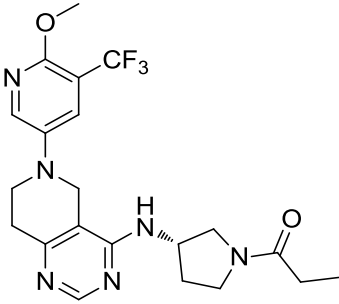
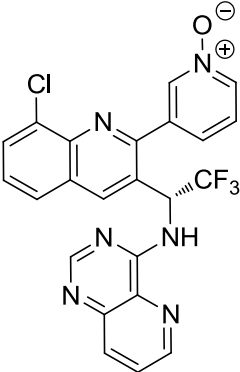
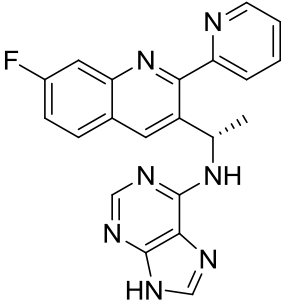
<p>Leniolisib³⁹⁻⁴¹</p> <p>16</p> <p>Novartis</p>		<p>Activated-PI3Kδ-Syndrome</p> <p>Sjögren's Syndrome</p> <p>Oral</p> <p>Phase II/III</p>	<p>PI3Kδ pIC₅₀ 7.6</p> <p>PI3Kα 11-fold</p> <p>PI3Kβ not reported</p> <p>PI3Kγ not reported</p>
<p>Seletalisib⁴²</p> <p>17</p> <p>UCB Pharma</p>		<p>Activated-PI3Kδ-Syndrome</p> <p>Sjögren's Syndrome</p> <p>Oral</p> <p>Phase I</p>	<p>PI3Kδ pIC₅₀ 7.9</p> <p>PI3Kα 303-fold</p> <p>PI3Kβ 177-fold</p> <p>PI3Kγ 24-fold</p>
<p>AMG319⁴³</p> <p>18</p> <p>Amgen</p>		<p>Oncology</p> <p>Oral</p> <p>Phase II</p>	<p>PI3Kδ pIC₅₀ 7.7</p> <p>PI3Kα 1833-fold</p> <p>PI3Kβ 150-fold</p> <p>PI3Kγ 47-fold</p>

Table 2 – Summary of literature clinical PI3K δ inhibitors. ^aData is taken from the original publication referenced in the name column.

CONFIDENTIAL – PROPERTY OF GSK – DO NOT COPY

A number of PI3K δ selective inhibitors are currently in clinical trials with indications in oncology and immune diseases, such as COPD and Sjögren's Syndrome. This shows the importance of the PI3K δ signalling pathway and its implication in many diseases. The available potency data suggests that for oral delivery a pIC₅₀ of greater than 7.5 is acceptable, with only the inhaled drug Nemiralisib **15**, exhibiting pK_i potency greater than 8. Selectivity of between 10-fold and >10,000-fold is observed for the other class I PI3K isoforms. This demonstrates that it is possible to achieve high selectivity for PI3K δ , however, is not necessarily required for progression into the clinic.

A number of the inhibitors (IC87114 **12**, Idelalisib **13**, Umbralisib **14**, Seletalisib **17** and AMG319 **18**) exhibit a similar chemotype with planar lipophilic substituents surrounding a chiral methyl or ethyl group. These compounds adopt a propeller-like structure, in which the nitrogen-rich heterocycle in each structure forms a hinge binding interaction with the backbone *N*-H of valine-828. Additionally, the purine *N*-H forms a hydrogen bonding interaction to the backbone carbonyl of glutamine-826. The quinoline or chromenone portion of the molecule is then pushed into a pocket known as the 'induced fit' pocket close to tryptophan-760 (Figure 9). Although these compound classes appear to exhibit reasonable potency and selectivity, they are deemed unlikely to be suitable for chronic dosing due to the high aromatic ring count. High aromatic ring count has been found to contribute to poor developability properties such as low solubility, high metabolic clearance and low selectivity.⁴⁴ This potentially accounts for why the development of these inhibitors have been limited to oncology.

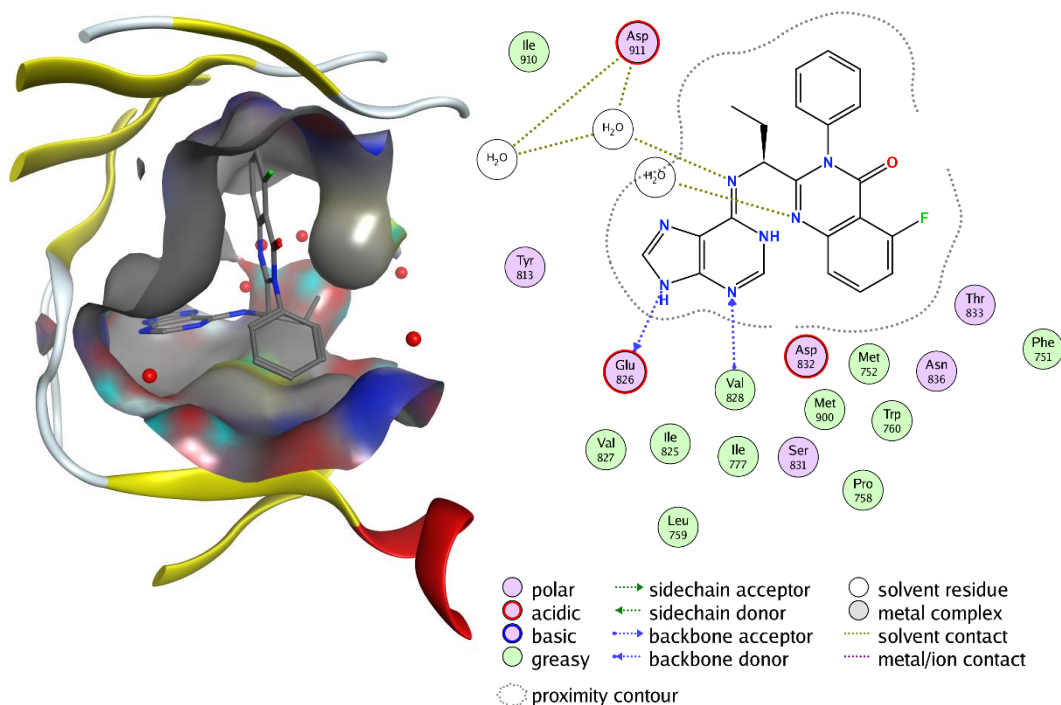


Figure 9 – X-ray crystal structure of Idelalisib 13, 4XE0 (2.43 Å). The following features are shown, as calculated by MOE: Hydrogen bond strengths $>1.0 \text{ kcal mol}^{-1}$, Ionic bond strengths $>1.5 \text{ kcal mol}^{-1}$, Residues within 4.0 Å.

Within our laboratories, a number of alternative chemical templates have been developed as PI3K δ inhibitors (Figure 10).⁴⁵ These include the ‘benzoxazine’ and ‘lactam’ series which will be discussed further in this thesis.

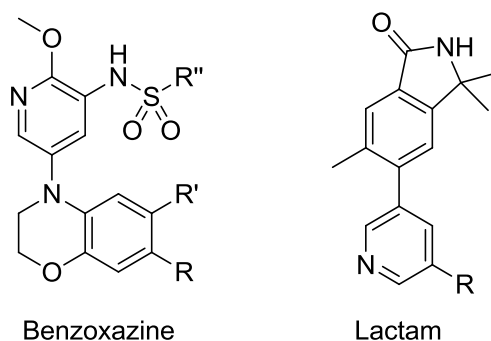


Figure 10 - Series of interest in the PI3K δ project.

Chapter 2. Benzoxazine Series

2.1 Introduction

2.1.1 Development of the Benzoxazine Series

The benzoxazine series was identified from a fragment screen;⁴⁵ a low molecular weight, but highly efficient starting point benzodioxine **19** was discovered. This fragment hit was then optimised to benzoxazine **20**, then further to lead compound **21** (Figure 11).

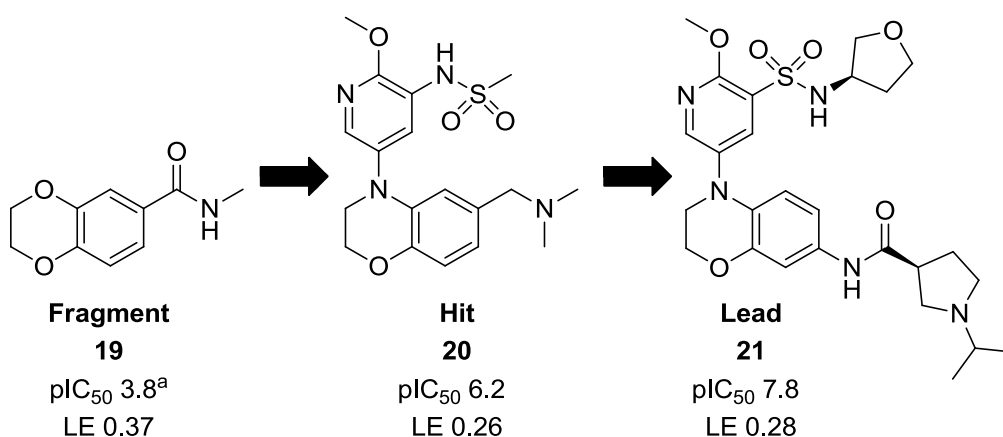


Figure 11- Summarised development of fragment screening hit 19 to lead compound 21. ^aDue to the small molecular size of this fragment, the biochemical screening was conducted using a higher maximum concentration than in the standard assay, giving a lower assay limit of pIC₅₀ ~2.8.

X-ray crystallography demonstrates the core of the molecule makes a number important interactions with the ATP binding site of PI3K δ (Figure 12). The key interactions are the benzoxazine oxygen in the hinge region, which participates in hydrogen bonding to the backbone *N*-H of valine-828, a water mediated hydrogen bond from pyridine nitrogen to aspartate-787 and -911 and interaction of protonated lysine-779 with sulfonamide oxygen. These interactions mimic the binding of ATP with the benzoxazine oxygen mimicking the interaction of one purine nitrogen and with the sulfonamide occupying the ATP phosphate region.

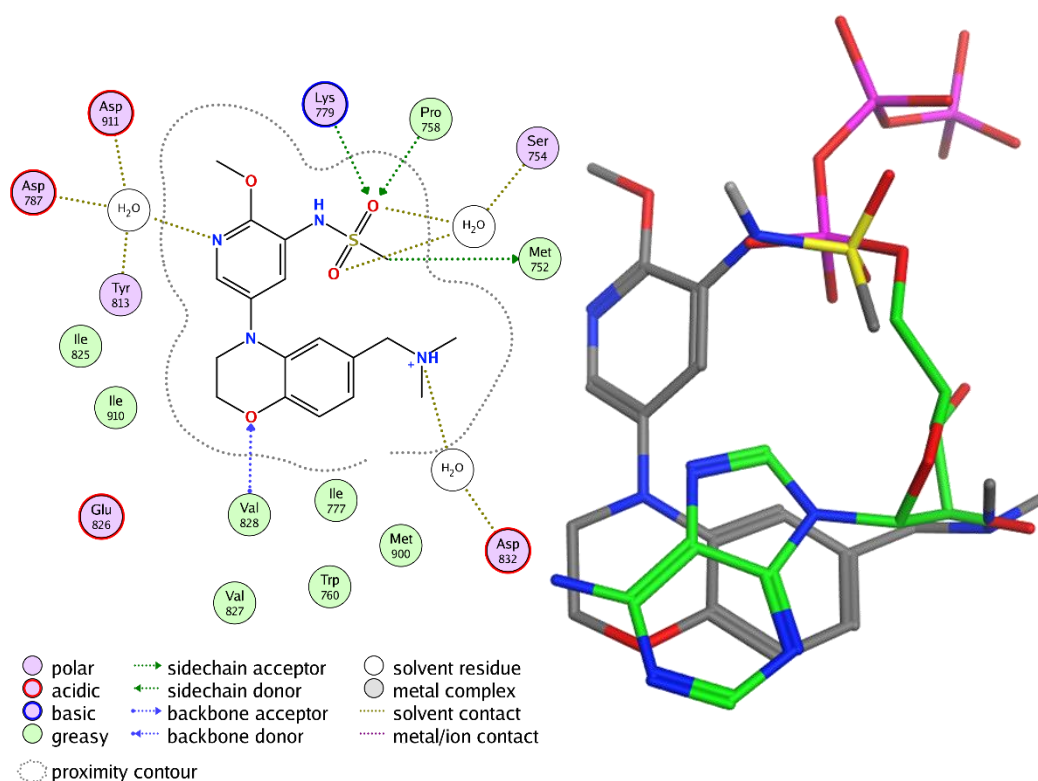


Figure 12 - The key interactions of benzoxazine 20 and an overlay of bound conformations of benzoxazine 20 (grey, 9GWLQ, 2.15 Å) and ATP 4 (green, 2IMFR, 2.23 Å) bound to PI3K δ . The following features are shown, as calculated by MOE: Hydrogen bond strengths >1.0 kcal mol $^{-1}$, ionic bond strengths >1.5 kcal mol $^{-1}$, residues within 4.0 Å.

One strategy employed, elsewhere within our laboratories, to synthesise molecules of increased potency and selectivity was to grow towards tryptophan-760. This residue is conserved across the class I PI3K isoforms; however, the surrounding residues are altered allowing more space for interactions in the δ -isoform. Interaction in the other PI3K isoforms requires displacement of protein sidechains, forming a strategy for achieving selective inhibition of PI3K δ .

This led to the development of benzoxazine **21** which forms an additional interaction with tryptophan-760, as well as maintaining key benzoxazine interactions. The interaction of a lipophilic *iso*-propyl group with tryptophan-760 provided a gain in potency and selectivity over the other class I isoforms (Figure 13).

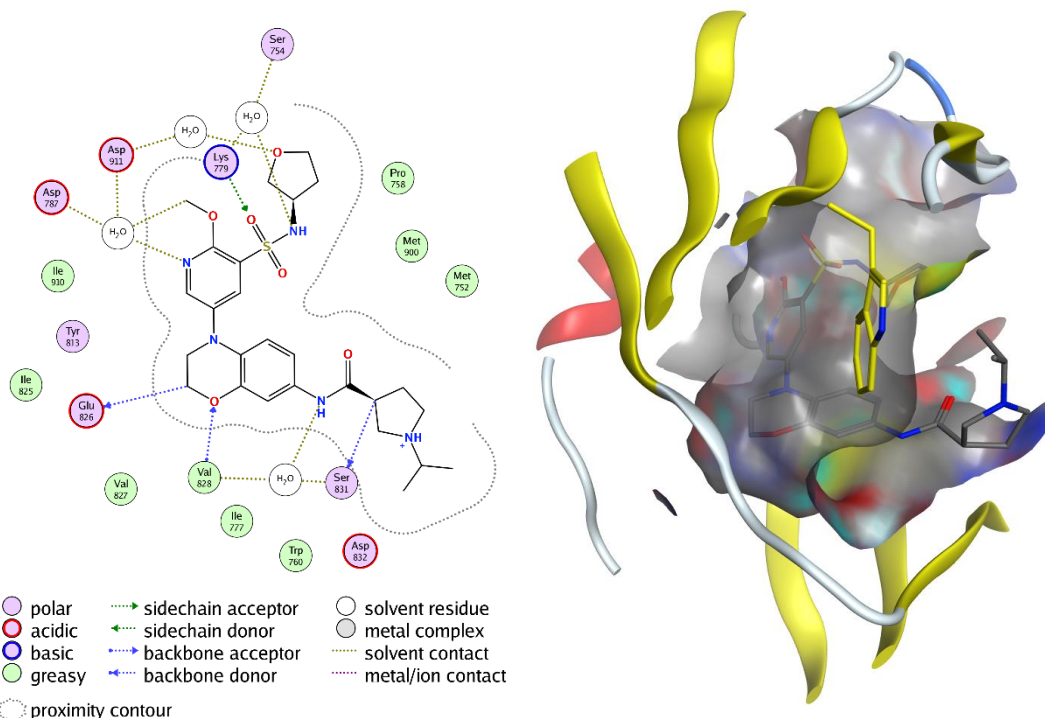


Figure 13 - The key interactions of benzoxazine 21 (9HZDX, 2.31 Å). The following features are shown, as calculated by MOE: Hydrogen bond strengths $>1.0 \text{ kcal mol}^{-1}$, Ionic bond strengths $>1.5 \text{ kcal mol}^{-1}$, Residues within 4.0 Å.

An analysis of protein bound X-ray crystal structures of molecules in the benzoxazine series led to an alternative hypothesis for optimising the series (Figure 14). The binding mode shows that the sulfonamide substituent and the benzoxazine 6-position substituent occupy adjacent regions of the protein, with the carbon atom of each methyl group separated by 3.3 Å. This resulted in the hypothesis that a macrocyclic approach may be employed to design further compounds with potentially improved properties such as permeability and clearance. The potential advantages that this approach offers are outlined in the subsequent sections.

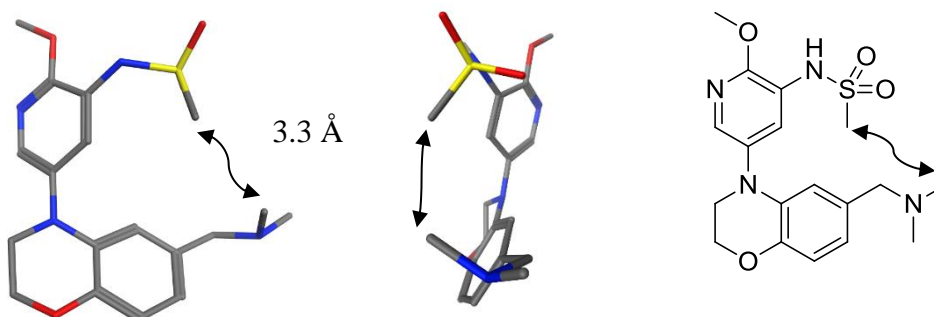


Figure 14 – Protein bound X-ray crystal structure of benzoxazine 20 (ligand only) (9GWLQ, 2.15 Å) and proposed macrocyclisation strategy.

2.1.2 Macrocycles in Drug Discovery

Macrocycles offer an exciting opportunity in drug discovery due to the potential for improved properties in many regards. Firstly, the increased conformational restriction in a macrocycle provides an opportunity for increased potency afforded by a reduced entropic cost of binding. The restriction in conformation may also result in increased selectivity due to a reduction in available conformations for binding to alternative sites.⁴⁶ Macrocycles have also shown promising drug-like properties with a number of such compounds being progressed to clinical trials.⁴⁷

The macrocycle pacritinib **22** (Figure 15) has been developed to target Janus Kinase 2 (JAK2), a protein kinase. This compound is currently in phase III clinical trials as a treatment for myelofibrosis, a bone marrow disease. This highlights the potential for macrocycles to target kinases, but also shows that macrocycles can exhibit favourable developability properties for progression as clinical candidates and ultimately to the market as a new medicine.⁴⁸ In this example, the authors chose to use macrocycles in order to gain structural novelty; the pyrimidine motif being well documented as a JAK2 inhibitor chemotype.⁴⁹ However, no data is available on directly comparable acyclic molecules and hence other benefits of macrocyclisation are more difficult to discern in this case.

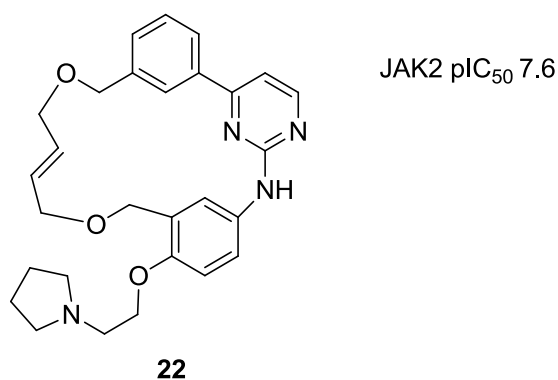


Figure 15 - The structure of pacritinib **22**.

Another example of a successful macrocyclic approach in which an increase in potency is seen, is in the area of beta-secretase 1 (BACE-1) inhibitors. Lead compound **23** was first simplified to give progenitor **24**. Macrocyclisation, by addition of a carbon-carbon

bond (**24** to **25**), offered a greater than 30-fold increase in potency and further optimisation led to a highly potent macrocycle **26** (Figure 16).⁵⁰

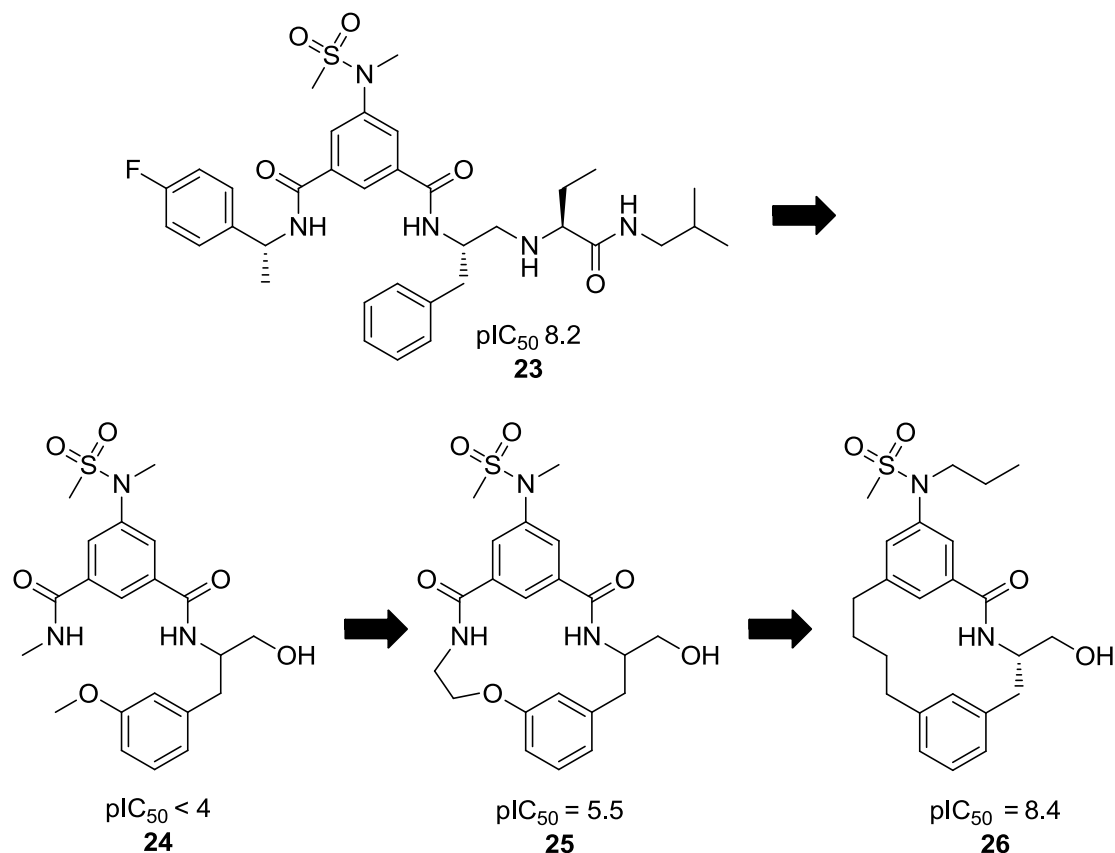


Figure 16 – Acyclic and macrocyclic inhibitors of BACE-1.

The authors hypothesise that a reduction in conformational freedom present in the macrocyclic inhibitor **25** compared to acyclic progenitor **24**, led to the potency increase observed.⁵⁰ This allowed the group to remove several binding functional groups from lead compound **23** and still maintain potency in macrocycle **26**.

Another recent example comes from Pfizer focusing on inhibitors of the Anaplastic Lymphoma Kinase (ALK).⁵¹ ALK is a tyrosine kinase in the insulin receptor family and is implicated in oncology.⁵² Here, Pfizer were searching for a central nervous system (CNS) penetrable molecule with high potency and selectivity. However, the authors encountered difficulty in achieving all these characteristics in a single acyclic molecule, hence, a macrocycle approach was utilised. The authors postulated that

reducing the number of rotatable bonds would make the molecules more compact with more buried surface area and, hence, could increase CNS penetration.⁵¹

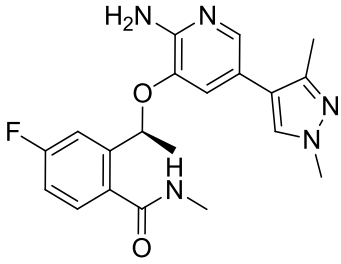
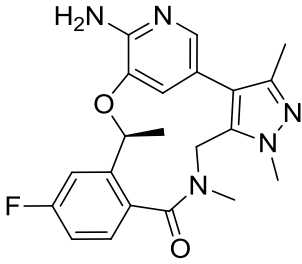
		
Compound Number	27	28
ALK pIC₅₀	8.6	>9.7
Cell pIC₅₀	6.9	9.2
log D_{pH 7.4}	2.1	2.2
LLE	3.7	5.7
Human liver microsomal clearance / mL min⁻¹ kg⁻¹	28	8.6
MDCK-MDR1 B→A/A→B ratio	17	4.2

Table 3 – Improvement in properties of ALK-inhibitor upon macrocyclisation.

Upon addition of a methylene linker to acyclic **27** to give macrocycle **28**, potency and efficiency are improved greatly, in both enzyme and in cell assays. The molecule also shows reduced metabolic clearance in microsomes, which could be a consequence of reduced accessibility of metabolic sites, or the restricted conformation of the macrocycle reducing promiscuous binding to metabolising enzymes such as cytochrome P450s. The MDCK-MDR1 ratio is also reduced; this assay uses modified Madin Darby canine kidney (MDCK) cells, transfected with MDR1 gene to express P-glycoprotein (P-gp), a key efflux transporter in the blood-brain barrier. The assay measures the rate at which compound moves from the basal (B, inside the blood-brain barrier) to the apical (A, outside the blood-brain barrier) side of a membrane and *vice-versa*. A smaller ratio indicates that the compound is effluxed at a slower rate, which indicates that the compound is less likely to be effluxed from the CNS *via* P-gp.⁵³

Hence, compounds with a smaller ratio are likely to be more brain penetrant and offer a more promising profile for CNS therapeutics.

Despite these improvements, it was found the macrocycle **28** had poor selectivity over a range of other related kinases. Hence the pyrazole was further elaborated to give the candidate macrocycle **29** with higher selectivity over related kinases.

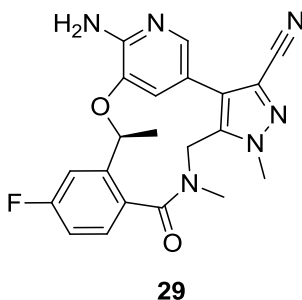


Figure 17 – Macrocycle **29** advanced into *in vivo* studies and later into Phase I/II clinical trials as an oral ALK inhibitor.

Macrocycle **29** was advanced to rat *in vivo* studies where it showed 100% oral bioavailability and high CNS penetration. Given, this promising profile, the molecule was later progressed to phase I/II clinical trials for non-small-cell lung carcinoma. This optimisation campaign shows the potential for macrocyclisation to positively impact a range of drug-like properties and provides a precedent for oral bioavailability with these cyclic scaffolds.

Workers at AstraZeneca have found that macrocyclisation strategies can also be applied to protein-protein interactions.⁵⁴ They have designed inhibitors of an interaction between B-Cell Lymphoma 6 (BCL6) and a corepressor protein, for oncology indications. Upon forming a macrocycle, the authors observe a greater than 200-fold increase in potency.⁵⁴

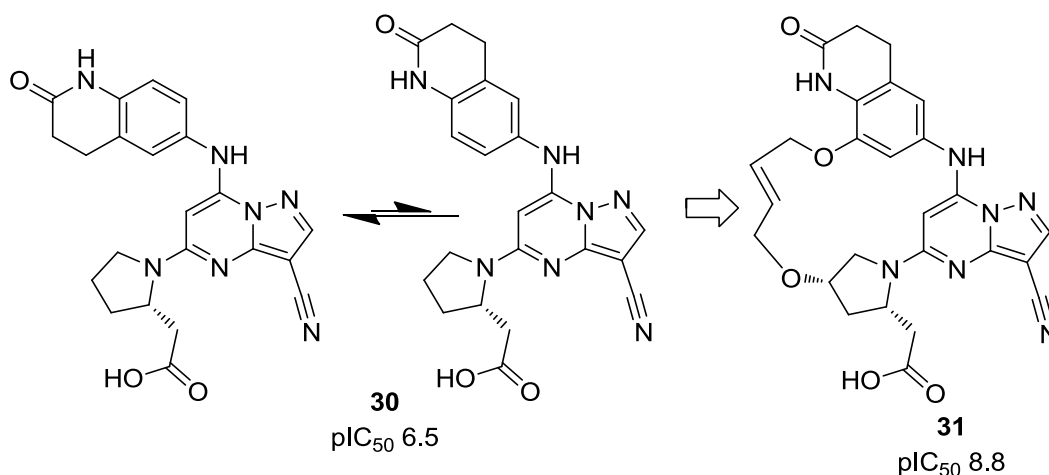


Figure 18 – Progenitor and macrocycle inhibitors of BCL6 protein-protein interaction.

The authors show in NMR studies that the main solution conformation of the progenitor compound **30** is with dihydroquinolinone portion in non-binding conformation (left) and therefore there is a barrier to access the required binding conformation (centre). However, the macrocyclic linker fixes the molecule in the favourable binding conformation removing this barrier. Hence, the overall energetics of binding are more favourable and the potency is higher.

Based on all the above, a macrocyclisation strategy was attractive for the benzoxazine lead series for PI3K δ , with the aim of enhancing potency and evaluating the impact of macrocyclisation on other drug parameters. The impact will then be examined to explore whether macrocycles provide an improved template for oral or inhaled compounds.

2.1.3 Existing PI3K δ Macrocycles

An initial set of macrocyclic benzoxazine PI3K δ inhibitors were designed⁵⁵ and synthesised⁵⁶ elsewhere in our laboratories, based on progenitor compound **20** (Table 4).

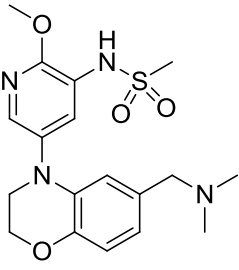
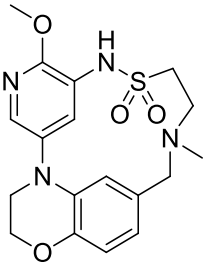
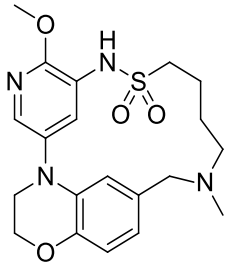
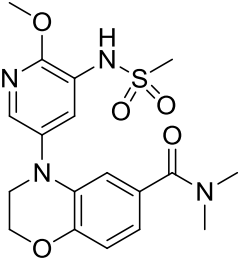
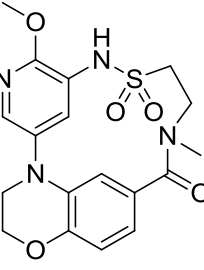
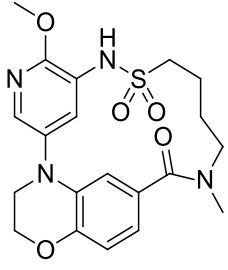
			
Compound no.	20	32	33
pIC₅₀ PI3Kδ	6.2	7.7	7.1
			
Compound no.	34	35	36
pIC₅₀ PI3Kδ	5.5	6.9	6.3

Table 4 – Initial potency data for macrocycles compared to progenitor molecules. All $n \geq 2$ unless otherwise indicated.

This data is analysed further in subsequent sections.

2.2 Aims

The aims for this chapter are:

- To design and synthesise a range of macrocyclic analogues of the benzoxazine series.

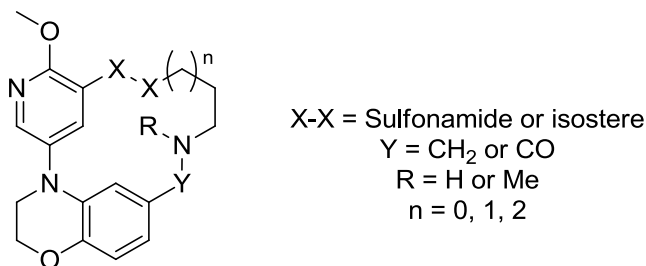


Figure 19 – Targets for synthesis in Chapter 2.

- To explore effects of macrocyclisation on potency and efficiency for PI3K δ inhibition.
- To assess whether the macrocyclic templates provide advantageous properties for oral or inhaled delivery, with a focus on solubility, permeability and metabolic clearance.
- To evaluate the effect of macrocyclisation on chemical properties such as acidity, basicity and lipophilicity.

2.3 Results and Discussion

2.3.1 Investigation into Potential for Macrocyclisation

Analysis of all the available PI3K δ potency data for macrocyclic compounds (Table 4) showed that the macrocycles exhibit increased potency when compared to the progenitor molecules. The two-carbon linked compounds **32** and **35** both had greater than 10-fold increase in potency, whereas the four-carbon linked compounds **33** and **36** exhibited a more modest increase. In all cases, the amine analogues were approximately 5-fold more potent than the amide analogues. This is possibly due to a balance being required between rigidity of amide linkers, providing entropic favourability, and flexibility of amine linkers, allowing more optimal interactions with the protein.

Initial interest centred on the most potent compound **32**, which showed a 30-fold increase in potency compared to its progenitor compound **20**. Investigations were conducted to determine the potential for further optimisation of the series, and to understand the nature of the potency increases observed. The initial hypothesis was that reduced entropic cost of binding due to the conformational restriction present in the macrocycle was driving increased potency, however it was not clear if further increases were possible.

In the first instance, crystal structures were generated for the macrocyclic compound **32** and progenitor molecule **20** bound to the PI3K δ enzyme.⁵⁷

2.3.1.1 X-Ray Crystallography

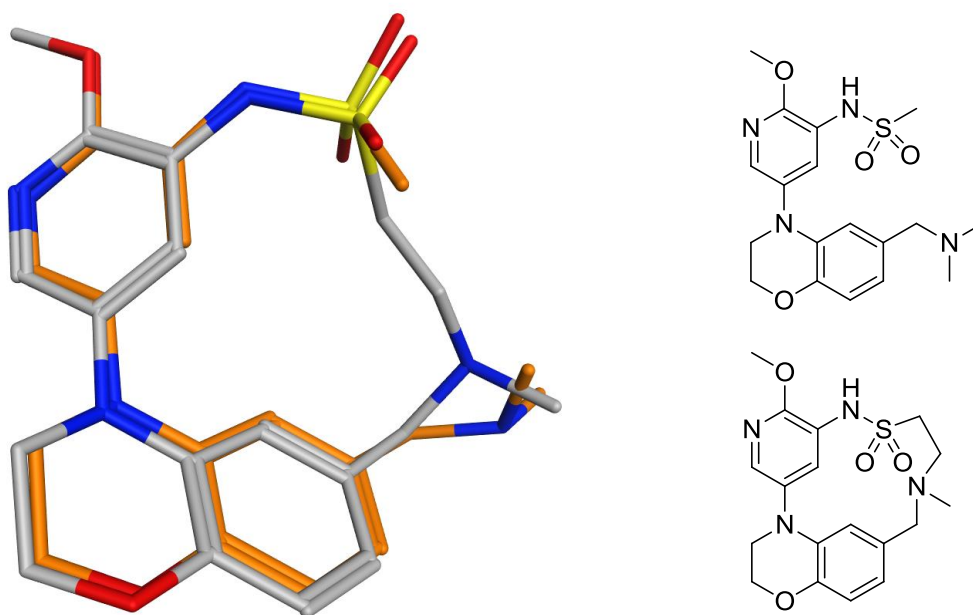


Figure 20 – Overlay of protein bound X-ray crystal structures of progenitor **20** (orange, 9GWLQ, 2.15 Å) and macrocycle **32** (grey, 3VLSE, 2.24 Å).

An overlay of the two crystal structures showed that both molecules share the same binding mode, with conserved interactions in the hinge and back pocket (see 1.4 Designing Selective PI3K δ Inhibitors). However, a number of differences are evident upon closer examination of the binding mode.

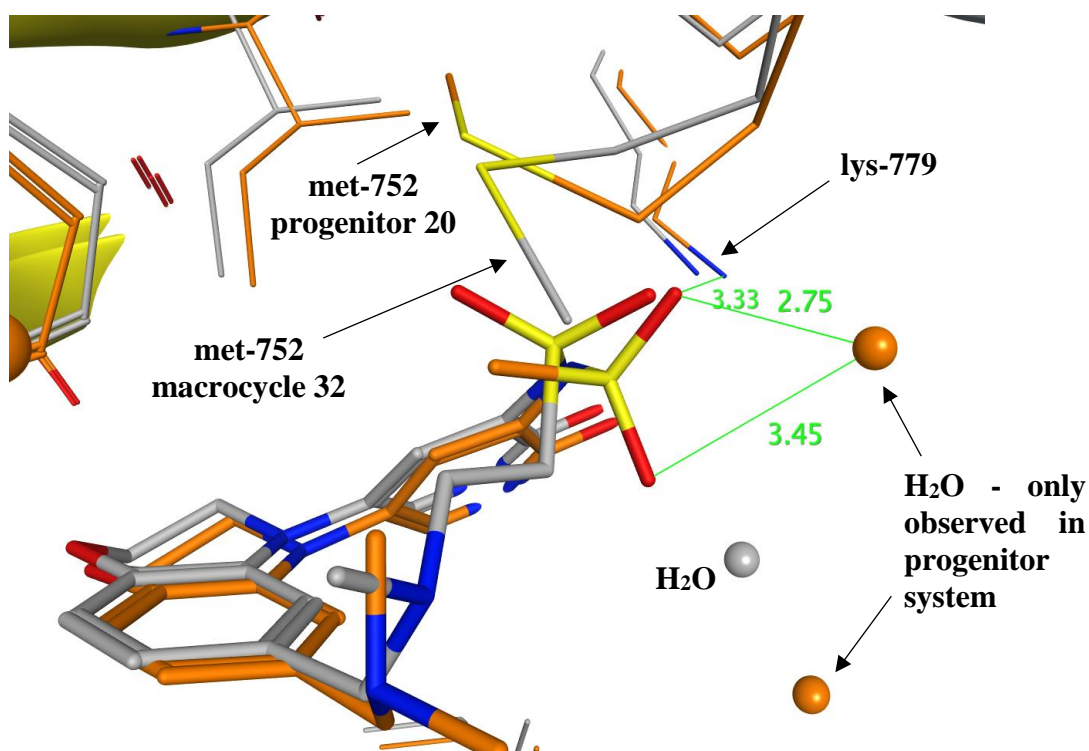


Figure 21 - X-ray crystal structures of progenitor **20** (orange, 9GWLQ, 2.15 Å) and macrocycle **32** (grey, 3VLSE, 2.23 Å) highlighting differences in sulfonamide conformation.

Firstly, the sulfonamide appears to be adopting an alternative conformation. Whilst the X-ray crystal structure is unable to differentiate the oxygen and methyl group on the progenitor sulfonamide, the structure is modelled in a conformation which enables a possible hydrogen bonding interactions with a water molecule in the crystal, and places the methyl group into a lipophilic interaction with methionine, seen at the top of the image. In the macrocycle, the ring constraint forces the sulfonamide to occupy a different conformation. This conformation still allows favourable interactions with lysine-779, shown at the back top of the image, however, fewer interactions are possible with the water molecule that is present in the progenitor crystal structure. Indeed, this water is not observed in the macrocycle crystal structure despite the crystal structures having similar resolution (9GWLQ, 2.15 Å and 3VLSE, 2.24 Å). This conformation also means that the sulfonamide oxygen is forced close to methionine-752, creating an unfavourable lipophilic-polar interaction and causing the methionine to flip. This loss of sulfonamide solvation and loss of lipophilic interaction would be expected to cause an enthalpic penalty to binding.

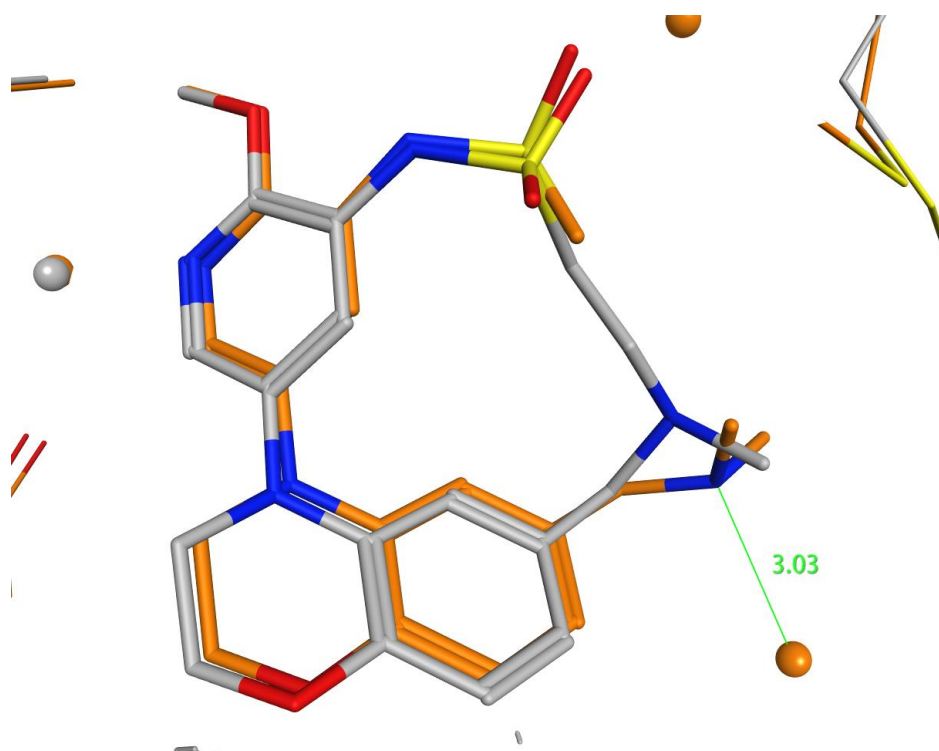


Figure 22 - X-ray crystal structures of progenitor **20** (orange, 9GWLQ, 2.15 Å) and macrocycle **32** (grey, 3VLSE, 2.23 Å) highlighting differences in amine conformation.

Secondly, the amine portion of the molecule appears to adopt a slightly different conformation. In the progenitor molecule **20**, the amine can make a hydrogen bonding interaction with a water molecule present in the structure which is not possible for the macrocycle. However, it should be noted that the electron density for the progenitor structure is not well defined in this region and therefore the modelled structure may not accurately reflect the dynamic range of possible conformations present in the crystal. Since the acyclic molecule shows disorder in the crystal, the loss of this interaction may not be significant, and care should therefore be taken not to overinterpret this observation.

Taken together, these observations in the subtle differences between the binding conformations of progenitor and macrocycle suggested that further optimisation of the macrocycle would be possible, with the aim of further improving potency of the cyclised compounds.

2.3.1.2 Biophysical Techniques

To further explore the differences in binding, the generation of thermodynamic data was explored. These experiments allow elucidation of the enthalpy and entropy of binding, giving a greater understanding of the overall binding event.

There are a number of methods for measuring binding thermodynamics experimentally. These include isothermal titration calorimetry (ITC)⁵⁸⁻⁶⁰ and surface plasmon resonance (SPR)^{61,62} techniques.

ITC gives a direct measure of the enthalpy of binding by measuring the heat change of binding and a direct measure of the binding affinity by measuring the concentration at which the binding takes place. The entropy and Gibbs free energy can then be calculated using the following relationship:

$$\Delta G = -RT \ln K_d = \Delta H - T\Delta S$$

where $R = 8.314 \text{ JK}^{-1}\text{mol}^{-1}$ and $T = \text{temperature} / K$

Equation 1 – Definition of Gibbs free energy

However, ITC experiments typically require a large amount of protein and hence were ruled out for this study due to issues with protein supply.

SPR is a versatile technique for analysing biological interactions.⁶³ SPR involves tethering of the protein of interest to dextran above a gold surface. The sensor chip is then irradiated with polarised light, resulting in reflection at a specific angle. The angle of reflection is dependent on the state of the gold surface, and therefore the state of the tethered protein. A ligand is then flowed across the surface of the gold allowing binding to take place. Changes in this angle of reflection are sensitive enough to detect a ligand binding to the protein, and therefore binding can be observed (Figure 23).

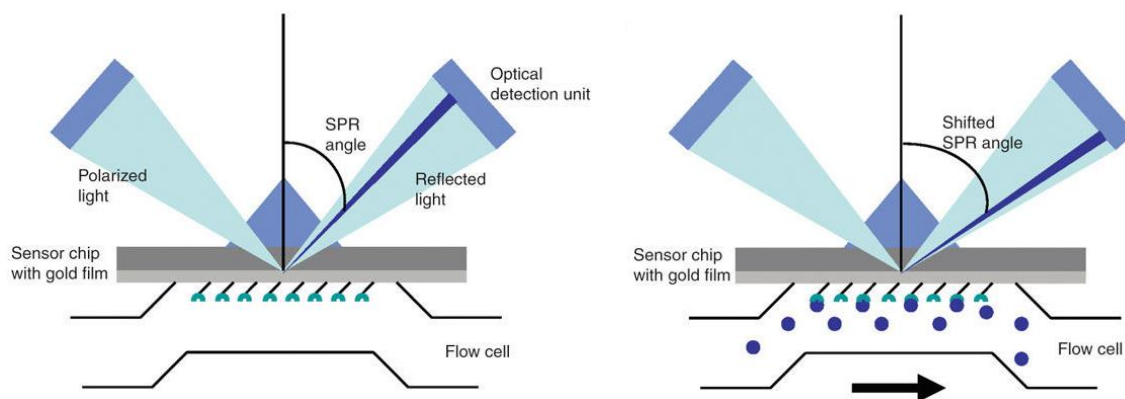


Figure 23 – Schematic illustrating the principle of surface plasmon resonance.⁶⁴

Changes in the angle of reflected light can be used to observe association and dissociation kinetics (Figure 24). Raw data is analysed using a computer model to generate fitted curves from which the on and off rates can be determined.⁶⁵ The known PI3K δ inhibitor **37**⁶⁶ was used as a positive control to test the assay.

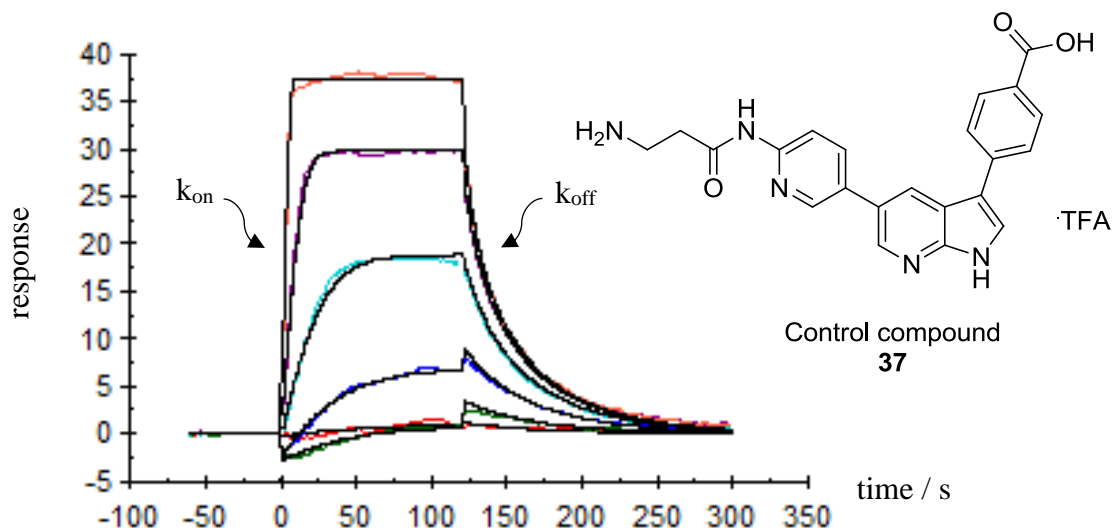


Figure 24 – Measured SPR curves (coloured) and fitted curves (black) for control compound **37** at 25 °C with different colours showing varying concentrations of compound **37**.

From these kinetics, the dissociation constant can be calculated using the following equation:

$$K_d = \frac{k_{on}}{k_{off}}$$

Equation 2 – Kinetic determination of equilibrium constant.

This then allows determination of the binding thermodynamics by using a Van't Hoff analysis. The experiment is conducted at varying temperature to establish a relationship between the equilibrium constant and temperature. Rearranging Equation 2 shows that a linear relationship is expected between the natural logarithm of the equilibrium constant and the reciprocal of temperature:

$$\ln K_d = -\frac{\Delta H}{RT} + \frac{\Delta S}{R}$$

where $R = 8.314 \text{ JK}^{-1}\text{mol}^{-1}$ and $T = \text{temperature} / \text{K}$

Equation 3 – The Van't Hoff relationship

Therefore, a plot of $\ln(K_d)$ vs. $1/T$ should have a gradient of $-\Delta H/R$ and an intercept of $\Delta S/R$ (Equation 3). This analysis makes the assumption that the enthalpy and entropy are constant across the experimental temperature range.

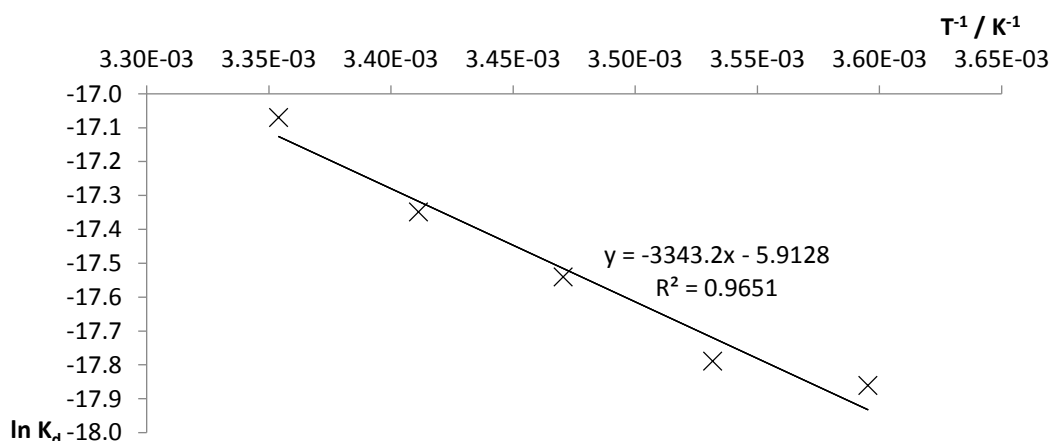


Figure 25 – Van't Hoff analysis for control compound **37**.

This experiment was conducted for the progenitor compound **20**, the macrocycle **32** and known PI3K δ inhibitor **37** using a temperature range of 5-25 °C.⁶⁷ The Van't Hoff analysis was then carried out and the data is summarised in Table 5.

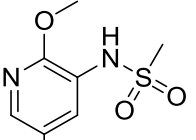
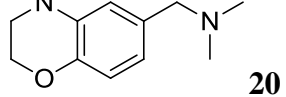
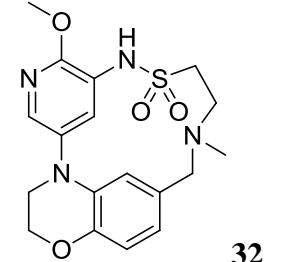
Entry	Compound	$\Delta H /$ kJ mol^{-1}	Error $\Delta H /$ kJ mol^{-1}	$\Delta S / \text{J K}^{-1}$ mol^{-1}	Error ΔS $/ \text{J K}^{-1}$ mol^{-1}	$\Delta G 25\text{ }^\circ\text{C} /$ kJ mol^{-1}	pK_d 25 $^\circ\text{C}$	pIC_{50}	pK_{app}
1		-55.2	8.0	-59.9	27.6	-37.4	6.6	6.2	6.8
2	 20	-62.5	4.9	-85.0	17.0	-37.1	6.5	6.2	6.8
3	 32	-1.0	35.8	163.9	125.3	-49.9	8.7	7.7	8.3
4		0.3	5.2	155.8	18.0	-46.1	8.1	7.7	8.3
5	Control 37	-27.8	3.1	49.2	10.6	-42.4	7.4	6.8	7.4
6		-23.3	1.1	64.9	3.8	-42.6	7.5	6.8	7.4
7		-15.6	1.3	91.1	4.4	-42.7	7.5	6.8	7.4

Table 5 – Results of SPR thermodynamic analysis.

Data generated from variable temperature SPR experiments for the control compound **37** (entries **5-7**) showed that some variation is present in the experiment. However, in general significant changes in observed values are much greater than the errors present. For the macrocycle **32**, an almost horizontal line was observed.

Based on our hypothesis that the increase in potency with macrocycle **32** was due to a reduced entropic cost of binding it was anticipated that the macrocycle would show a larger entropic contribution than progenitor **20**. This is observed in the experiment, with the macrocycle gaining 215.3-248.9 J K⁻¹ mol⁻¹ in entropic contribution and this is indeed consistent with reduced conformational flexibility in the unbound state.

The macrocycle **32** was expected to lose some enthalpic contribution due to the restricted conformation not being able to make as optimal interactions with the protein as the progenitor **20**. This is indeed observed, with the macrocycle losing 54.2-62.6 kJ mol⁻¹, however the magnitude of this change was unexpected. These results suggest the macrocycle has minimal enthalpic contribution to binding.

An analysis of hydrogen bond energies indicates a bond strength of approximately 4-5 kcal mol⁻¹ (16-21 kJ mol⁻¹) is typical.⁶⁸ However, these figures are approximate and in a macromolecular system, such as an enzyme binding to a reversible inhibitor, there are a large number of interactions. Hence, this complexity means that firm conclusions cannot be drawn, but some inferences can be made. The difference observed in the enthalpy would correspond to approximately three hydrogen bonds being lost. Two of these could originate from the sulfonamide and amine. These are likely to be solvated by water in the unbound state, however become unable to form hydrogen bonds in the bound state. The remaining value could be made up from the macrocyclic restrictions, these may prevent the core of the molecule from making the same optimal interactions as the acyclic precursor with the hinge region for example.

A similar analysis has been carried out by Sasikala *et al.* to analyse the entropy gain upon displacing each of eight water molecules present in the streptavidin cavity.⁶⁹ This analysis indicates entropy components of between 12.5 and 18.2 cal K⁻¹ mol⁻¹ (52.5 to 76.1 J K⁻¹ mol⁻¹) per water molecule.⁶⁹ Assuming the water molecules in PI3K δ have a similar degree of order in their conformation, the differences in entropy would

correspond to 3 to 5 water molecules being displaced. Considering the sulfonamide and amine interactions discussed previously, two water molecules are present in the crystal structure for the progenitor compound **20**, that are not present for the macrocycle **32**. The remaining entropic gain could be explained by the conformational restrictions present in the macrocycle, compared to the progenitor.

These data suggest that the macrocycle is indeed gaining potency due to entropic gains, however enthalpic losses are observed. It is therefore hypothesised that by optimising the macrocyclic linker, improved compounds could be designed. If the optimal enthalpic and entropic components of the two molecules could be combined, a hypothetical ΔG of $-111.3 \text{ kJ mol}^{-1}$ would be obtained corresponding to a pK_d of >19 . Whilst this theoretical combination is likely to be beyond the maximal efficiency possible for any ligand,⁷⁰ this demonstrates the potential of this approach for synthesising highly potent compounds.

2.3.2 Initial Exploration of Ring Size

Initial optimisation of macrocycle **32** focused on exploration of linker length. Targets were designed to probe the balance between maximal conformational restriction and maximal interactions with the binding site. In addition to amine linkers, it was also hypothesised that amide macrocycles may provide additional conformational restriction and therefore were also targets of interest. It was also anticipated that amide macrocycles could reduce the cost of desolvation of the amine, due to the reduced hydrogen bond donor ability in an amide.

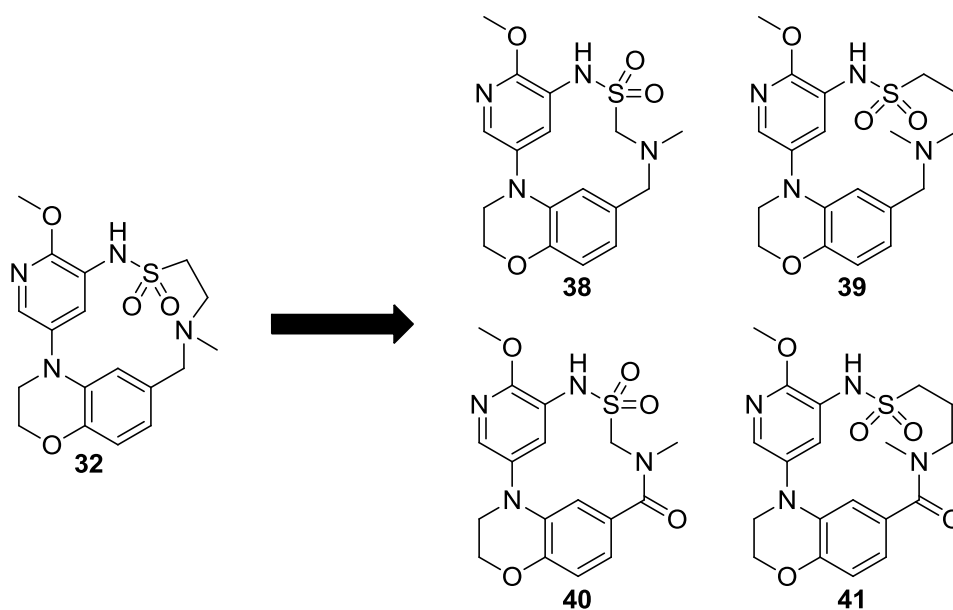
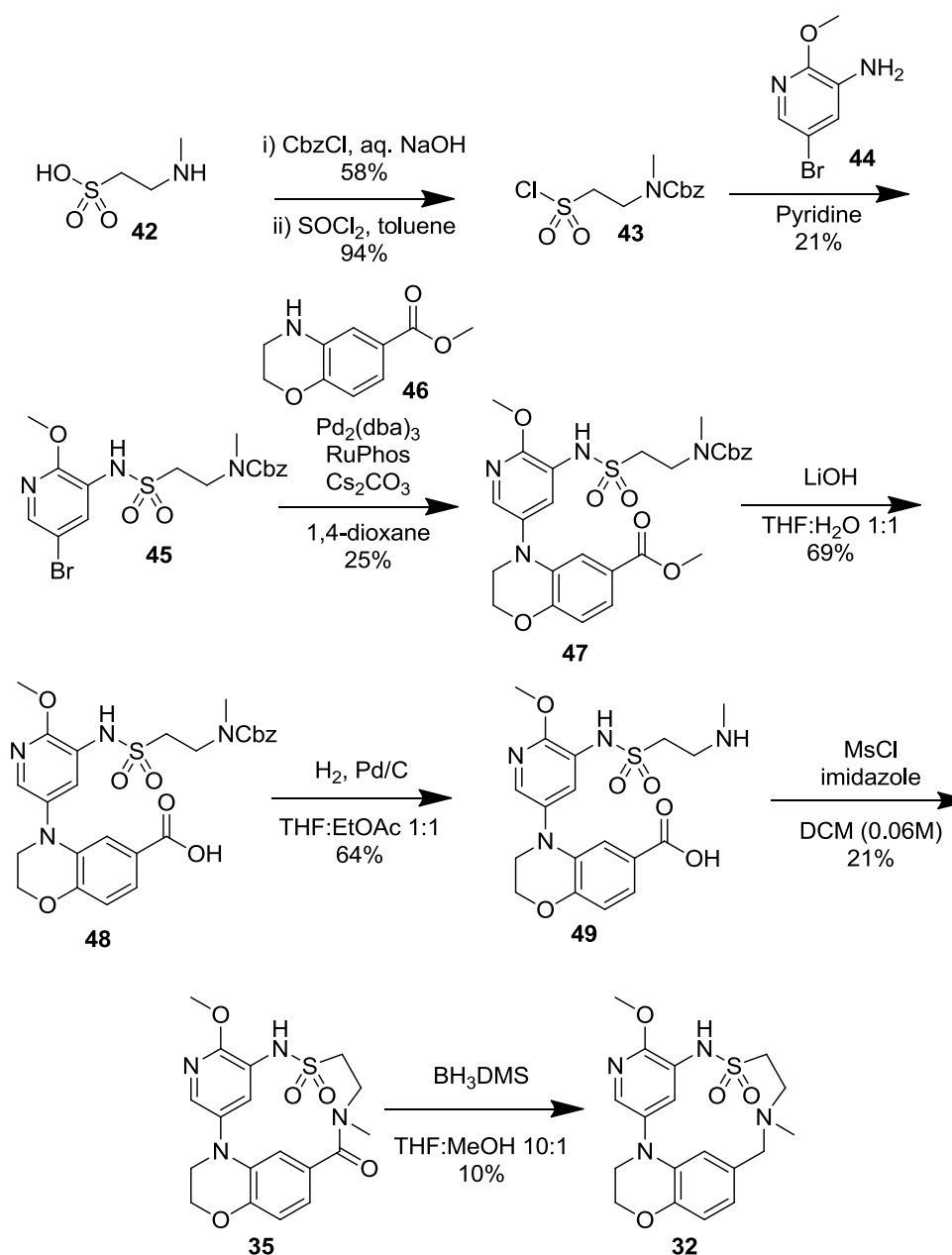


Figure 26 – Initial design of analogues of two-carbon linked macrocycle **32**.

Additionally, both the amine and amide macrocycles could be accessed using an analogous synthesis to the two-carbon linked macrocycle **32** designed within our laboratories⁵⁵ and synthesised externally (Scheme 4).⁵⁶



Scheme 4 – Synthesis of two-carbon linked macrocycle conducted elsewhere in our laboratories.

Analysis of the route used to synthesise two-carbon linked macrocycle **32** identified several areas where improvements could be made.

Firstly, the total number of steps in the route could be reduced by using commercially available sulfonyl chlorides *tert*-butoxycarbonyl **51** and phthalimides **50** and **52** (Figure 27). This removed the need for carboxybenzyl protection and sulfonyl chloride formation, however, introduced the need for an *N*-methylation step. This approach

would also allow conversion of late stage intermediates to form both the *N*-H and *N*-Me analogues for screening.

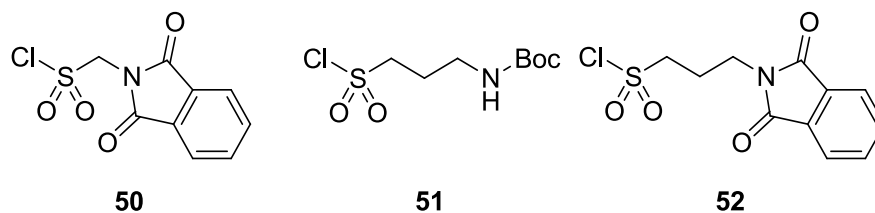
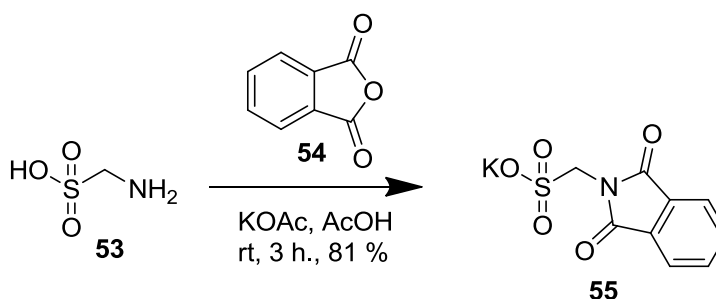


Figure 27 – Commercially available sulfonyl chlorides utilised in the synthesis of one- and three-carbon analogues.

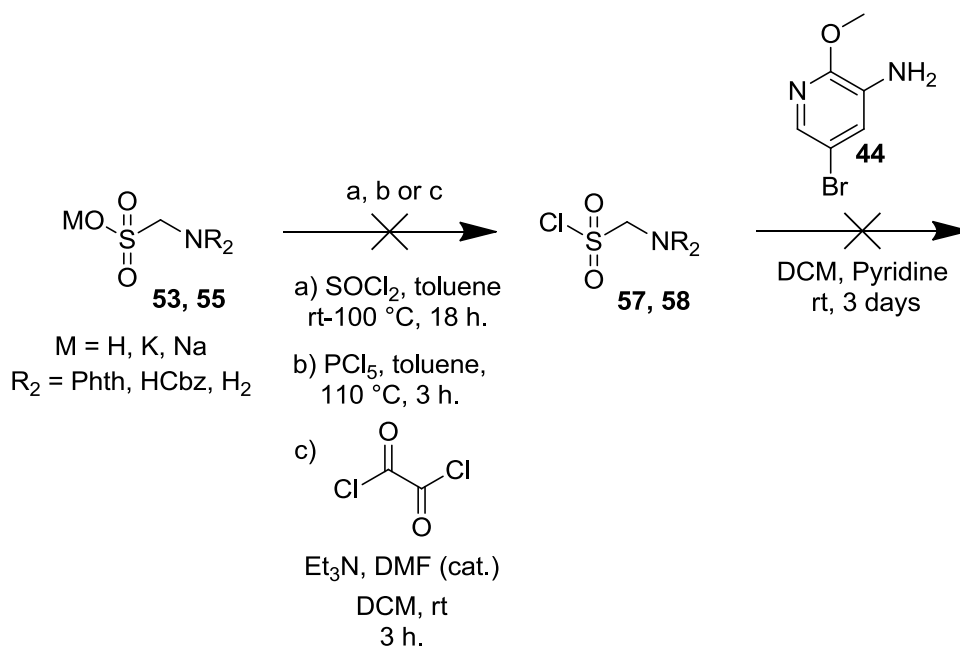
However, attempts to synthesise *geminal* sulfonyl chloride-protected amine **50** were unsuccessful. The material could not be provided from a commercial source due to issues of instability.

Aminomethane sulfonic acid **53** could be readily protected to yield phthalimide **55** or carboxybenzyl **56** protected amine (Scheme 5).



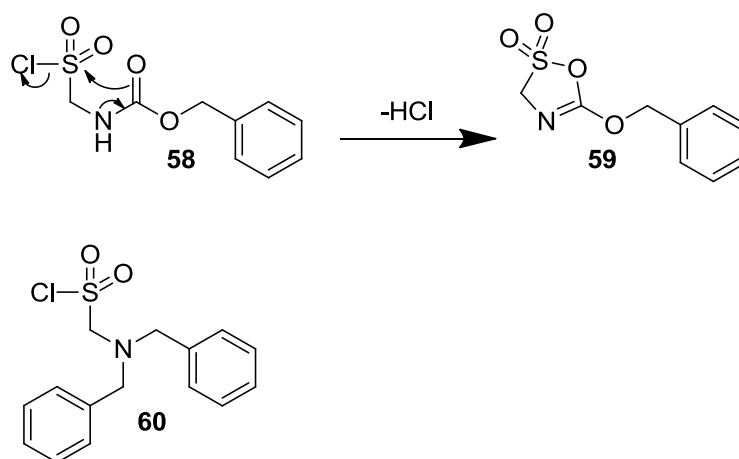
Scheme 5 – Preparation of protected amine substrate for sulfonyl chloride formation reaction.

Treatment of aminomethane sulfonic acid **53** with phthalic anhydride in the presence of acetic acid and potassium acetate⁷¹ gave phthalimide protected potassium salt **55** in good yield (Scheme 5). Alternatively, treatment with carboxybenzyl chloride in aqueous sodium hydroxide⁷² gave carboxybenzyl protected sodium salt **56** in quantitative yield (Scheme 6). These substrates were then progressed in an effort to form the corresponding sulfonyl chloride derivatives. (Scheme 6).



Scheme 6 – Summary of attempts to synthesise geminal sulfonyl chloride-amine compounds.

Treatment of sulfonic acid salts **55/56** with thionyl chloride,⁷³ phosphorus pentachloride,⁷⁴ or oxalyl chloride⁷⁵ led to a new species observed by LCMS. However, this material could not be isolated *via* silica gel chromatography or *via* extraction as the species appeared to be decomposing to form a complex mixture of products. Attempts to telescope the crude concentrated reaction mixtures into sulfonamide formation with amine **44** also failed with no sulfonamide product being observed in any case. It is hypothesised that upon formation of the sulfonyl chloride an intramolecular cyclisation to yield 5-membered ring intermediate could take place (Scheme 7).



Scheme 7 – Proposed cyclisation and proposed protecting group to prevent cyclisation.

It is possible that a 5-exo-tet cyclisation is taking place to form sulfonic ester ring **59**. Removal of the nucleophilic group in this position by changing to a benzyl protecting group may prevent this reaction. It is hypothesised that a dibenzyl protected **60** will be required since *mono*-benzyl amine would be expected to be a good nucleophile and may react with sulfonyl chloride functionality. However, this was not investigated further and the use of an alternative alkyl chloride commercial starting material **61** was explored.

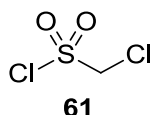
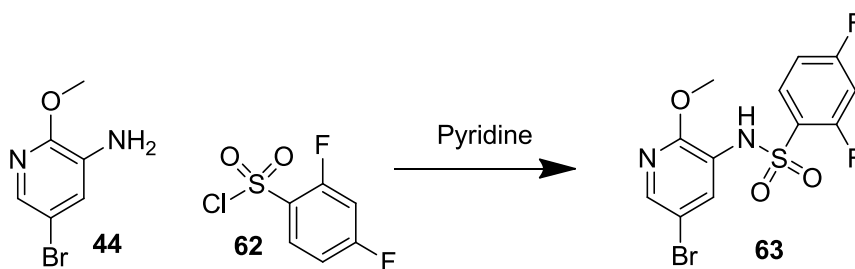


Figure 28 – Commercial one-carbon building block.

A range of conditions for sulfonamide formation with three carbon building blocks **51** and **52** as well as one-carbon building block **61** were explored. It was hypothesised that the amine **44** may be a poor nucleophile and hence forcing conditions may be required. A literature search revealed a wide range of yields reported for very similar conditions in sulfonamide couplings with the amine **44** (Table 6).

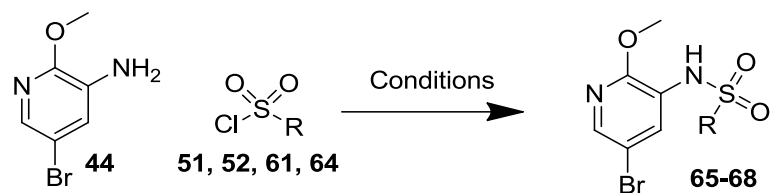


Temperature / °C	Time	Yield	Author
0-20	24 h	86	Fan <i>et al.</i> ⁷⁶
20	20 h	83	Botyanski <i>et al.</i> ⁷⁷
20	0.25 h	72	Leivers <i>et al.</i> ⁷⁸
0-20	16 h	46	Wang <i>et al.</i> ⁷⁹
0-20	16.25 h	32	Parish <i>et al.</i> ⁸⁰

Table 6 – Literature yields for sulfonamide coupling between amine **44** and sulfonyl chloride **62**.

A wide range of yields have been observed with almost identical conditions indicating the irreproducibility of the reaction. Although the reaction appears to be a simple transformation there may be complex processes occurring.

A range of conditions were selected and screened (Table 7).



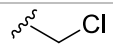
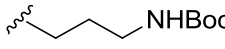
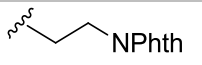
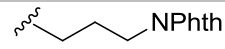
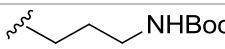
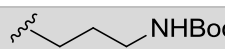
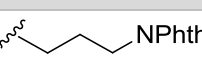
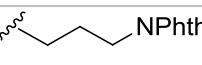
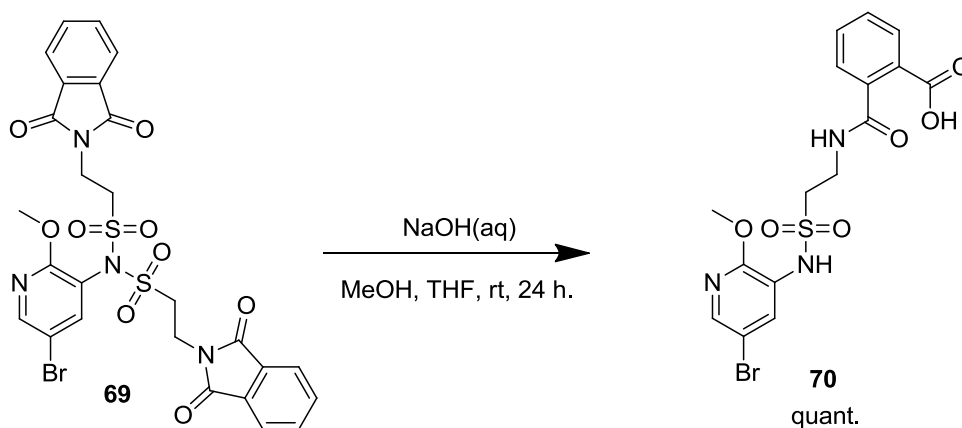
Entry	R =	Base	Solvent	T / °C	Time	Additive	Conversion /% ^a		
							Product	SM	Bis-sulfonamide
1	 61	Et ₃ N	1,4-dioxane	RT	2 h		15	40	44
2	 51	Pyridine	1,4-dioxane	RT	3 days		8	92	0
3	 64		Pyridine	RT	18 h.		20	60	3
4	 52		Pyridine	60	16 h.		25	35	5
5	 51		Pyridine	RT	3 days	DMAP	6	48	22
6	 51	Pyridine	DCM	rt	18		26	73	0
7	 52	NaH	THF	RT	16 h.		12	43	10
8	 52		MeCN	80	16 h.	Indium ⁸¹	2	51	0

Table 7 – Condition screening for sulfonamide coupling. ^aPercentage by LCMS.

Initial screening with triethylamine (entry **1**) showed that even after short reaction times *bis*-sulfonamide formation was observed. It was hypothesised that triethylamine was a strong enough base to deprotonate the sulfonamide product and would therefore lead to *bis*-sulfonamide formation. Hence, pyridine was employed for the subsequent reactions. Pyridine prevented *bis*-sulfonamide formation, however led to decreased conversion with large quantities of starting material remaining after three days of reaction (entry **2**). The equivalents of pyridine were increased, including use of pyridine as solvent (entry **3**). This led to slightly increased conversion to product. Next, the temperature was increased (entry **4**) to try to increase the rate of reaction. Again, this led to a slight increase in product formation. Following this, dimethylamino-pyridine (DMAP), a nucleophilic catalyst, was explored (entry **5**). It was hoped that DMAP may activate the sulfonyl chloride component leading to a more reactive electrophile. However, this unfortunately led to lower conversions. Use of pyridine in dichloromethane led to the highest conversions (entry **6**), with the cleanest reaction profile. However, conversion stalled at 26% even upon addition of further base and sulfonyl chloride at this stage.

It was hypothesised that formal deprotonation of amino pyridine **44** with sodium hydride may lead to increased nucleophilicity and hence reactivity (entry **7**). However, some degradation to by-products was observed, and low conversion to product was seen; hence these conditions were not explored further. Alternative indium-mediated sulfonamide formation conditions⁸¹ were also explored (entry **8**), however proved unproductive for this system.

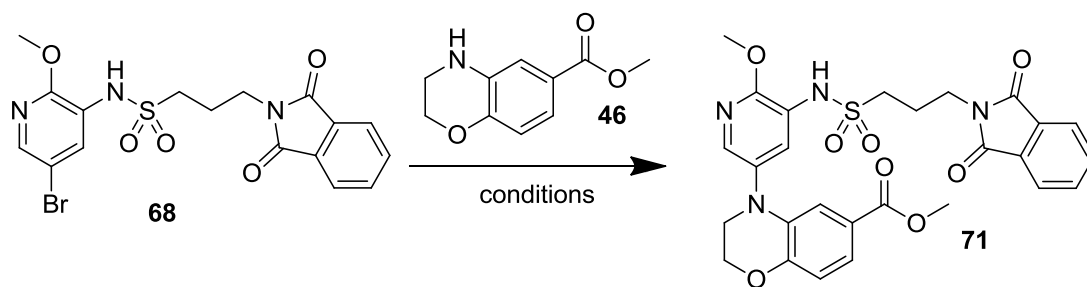
Use of *bis*-sulfonamide species was also explored. It was hypothesised that *bis*-sulfonamide species could be converted to *mono*-sulfonamide by reaction with aqueous base (Scheme 8).



Scheme 8 – Reaction of bis-sulfonamide **69** with aqueous sodium hydroxide.

Attempts to hydrolyse *bis*-sulfonamide **69** resulted in clean conversion to ring-opened *mono*-sulfonamide **70**. Although, this was not the desired *mono*-sulfonamide product the reaction shows that hydrolysis of *bis*-sulfonamide is possible and may be an alternative method to improve the yield from sulfonamide coupling reaction. This reaction also showed the possibility that the phthalimide protecting group may be labile under basic conditions. This was therefore explored further in later sections. However, the optimal *mono*-sulfonamide forming conditions of pyridine in dichloromethane were used for further reactions.

Next, a range of conditions were explored for the Buchwald-Hartwig amination step. A focused set of screening conditions were selected based on Buchwald's 'user's guide'.⁸² The ligand RuPhos is recommended for secondary anilines, such as the amine found in benzoxazine **46**. Accordingly, this ligand was prioritised for screening. It was hypothesised that efficient formation of active catalyst species from Pd₂(dba)₃ may be problematic and that dibenzylideneacetone may be inhibiting the reactions. Hence, use of the second generation RuPhos palladium precatalyst was explored. Buchwald also shows that use of stronger bases can give faster reaction rates.⁸³ However, stronger bases also have lower functional group tolerance. Sodium *tert*-butoxide is often found to give the highest reaction rates and to permit the lowest catalyst loadings, whilst caesium carbonate provides the highest reaction rate of the weaker bases and provides increased functional group tolerance.⁸² These bases were hence selected for further studies (Table 8).



Entry	Catalyst (0.2 eq.)	Ligand (0.4 eq.)	Solvent	Base (3 eq.)	T / °C	Time / hours	Conversion ^a
1	Pd ₂ (dba) ₃	RuPhos	1,4- dioxane	Cs ₂ CO ₃	130	3	4
2	Pd ₂ (dba) ₃	RuPhos	1,4- dioxane	NaO ^t Bu	130	3	0
3	RuPhos Pd G2	RuPhos	1,4- dioxane	Cs ₂ CO ₃	130	3	56
4	RuPhos Pd G2	RuPhos	1,4- dioxane	NaO ^t Bu	130	3	0

Table 8 – Screen of conditions for Buchwald-Hartwig amination of aryl bromide **68** with amine **46**. ^aPercentage product by LCMS, all peaks were included in analysis.

Screening of a range of conditions showed that the precatalyst gave improved conversions to coupled product **71**. Caesium carbonate (entries **1** & **3**) was found to give higher yields than sodium *tert*-butoxide (entries **2** & **4**). It was hypothesised that the electrophilic methyl ester present in the benzoxazine **46** may be sensitive to the nucleophilic *tert*-butoxide anion. Use of RuPhos Pd G2 in combination with caesium carbonate (entry **3**) gave a significant improvement in yield and could therefore be used in future reactions.

Following on from this, the ring closing amide coupling was then explored. First, a literature search was used to identify macrolactamisation reagents to synthesise ring sizes of between 10 and 20 atoms (Table 9).

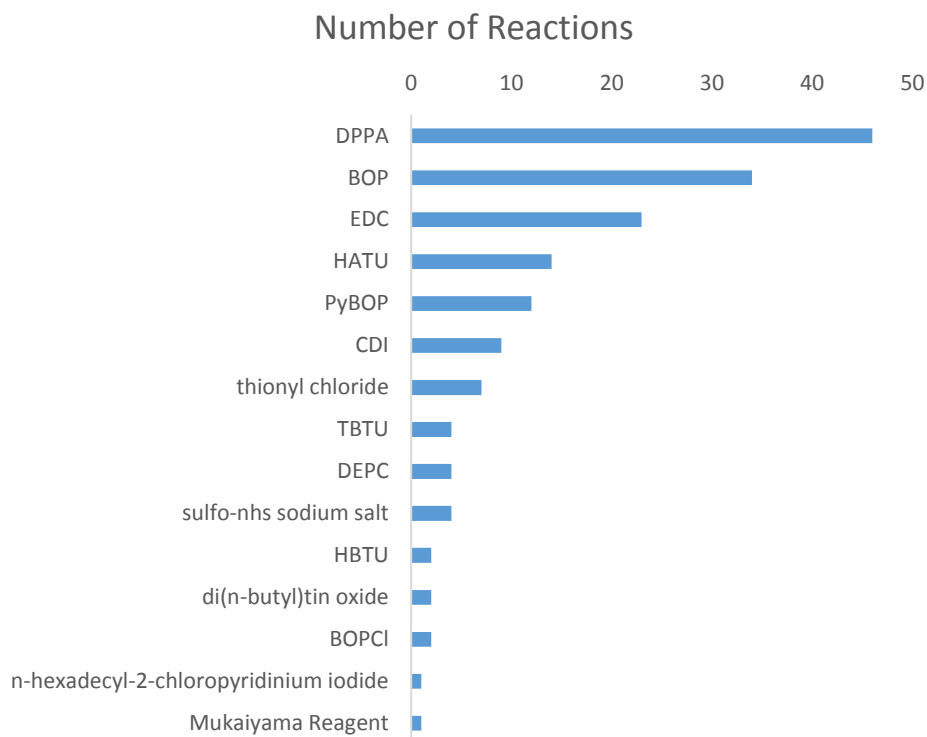
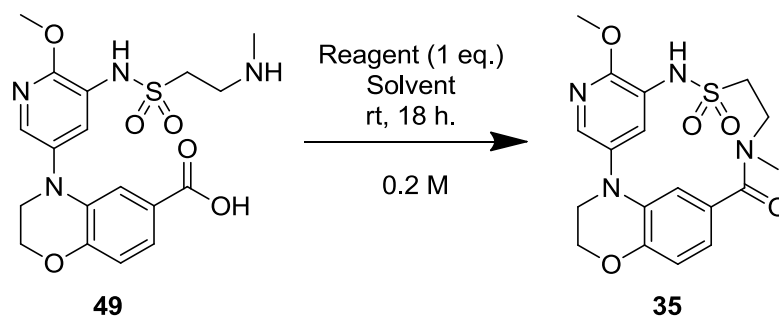


Table 9 – An analysis of all lactamisation reactions indexed in Reaxys to form ring sizes of between 10 and 20 atoms.

This identified 165 reactions using 16 different coupling agents. A selection of these agents were trialled, along with a number of general amide coupling agents (see appendix for structures) (Table 10).



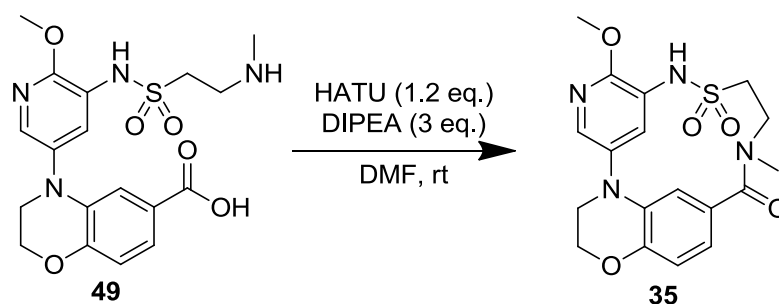
Entry	Reagent	Solvent	Additive/ Variation in Standard Conditions	Conversion /% ^a
1	Ghosez ⁸⁴	DCM		0
2	Mukaiyama ⁸⁵	DCM	Et ₃ N	1
3	TFFH ⁸⁶	DMF	DIPEA	0
4	DMTMM ⁸⁷	MeOH		3
5	COMU ⁸⁸	DMF	DIPEA	16
6	SucOCOOSuc ⁸⁹	MeCN	Et ₃ N	0
7	EEDQ ⁹⁰	DCM	40 °C	28
8	BOP ⁹¹	DMF	Et ₃ N	0
9	Thionyl chloride ⁹²	EtOAc		0
10	DPPA ⁹³	DMF	Et ₃ N 4Å Molecular sieves	5
11	EDC ⁹⁴	DCM	Et ₃ N DMAP	1
12	T3P ⁹⁵	THF	DIPEA	0
13	HATU ⁹⁶	DMF	DIPEA	28
14	PyBOP ⁹⁷	DMF		21
15	CDI ⁹⁸	DCM		0
16	Mesoporous silica MCM-41 ⁹⁹	Toluene	110 °C	0

Table 10 – Screening of conditions for ring closing amide coupling. ^aConversion is reported by LCMS with peaks attributed to coupling reagent removed.

In summary, most coupling reagents selected showed no presence of the expected macrocycle product. It was hypothesised that carboxylic acid activation is taking place in some cases, however intramolecular restrictions do not allow the amine to access the conformation required to attack this species. In others cases, it is reasoned that the presence of nucleophilic amine functionality throughout the reaction may be

CONFIDENTIAL – PROPERTY OF GSK – DO NOT COPY

problematic. Preactivation of carboxylic acid functionality is not possible with these systems, meaning the nucleophilic amine may be reacting with the coupling reagent causing side-reactions and by-product formation. However, COMU, HATU, EEDQ and PyBOP showed some conversion to expected product. HATU was selected for further studies due to identification of a major by-product as a dimeric species by LCMS. It was hypothesised that this could be controlled by adjusting the concentration at which the reaction was performed and therefore, a screen was carried out (Table 11).



Entry	Concentration / mM	% Product ^a	% Dimeric species ^a
1	190	28	56
2	95	61	17
3	47	72	10
4	24	65	5
5	12	70	3
6	6	64	2
7	3	56	0
8	1.5	35	0

Table 11 – Screening of concentration for HATU mediated ring closing reaction. ^aBy UV peak area in LCMS.

Varying the reaction concentration showed that the dimerisation product formation could be controlled. Reaction concentrations of between 10 and 50 mM were found to be optimal for conversion to ring closed monomeric product. At lower concentrations reduced conversion is hypothesised to be due to reduced reaction rates, implying long reaction times would be necessary for these reactions.

The final reaction to be explored in further depth was the amide reduction. Borane-tetrahydrofuran complex was used to prepare macrocycle **32**, however yields were low. Again, an analysis of a literature conditions for amide to amine reduction in ten to twenty membered rings was explored *via* Reaxys.

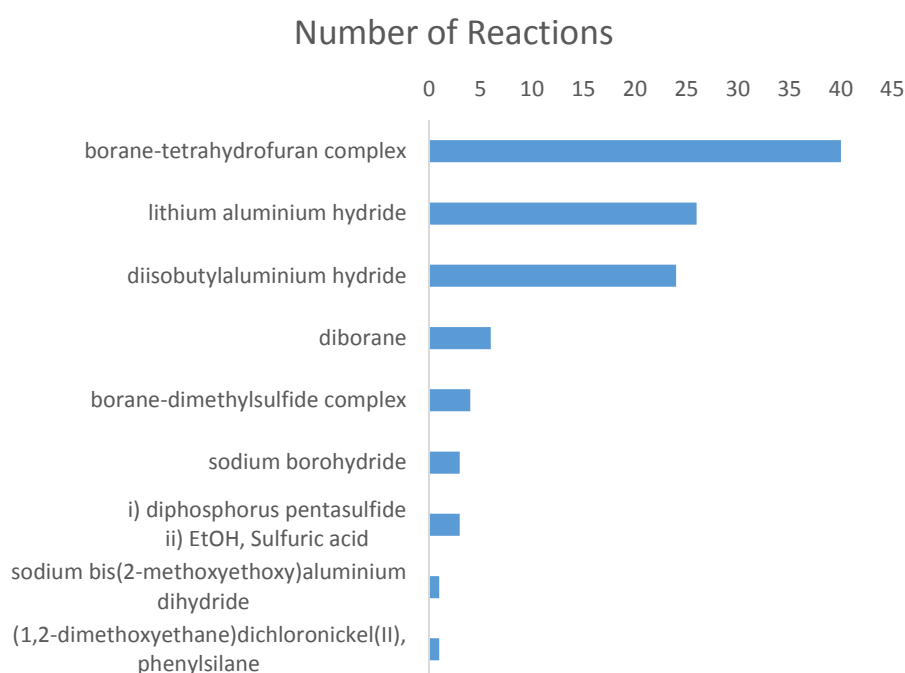


Table 12 – An analysis of reagents used for reduction of ten to twenty membered lactams to cyclic amines.

This analysis identified 102 reactions using nine different reagents. A range of reducing agents have been used, with borane based reagents the most widely utilised. However, nucleophilic hydride reagents were also employed, as well as conversion to a thioamide and a nickel-phenylsilane combination.

CONFIDENTIAL – PROPERTY OF GSK – DO NOT COPY

In the benzoxazine series, this reduction was anticipated to be a difficult transformation due to the conformation of the macrocycle and the angle required for attack of the carbonyl. The most favourable angle for a nucleophile to attack a carbonyl is the Bürgi-Dunitz trajectory of 107° .¹⁰⁰ The computationally produced lowest energy conformation of the amide macrocycle (Figure 29) shows that to access this angle the nucleophile must approach from a highly sterically hindered trajectory, reducing the reactivity of this amide. It was reasoned that this problem could be overcome by using elevated temperatures to increase the number of accessible conformations for the macrocycle. Alternatively, reducing agents which deliver the hydride directly from a co-ordinated intermediate could also solve the problem.

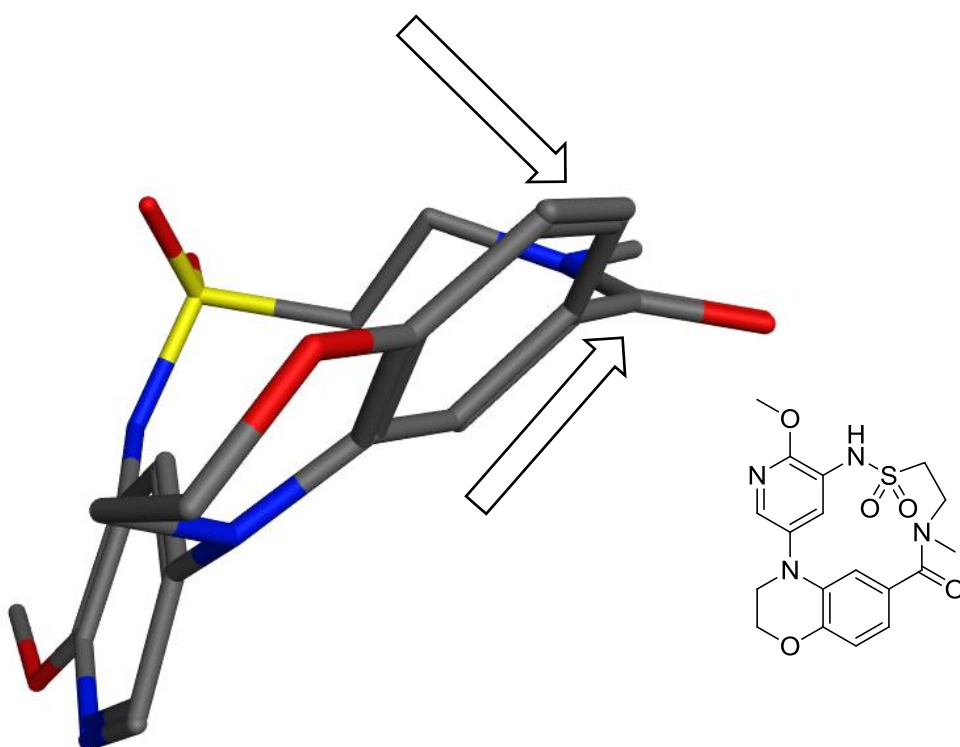
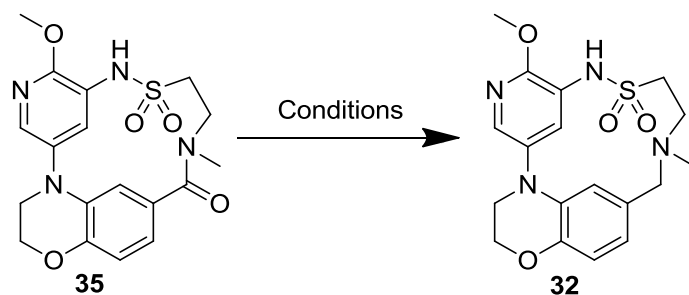


Figure 29 - Lowest energy conformation of amide **35** minimised using AMBER10:EHT in MOE.¹⁰¹ The approximate Bürgi-Dunitz trajectory for attack on the carbonyl is indicated.

Based on the above, a range of reducing agents and conditions were selected and were screened for this transformation (Table 13).

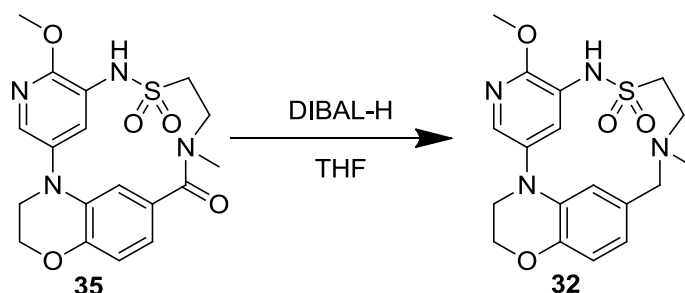


Entry	Reagent	Temperature	Solvent	Starting Material ^a	Product ^a
1	NaBH ₄	rt	THF	68	0
2	LiAlH ₄	rt	THF	0	0
3	Borane.THF	rt	THF	55	20
4	Borane.DMS	rt	THF	15	21
5	DIBAL-H	rt	THF	25	45
6	LiBH ₄	rt	THF	27	0
7	L-Selectride	rt	THF	41	0
8	LiBHEt ₃	rt	THF	0	0
9	Red-Al	rt	THF	0	0
10	Zn(OAc) ₂ / (EtO) ₃ SiH	rt - 40	THF	67	0
11	NaB(OAc) ₃ H	rt	THF	68	0
12	NaB(CN)H ₃	rt	THF	68	0
13	Tf ₂ O/ HEH ^{102,103}	rt	DCM	0	7
14	-	rt	THF	96	0

Table 13 – Screening of reagents for lactam reduction. ^aBy UV peak area in LCMS.

LCMS analysis of the reaction mixtures showed a range of conversions to the expected product. An interesting observation was the instability of the starting material to all reducing conditions. This resulted in starting material degradation in all cases compared to a reference system containing no reductant. The strongest reducing agents were found to form a large number of by-products with complete starting material consumption. However, more mild reducing agents such as DIBAL-H, yielded moderate conversion to product with some starting material remaining. Hence, DIBAL-H was selected for further study.

A range of equivalents of DIBAL-H from the theoretical two equivalents required for the reaction up to 6 equivalents were selected. It was anticipated that the higher equivalents would lead to faster reduction, however with more potential for by-products. A range of temperatures from room temperature to 60 °C were also selected. It was hypothesised that higher temperatures may provide activation energy to allow the macrocycle to adopt more reactive conformations.



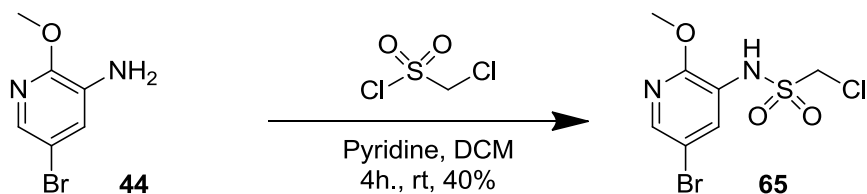
		% product (% starting material) ^a		
		Equivalents		
		2	4	6
Temperature / °C	rt	7 (67)	8 (37)	38 (26)
	40	12 (51)	15 (12)	28 (2)
	60	28 (34)	37 (4)	10 (3)

Table 14 – Screening of conditions for DIBAL-H mediated macrolactam reduction.
^aBy LCMS UV peak area.

Increasing the equivalents did in general lead to an increase in product formation, however also led to more by-products. Similarly, increasing temperature led to more starting material consumption however not always more product formation. It was hypothesised that the product may not be stable at elevated temperatures in the presence of DIBAL-H. Hence six equivalents of DIBAL-H at room temperature was selected.

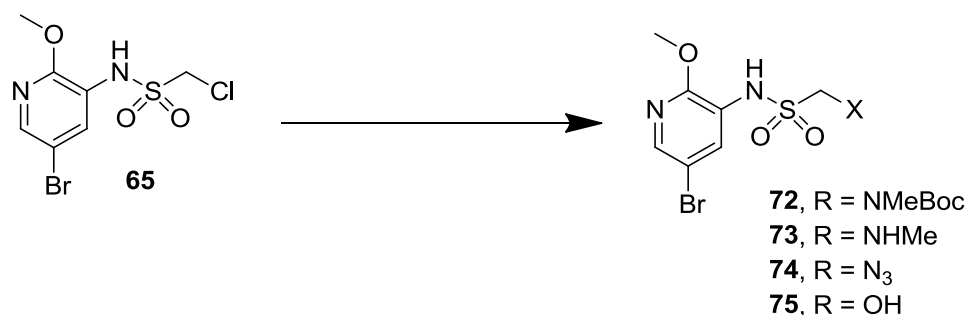
CONFIDENTIAL – PROPERTY OF GSK – DO NOT COPY

Reaction optimisation has identified conditions using pyridine in dichloromethane for sulfonamide coupling, Buchwald-Hartwig amination using second generation RuPhos palladium precatalyst, HATU mediated lactamisation under dilute conditions and DIBAL-H mediated reduction as the most productive conditions. With this optimised route to the macrocycles in hand, synthesis of the one- and three-carbon linked *N*-H and *N*-Me macrocycles was commenced.



Scheme 9 – Synthesis of one-carbon macrocycle precursor **65**.

Sulfonamide **65** was synthesised using optimised pyridine-dichloromethane conditions in moderate yield (Scheme 9). Next, displacement of the chloride group α - to the sulfonamide group was explored. A number of nitrogen nucleophiles were selected and the precursor was subjected to alkylation conditions (Table 15). It was thought that substitution would be favourable due to the absence of possible elimination.



Entry	Nucleophile	Base	Solvent	Time / Temperature	Conversion /% ^a		
					65	72/73/ 74	75
1	MeNHBoc	NaH	THF	24 h. rt	86	0	0
2				Then 18 h. 60 °C	87	0	0
3	MeNHBoc	NaH	DMF	18 h. 90 °C	50	0	40
4	MeNHBoc	Cs ₂ CO ₃	DMF	18 h. 90 °C	58	0	26
5	MeNHBoc	KO ^t Bu	DMF	18 h. 90 °C	93	0	5
6	MeNHBoc	NaH	THF	24 h. rt	82	0	0
7		TBAI		Then 18 h. 60 °C	81	0	0
8	MeNH ₂	NaH	THF	24 h. rt	100	0	0
9				Then 3 d. 60 °C	100	0	0
10	NaN ₃ ¹⁰⁴	15-crown-5	DMF	18 h. 100 °C	98	0	0

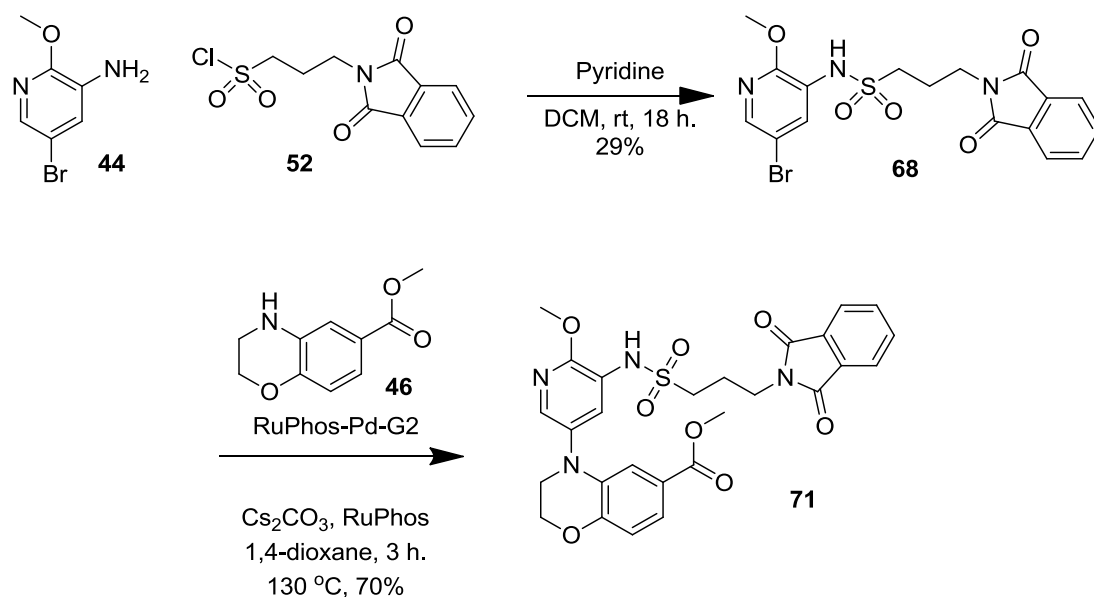
Table 15 – Summary of attempted reactions for nucleophilic displacement of chloride in one-carbon system. ^aBy LCMS.

Screening initially focused on displacement with Boc-methylamine due to precedence for α -chlorosulfones being displaced by amides.¹⁰⁵⁻¹⁰⁸ Firstly, a range of different bases

CONFIDENTIAL – PROPERTY OF GSK – DO NOT COPY

and reaction temperatures were explored. However, in all cases no product was observed with the only non-starting material mass corresponding to the product from displacement of chloride with hydroxide. This showed that displacement may be possible. Next, tetra-*n*-butyl ammonium iodide was used as an additive, as it was hypothesised that iodide may displace the chloride in the substrate creating a more electrophilic species and acting as a nucleophilic catalyst. However again, no product was observed. It was then thought that a stronger nucleophile may be required and hence, methylamine was examined. However, only starting material was observed by LCMS. There was literature precedence for using azide as a nucleophile in this type of reaction¹⁰⁴ and it was hoped that the azide product could be reduced under Staudinger conditions^{109,110} to the corresponding amine. However, no product was observed with this system.

Since conditions could not be established for productive displacement, focus turned to synthesising three-carbon linked analogues (Scheme 10).



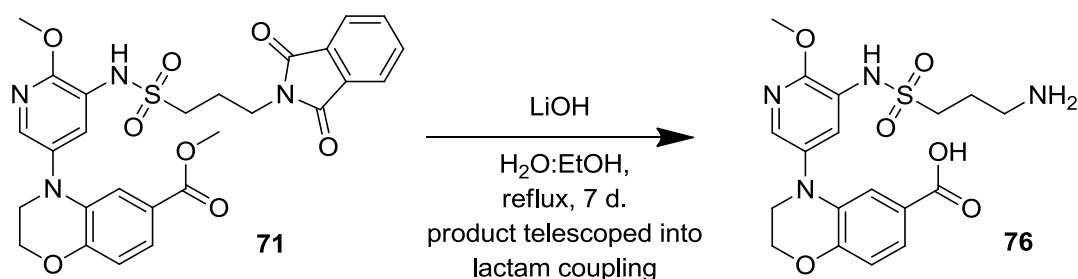
Scheme 10 – Use of optimised conditions to synthesise three-carbon macrocycle precursor **71**.

Optimised sulfonamide coupling conditions were employed to synthesise sulfonamide **68** in low yield. This material could then be coupled onto benzoxazine **46** *via*

CONFIDENTIAL – PROPERTY OF GSK – DO NOT COPY

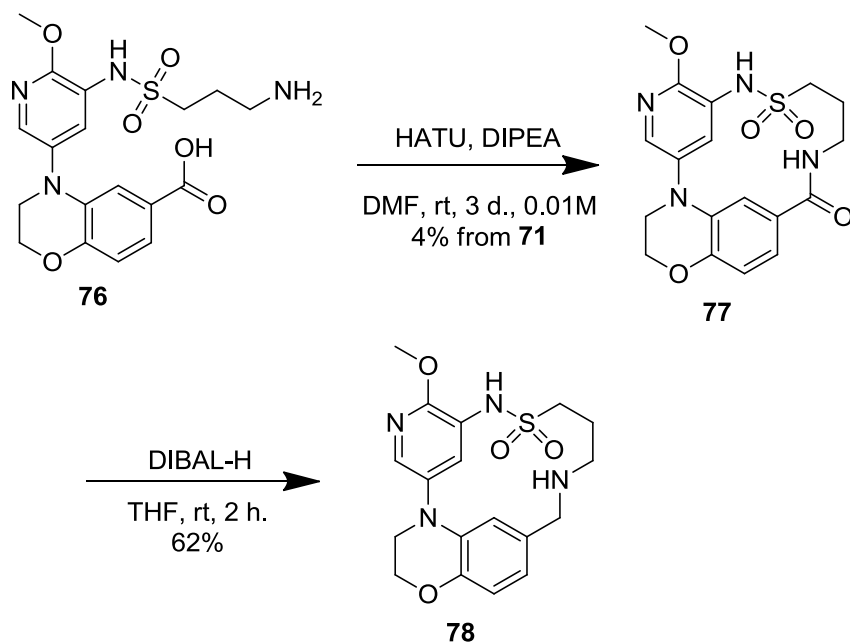
Buchwald-Hartwig amination in good yield. Ester hydrolysis and phthalimide deprotection of this compound was then explored in further depth.

It was hypothesised that due to phthalimide ring opening observed under hydrolysis conditions (Scheme 11) that this group may be labile under forcing basic conditions. This would allow concomitant phthalimide deprotection and ester hydrolysis and would make isolation of the Zwitter-ionic amino acid species more facile. This route would negate the use hydrazine hydrate, substituting a highly toxic and explosive reagent for much less hazardous conditions.



Scheme 11 – Concomitant ester hydrolysis and phthalimide deprotection performed under forcing conditions.

It was found that by subjecting phthalimide to reflux conditions in the presence of excess lithium hydroxide ester hydrolysis occurred, followed by phthalimide ring opening, then hydrolysis of the resulting amide. The solvent could then be evaporated and the residue isolated using an isolute-103 cartridge. This cartridge allows separation of zwitter-ionic organic species from inorganic species. With the amino acid product in hand, attention turned to the lactam formation and reduction (Scheme 12).



Scheme 12 – Synthesis of three carbon linked macrocycles **77** and **78**.

Employment of optimised lactam formation conditions yielded amide macrocycle **77** in low yield. Subsequent lactam reduction led to amine macrocycle **78**, in moderate yield. However, sufficient material was obtained for biological profiling and the reactions were not optimised further.

In vitro PI3K δ enzyme assay results for sulfonamide compounds

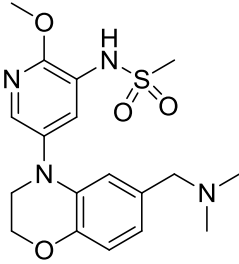
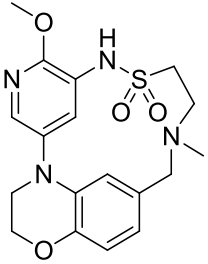
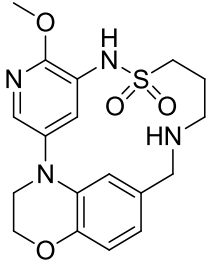
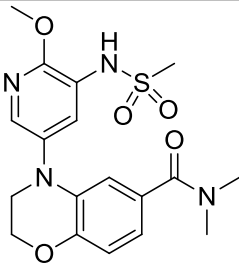
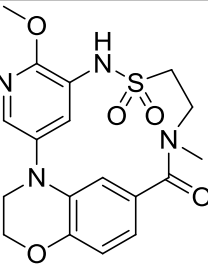
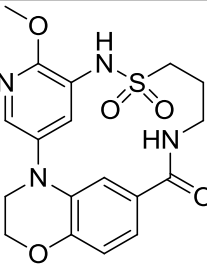
			
Compound no.	20	32	78
pIC₅₀	6.2	7.7	7.0
PI3Kδ			
			
Compound no.	34	35	77
pIC₅₀	5.5	6.9	7.8
PI3Kδ			

Table 16 – Biological data for three-carbon linked macrocycles in comparison to progenitor molecules and two-carbon linked macrocycles. All $n \geq 2$ unless otherwise indicated.

Data for three-carbon linked macrocycles show the amide macrocycle **77** displayed a 200-fold increase in potency over the progenitor **34**. Whereas in the amine series, macrocycle **78** exhibits an approximate 10-fold increase in potency compared to progenitor **20**. However, when the ring sizes are compared, differences are observed. Within the amine series two-carbon linked macrocycle **32** is more potent than three-carbon linked macrocycle **78**, whereas in the amide series the three-carbon macrocycle **77** is more potent than two-carbon **35**. It is possible that this is due to the additional conformational restriction of amide compared with amine requiring a more flexible linker to maintain key interactions with the protein. Whereas, the flexibility of the amine allows these interactions to be made with the shorter two-carbon linker, and hence the conformational restriction present in this system gives an additional entropic benefit to binding. Hence, shorter linkers seem to be preferred with more flexible groups, whereas with less flexible groups longer linkers are preferred.

CONFIDENTIAL – PROPERTY OF GSK – DO NOT COPY

Comparison of physicochemical profiles of the compounds, expanded upon in subsequent sections, showed one key finding relating to lipophilicity. Upon moving from *N*-Me amine macrocycle to *N*-H amine macrocycle lipophilicity has a large decrease (see Page 127). This led to the hypothesis that *N*-H amine macrocycles may be preferred and therefore were explored further in future sections.

2.3.3 Transposition of Sulfonamide

Another area of exploration was in the sulfonamide portion of the linker. It was proposed that desolvation of the sulfonamide was a cause for an enthalpic cost of binding, therefore it was decided to next explore whether the sulfonamide could be reversed. Analysis of crystal structures of existing molecules provides additional rationale. The protein-bound X-ray crystal structures of two-carbon macrocycle **32** and reversed sulfonamide **79** show for the macrocycle **32**, that the one of the sulfonamide oxygens in each structure occupies a very similar location in space (Figure 30). In the acyclic forward sulfonamide **20**, neither sulfonamide oxygen occupies this position (see section 2.3.1.1). This is hypothesised to be a lipophilic pocket and hence, it may not be maximally favourable for a polar oxygen to be placed in this region. However, in the reversed sulfonamide acyclic compound **79**, the sulfonamide already occupies this position, and it is therefore anticipated that there will be a reduced penalty for macrocycles occupying this conformation.

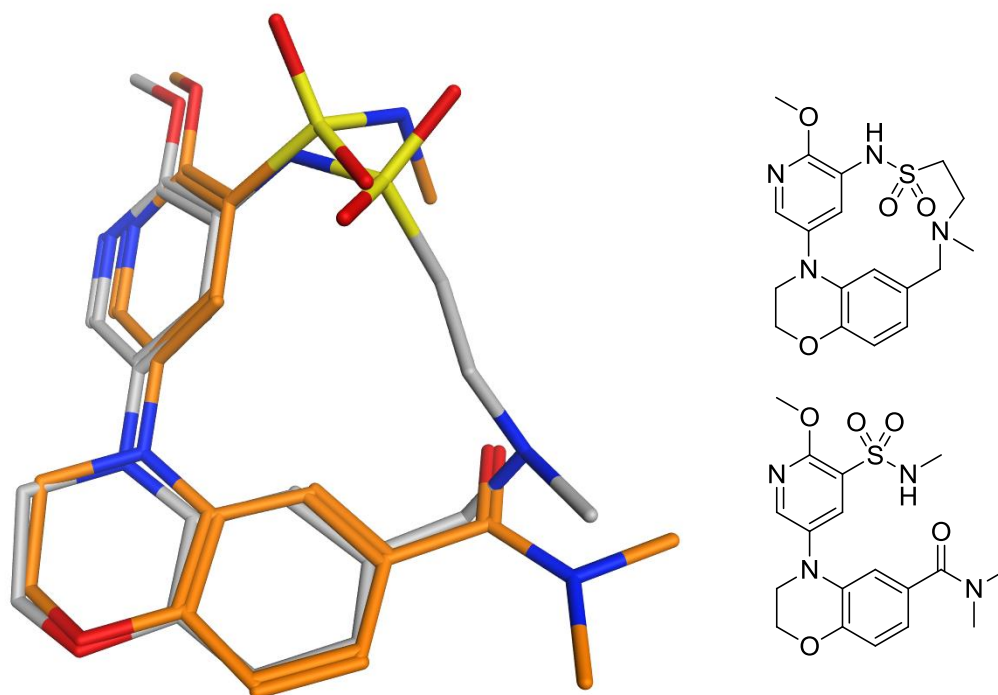


Figure 30 – Protein bound X-ray crystal structures of two-carbon linked sulfonamide macrocycle **32** (grey, 3VLSE) and reversed sulfonamide **79** (green, 2IHJ, 2.40 Å)

Therefore, the next synthetic plans were to prepare reversed sulfonamide equivalents of each of the sulfonamide analogues. Since, *N*-methylation was found to be unfavourable for lipophilicity, secondary amines were synthesised in the first instance. However, the possibility of *N*-alkylation was still open as a final step in the synthesis, should these compounds be of interest.

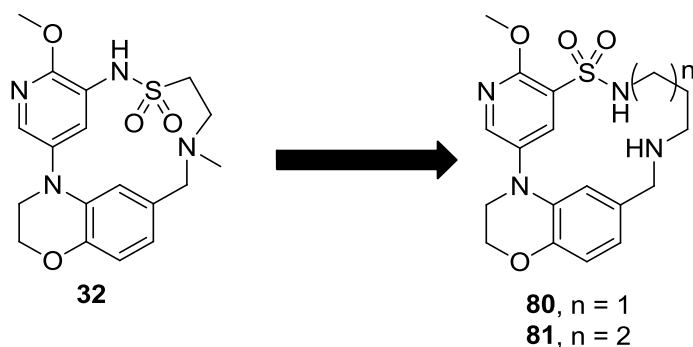
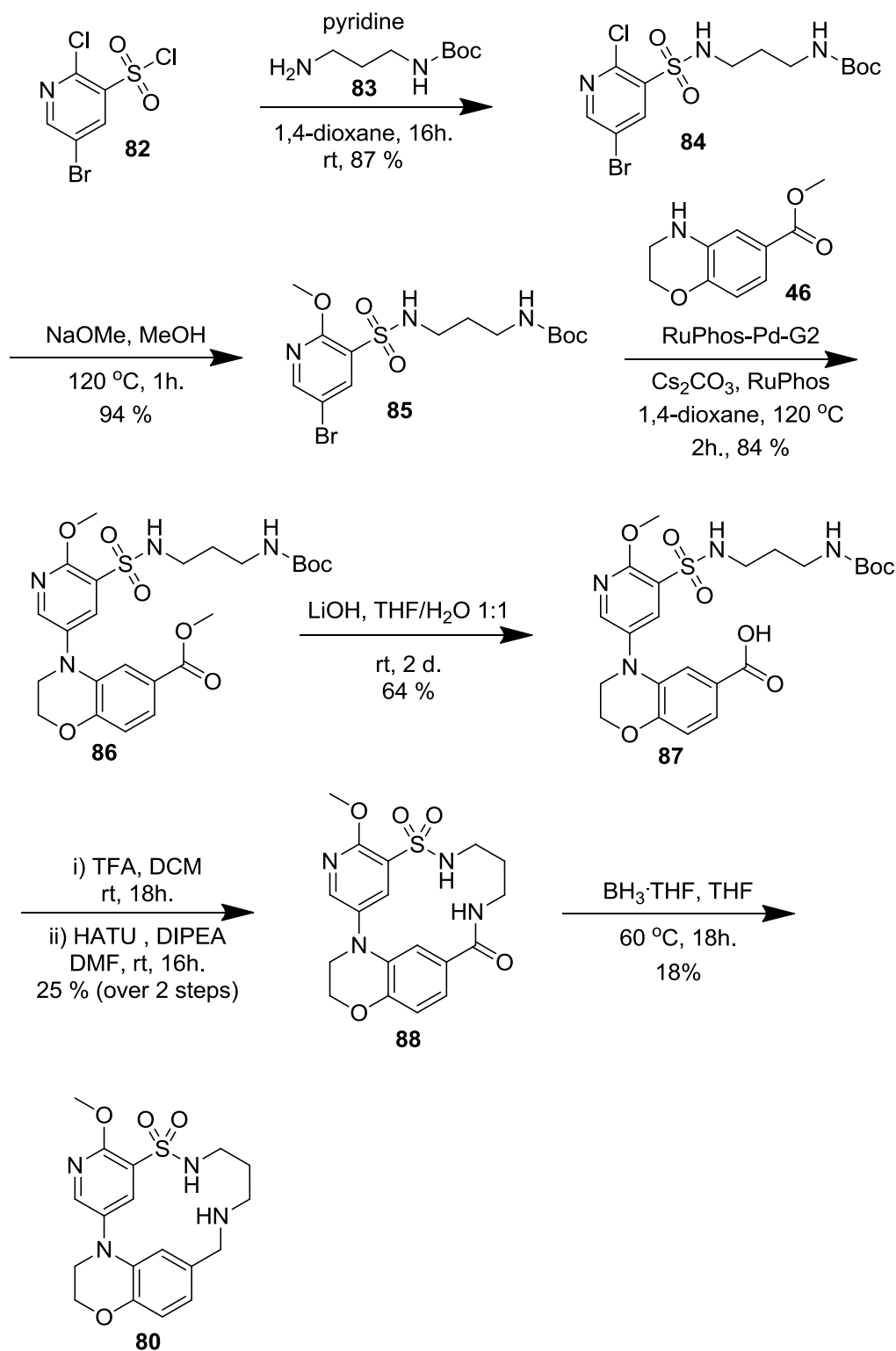


Figure 31 – Reversal of sulfonamide in macrocycles.

It was planned to explore a variety of linker lengths to generate more acyclic and macrocyclic pairs for comparison and to yield a larger data set to examine the effect on common physicochemical properties.

A similar synthetic route to that already described was utilised to access these reverse sulfonamide analogues (Scheme 13).

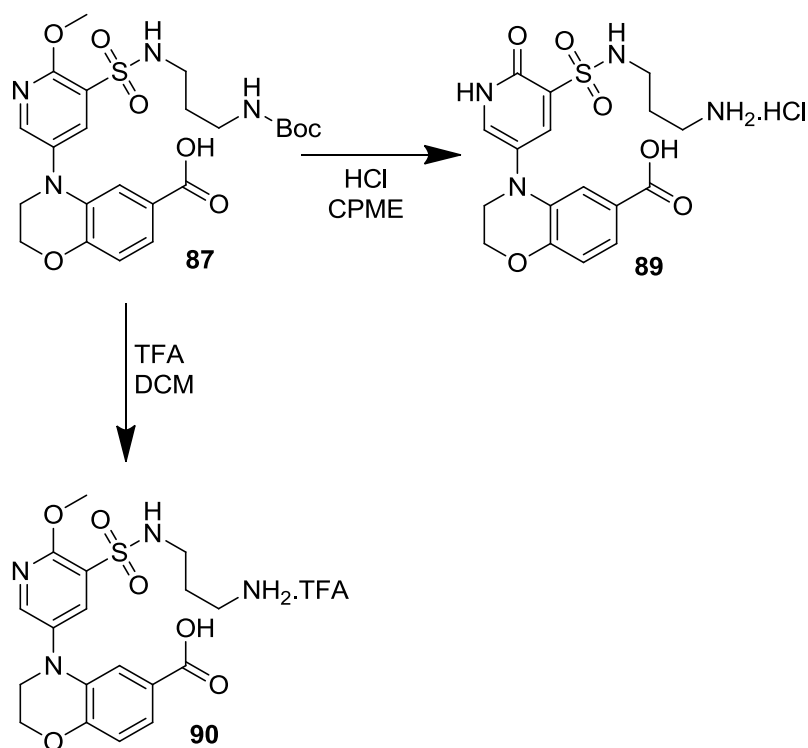


Scheme 13 - Route to three-carbon linker reverse sulfonamide analogues.

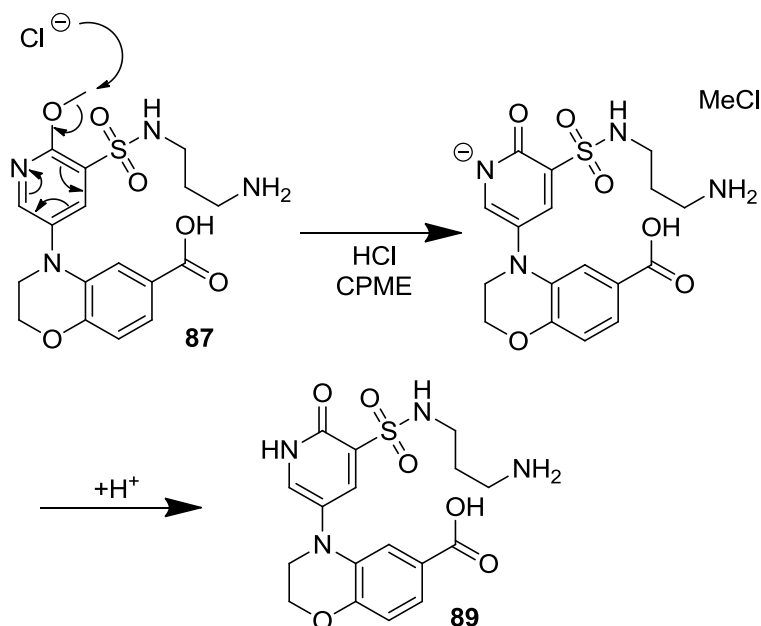
A sulfonamide coupling was employed between the commercially available sulfonyl chloride **82**,¹¹¹ followed by nucleophilic aromatic substitution¹¹² to yield

CONFIDENTIAL – PROPERTY OF GSK – DO NOT COPY

intermediate **85**. This was then coupled *via* a Buchwald-Hartwig amination to benzoxazine **46**.⁵⁶ Subsequent ester hydrolysis followed by Boc-deprotection led to TFA-salt **90** which was not isolated. Hydrochloric acid in cyclopentylmethyl ether was initially used to allow isolation of the product by evaporation rather than aqueous extraction, which was of concern for an amino acid product. However, these conditions led to deprotection and demethylation of the pyridine as determined by LCMS, with pyridone **89** (Scheme 14) the proposed structure. Based on this, alternative reaction conditions were sought and deprotection with trifluoroacetic acid yielded exclusively product **90**. The absence of by-product formation in this case is thought to be due to the decreased nucleophilicity of the conjugate base, between trifluoroacetate and chloride.



Scheme 14 – Byproduct formed by attempted Boc-deprotection using hydrochloric acid in cyclopentylmethylether.



Scheme 15 – Proposed mechanism for demethylation under hydrochloric acid conditions.

Subsequent HATU mediated amide bond formation⁹⁶ under dilute conditions yielded amide macrocycle **88** (Scheme 13) in relatively low yield due to dimerisation product **92** (Figure 32) observed by LCMS, despite the reaction being performed at 0.01 M concentration. However, a sufficient quantity of product was obtained to take through to the next stage of the synthesis.

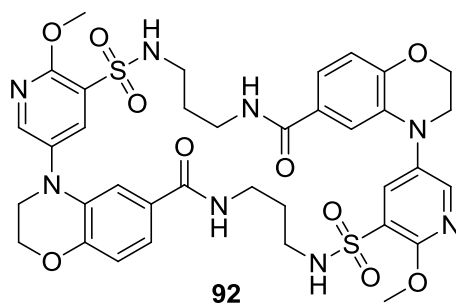
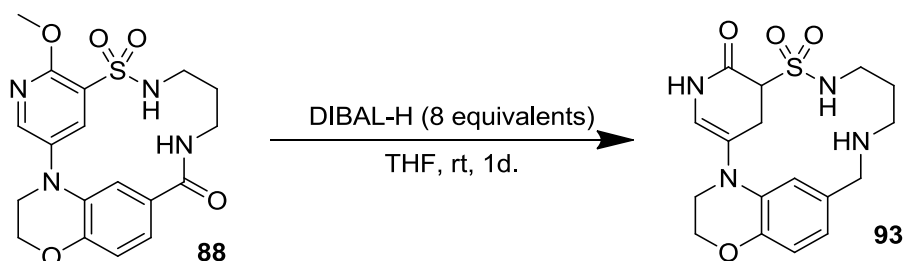


Figure 32 – Dimerisation product **92** observed via LCMS in HATU mediated amide bond formation reaction.

Reaction of amide **88** with DIBAL-H (4 equivalents) led to partial conversion to the desired amine macrocycle **80** (30% by UV, 20% starting material, 40% imine intermediate) however upon addition of further DIBAL-H (2 x 2 equivalents) to force the reaction to completion, reduction of the pyridine ring and demethylation was

CONFIDENTIAL – PROPERTY OF GSK – DO NOT COPY

observed, leading to over-reduction product **93** (63% by UV, 0% starting material, 0% product, 0% intermediate, Scheme 16) identified by NMR.



Scheme 16 – Product obtained from DIBAL-H reduction.

However, the use of borane tetrahydrofuran complex at 60 °C (Scheme 13), gave acceptable conversion to expected product and the reaction was stopped before completion to ensure over reduction did not take place.

With a route to the macrocyclic products in hand, a similar strategy was employed in the synthesis of four carbon linked analogues **81** and **99** (Scheme 17).

CONFIDENTIAL – PROPERTY OF GSK – DO NOT COPY

Analogous chemistry using a butyl derived linker rather than propyl, led to the isolation of macrocycles **99** and **81**, in similar yield. Again, a relatively low yield in ring closing amide coupling was seen due to competing dimerisation being observed, despite again performing the reaction under high dilution.

In the preparation of amine **81**, amide reduction was stopped at 25% conversion by LCMS to prevent the possibility of over reduction, however, this led to a low yield of the desired product. A sufficient quantity of product **81** was obtained to enable biological evaluation, therefore further optimisation was not pursued at this stage.

***In vitro* PI3K δ enzyme assay results for reverse sulfonamide compounds**

PI3K δ potency data for these macrocycles were obtained (Tables **17** and **18**).

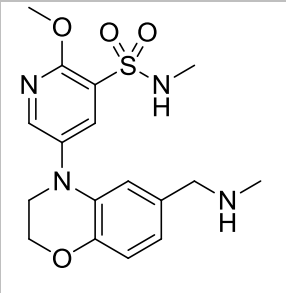
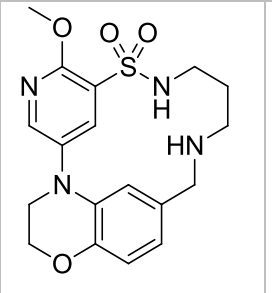
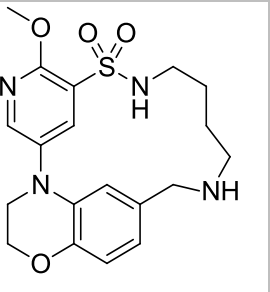
				
Compound no.		100	80	81
pIC₅₀	PI3Kδ	5.9	6.2	6.8

Table 17 – pIC₅₀ data for alkyl linked sulfonamide-amine macrocycles and acyclic analogue. All n \geq 2 unless otherwise indicated.

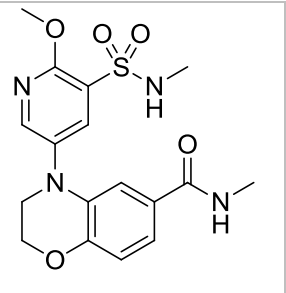
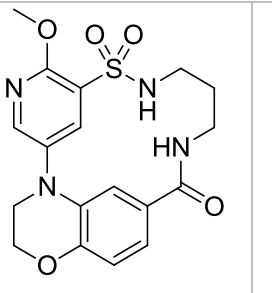
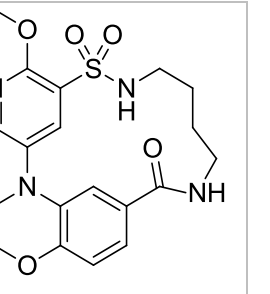
				
Compound no.		101	88	99
pIC₅₀	PI3Kδ	7.4	6.3	7.2

Table 18 - pIC₅₀ data for alkyl linked sulfonamide-amide macrocycles and acyclic analogue. All n \geq 2 unless otherwise indicated.

The data for the N-H analogues show that sulfonamide reversal is well tolerated. Macrocycle **81** has a ten-fold increase in potency compared to the progenitor acyclic molecule **100**, and it is proposed that this is again due to the decreased entropic cost of binding. However, macrocycle **80**, containing a three-carbon linker, does not see quite as large an increase in potency. This is could be due to the three-carbon linker forcing the pyridine and benzoxazine portions of the molecule to adopt more unfavourable conformations. This does not allow all the interactions with the kinase to be made effectively.

Interestingly, acyclic progenitor **101** has a surprisingly high potency compared to other progenitor compounds. It was hypothesised that this could be due to the aromatic amide giving this compound a more restricted conformation compared to the amine analogue **100**. Analysis of the X-ray crystal structures⁵⁷ of progenitor **101** and macrocycle **99** shows that the amide occupies a different conformation in macrocycle **99** compared with methyl amide **101** (Figure 33). This conformational preference of macrocycle **99**, is expected to translate to other macrocycles due to conformational restrictions imposed by ring formation. This could explain the reduction in potency observed between the progenitor amide **101** to macrocycles **88** and **99**.

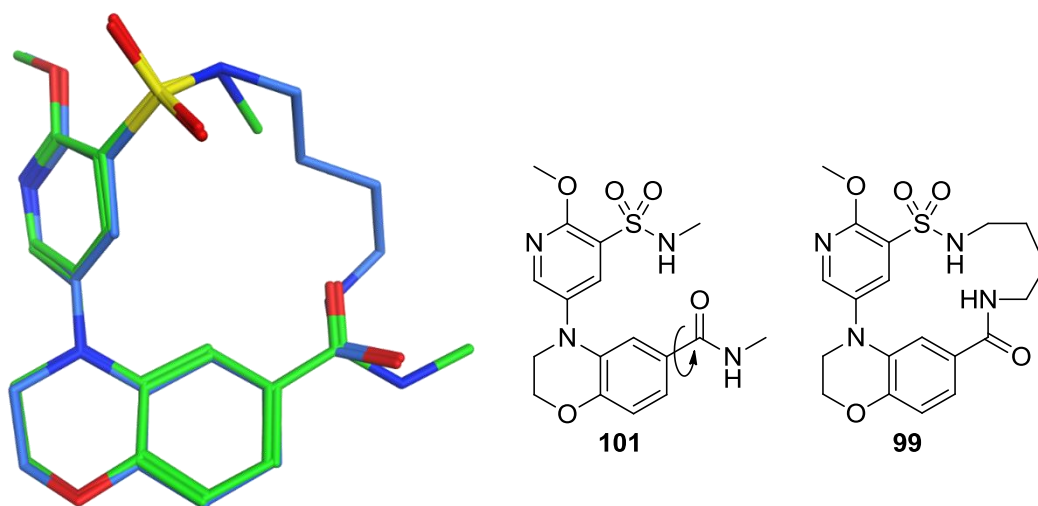


Figure 33 – X-ray crystal structure showing compounds **101** (green, 8IXIX, 1.98 Å) and **99** (blue, 9AXZY, 1.98 Å) in the PI3K δ binding site with the change in amide conformation highlighted.

CONFIDENTIAL – PROPERTY OF GSK – DO NOT COPY

Whilst macrocycle **99** appears relatively potent, it has similar activity compared to its progenitor system **101**. However, it is ten-fold more potent than macrocycle **88**, again owing to the more flexible linker. This data shows that macrocyclisation can increase potency and selectivity, however it can also be detrimental to potency if the linker is not optimised.

In summary, this short survey shows that whilst macrocyclisation is shown to increase potency in some cases, the nature of the linker and the conformational restrictions it imposes vary on a substrate specific basis. It was hence decided to explore introducing additional linker restriction to the most potent reverse sulfonamide macrocycle **99**.

2.3.4 Restriction of linker

An analysis of protein bound X-ray crystal structure for four-carbon linked reverse sulfonamide-amide macrocycle **99** provides a robust rationale for restriction of the linker. This structure shows that the four carbons of the linker appear to occupy a planar arrangement (Figure 34). This suggests that a planar *E*-alkene may lock this conformation, providing a more favourable entropic change in binding and therefore increased potency. Additionally, the strong precedent for use of ring closing metathesis to provide macrocyclic scaffolds meant alkene containing compounds were targeted (Figure 35).

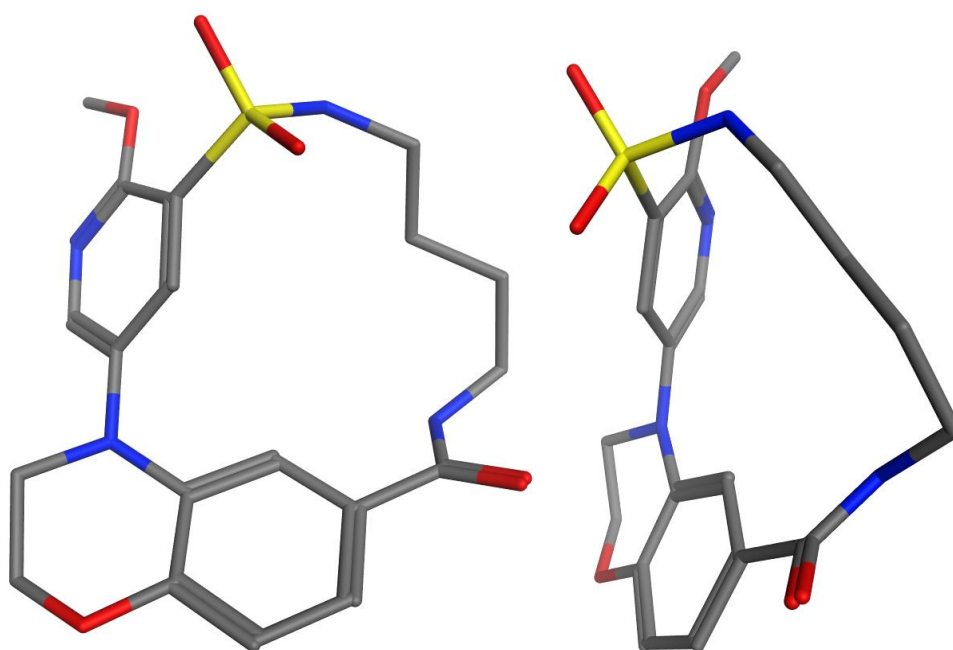


Figure 34 – Protein bound X-ray crystal structure of four carbon linked reverse sulfonamide-amide macrocycle **99** (9AXZY, 1.98 Å).

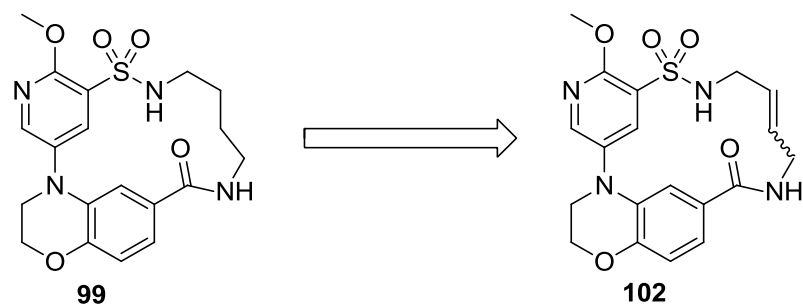
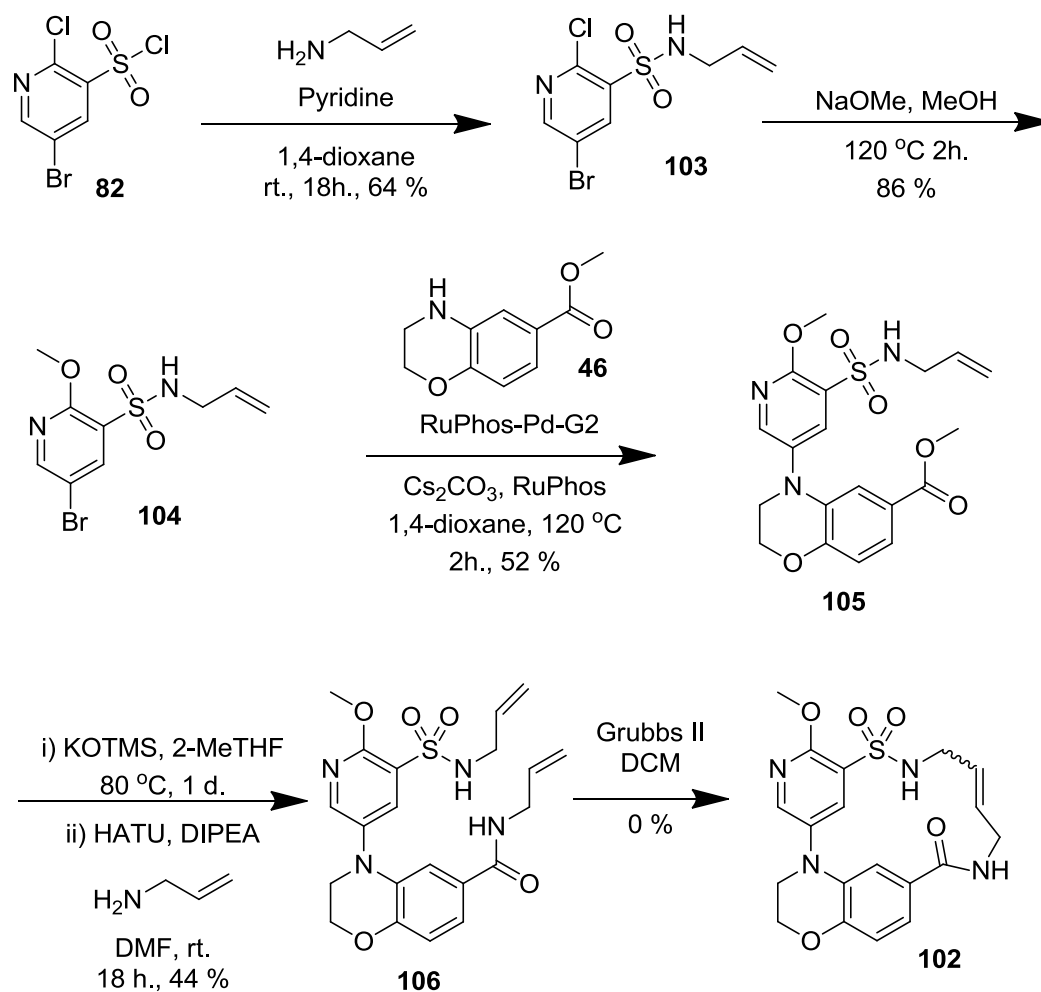


Figure 35 – Introduction of an alkene to increase restriction in linker.

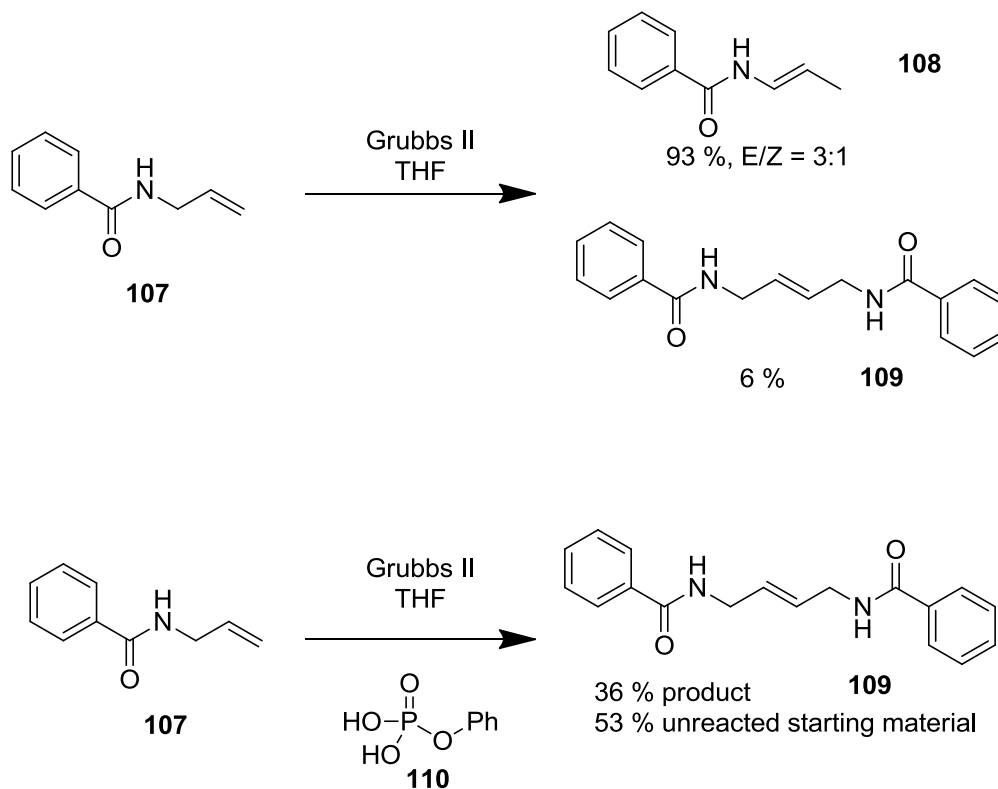
Ring closing metathesis has been widely used in synthesis with examples of a range of structurally diverse substrates with a range of ring sizes being synthesised.¹¹³⁻¹¹⁷ Despite the encouraging precedent, attempts to synthesise macrocycles containing an alkene linker within the current series proved problematic (Scheme 18).



Scheme 18 – Synthesis of alkene linked macrocycle.

Access to the requisite dialkene **106** was enabled using a similar strategy of sulfonamide coupling and Buchwald-Hartwig amination to synthesise intermediate ester **105**. In this synthetic sequence, potassium trimethylsilanoate was used in order to facilitate anhydrous conditions for ester hydrolysis and to remove the need for aqueous extraction.¹¹⁸ HATU mediated amide coupling was then employed to yield the ring closing metathesis precursor **106**. However, metathesis using second generation Grubbs catalyst¹¹⁹ failed to yield macrocycle **102**. Further exploration of the literature suggested the potential for allyl groups to isomerise under metathesis conditions.¹²⁰ This isomerisation could be detected by LCMS, as a shift in retention time with the same mass ion peaks and was observed upon treatment of dialkene **106** with Grubbs II.

Formentin *et al.* report this isomerisation phenomenon on similar allyl amide substrate **107** (Scheme 19).¹²⁰ In this same study, the group also reports that addition of phenyl phosphate **110** inhibits alkene isomerisation, whilst still allowing metathesis to take place.



Scheme 19 – Alkene isomerisation reported by Formentin *et al.* in a similar allyl amide and additive reported to reduce by-product formation.

Further literature reports proposed that the mechanism for isomerisation proceeds through a ruthenium hydride intermediate.¹²¹ Two potential reactions manifolds are also suggested (Figure 36).

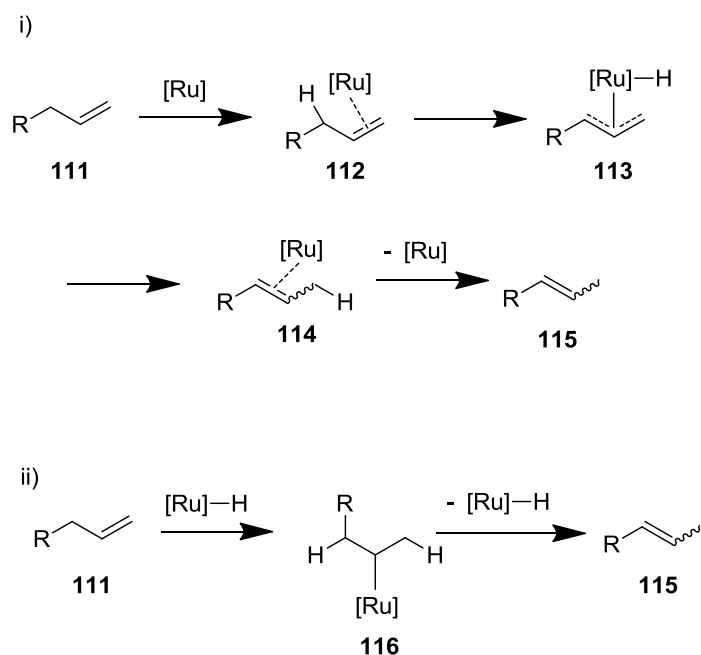


Figure 36 – i) Proposed mechanism of isomerisation through ruthenium hydride intermediate. ii) Proposed mechanism through ruthenium hydride catalyst impurity.

The first mechanism (Figure 36i) proceeds *via* ruthenium catalyst coordination followed by C-H insertion to give an η^3 intermediate **113**. Reductive elimination gives η^2 complex **114**, with subsequent catalyst dissociation regenerating the active catalyst and isomerised product **115**.¹²¹ An alternative mechanism (Figure 36ii), utilising a ruthenium hydride complex, proceeds *via* hydrometallation, followed by β -hydride elimination. It is proposed that this ruthenium hydride complex could be present as a by-product of catalyst synthesis¹¹⁴ or that it could be formed from degradation of catalyst under reaction conditions.¹²¹

In a related study, Grubbs *et al.* report that addition of a benzoquinone additive prevents isomerisation.¹²²

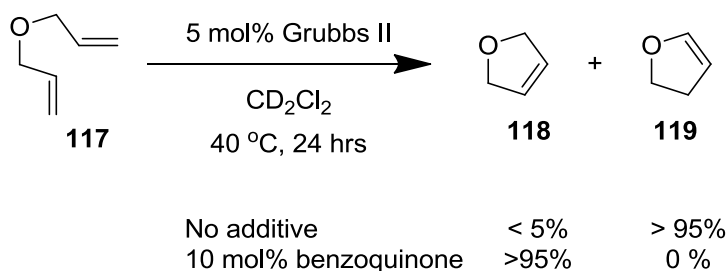
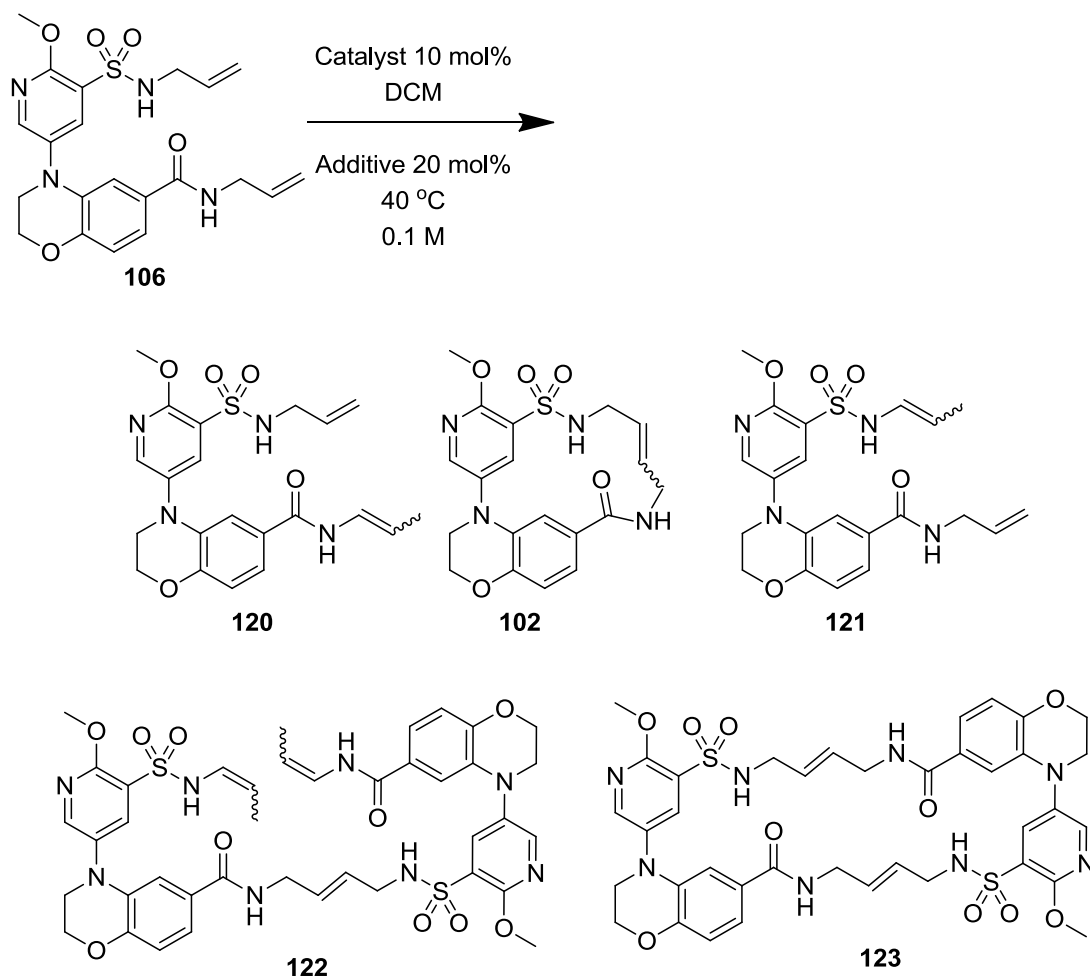


Figure 37 – A report by Grubbs that benzoquinone additive suppresses the rate of isomerisation.

In this case, the benzoquinone additive prevents isomerisation of the product **118** to the more stable conjugated alkene **119**. It is known that benzoquinone can be reduced by ruthenium hydride species,¹²³ and this results in an observed hydroquinone product. This quenches any ruthenium hydride species which may be present and hence prevents isomerisation. It is also reported that acetic acid can quench the ruthenium hydride species, by an acid/base quench.¹²²

In addition to this, it has been suggested by Yamamoto *et al.*, that increasing the temperature can increase the rate of monomer cyclisation against dimerisation.¹²⁴ An increase in temperature increases the entropic component to the activation energy and if the monomer formation is more entropically favoured this should increase the ratio of cyclised product. The entropic component of reaching the transition state is thought to be less for the monomer since only one molecule must be conformationally constrained, however for the dimer formation two molecules must be constrained.

From consideration of the above literature precedent, a screen of catalysts and additives was carried out to explore the best conditions for the metathesis reaction. (Table 19)



Entry	Catalyst	Additive	SM 106	Isomerisation 120/121	Product 110	Dimer 122	Cyclic Dimer 123
1	Grubbs I	None	29	19	2	38	0
2	Grubbs II	None	10	35	2	12	0
3		Phenyl Phosphate	93	0	0	0	0
4		Benzoquinone	30	0	2	32	0
5		Acetic Acid	35	8	2	22	0
6	Hoveyda- Grubbs I	None	29	10	3	19	0
7		None (80 °C, toluene)	9	0	1	82	0
8		benzoquinone	29	0	2	19	0

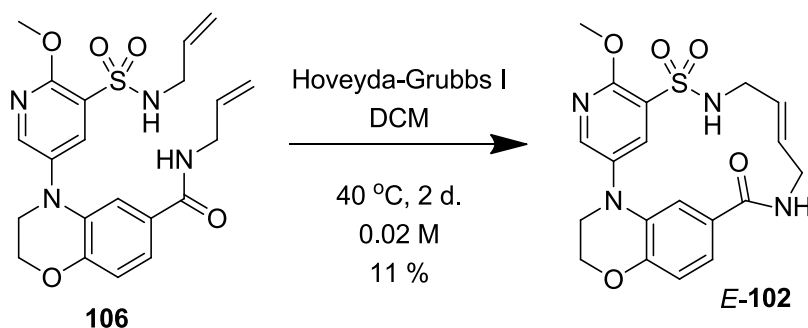
CONFIDENTIAL – PROPERTY OF GSK – DO NOT COPY

9	Hoveyda-Grubbs II	None	10	40	2	12	0
10	Zhan 1B	None	4	0	0	0	25

Table 19 – Results from an additive screen with the aim of reducing isomerisation of alkene. Proportions are given as a percentage by UV LCMS trace.

It was noted that upon variation of catalyst and additive the proportion of by-products changes, however, the proportion of desired product does not increase. Addition of benzoquinone appears to reduce isomerisation (entry **4** & **8**), however does not lead to increased product formation. An increase in temperature (entry **7**) resulted in increased dimer formation suggesting the entropic component of dimer formation is more favourable in this system.

Based on the screening data in Table 19, it was chosen to use the Hoveyda-Grubbs I catalyst (entry **6**) since this system resulted in low isomerisation with low dimerisation at 40°C. It was reasoned that dimerisation could be controlled by tuning reaction concentration. When concentration was reduced from 0.1 to 0.02 M the product could be isolated in useful quantities, despite competing isomerisation and dimerisation reactions (Scheme 20).



Scheme 20 – Successful metathesis using Hoveyda-Grubbs I.

Use of Hoveyda-Grubbs 1st generation was found to give exclusively the thermodynamic *E*-isomer **102** ($^3J_{\text{H-H}} = 15.4$ Hz, confirming the *trans* nature of the double bond) in ring closing metathesis.

In vitro PI3K δ enzyme assay results for restricted linker compounds

Compound no.		100	101	81
pIC₅₀	PI3K δ	5.9	7.4	6.8
Compound no.		99	102	106
pIC₅₀	PI3K δ	7.2	6.8	8.0

Table 20 – Effect of conformational restriction of macrocycle by addition of a *trans* alkene into the ring. All $n \geq 2$ unless otherwise indicated.

With a sufficient quantity of the target alkene containing macrocycle **102** in hand, attention turned towards biological profiling of this analogue (Table 20).

Upon increasing constraint from amine **100** to amide **101**, there is a significant increase in potency. This is thought to be due to reduced conformational flexibility of an aryl amide compared with a benzylic amine. Upon macrocyclisation, a ten-fold increase in potency is observed between amine **100** and macrocycle **81**. Introduction of an amide into macrocycle **99** gives a slight increase in potency, however this is not as significant as the increase previously observed with the acyclic molecules. Introduction of an alkene then results in a reduction in potency back to the level of amine macrocycle **81**

CONFIDENTIAL – PROPERTY OF GSK – DO NOT COPY

and not as potent as acyclic amide **101**. It is thought that the presence of an alkene in the linker locks the sulfonamide and amide in unfavourable conformations and hence is not preferable. Screening of metathesis precursor **106** shows that acyclic alkene derivatives can potentially make favourable interactions with the protein.

Based on all of the above, it has been shown that macrocycles can offer an increase in potency in some cases and therefore macrocycles may provide a good template for developing novel PI3K δ inhibitors. Since the reversed sulfonamide was tolerated, removal of the sulfonamide and replacement with another functionality was considered.

2.3.5 Sulfonamide Replacements

Due to the promising results in reversal of the sulfonamide, it was reasoned that other groups may also be tolerated in this position.

The pyridine sulfonamide moiety is a conserved feature in many potent and selective PI3K δ inhibitors, acting as mimic for the phosphate portion of ATP.

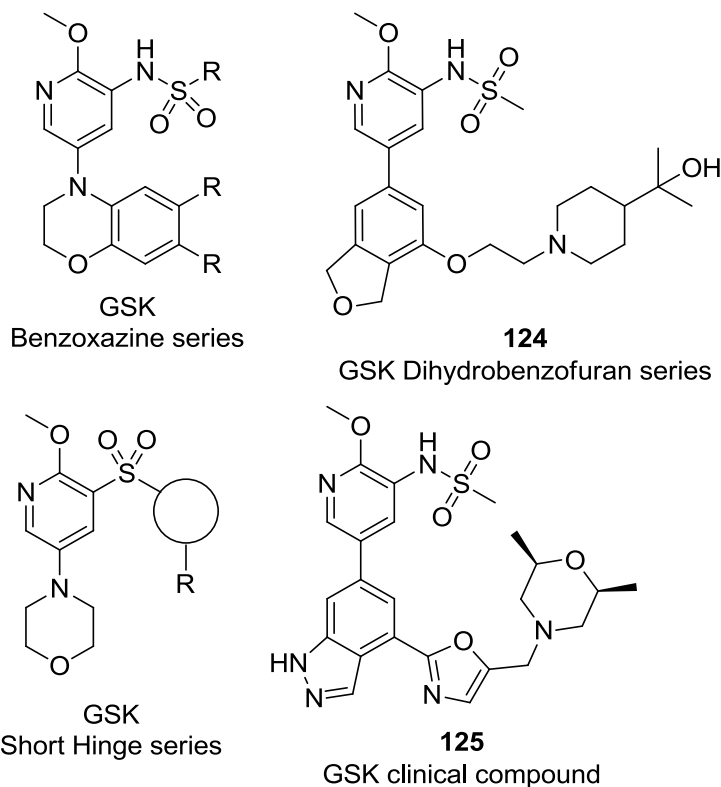


Figure 38 – Prevalence of pyridine sulfonamide in current GSK series and GSK clinical candidates.

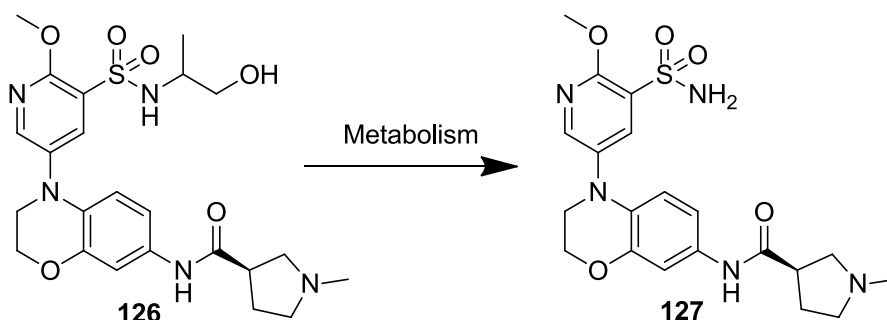
The sulfonamide moiety is present in almost all molecules in benzoxazine and short hinge series as well as being present in a GSK clinical compound **125**. An analysis of all proprietary PI3K δ screening data, prior to the commencement of this project, showed that as the potency threshold increases the proportion of molecules containing a sulfonamide increases greatly (Table 21).

pIC₅₀ PI3Kδ	>6	>7	>8	>9
Number of molecules with a sulfonamide	1814	984	431	88
Total number of molecules	3592	1522	552	93
Percentage	51%	65%	78%	95%

Table 21 – Total number of GSK molecules exceeding potency thresholds before 01/10/14 and the prevalence of sulfonamide moiety in these compounds.

The high proportion of potent compounds containing a sulfonamide means that if an issue with the sulfonamide moiety were to be identified, there are not likely to be suitable back-up compounds available which are chemically distinct from the current assets.

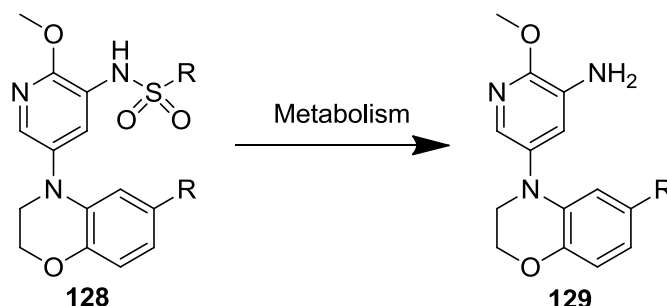
One such problem could be the clearance of sulfonamide molecules. An *in house* study has shown that a major route of metabolism *in vitro* for benzoxazine **126** is *via* sulfonamide *N*-dealkylation (Scheme 21).¹²⁵



Scheme 21 – Metabolite **127** of benzoxazine **126**, identified in a metabolite identification *in vitro* study.

This *N*-dealkylation could be avoided by changing the sulfonamide moiety for another functional group, and this could potentially result in a reduction in metabolic clearance.

Having stated this, another concern comes from the pyridyl *N*-linked sulfonamide. In this case, sulfonamide cleavage could result in a potentially genotoxic aniline functionality (Scheme 22).^{126,127}



Scheme 22 – Release of potentially genotoxic aniline moiety by metabolism of sulfonamide.

The possibility that aniline **129** could be genotoxic^{126,127} results in further testing being required for molecules of this type to determine if the potential aniline metabolite is mutagenic and to confirm if it is released *in vivo*. This is further complicated by metabolism in other parts of the molecule potentially leading to several different aniline fragments being released which must be characterised and tested. Based on all the above, avoidance of these potential problems would be advantageous.

Another potential problem for the aryl sulfonamide comes from the pK_a of the sulfonamide proton (Figure 38). The high acidity of this proton results in the molecule being at least partially ionised at biological pH, resulting in lower permeability since ionic compounds cannot easily passively permeate biological membranes.

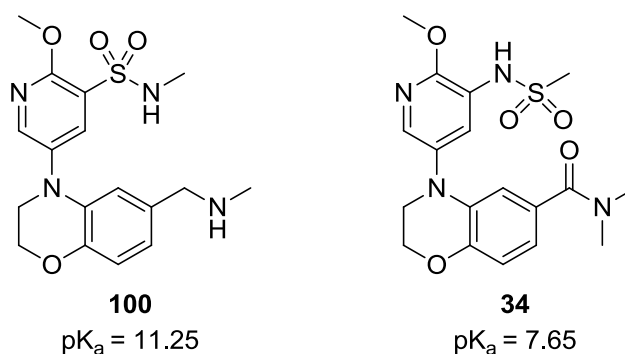


Figure 39 – Measured pK_a of sulfonamide moiety.

CONFIDENTIAL – PROPERTY OF GSK – DO NOT COPY

The sulfonamide group also has a high mass with the heavy sulfur atom and three period two elements. The large number of heavy atoms means that the sulfonamide must make strong interaction to have high ligand efficiency. Hence introduction of an alternative functional group may improve this.

In terms of replacing the sulfonamide, adopting a macrocyclisation strategy may offer additional functional group tolerance by forcing the pyridine to exhibit one conformation rather than being able to rotate (Figure 40).

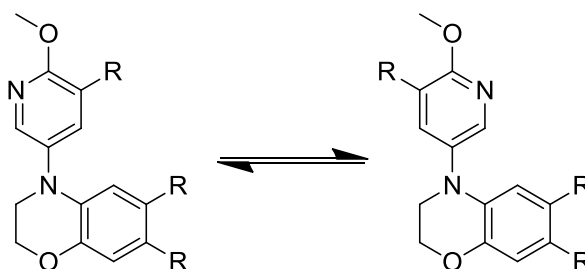


Figure 40 – Potential rotation prevented by working within a macrocyclic template.

A macrocycle would fix the rotational conformation preventing rotation and potentially allowing a larger range of functionality to be tolerated, by spatially restricting the location of the isostere, and increasing the probability of making similar interactions with the kinase.

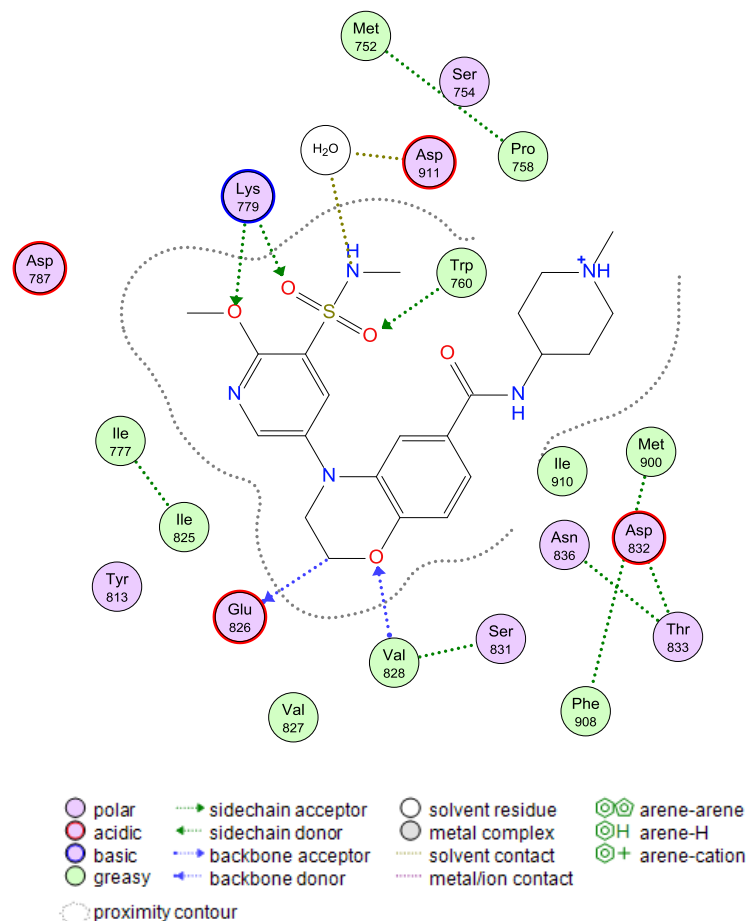


Figure 41 – Interactions made by the sulfonamide portion of the molecule in a typical benzoxazine compound (1LVRZ). The following features are shown, as calculated by MOE: Hydrogen bond strengths $>1.0 \text{ kcal mol}^{-1}$, Ionic bond strengths $>1.5 \text{ kcal mol}^{-1}$, Residues within 4.0 \AA .

The interactions made by the sulfonamide are summarised in Figure 41 and consist primarily of a hydrogen bond from sulfonamide oxygen to lysine-779 and a water mediated hydrogen bond to asparagine-911. Substitution of the sulfonamide for other functional groups will allow the importance of these interactions on potency and selectivity to be explored.

Figure 42 shows some possible replacements for the sulfonamide system which may address several of the issues outlined above.

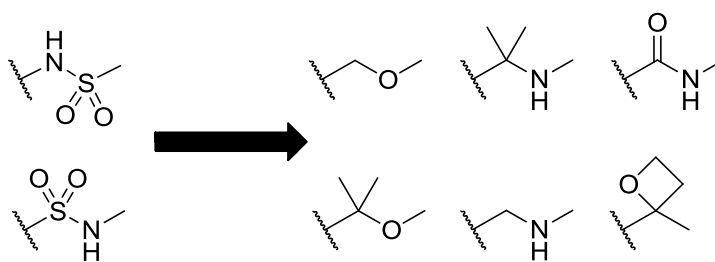


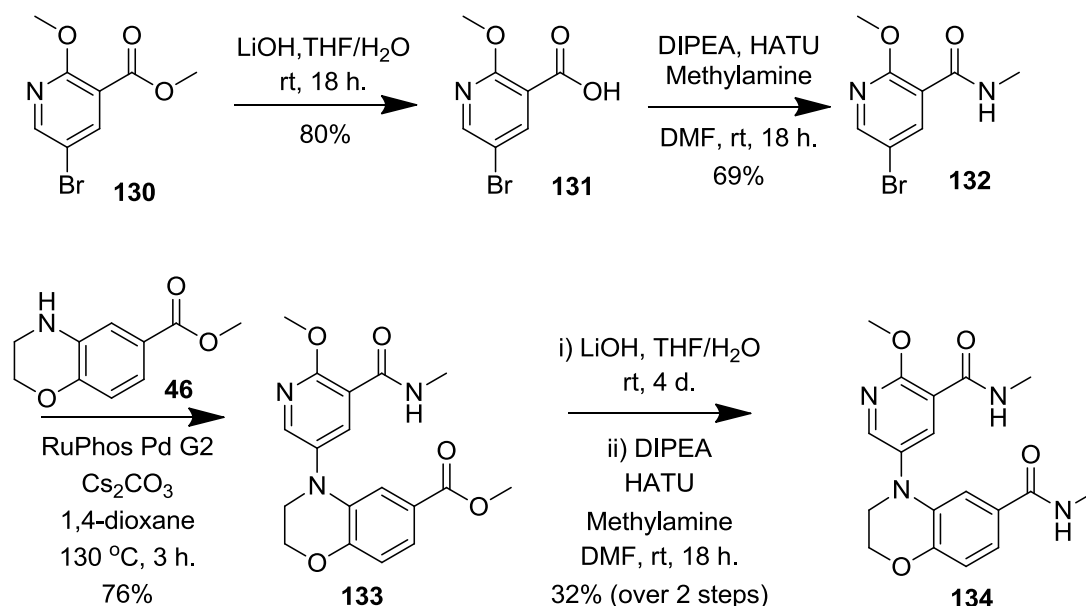
Figure 42 - A selection of possible sulfonamide replacements.

Based on synthetic expediency, it was decided to initially consider a range of acyclic analogues to judge which sulfonamide replacements would be best to progress to macrocycles. The first replacement considered was an amide moiety (Figure 43).



Figure 43 – Sulfonamide to amide replacement.

As only one sulfonamide oxygen makes a bonding interaction with lysine-779 (Figure 41), it was hypothesised that replacement with an amide would allow this interaction to be maintained. It was also anticipated that by maintaining an *N*-H functionality, water mediated hydrogen bond to asparagine-911 could be retained. However, it was known that the aryl amide was likely to occupy different conformations to the aryl sulfonamide due to the π -overlap between aromatic ring and amide. The amide also has a different spatial arrangement to the sulfonamide, with the sulfonamide adopting a tetrahedral geometry and the amide a trigonal planar arrangement. As a trade-off to these concerns, amide synthesis was expected to be facile and hence this compound was made (Scheme 23).



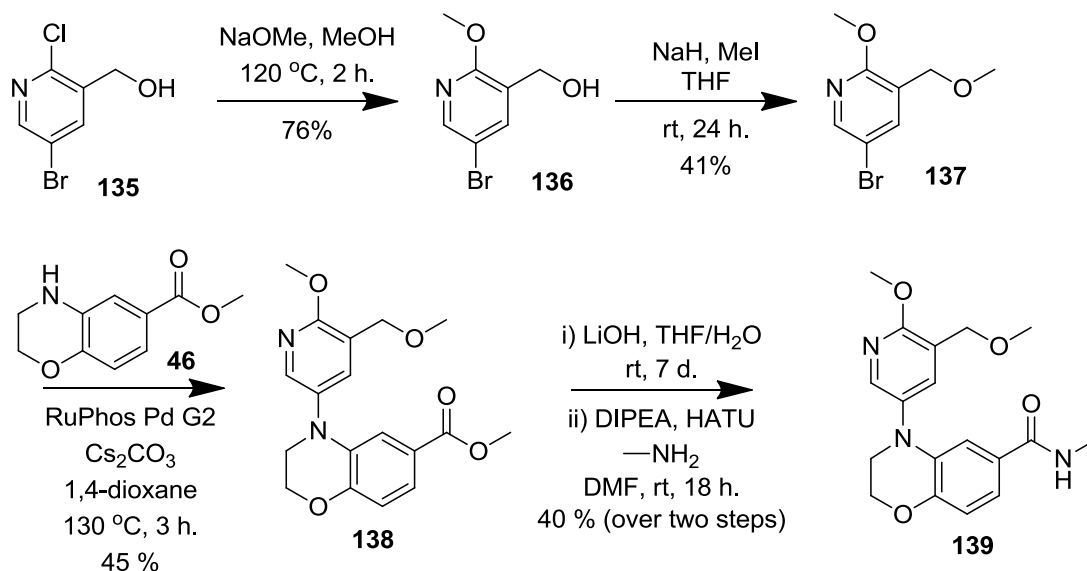
Scheme 23 – Synthesis of amide as a sulfonamide replacement.

Synthesis of amide **134** proceeded *via* ester hydrolysis of commercially available pyridine building block **130** to yield pyridyl acid **131**. Subsequent HATU mediated amide coupling gave amide **132**. This was then coupled *via* Buchwald-Hartwig amination to benzoxazine **46** in good yield.¹²⁸ Finally, ester hydrolysis and amide coupling yielded amide **134**.



Figure 44 – Sulfonamide to ether replacement.

It was hypothesised that the water mediated hydrogen bond between the sulfonamide N-H and asparagine-911 and hydrogen bond between sulfonamide O and lysine-779 are weak. This is due to the flexibility of the long lysine chain meaning forming a bond is entropically disfavoured. Hence, these interactions may not be required for potency or selectivity. Based on this, it was proposed that a simple methylene unit containing oxygen as a potential growth vector could maintain potency (Figure 44). Accordingly, the ether linker was also prioritised for synthesis (Scheme 24).



Scheme 24 – Synthesis of ether **139** as a sulfonamide replacement.

Synthesis of the target ether analogue **134** proceeded by nucleophilic aromatic substitution on commercially available pyridyl chloride **130**. This was followed by *O*-alkylation *via* nucleophilic substitution, which gave low yield owing to competing pyridine *N*-alkylation resulting in a pyridinium salt observed as a highly polar species by LCMS. Buchwald-Hartwig amination then yielded aminopyridine **133**, with similar ester hydrolysis and amide coupling steps to yield the target ether **134**.

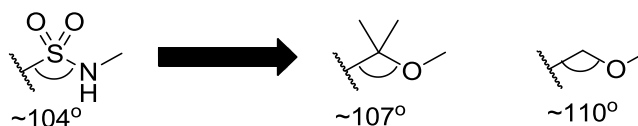
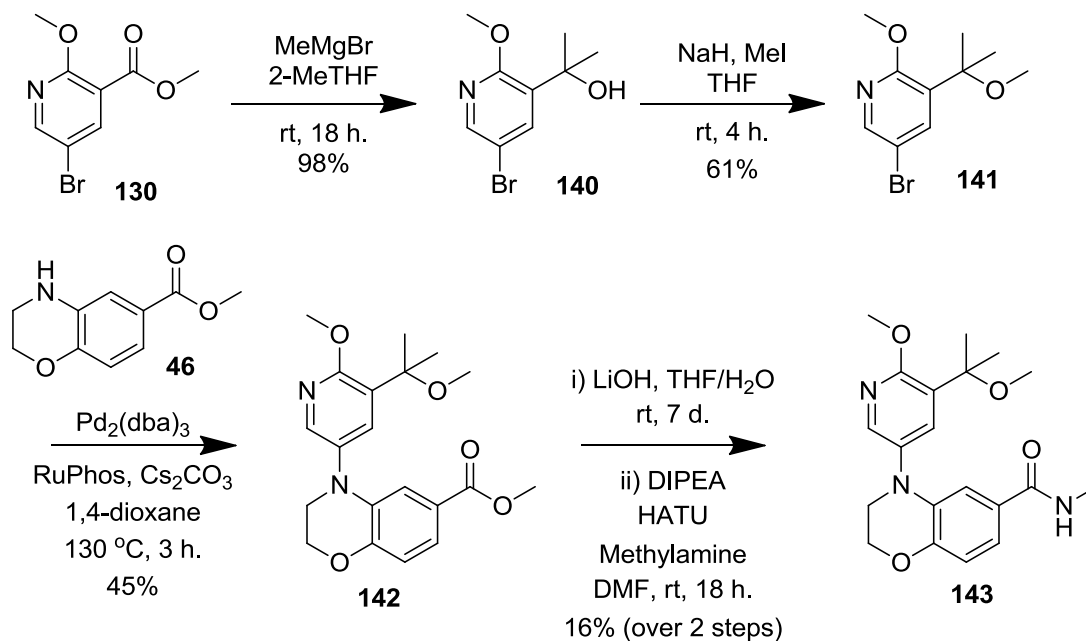


Figure 45 – Sulfonamide to dimethyl ether replacement.

In addition to the target methylene ether analogue, it was hypothesised that adding methyl groups to the ether would reduce the angle at the carbon centre to make the methyl vector similar to the sulfonamide (Figure 45). Accordingly, this compound was also synthesised using an analogous synthetic sequence. (Scheme 25)



Scheme 25 - Synthesis of geminal dimethyl ether **143** as a sulfonamide replacement.

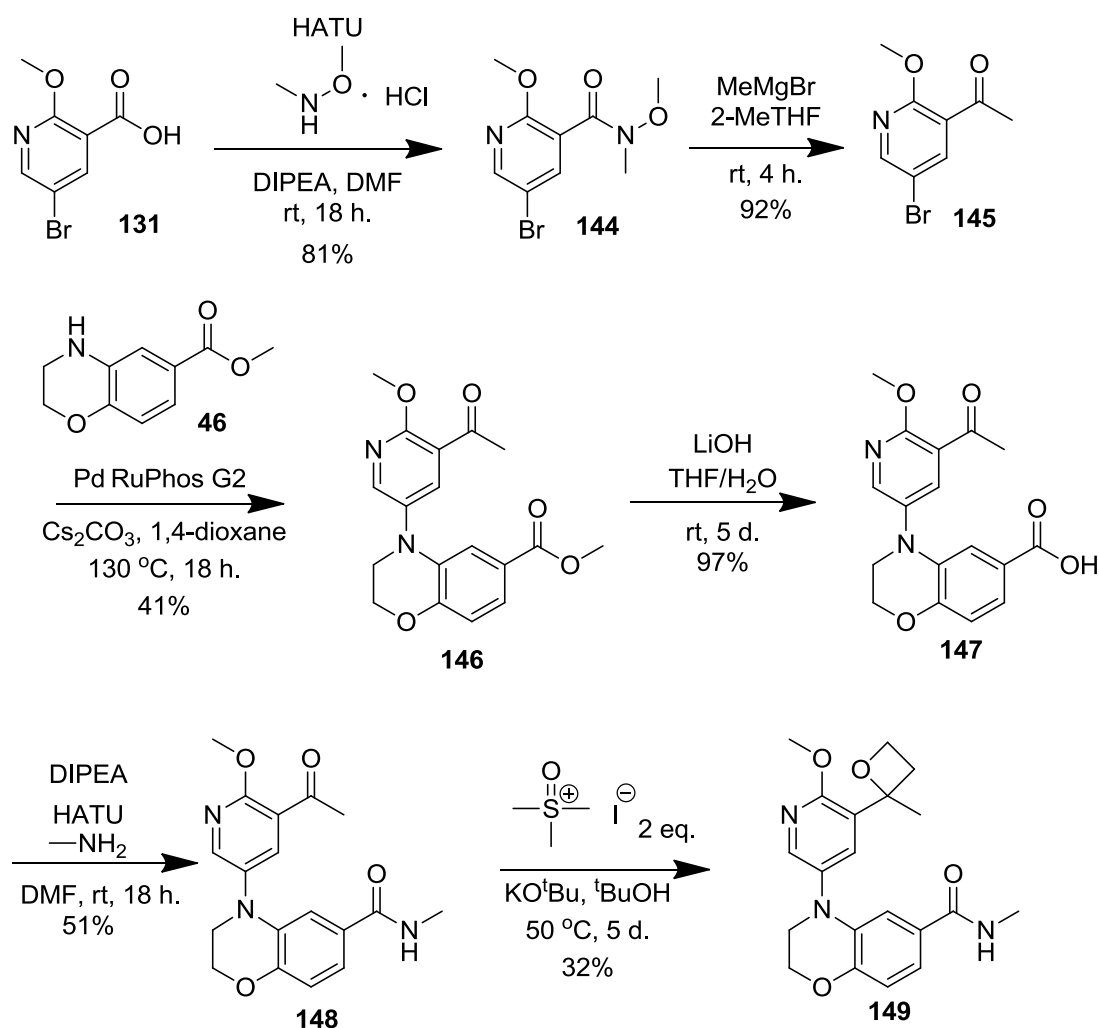
Geminal dimethyl ether synthesis proceeded *via* a double Grignard addition into ester **130**, and the resulting alcohol **140** was then alkylated *via* nucleophilic substitution to yield ether **141**. Buchwald-Hartwig amination using the RuPhos Palladacycle did not yield the desired product and hence Pd₂(dba)₃ with RuPhos ligand was employed with more success. This observation can potentially be rationalised by the electronics of the aryl bromide affecting the best catalyst system for the reaction. The geminal dimethyl ether is likely to be more electron donating than the methylene and the sulfonamide, thus changing the electronics of the ring system. The modified conditions gave benzoxazine **142** in relatively low yield compared to related Buchwald-Hartwig products, however, a sufficient quantity of product was isolated to proceed with the synthesis. Subsequent ester hydrolysis and amide coupling then gave final compound **143**.



Figure 46 – Sulfonamide to oxetane replacement.

CONFIDENTIAL – PROPERTY OF GSK – DO NOT COPY

As stated previously, it was observed that since both sulfonamide oxygens appeared to be interacting with different residues, that both interactions may not be required. Hence an oxetane was considered (Figure 46), and it was anticipated that the oxetane oxygen would potentially mimic one of the sulfonamide oxygens. 2,2-Substituted oxetanes were selected in preference to the isomeric 3,3-substituted oxetane to try to retain the oxetane oxygen in an orientation proximal to the sulfonamide oxygen. Based on this, the requisite oxetane was then synthesised (Scheme 26) with intermediate ketone **148** also being submitted for screening.



Scheme 26 – Synthesis of oxetane **149** as a sulfonamide replacement.

CONFIDENTIAL – PROPERTY OF GSK – DO NOT COPY

Starting from common intermediate **131**, a Weinreb amide was formed, followed by nucleophilic attack of methyl magnesium bromide to yield ketone **145**.¹²⁹ Subsequent Buchwald-Hartwig amination, ester hydrolysis and amide coupling yielded amide **148**. The ketone was then converted to oxetane **149** via a double Corey-Chaykovsky addition (Figure 47) described by Okuma *et al.*¹³⁰

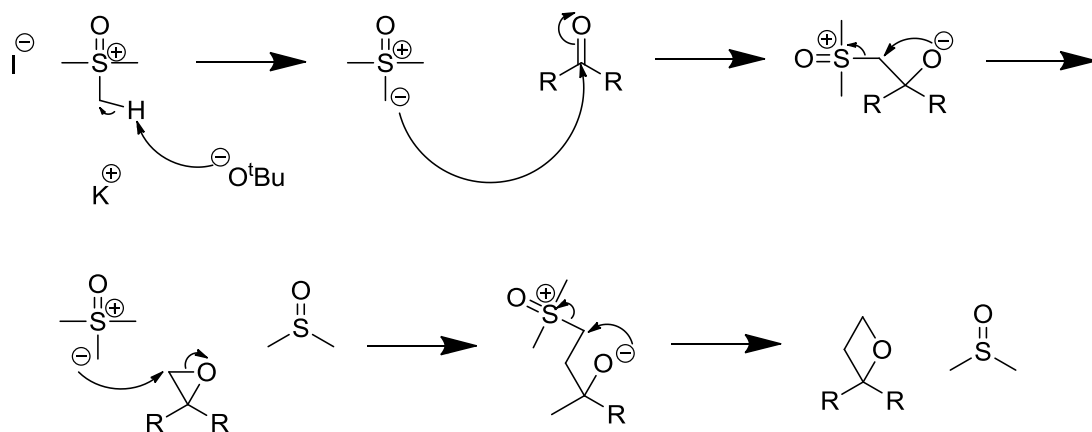


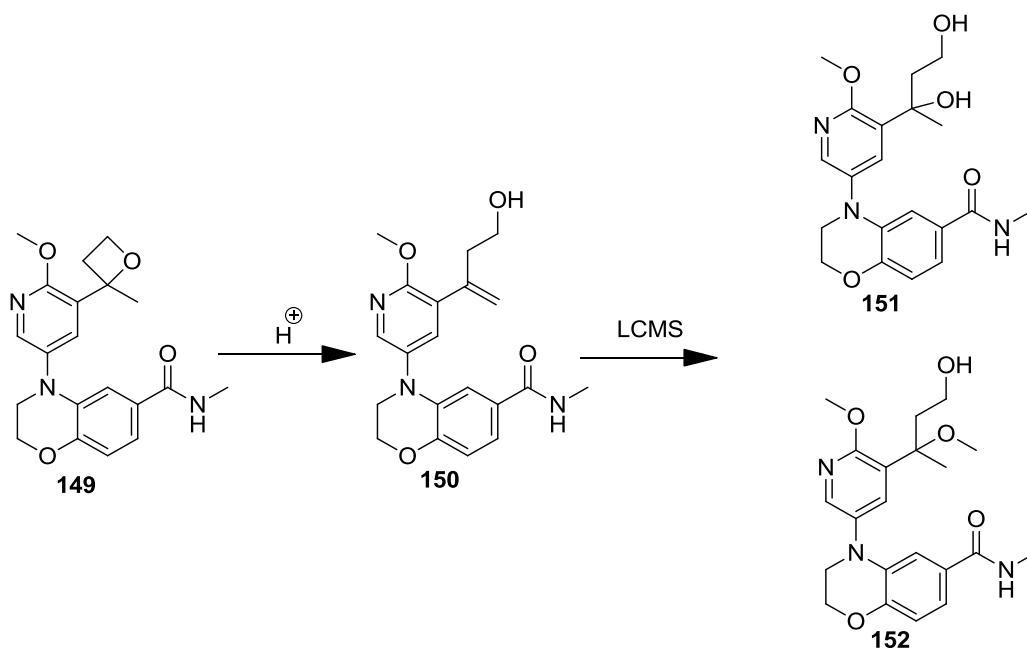
Figure 47 – Mechanism for oxetane formation via double Corey-Chaykovsky addition to ketone.

The reaction mechanism for the formation of the oxetane starts with formation of a sulfur ylide from deprotonation of the Corey-Chaykovsky reagent by potassium *tert*-butoxide. The ylide can then perform a nucleophilic attack on a ketone, followed by displacement of neutral dimethyl sulfoxide leaving group and formation of an epoxide intermediate. The epoxide can then be opened by a further equivalent of the ylide and another molecule of dimethyl sulfoxide displaced to yield the desired oxetane.

Oxetane **149** was then analysed by chiral chromatography to explore whether separation of the enantiomers would be possible. However, it was found that oxetane **149** was degrading to an achiral product under the analysis conditions. Based on this, further stability studies were conducted. A small amount of oxetane **149**, was then left in methanol solution and no degradation was observed by LCMS after 7 days. A small amount was then exposed to acidic and basic conditions, with the acidic sample showing instantaneous degradation and the basic sample showing no degradation after 7 days. The acidic conditions were then scaled up to 10 mg oxetane input and two products were isolated by mass directed HPLC purification. Subsequent NMR and

CONFIDENTIAL – PROPERTY OF GSK – DO NOT COPY

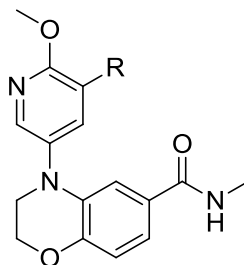
mass spectrometry analysis identified the structures as ether **152** and alcohol **151** (Scheme 27) with the structure of the achiral intermediate hypothesised to be alkene **150**. This degradation under acidic aqueous conditions could mean the oxetane may not be suitable for oral dosing due to the low pH encountered in the stomach, however initial biological profiling was completed as the compound was found to be stable under assay conditions.



Scheme 27 – Proposed degradation of oxetane under acidic conditions.

In vitro PI3K δ enzyme assay results for sulfonamide replacement compounds

With a range of sulfonamide replacements in hand, these new compounds were then evaluated in the PI3K δ assay.

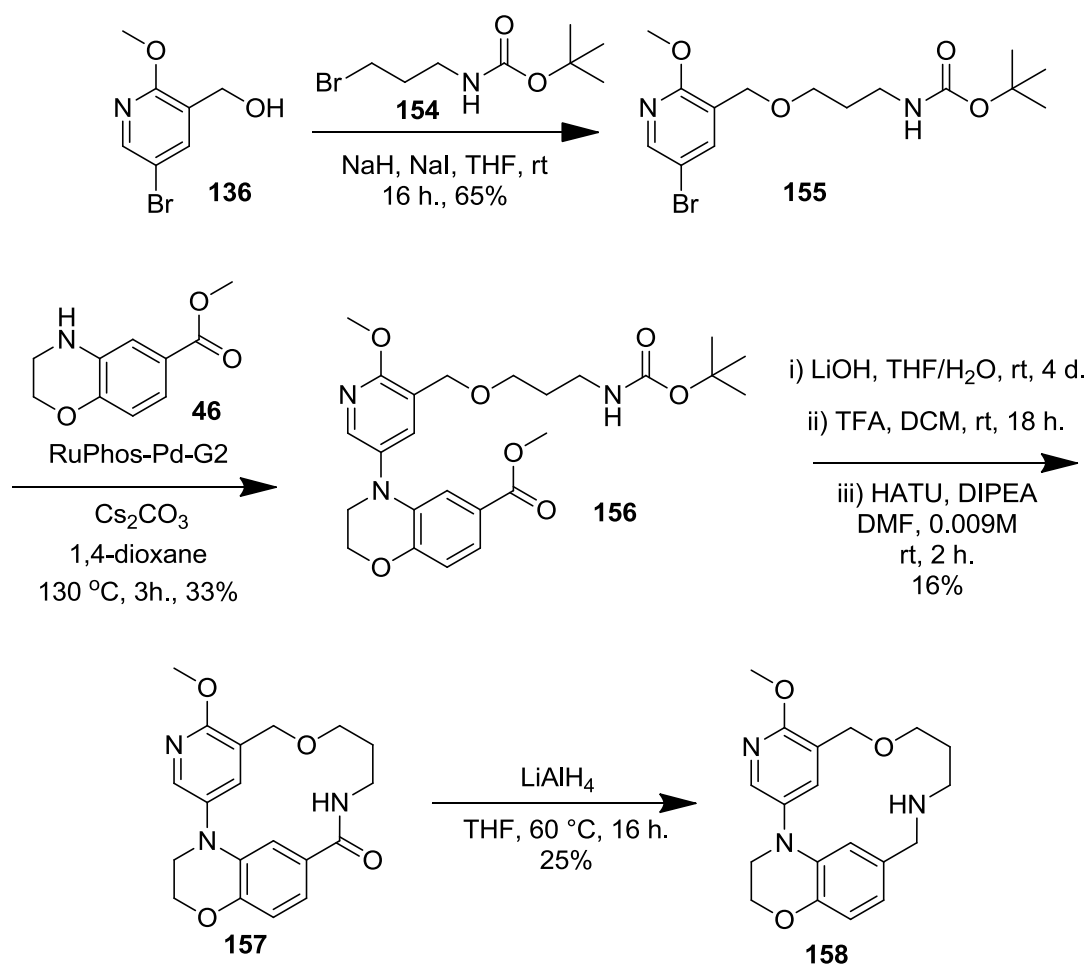


R=							
Compound no.	101	153	134	139	143	149	148
pIC₅₀ PI3Kδ (LE)	7.4 (0.38)	7.3 (0.37)	5.8 (0.28)	7.2 (0.39)	6.8 (0.35)	5.9 (0.30)	6.3 (0.35)

Table 22 – PI3K δ pIC₅₀ for sulfonamide replacements. All n \geq 2 unless otherwise indicated.

Initial data for the sulfonamide replacements was encouraging and showed that ligand efficiency can be maintained without the sulfonamide being required. Ether replacement **139** showed a small increase in efficiency, and dimethyl ether **143** showed comparable potency. However, amide **134** and oxetane **149** gave reduced potency and efficiency compared to sulfonamides **101** and **153**. These data led to the ether moiety being selected for macrocyclisation as it provided improved ligand efficiency (*vide infra*).

An analogous synthesis to those used for sulfonamide macrocycles was employed to synthesise three-carbon linked ether macrocycles (Scheme 28).

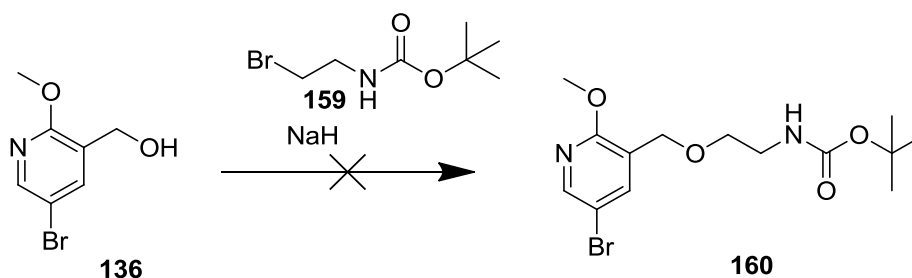


Scheme 28 – Synthesis of three-carbon ether linked macrocycles.

The synthesis commenced with alkylation of alcohol **136** using alkyl bromide **154** in the presence of sodium iodide, a nucleophilic catalyst, giving product **150** in good yield. Buchwald-Hartwig amination under the optimised conditions yielded benzoxazine **156** in low yield. This may be due to the electronics of the aryl bromide **155** being altered by presence of an alkyl substituent as opposed to a sulfonamide. Ester hydrolysis and Boc-deprotection gave amino acid intermediate, which was not isolated. Cyclisation with HATU under dilute conditions yielded amide macrocycle **157** in low yield. However, enough material was obtained to biologically profile the compound and to conduct reduction with lithium aluminium hydride to yield amine macrocycle **158**.

Despite the success in preparing the propyl linked system, synthesis of two-carbon linked macrocycles required an alternative strategy. Attempted alkylation of alcohol

136 with ethyl alkylation agent **159** resulted in no alkylation product by LCMS (Scheme 29).



Scheme 29 – Attempted alkylation of pyridyl methanol **131**.

The absence of product may be due to elimination of the alkyl bromide to give conjugated system **161** (Figure 48). It was thought that this could be avoided by reversing the alkylation (Figure 48).

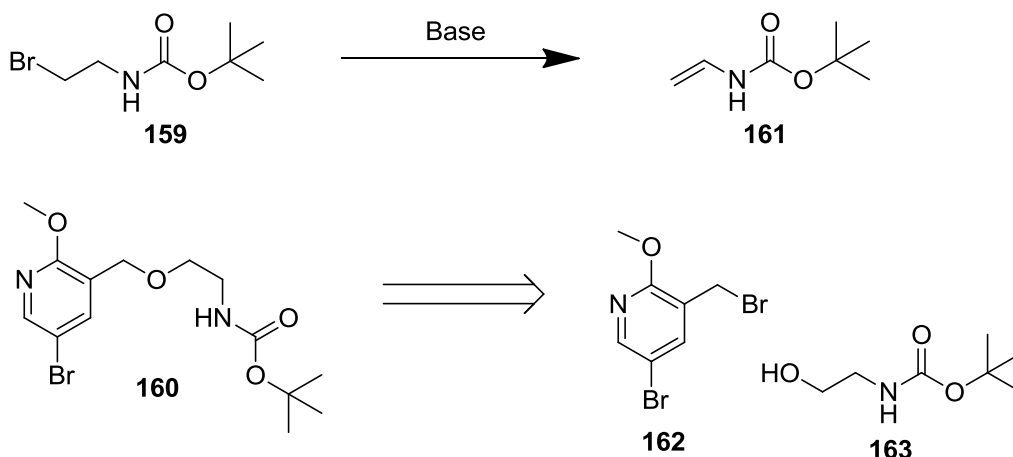
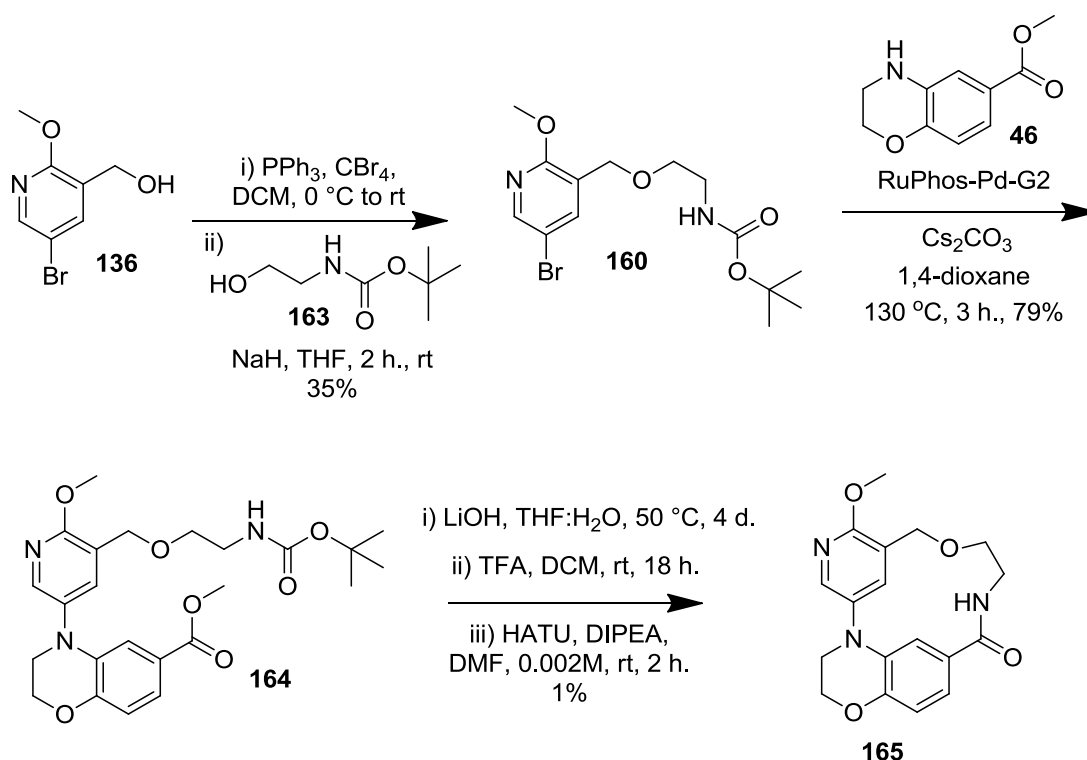


Figure 48 – Proposed explanation for unsuccessful alkylation reaction and proposed reversal of alkylation conditions to access ether **165**.

Reversal of the alkylation reaction would mean the benzyl alkylating agent could no longer eliminate. The benzyl halide is also likely to be more electrophilic due to overlap of the C-Br antibonding orbital with the π -system of the aromatic ring.

This method was therefore used for the synthesis of two-carbon linked macrocyclic ether molecules (Scheme 30).



Scheme 30 – Synthesis of two-carbon linked ether macrocycle **162**.

Pyridyl bromide was synthesised by an Appel reaction.¹³¹ This was then alkylated with alcohol **163** in moderate yield with most losses occurring in bromination step; the alkylation is probably successful due to the elimination pathway not being possible. Buchwald-Hartwig amination proceeded in good yield for this system, and subsequent ester hydrolysis followed by Boc-deprotection gave amino acid intermediate, which was not isolated. However, cyclisation in the presence of HATU under dilute conditions resulted in a very low yield of macrocycle **165**. The major species observed by LCMS corresponded to the mass of dimer **166**.

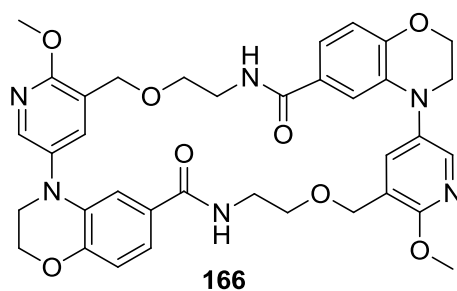
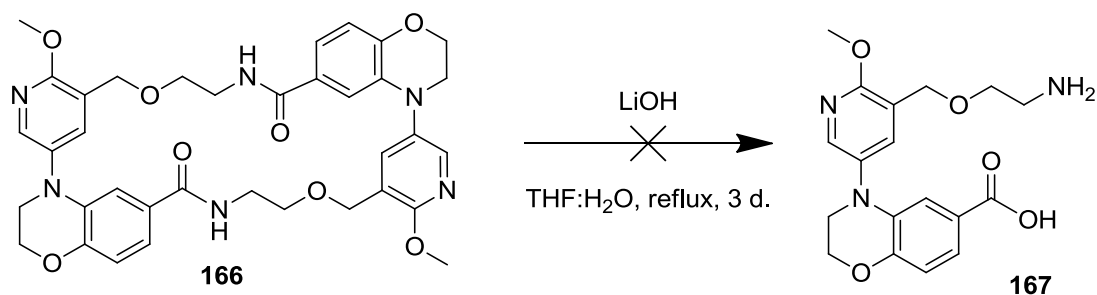


Figure 49 – Proposed structure of main product in macrocyclisation sequence from ester **164**.

It was thought that the ring strain present in the two-carbon linked ether macrocycle provides a large barrier to forming the monomer macrocycle **165**, meaning the dimer **166** is the major product even under high dilution.

Despite this, it was anticipated that hydrolysis back to the amino acid **167** may be possible (Scheme 31).



Scheme 31 – Attempted hydrolysis of dimer **166**.

However, after three days of refluxing in base, no trace of the amino acid was observed by LCMS. Nevertheless, despite the poor yield of the cyclisation step, enough monomer macrocycle was obtained to proceed to biological testing.

In vitro PI3K δ enzyme assay results for sulfonamide replacement macrocycles

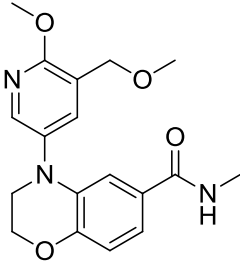
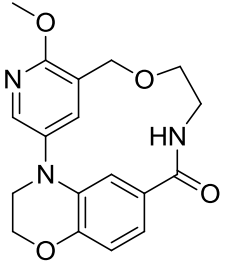
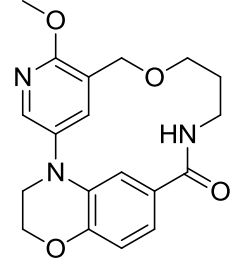
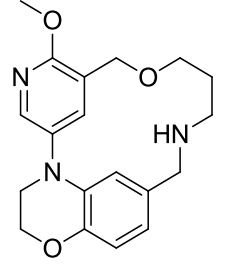
			
Compound no.		139	162
pIC₅₀	PI3Kδ	7.2	5.2*
			
Compound no.		157	158
pIC₅₀	PI3Kδ	5.7	5.7

Table 23 – Potency of ether macrocycle compounds. All $n \geq 2$ unless otherwise indicated.* $n=1$

Macrocyclisation of the ether modified compounds proved to be detrimental to potency. It was found that between 30- and 100-fold drop in potency was observed for all ether containing macrocycles. This may be due to the conformation of the ether oxygen in the active site changing from acyclic to macrocyclic compounds, meaning possible beneficial hydrogen-bonding interactions with Lys-779 are lost (Figure 50). Therefore, synthesis of ether macrocycles was halted at this stage, however it is proposed that macrocycles linked through carbon may be able to overcome this (Eg. compound **168**, Figure 50).

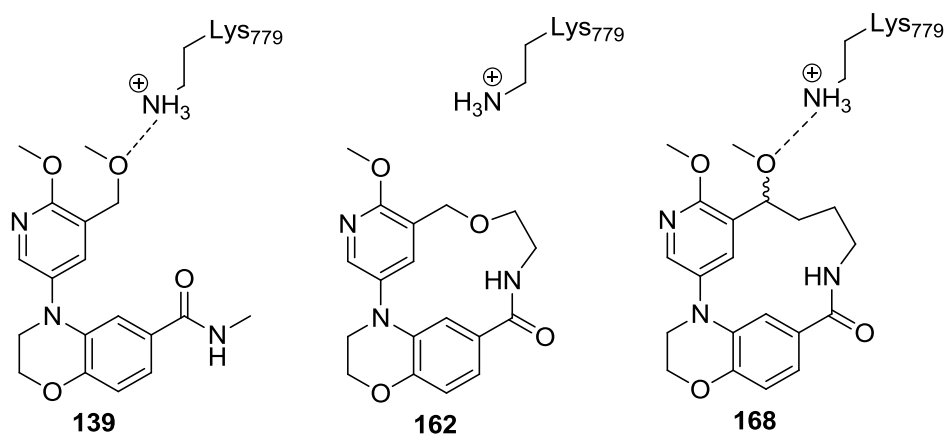


Figure 50 – Proposed lost interactions of ether with lysine-779 and proposed macrocyclic target to overcome this loss.

In summary, the ether linked acyclic compound proved to be a viable alternative for sulfonamides. These compounds may be able to overcome the problems with metabolism, potential genotoxicity and poor permeability associated with sulfonamide compounds within this series. However, the ether cannot be directly translated into macrocyclic compounds, meaning further studies are required to explore macrocyclisation within this template.

2.3.6 Effect of Macrocyclisation on Drug Properties

Having established a biochemical profile for a range of macrocyclic compounds, the impact of macrocyclisation on a range of important physicochemical properties was then assessed.

In respiratory disease, there are two main pathways of delivery, oral and inhaled, for which the desirable properties vary. Our laboratories currently have an inhaled PI3K δ inhibitor in the clinic¹³² as well as an inhaled back-up compound,¹³³ however, further inhaled and additional oral molecules are being sought.

Oral drugs offer some advantages over inhaled drugs for patients, particularly in respiratory disease where patients may struggle to breathe in the inhaled drug. As stated previously, inhalers are also difficult to operate and give varying dose, dependant on the technique used.^{9,11} Oral drugs are therefore much easier for the patient to administer and hence typically give higher patient compliance.

Having stated this, inhaled drugs are also sought in the respiratory field as they offer direct administration to the site of action in the lung. Careful design of pharmacokinetic properties allows minimisation of systemic exposure, thus reducing the chances of side effects.

Hence, for the reasons outlined above, the effect of macrocyclisation on developability properties both for oral and inhaled drugs was investigated. In the initial hypothesis, and based on earlier literature precedent,^{46-48,50,51,54} it was anticipated that macrocyclisation could offer differentiation in many drug properties such as increased permeability, reduced clearance and increased potency, whilst maintaining similar lipophilicity. Accordingly, appropriate data for all macrocycles and acyclic analogues were generated and some illustrative examples selected with the aim of elucidating whether a macrocyclic template offers an improved profile for oral or inhaled dosing.

For the purpose of this analysis macrocycles were matched to their corresponding progenitor parent compound, by sulfonamide orientation, amide or amine and by *N*-methylation state. This enabled direct comparisons of closely related compounds to determine the effect of macrocyclisation.

CONFIDENTIAL – PROPERTY OF GSK – DO NOT COPY

The first property to be considered in further depth was potency. In both oral and inhaled drugs, high potency is a key requirement. Potency is a good preclinical indicator of efficacy¹³⁴ and also allows the administered dose to be as low as possible. This reduces the chance of any off-target interactions and, therefore, means side-effects may be reduced. Experience from within our laboratories shows that a pIC₅₀ of greater than 9 is desired for inhaled and greater than 8 for oral. The potency must be higher for inhaled compounds since the maximum single dose is limited to 1 mg due to the design of the inhaler used to administer the drug to humans.

It was hypothesised that a macrocyclic template may provide improved potency due to restrictions in conformation thus providing a reduced entropic cost of binding. However, it was also known that restricting the compound in a non-binding conformation would cause a large reduction in potency.

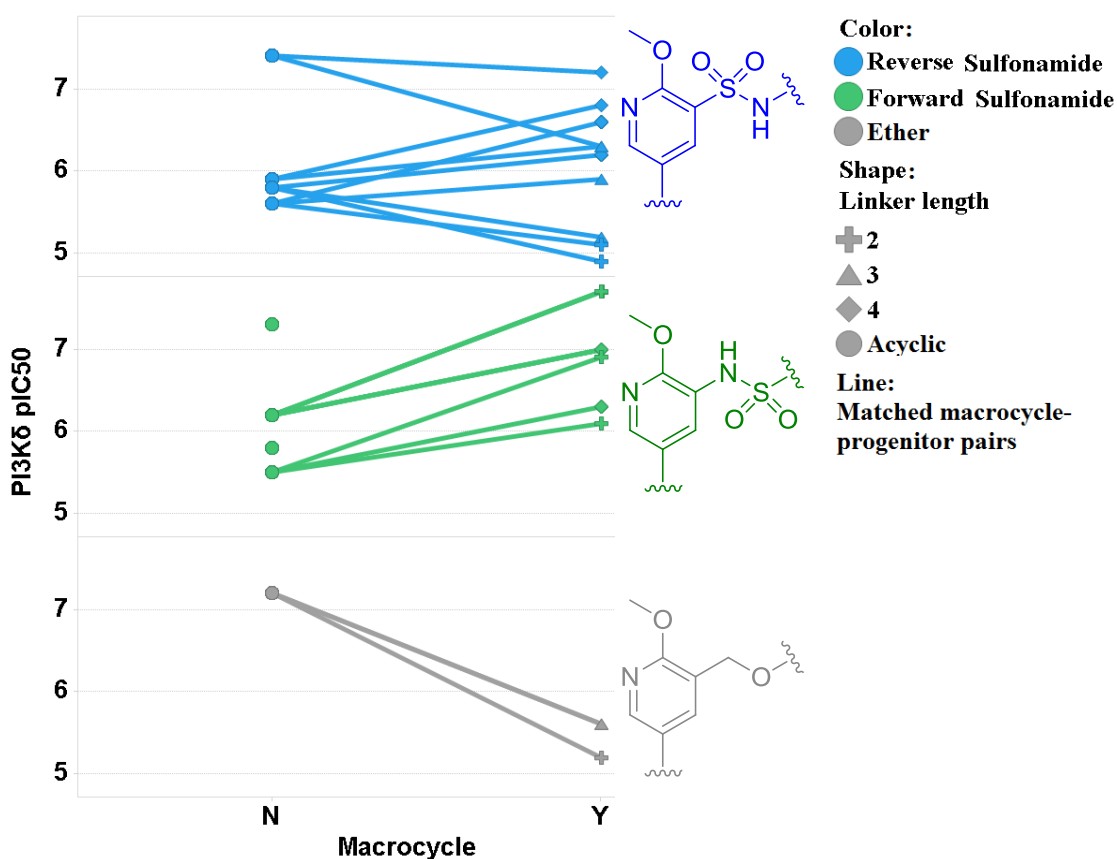


Figure 51 – A visualisation of the effect of macrocyclisation on the potency at PI3Kδ.

Analysis of the potency data (Figure 51) shows that several matched pairs gain potency upon formation of a macrocycle, however a number of pairs also lose potency. It was

thought that macrocyclisation in the ether template was unfavourable due to macrocyclic restriction forcing the molecule into a non-binding conformation.

All the forward sulfonamide compounds were found to have a significant increase in potency. However, in the case of the reversed sulfonamide the results are more mixed. In general, the longer linker compounds are more favoured with gain in potency or at worst small reductions observed. Whereas, short two-carbon linkers result in large reductions in potency. It was expected that the forward and reverse sulfonamides would occupy similar conformations and therefore, linker length SAR would be transferable. However, this was not the case, and significant differences in SAR were observed. All compounds lie below the desired potency thresholds for oral or inhaled compounds, however, since the compound are generally $M_w \sim 400$, there is scope for potency enhancement by further optimisation or growth of the compounds. As such, ligand efficiency metrics may provide a better understanding of where the compounds are placed in terms of potency. Additionally, since some macrocyclic systems contain additional atoms, efficiency may provide a more direct comparison between acyclic and macrocyclic compounds.

A number of ligand efficiency metrics allow a comparison of whether increasing molecular weight is compensated by a significant increase in potency.¹³⁵ The most widely considered is ligand efficiency (LE), defined in Equation 4.

$$LE = -\frac{RT \ln IC_{50}}{N} = -\frac{1.37pIC_{50}}{N}$$

where N is the number of non Hydrogen atoms

Equation 4 – The definition of ligand efficiency.

Ligand efficiency is a measure of the Gibb's free energy of binding per heavy atom in the molecule. This provides a guide as to whether additional molecular weight is providing the desired increase in binding affinity. Typically, an LE value greater than 0.3 for a lead compound is desired.¹³⁶

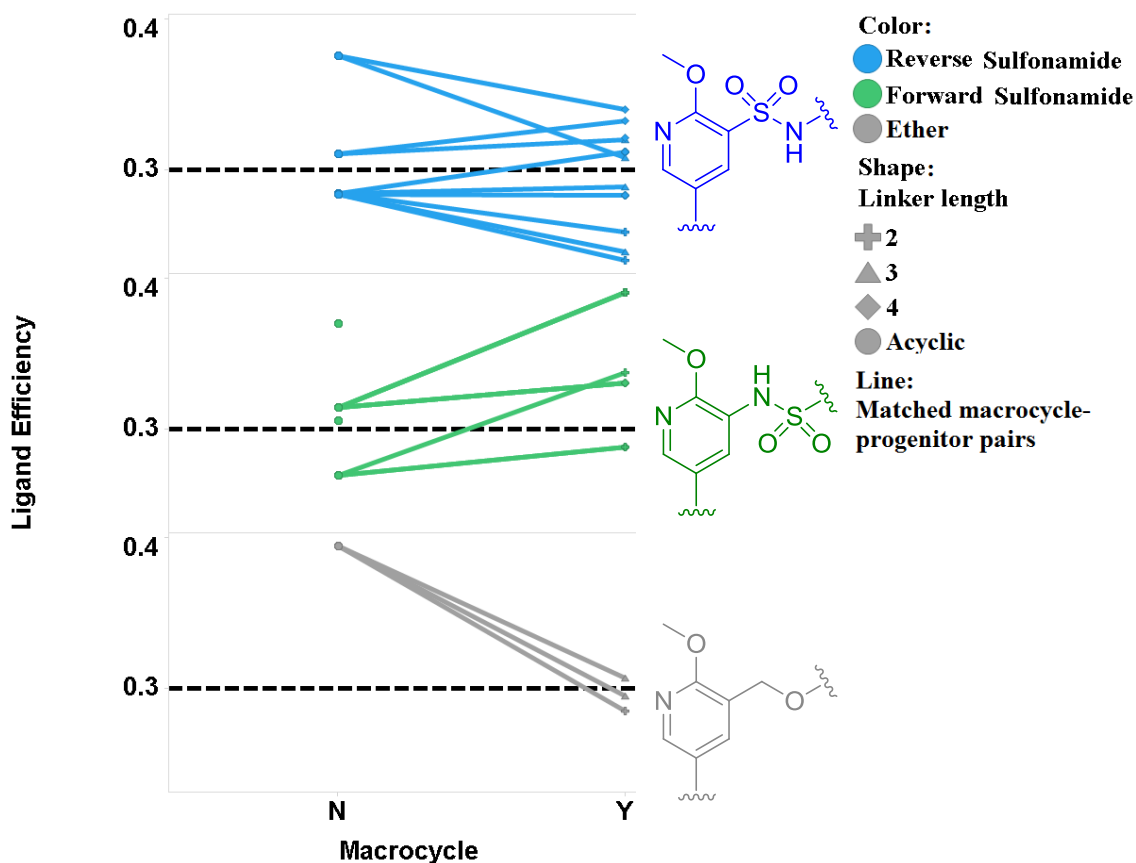


Figure 52 – A visualisation of the effect of macrocyclisation on the ligand efficiency at PI3K δ .

In an analogous manner to potency, the ether macrocycles become significantly less ligand efficient. The forward sulfonamide compounds exhibit increased efficiency, as well as an increase in potency, showing that the observed increase is gained through useful ligand-protein interactions. The reverse sulfonamide compounds again show a mixture of small improvement and loss in efficiency. This analysis indicates that macrocyclisation can result in significant increases or decreases in efficiency dependent on the precise nature of the template. Despite the fact the compounds do not reach the threshold for potency, they are above the desired ligand efficiency threshold, which indicates they are a suitable starting point for further optimisation to obtain analogues with the desired potency levels for oral or inhaled drugs.

Selectivity is also an important part of the compound profile; a compound must be highly selective to reduce the chance of off-target binding which can often be associated with

CONFIDENTIAL – PROPERTY OF GSK – DO NOT COPY

side effects, thus reducing the likelihood of toxicity. In the current study, a selectivity of >100-fold over the other PI3K isoforms and >1000-fold over other kinases was desired.

It is hypothesised that a macrocyclic template may provide improved selectivity over structurally unrelated enzymes, due to macrocyclic constriction reducing the number of available binding conformations. However, the binding mode within the PI3K family of enzymes, as well as the lipid kinase family in general, is likely to be similar, and macrocyclisation may not impart improved selectivity, depending on protein flexibility and amino acid residue changes in the appropriate region of the protein.

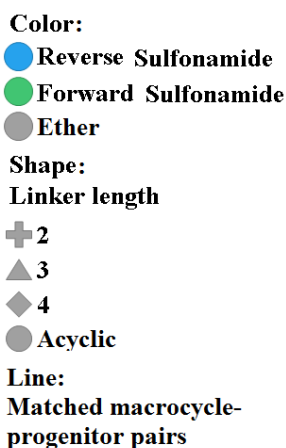
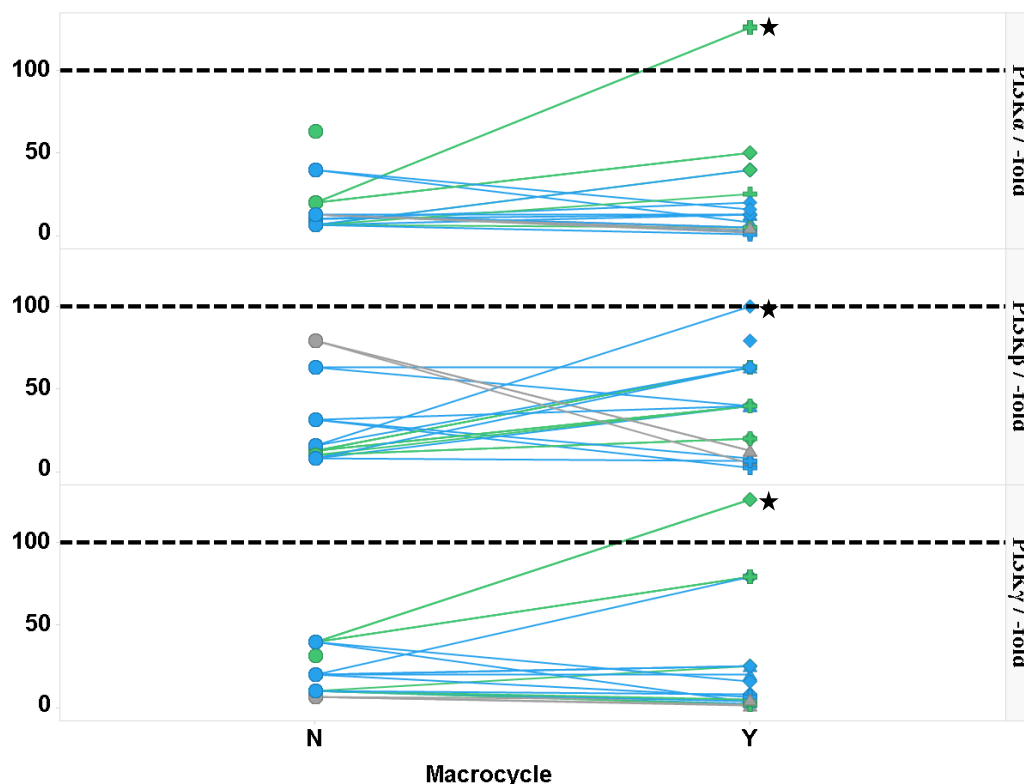


Figure 53 - A visualisation of the effect of macrocyclisation on the selectivity over other PI3K isoforms. Selectivity data is calculated using mean pIC_{50} , from which values below the assay threshold ($pIC_{50} < 4.5$) have been excluded. Where all data fall below the assay threshold the pIC_{50} is assumed to be 4.5, meaning some of the selectivities are in fact greater than or equal to the value stated.

Analysis of the data (Figure 53) revealed that macrocyclisation does not have a significant effect on the selectivity over the other PI3K isoforms. Most of the variation observed is not significant, especially when biological error on the assay data is considered. Having stated this, a small number of compounds (indicated by a star)

appear to have small, but significant increases in selectivity. These compounds do not have consistent increases in selectivity over all the isoforms; it is therefore hypothesised that some linkers prevent access to the subtly different binding modes in each of the isoforms.

A number of physicochemical properties have been found to be important for drug development. An oral molecule should have high solubility, since it must be in solution in the gastrointestinal tract in order to be absorbed.¹³⁷ A high solubility is defined as the maximal dose dissolving in 250 mL of aqueous media,¹³⁸ this leads to greater than 100 $\mu\text{g mL}^{-1}$ or 200 μM being desired for 25 mg dosing of a compound with molecular weight of 500. For inhaled drugs solubility is less important since the drug can be administered as a dry powder and small solid particles can diffuse into lung tissue.^{139,140} These solid particles are often slow to diffuse and therefore can result in a long duration of action for the drug. However, the presence of solid particulates in the lung can cause toxicity, meaning solubility for inhaled compounds is complex, with factors such as lung retention competing with potential toxicity.¹⁴¹

It was initially thought that macrocyclisation would reduce solubility; steric restrictions in the macrocyclic template could reduce the ability for water to solvate polar groups. It was also hypothesised that the macrocyclic restriction would force the molecules to adopt a flatter conformation, which could promote π -stacking and stabilise the crystalline form of the compounds, resulting in poor crystalline solubility.

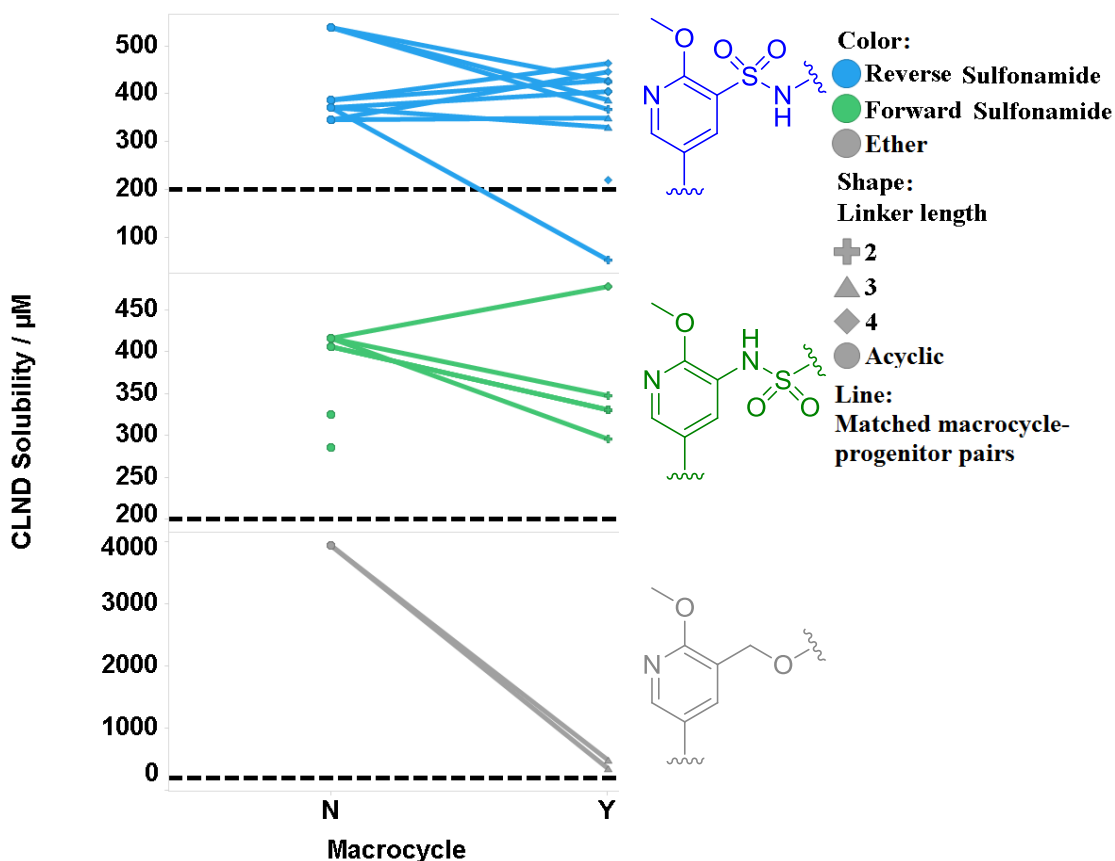


Figure 54 - A visualisation of the effect of macrocyclisation on the CLND solubility.

Analysis of kinetic solubility data (Figure 54), measured using a chemiluminescent nitrogen detection assay, shows that macrocyclisation has a variable effect on solubility depending on the nature of the macrocycle. In ether compounds, dramatic decreases from highly soluble acyclic compounds are observed. However, in forward and reverse sulfonamide series, macrocyclisation results in compounds of similar solubility in most cases. In fact, most acyclic and macrocyclic compounds exhibit greater solubility than the 200 μM threshold for candidates within our laboratories. However, the kinetic solubility assay, whilst being high throughput, measures precipitation of compound from a solution of DMSO and therefore the energy barrier for dissolution is not important. This means factors such as the crystallinity of the compound, which increases the size of this barrier, are not accounted for in the the solubility measured in this assay.

High permeability is also required for oral molecules in order for the molecule to move from the gut into the systemic circulation.¹³⁷ An analysis by Hwang *et al.* of 93

marketed drugs shows that molecules with artificial membrane permeability greater than 30 nm s^{-1} have a high probability of achieving good bioavailability and all compounds with permeability greater than 200 nm s^{-1} exhibit bioavailability of greater than 90%.¹⁴² However, most assays generally measure passive permeability through an artificial membrane, neglecting any active transport, which is considered by some to be the main mechanism *in vivo*.¹⁴³ For inhaled compounds permeability can be less important with low permeability compounds often showing good efficacy and long residence times within the lung¹⁴⁴ as long as the compound can reach the target.

It was proposed that macrocyclisation would result in an increase in permeability, due to the restricted conformation reducing the number of rotatable bonds, meaning that the macrocycle may occupy a smaller volume in space and therefore may permeate more easily.

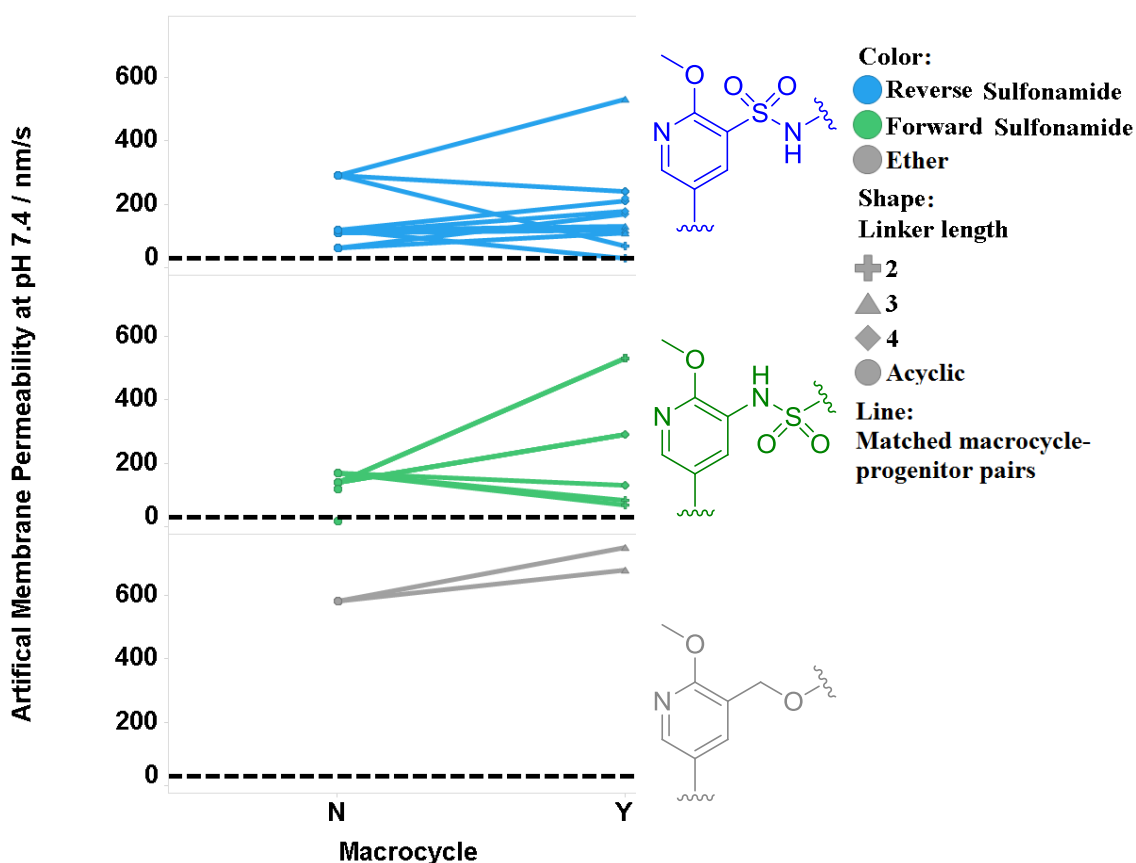


Figure 55 - A visualisation of the effect of macrocyclisation on the artificial membrane permeability.

CONFIDENTIAL – PROPERTY OF GSK – DO NOT COPY

Analysis of artificial membrane permeability data (Figure 55) shows that macrocyclisation has a mixed effect on permeability. A small number of compounds show a slight reduction in permeability, however many compounds show increases in permeability as expected. All compounds studied are in the desired permeability range for oral compounds.

A further important factor in drug discovery, particularly in oral compounds, is plasma protein binding. If a drug molecule is bound to plasma protein it is not free to interact with the target and hence a binding of less than 99% is desired. However, inhaled compounds do not have to enter the blood to reach their site of action and therefore blood protein binding is a less important factor.¹⁴⁵ Human Serum Albumin (HSA) and α -1-acid glycoprotein (AGP) are the most widely studied plasma proteins, with HSA the protein of further study within this thesis. HSA has a number of binding sites and a number of flexible groups which allow it to bind a wide range of ‘drug-like’ molecules.¹⁴⁶

Since drug molecules are expected to make non-specific interactions with HSA, it was anticipated that macrocyclisation would not cause large differences to this binding.

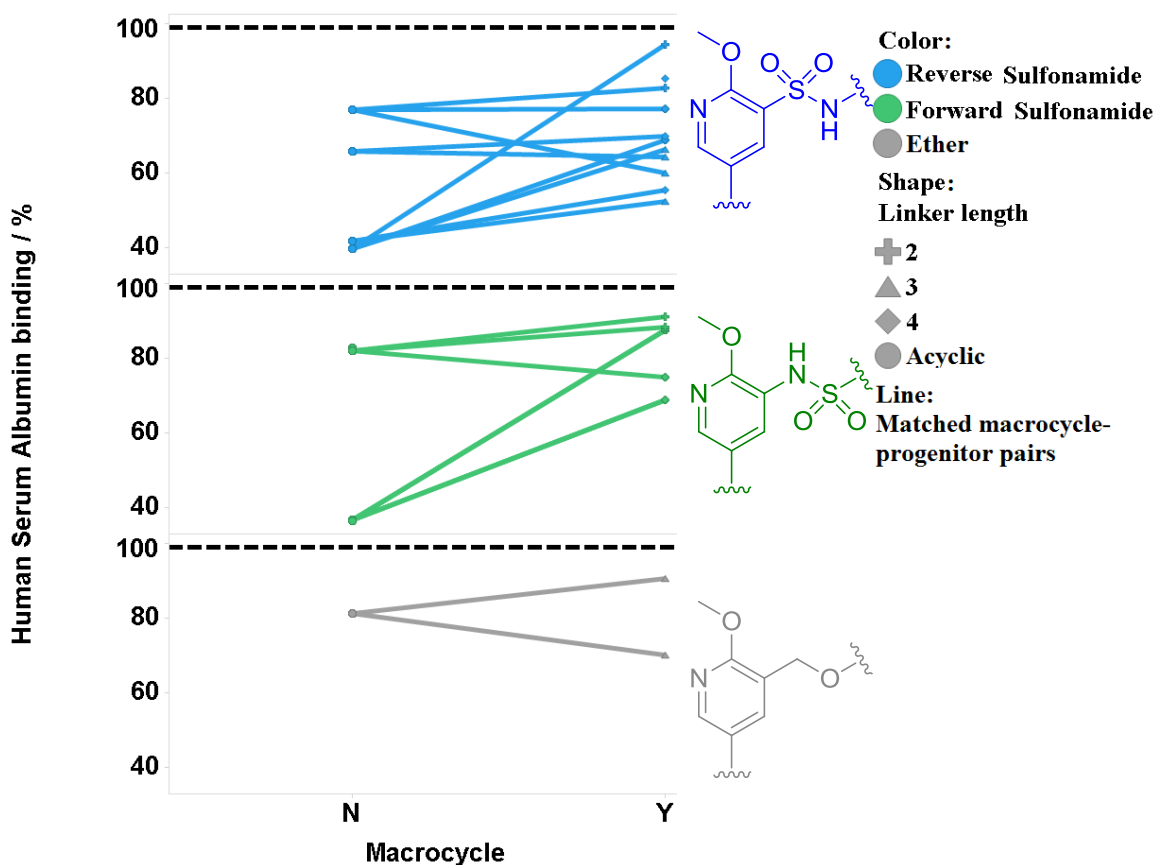


Figure 56 - A visualisation of the effect of macrocyclisation on human serum albumin binding.

Visualisation of the binding data for compounds (Figure 56) shows that the binding to HSA increases upon macrocyclisation in most cases. However, all values measured remain within acceptable range for oral dosing.

One further important consideration in drug discovery is the clearance of the molecule by the body. The liver contains many metabolising enzymes, which in general make the compound more polar and lead to excretion. It is clear that the length of time before a drug is metabolised into an inactive form is important for both oral and inhaled delivery. For oral delivery, a low clearance is desired since the drug must be transported from the gut to the site of action without being metabolised and then must remain at the site of action for long enough to have a meaningful effect. By contrast, for inhaled compounds a moderate to high clearance is desired, since it is beneficial for the drug to be metabolised quickly once it reaches systemic circulation from the lung, as this reduces the chance of side effects from on- or off-target interactions

CONFIDENTIAL – PROPERTY OF GSK – DO NOT COPY

outside of the lung. Generally, molecules are initially analysed *in vitro* in rat, minipig and human microsomes and hepatocytes. Microsomes contain a variety of cytochrome P450 enzymes isolated from fragmented endoplasmic reticulum and data generated indicates phase I metabolism only. This includes oxidation, reduction and hydrolysis. Hepatocytes are liver cells and can give an indication of both phase I (see above) and phase II metabolism. This consists of, in addition to the above, conjugation to other molecules, including methylation, glucoronidation or acetylation. Experience within our laboratories indicates that values below 35% liver blood flow are desirable for oral delivery.

It was proposed that macrocyclisation could affect clearance in a number of ways. Firstly, it was hoped that the conformational restriction from macrocyclisation may prevent binding to some metabolising enzymes. It was also hypothesised that any sites of metabolic weakness in the progenitor compounds may be impacted by macrocyclisation; if these sites were located on the inside of the macrocyclic ring they may no longer be accessible for metabolism. Conversely, if these sites are located on the outside of the ring, they may be more accessible and therefore clearance could increase.

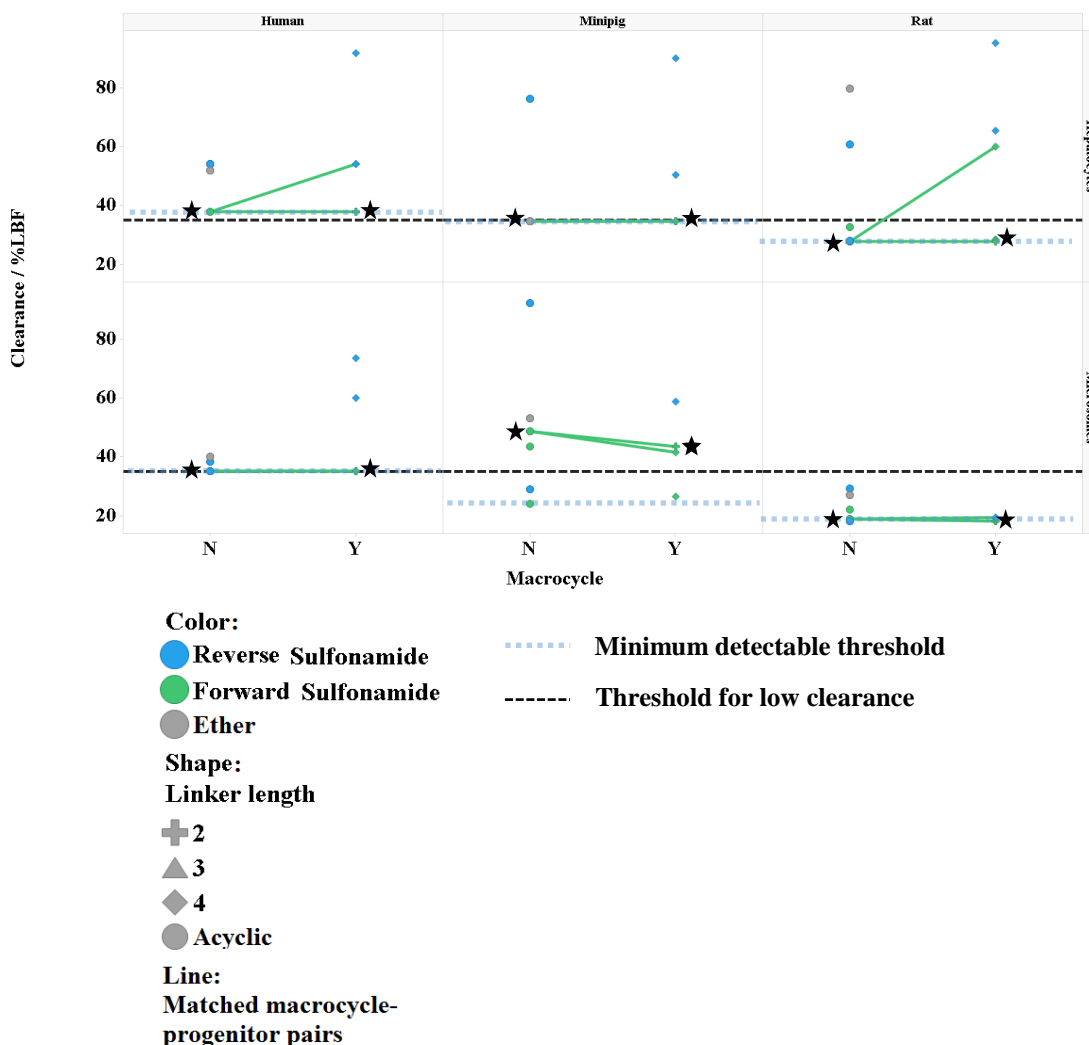


Figure 57 – A visualisation of the effect of macrocyclisation on clearance in microsomes and hepatocytes derived from human, minipig and rat.

The data (Figure 57) shows that many of the compounds lie above the desirable low clearance desired for oral delivery. However, a number of values lie close to the minimum detectable limit of these assays, above the desirable threshold, meaning some clearances may fall below the desirable limit, but cannot be detected within the assay. In general, the matched macrocycle and acyclic pairs show that there is not much difference between the progenitor and macrocycle compounds. However, when forward and reverse sulfonamide pairs are compared more insightful results are obtained.

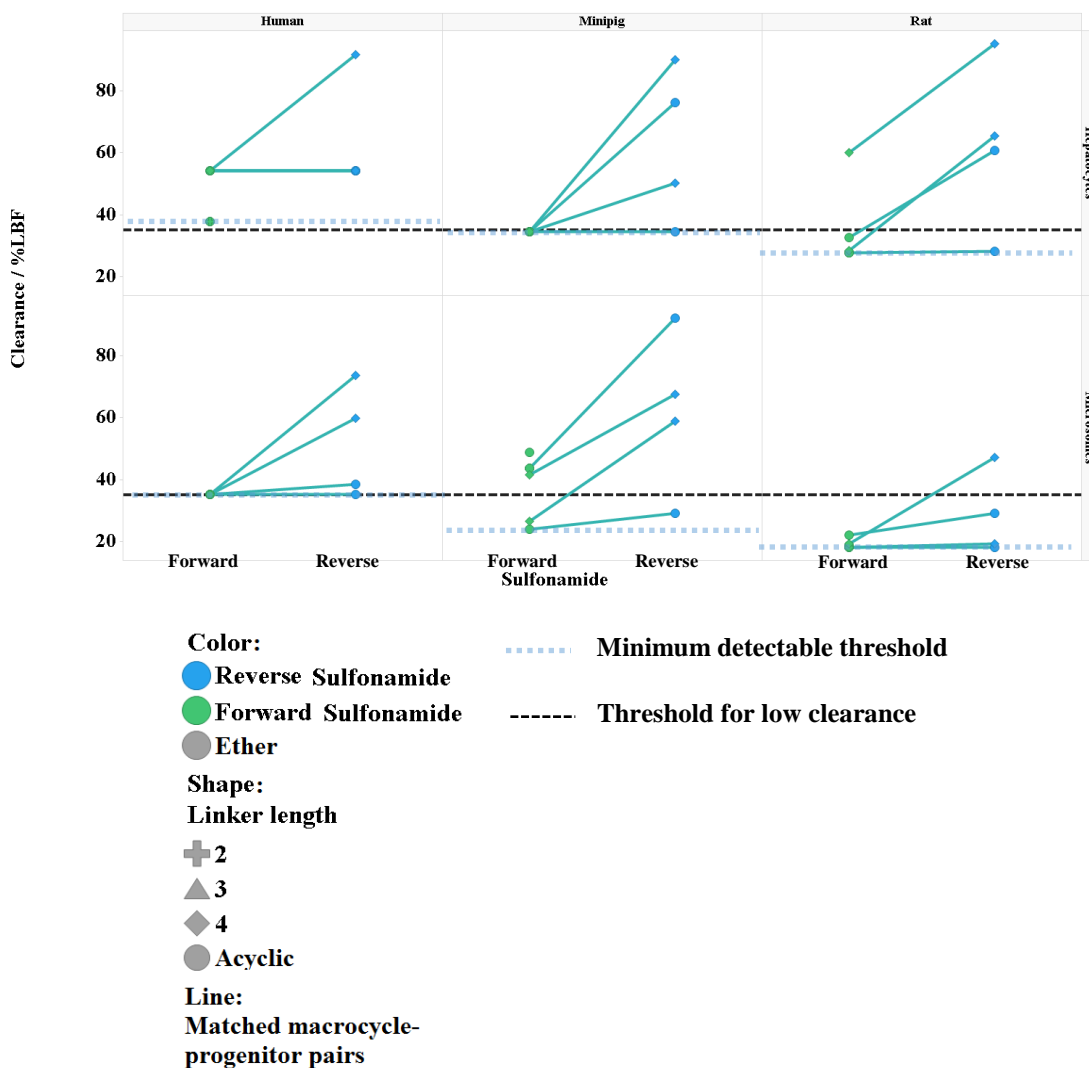


Figure 58 - A visualisation of the effect of sulfonamide isomer on clearance in microsomes and hepatocytes derived from human, minipig and rat.

Visualisation comparing forward and reverse sulfonamides matched pairs (Figure 58) shows that greater clearance is observed in the reverse than the forward sulfonamide in all cases. This suggests that the main pathway of metabolism involves the sulfonamide, with the possibility of sulfonamide cleavage or *N*-dealkylation (Figure 59). Both forward and reverse sulfonamides would be expected to be capable of undergoing sulfonamide cleavage, with possible subtle differences in rate caused by differences in binding. However, only the reverse sulfonamide can undergo an oxidative *N*-dealkylation pathway, since the forward sulfonamide cannot be oxidised adjacent to sulfonamide nitrogen (Figure 59). This is a possible explanation for the differences in clearance observed between the two series.

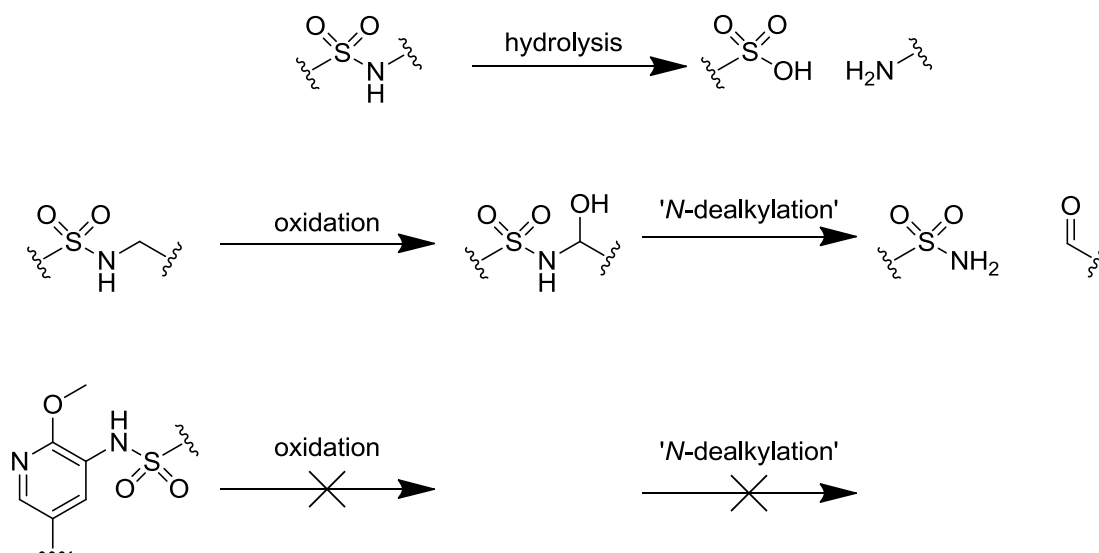


Figure 59 – Possible mechanisms of sulfonamide metabolism and rationale for lower clearance within reverse sulfonamide systems.

These data suggest the forward sulfonamide provides the preferred template for oral delivery (lower clearance) and the reverse sulfonamide for inhaled delivery (higher clearance).

Since, a number of the compounds fall close to the minimum detectable threshold, two compounds, macrocycle **32** and progenitor **20** (starred in Figure 57), were selected for further study *in vivo*. The macrocyclic compound **32** was dosed at two concentrations (0.23 mg kg⁻¹ and 2.92 mg kg⁻¹) whilst the progenitor **20** was dosed at one concentration (1.04 mg kg⁻¹). After intravenous dosing to rats, the blood concentration was analysed at time points up to 24 hours. These concentrations were then normalised to a dose of 1.00 mg kg⁻¹ and the data is presented in Figure 60.

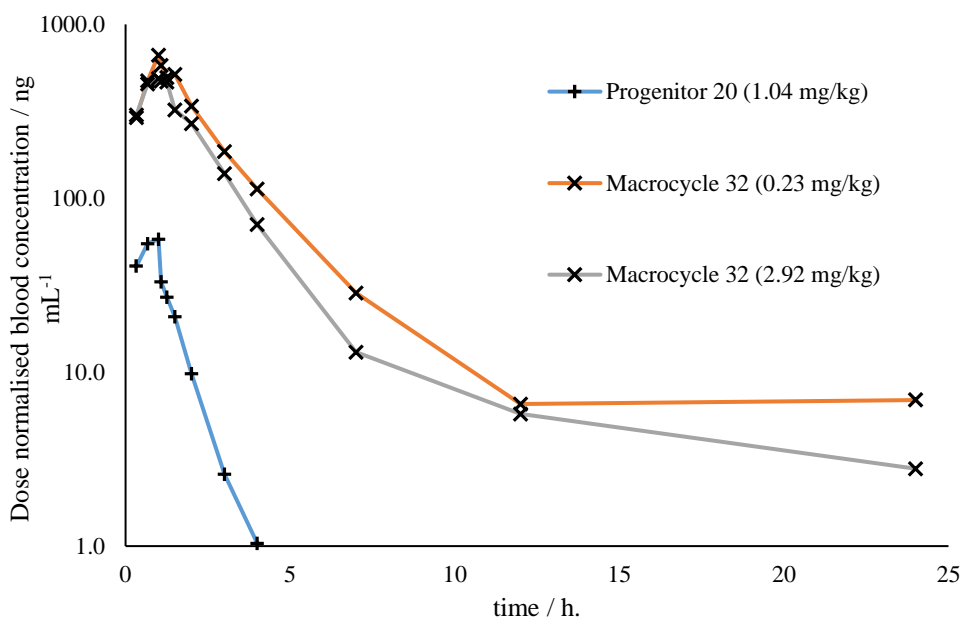


Figure 60 – Results of intravenous dosing of macrocycle **32** and progenitor **20** to rat.

The data shows that the concentration of the macrocycle declines more slowly than the progenitor. This indicates that the macrocycle is cleared slowly *in vivo* and the progenitor is cleared very rapidly. This clearance suggests that the macrocycle has a PK profile suitable for oral dosing. It is possible that these large differences are caused by the macrocyclic restrictions preventing access to conformations required to bind to metabolising enzymes. This would hence prevent some routes of metabolism, meaning the clearance is reduced.

Another important parameter in drug discovery is the lipophilicity of compounds. Lipophilicity affects a number of other drug-like properties, with solubility and passive permeability strongly dependent on lipophilicity.¹⁴⁷ Highly permeable compounds are generally moderately lipophilic, since the compounds need to permeate through both polar and lipophilic groups in the lipid bilayer. Highly soluble compounds generally have low lipophilicity, since soluble compounds have an affinity for the aqueous environment. As stated above, highly lipophilic compounds are also found to make non-specific interactions with targets, leading to poor selectivity. Based on this, a $\log D_{pH7.4}$ of less than 4 is desired.

It was hypothesised that a number of macrocyclic compounds would be more lipophilic than the corresponding acyclic compounds, since some linkers contain

additional methylene units. It is also suspected that macrocycles may be more lipophilic due to polarity being shielded from solvation due to the sterics imposed by the macrocycle.

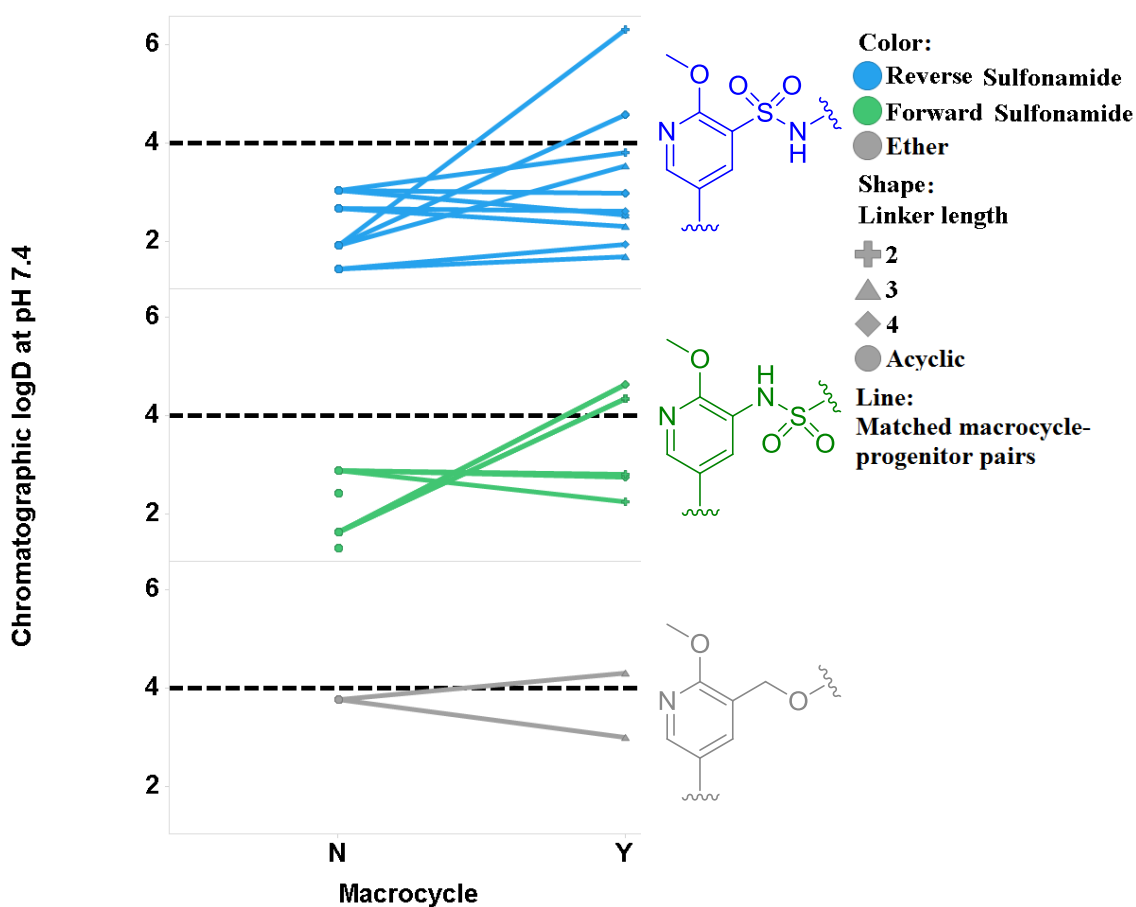


Figure 61 - A visualisation of the effect of macrocyclisation on chromatographic distribution coefficient at pH 7.4.

Initial analysis of data shows that macrocycles do indeed generally have higher lipophilicity than acyclic analogues. However, the magnitude of these changes, with up to ten thousand-fold, was not expected. Further analysis identified that compounds containing an amine had the most significant increases in logD (Figure 62).

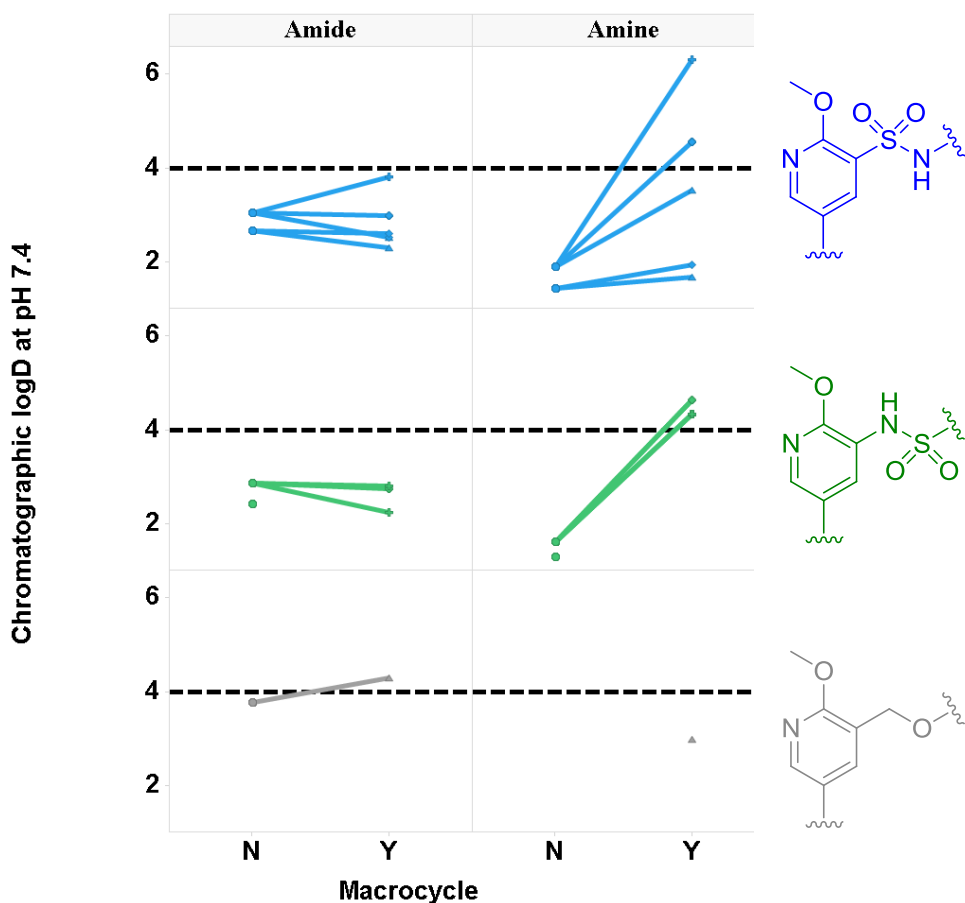


Figure 62 - A visualisation of the effect of macrocyclisation and the presence of an amide or an amine on chromatographic distribution coefficient at pH 7.4.

Based on this, it was thought that pK_{aH} may be impacting lipophilicity, therefore pK_a was measured for a number of acyclic and macrocyclic compounds.

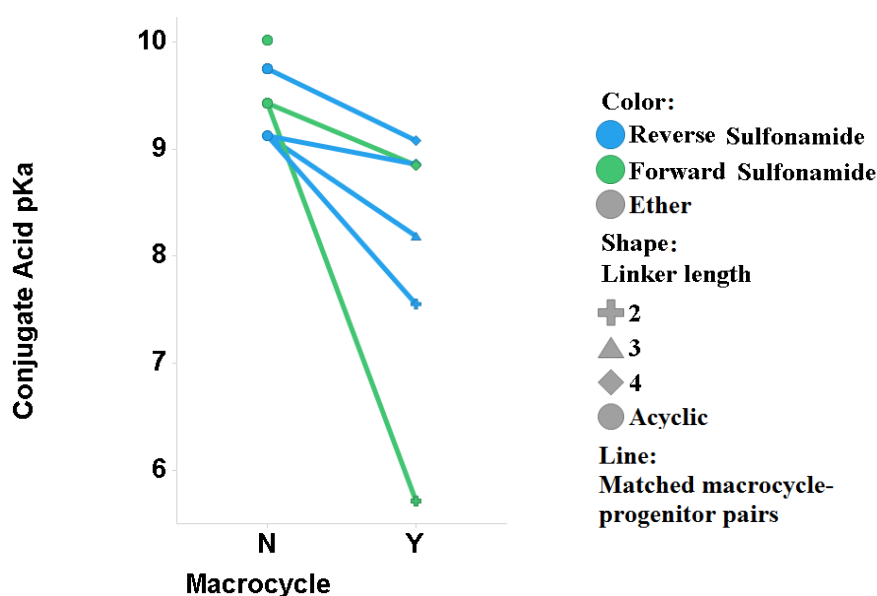


Figure 63 - A visualisation of the effect of macrocyclisation on the basicity of amine compounds.

An analysis of measured pK_a values for macrocyclic and acyclic analogues shows that for all compounds the macrocyclic compounds are less basic than the progenitor compounds. It was hypothesised that this may be due to accessibility of the amine lone-pair within the macrocyclic template. Particularly large differences were observed for compounds **20** and **32** (Figure 66), where almost two log unit change in pK_{aH} was observed. Whilst both compounds contain tertiary amines, the only difference is the macrocyclic connectivity. This difference can be rationalised by observing the lowest energy conformation for the macrocyclic compound **32** (Figure 65).

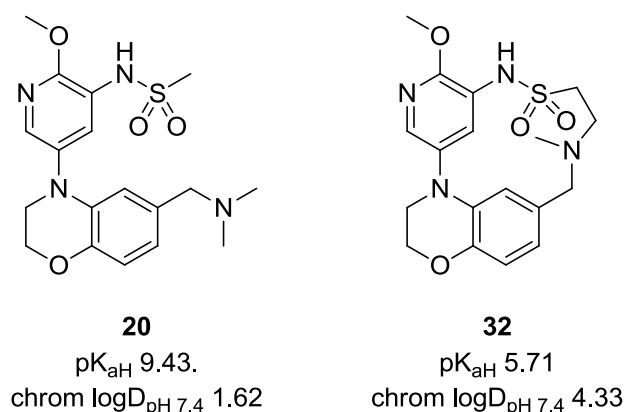


Figure 64 - Differences in pK_{aH} and $\text{chrom} \log D_{pH\ 7.4}$ of compound **20** and **32**.

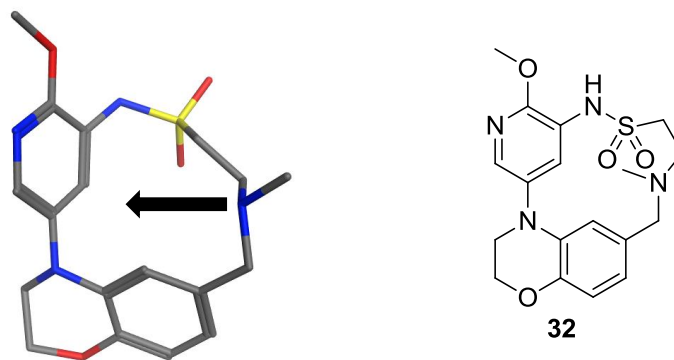


Figure 65 – Lowest energy conformation of macrocycle **32**, with position of amine lone-pair highlighted.

The lowest energy conformation of macrocycle **32** is a conformation in which the amine lone-pair is directed towards the inside of the macrocycle ring. This means that the lone-pair is very sterically hindered and cannot easily be protonated, reflected in the much lower pK_{aH} for the macrocycle. This lower pK_{aH} impacts the logD due to the percentage ionisation at pH 7.4.

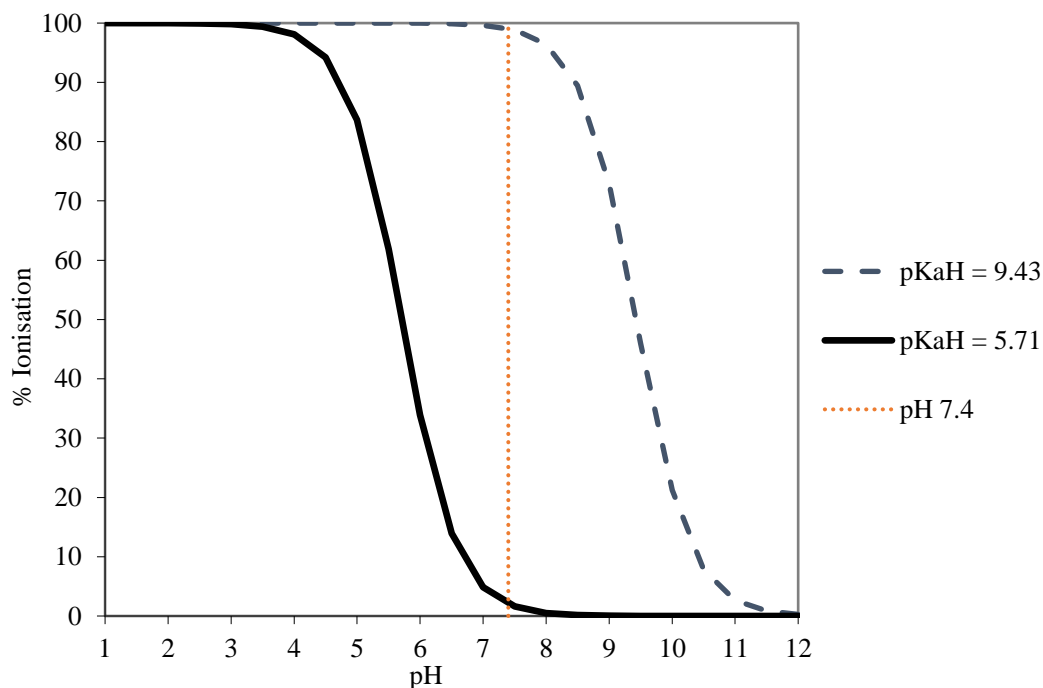


Figure 66 – The expected ionisation over a pH range, highlighting the differences in ionisation expected at pH 7.4 for compounds with measured pK_{aH} corresponding to compounds **20** and **32**.

CONFIDENTIAL – PROPERTY OF GSK – DO NOT COPY

An analysis of expected ionisation with respect to pH (Figure 66) for compounds with measured pK_{aH} of 9.13 and 7.55 shows the proportion of ionised species across a pH range. This analysis shows that at pH 7.4 compound **20** is 99.1% in the ionic form, reducing the $\log D_{pH\ 7.4}$ lipophilicity. Whereas compound **32** is only 2.0% ionised, leading to a higher measured lipophilicity. However, assuming that all the ionised form is in the aqueous phase and all the neutral form is in the organic phase, this would correspond to a difference in lipophilicity of ~ 1.7 log units. The observed difference is greater than this suggesting there are additional factors at play. Such factors could be the polarisability of the molecule and the accessibility for solvent co-ordination. The macrocycle would be expected to be less polarisable since the conformation is restricted, whereas, the acyclic compound can more easily change conformation and can therefore become more polarised and enter the aqueous phase. The macrocycle is also expected to sterically shield some potential hydrogen bond donors and acceptors within the macrocycle ring, as observed with the lowest energy conformation of compound **32** (Figure 65). This leads to an inability for water to solvate and therefore a reduced concentration in the aqueous phase. These factors combined are likely to cause the increase in lipophilicity observed.

The lipophilicity can also be incorporated into efficiency calculations to generate metrics analogous to ligand efficiency. One such measure, developed by Astex,¹³⁶ the lipophilic ligand efficiency (LLE) considers the lipophilicity of the compound, as well as the potency and number of heavy atoms. Increasing lipophilicity is generally found to increase potency, however can also negatively impact some of the other drug-like properties discussed in previous sections. Hence, increasing potency without excessively increasing lipophilicity is desired. The equation also contains scaling factors to align the desirable value for lead compounds with the standard ligand efficiency metric previously described as greater than 0.3.

$$LLE_{ASTEX} = 0.111 + 1.37 \frac{pIC_{50} - clogP}{N}$$

Equation 5 – The definition of Astex lipophilic ligand efficiency.

It was hoped that the macrocycles would show improvements in this efficiency measure, due to improvements in potency coming from entropy gains in binding rather

than increased lipophilicity. The definition of LLE uses clogP, a calculated value, which does not take into account the complex effects of macrocyclisation on lipophilicity discussed above. Therefore, this measure may not provide an accurate picture of the efficiency with respect to the true lipophilicity of the molecules at physiological pH.

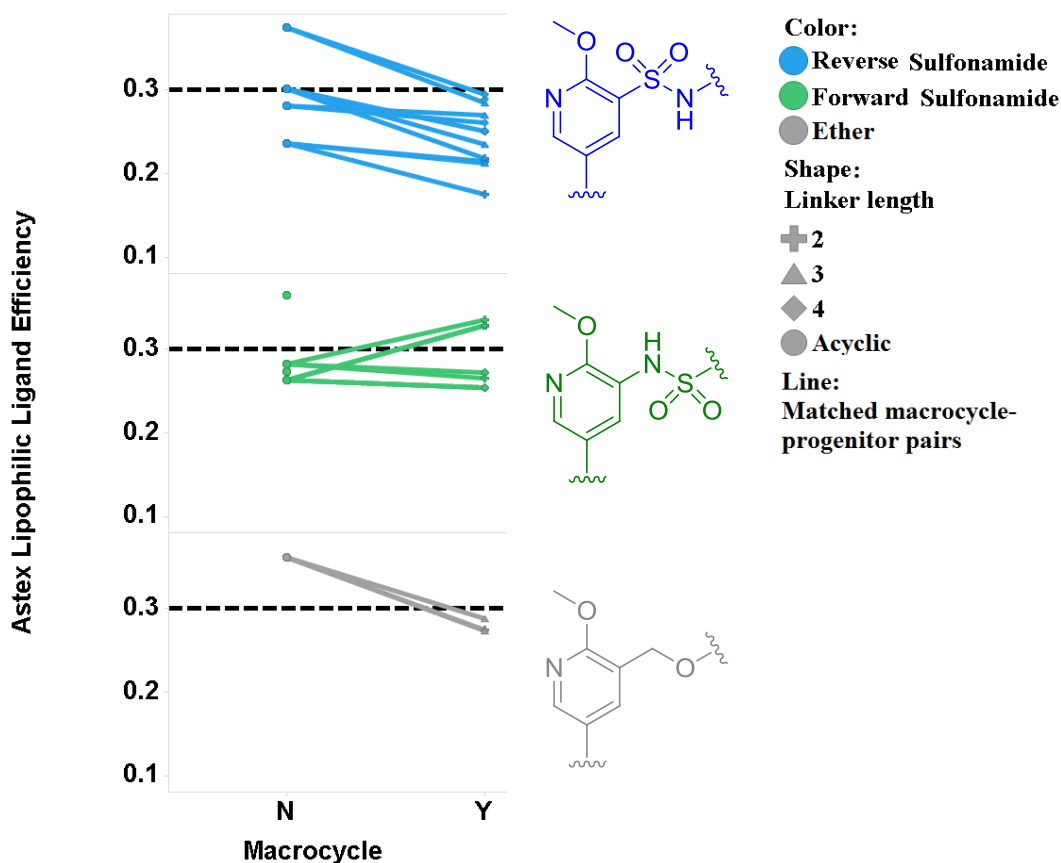


Figure 67 - A visualisation of the effect of macrocyclisation on the lipophilic ligand efficiency at PI3K δ .

In terms of lipophilic ligand efficiency, the compounds generally fall in efficiency upon macrocyclisation, with the exception of the forward sulfonamide compounds, some of which show an increase from below the threshold of 0.3 to above it.

Overall, the macrocyclic template leads to a number of changes to drug-like properties. Particularly within the forward sulfonamide series, improvements in potency and efficiency were observed. Macrocyces generally lie within similar solubility and permeability space to the progenitor compounds. Binding to plasma proteins generally

CONFIDENTIAL – PROPERTY OF GSK – DO NOT COPY

increases, however still remains within acceptable limits for both macrocycles and acyclic progenitors. Macrocyclisation appears to have little effect on *in vitro* clearance which is more reliant on chemical structure, such as orientation of the sulfonamide. However, within a pair of compounds taken into *in vivo* studies in rats, the macrocycle has significantly lower clearance than the progenitor compound. A subset of macrocycles are found to be significantly more lipophilic than would be otherwise expected, however this high lipophilicity does not translate into low solubility and high clearance. This indicates the complexity of interpretation of physicochemical properties, particularly within macrocyclic series.

Overall, these data support macrocycles as a good starting template for oral or inhaled delivery for inhibition of PI3K δ . The properties can be modulated by a number of variable groups within the macrocyclic template to generate compounds with low/high clearance, high permeability, good solubility and high potency. Therefore, macrocycles should be explored further within the PI3K δ programme.

2.4 Summary and Conclusions

In summary, flexible synthetic routes have been developed to synthesise a range of target compounds with the aim of exploring the effect of macrocyclisation on PI3K δ inhibition. A number of macrocycles have been synthesised and the biochemical potency analysed.

Macrocycles have been discovered with improved potency and comparable selectivity to progenitor compounds. This showed the potential for developing a highly potent candidate compound starting from the macrocyclic core.

The general differences in pharmacologically relevant properties between macrocycles and acyclic progenitor molecules have also been discussed. Macrocycles have been shown to be soluble and permeable, whilst sulfonamide functionality can be adjusted to generate high or low clearance compounds.

This work shows that macrocycles **32**, **77** or **99** and ether **139** would provide excellent lead-like compounds, which could likely be optimised within a lead optimisation programme to generate candidate compounds. These molecules represent an improved starting point for optimisation than acyclic sulfonamide progenitor molecule **20** (Table 24).

All of the compounds selected are more than ten times as potent as the progenitor **20**, with associated increase in LE showing this is meaningful. The compounds have similar selectivity, which could be optimised using existing knowledge from within our laboratories. The compounds are all highly soluble, permeable and have acceptable plasma protein binding. When macrocycle **32** and acyclic **20** were dosed *in vivo*, macrocycle **32** exhibited lower clearance, indicating that macrocycles may provide a good template for oral delivery of PI3K δ inhibitors.

Compound Number	20	32	77	99	139
pIC₅₀ PI3Kδ (LE)	6.2 (0.31)	7.7 (0.39)	7.7 (0.38)	7.2 (0.34)	7.2 (0.39)
Selectivity α, β, γ, -fold	20, 13, 40	126, 63, 79	32, 50, 16	16, 63, 16	13, 17, 6
logD_{pH 7.4}	1.62	4.33	2.66	2.61	3.76
CLND solubility / μM	≥ 406	≥ 331	≥ 724*	≥ 465	≥ 3935
AMP / nm s⁻¹	140	530	250	180	580
HSA / AGP binding /%	37 / 64	88 / 70	86 / 62	70 / 60	81 / 73
<i>In vivo</i> clearance t_{1/2} / h.	0.6	1.5	ND	ND	ND

Table 24 – Summary of properties of selected compounds. *solubility measured by Charged Aerosol Detection (CAD).

2.5 Further Work

The benzoxazine macrocycles explored in this thesis require further optimisation to move them from lead-like space to drug-like space, which could enable targeting for oral or inhaled delivery.

Previous work, within our laboratories, has shown that interaction with tryptophan-760 is a good strategy for generating highly potent and selective inhibitors of PI3K δ (see compound **21**, Figure 13). Therefore, introduction of known tryptophan binding groups could improve the macrocyclic benzoxazine scaffold into novel space with the combination of macrocyclic advantages and the high potency and selectivity derived from this interaction. This could be achieved by growing from the macrocyclic linker to generate compounds such as piperazine **169** or morpholine **170** (Figure 68).

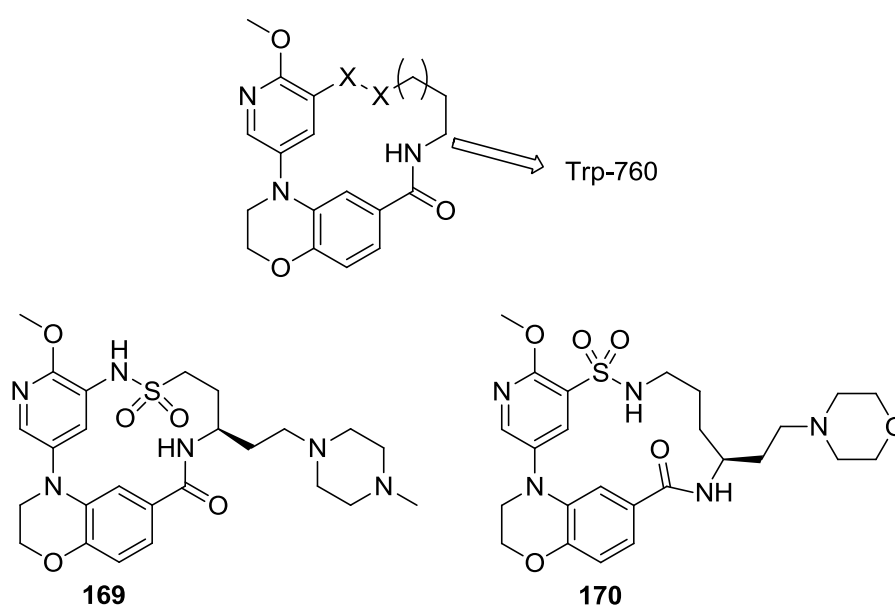


Figure 68 – An example of a compounds to combine macrocyclisation with knowledge of acyclic compounds.

Growth from the linker would provide a restricted vector directing known tryptophan binding groups, such as piperazine and morpholine, towards the selectivity pocket in PI3K δ . However, some optimisation would be required around the positioning of the saturated heterocycle and the distance from the macrocyclic scaffold.

CONFIDENTIAL – PROPERTY OF GSK – DO NOT COPY

Within the ether series, the next steps would be to synthesise compounds to explore the reason for loss of potency upon macrocyclisation. One proposal could be to design compounds with the ether group not part of the macrocycle (Figure 69).

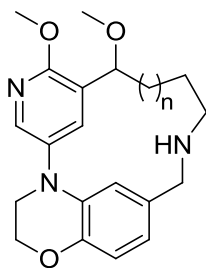


Figure 69 – The structures of compounds to explore ether binding further.

Synthesis of carbon linked ether macrocycles would explore the hypothesis that macrocyclisation forced the ether into an unfavourable conformation for participation in hydrogen bonding. It is hypothesised that the non-macrocyclic ether group will be able to make more favourable interactions with lysine-779. Optimisation of this series would allow a combination of the advantages of macrocyclisation and the advantageous properties of the ether template, compared to the sulfonamide compounds.

Chapter 3. Lactam Series

3.1 Introduction

3.1.1 Development of the Lactam Series

Work within our laboratories has identified the lactam series as another promising template to target PI3K δ (Figure 70). A number of key SAR findings emerged within early optimisation development. Firstly, the methyl group at the 3-position of the lactam core induces a twist between lactam ring and aryl ring, which was found to be important for potency. It was also found that substitution of the lactam *N*-H was not tolerated, however a range of aryl groups could be tolerated at the 4-position of the core.

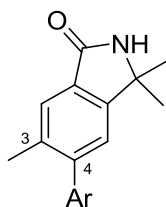


Figure 70 – The general structure of compounds within the lactam series.

An overlay of X-ray crystal structures of lactam compound **171** and benzoxazine **21** shows the similarities in the binding modes (Figure 71). The dimethyl lactam portion of the molecule occupies the back-pocket region of the kinase and the pyridine forms the hinge binding interaction with valine-828. The lactam series was also developed to interact with tryptophan-760 in an attempt to increase potency and selectivity. This binding mode is also shown in a ligand interaction diagram (Figure 72).

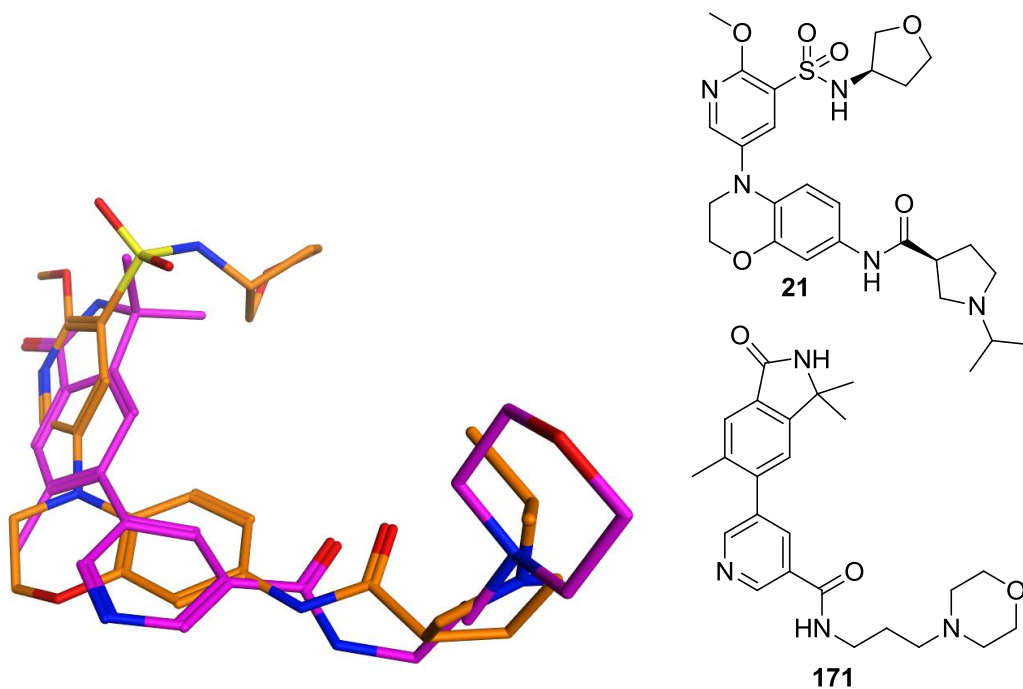


Figure 71 – An overlay of protein bound X-ray crystal structures of benzoxazine **21** (orange, 9HZDX, 2.15 Å) and lactam **171** (purple, 4MHLK, 1.86 Å).

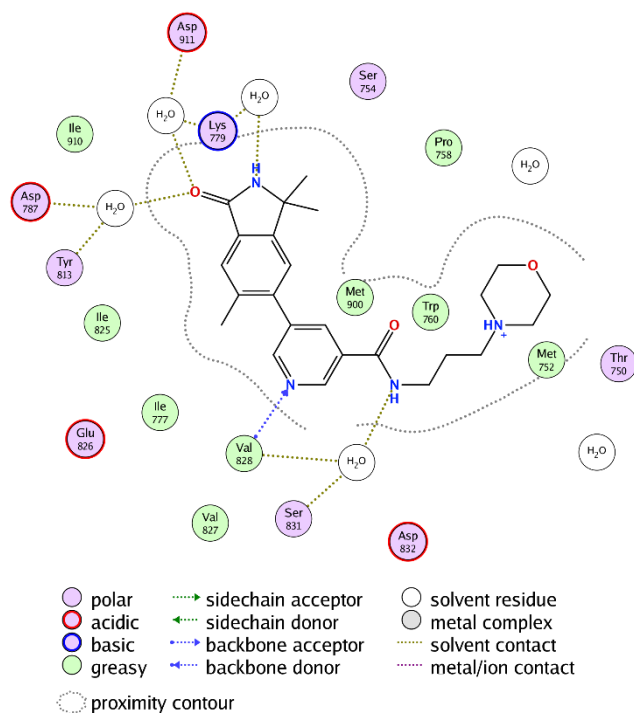
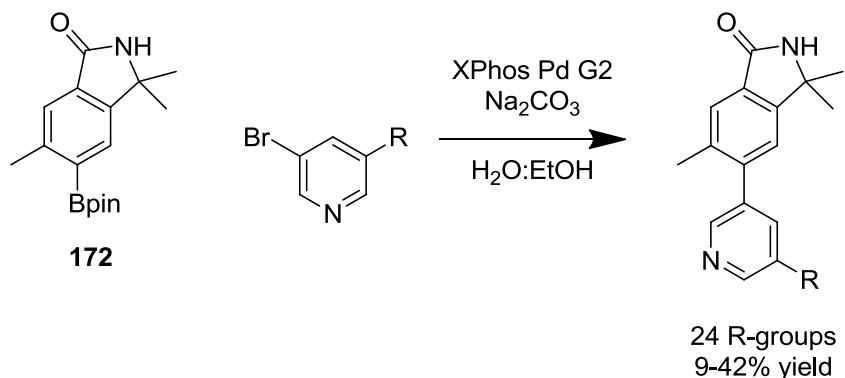


Figure 72 – Interaction diagram for lactam **171**. The following features are shown, as calculated by MOE: Hydrogen bond strengths $>1.0 \text{ kcal mol}^{-1}$, ionic bond strengths $>1.5 \text{ kcal mol}^{-1}$, residues within 4.0 \AA .

Since functionalisation at the 5-position of pyridine was found to approach tryptophan-760, a key residue for potency and selectivity, substitution at this position was investigated further. This was explored *via* an array carried out elsewhere within our laboratories (Scheme 32).¹⁴⁸



Scheme 32 – An array carried out to explore growth from pyridine 5-position in the lactam series.

A range of 5-substituted 3-bromo-pyridines were coupled to the lactam core **166** *via* a Suzuki-Miyaura cross coupling array. The results from this array identified cyclopropyl pyridine **167** (Figure 73) as a promising lead compound.

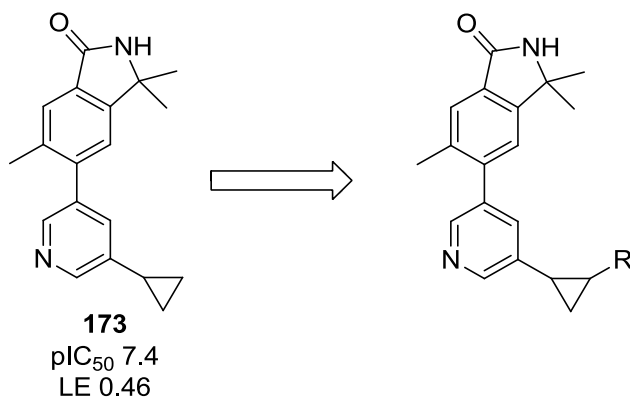


Figure 73 – A promising cyclopropyl compound identified from an array and proposal for further elaboration of this template.

It was reasoned that further elaboration of this template could be used to grow towards tryptophan-760 and could improve upon drug-likeness. Cyclopropyl rings have a number of attractive properties which makes the structure interesting for drug discovery¹⁴⁹ and this is discussed further in the following section.

3.1.2 Cyclopropyl Rings in Drug Discovery

Cyclopropyl rings are ubiquitous motifs in natural products and bioactive molecules.¹⁴⁹ The motif has been found in compounds known to affect a wide range of biological properties including enzyme inhibition, insecticidal, antibacterial, antitumor and antiviral properties.¹⁴⁹

Cyclopropyl rings are prevalent in marketed drug compounds, with eight of the 200 bestselling FDA drugs containing a cyclopropyl ring, and the cyclopropyl motif being the tenth most common ring system in all FDA approved drugs.¹⁵⁰ There are approximately 46 cyclopropyl containing drugs currently on the market indicating the functionality does not contain innate toxicity, mutagenicity or other undesirable medicinal properties.

There are several compelling reasons for introducing cyclopropyl groups in drug discovery efforts. These include increased metabolic stability, chemical stability, providing a constrained growth vector, and as an isostere for alkenes, phenyl rings, methyl or *iso*-propyl groups. Some examples of which are discussed in the following section.

One such drug is Montelukast **174**, an oral leukotriene receptor antagonist used in treatment of asthma. This molecule contains a 1,1-disubstituted cyclopropyl ring. This was introduced at a methylene position to reduce liver toxicity associated with peroxisomal enzyme induction (PEI). This enzyme oxidises the *beta*-position on carboxylic acids; prevention of which resulted in reduced liver toxicity.¹⁵¹

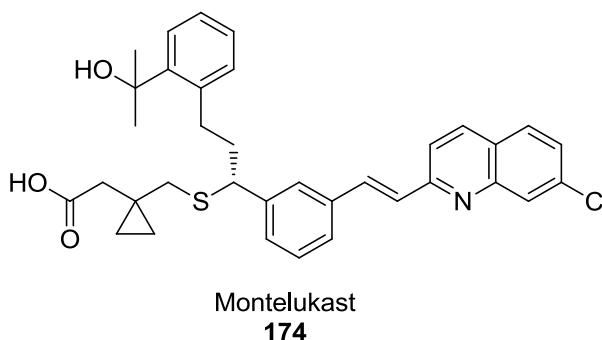


Figure 74 - Montelukast **174**, an approved drug for treatment of asthma.

CONFIDENTIAL – PROPERTY OF GSK – DO NOT COPY

In development of Polo-like kinase 4 (PLK4) inhibitors Sampson *et al.* have shown that the cyclopropyl ring can act as an alkene bio-isostere (Figure 75).¹⁵² Initial hit alkene **175** was found to have poor pharmacokinetic properties and the enone was found to isomerise yielding *E/Z* mixtures *in vivo*. Hence, the alkene was replaced with a cyclopropane. This analogue **176** showed similar potency and increased solubility, rationalised by the cyclopropyl ring disrupting π -stacking of the aromatic ring systems. The molecules were also found to be stable to isomerisation *in vivo* and thus an orally bioavailable analogue **177** could be developed.¹⁵² Analysis of binding modes generated from docking of analogues showed the conformational similarity of these structures.¹⁵²

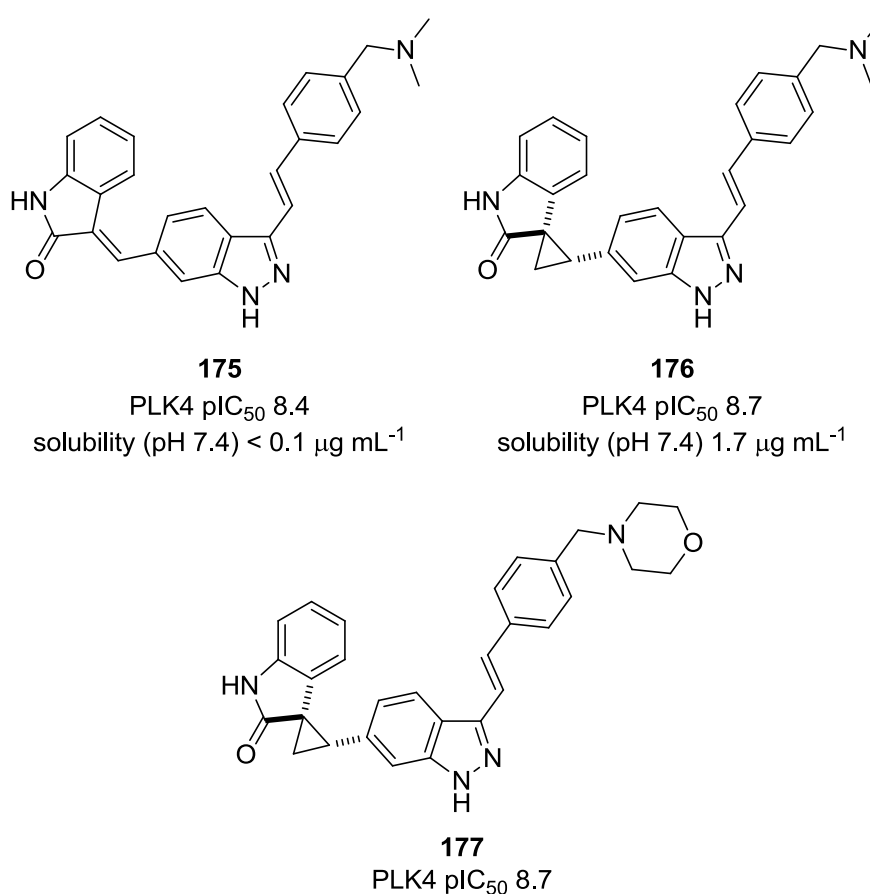


Figure 75 - Development of PLK4 inhibitors by replacement of an alkene with a cyclopropyl ring.

Abe *et al.*¹⁵³ have shown that a cyclopropyl ring can act as a phenyl isostere. Development of mitogen-activated protein kinase (MEK) inhibitors started with highly lipophilic phenyl substituted pyridopyrimidine core **178**. However, upon replacement

of a phenyl ring with a cyclopropyl ring **179**, an increase in potency and concurrent decrease in lipophilicity was observed. This was further developed into marketed drug trametinib **180**, licensed for the treatment of metastatic melanoma.

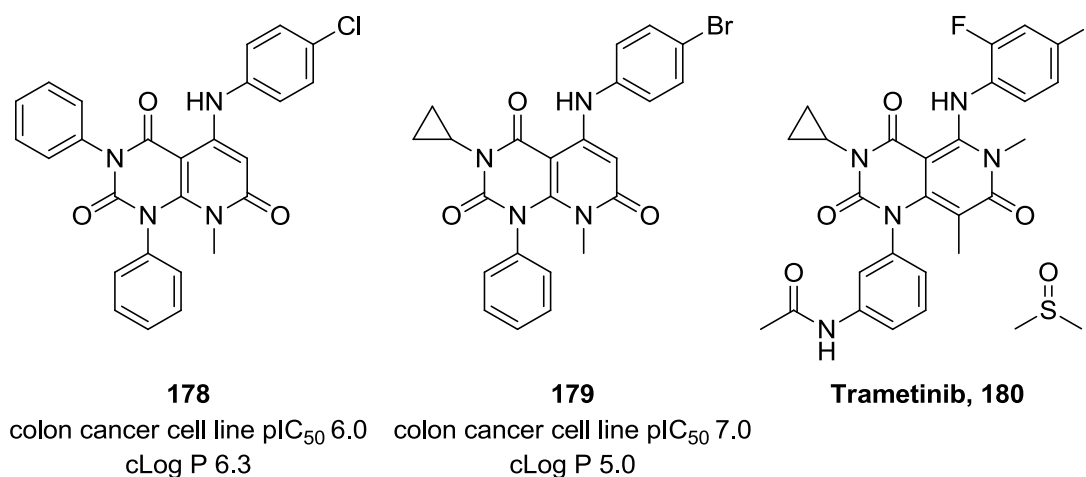
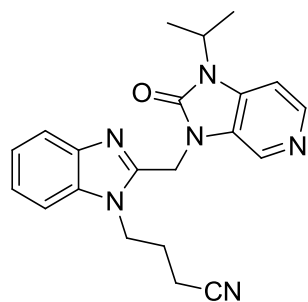


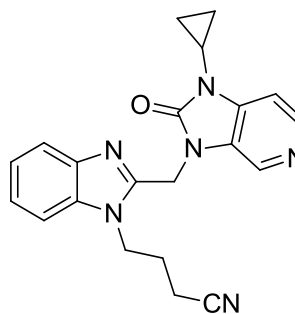
Figure 76 - Development of MEK inhibitors by replacement of a phenyl ring with a cyclopropyl ring.

A cyclopropyl ring is also predicted to have increased metabolic stability over methyl or *iso*-propyl analogues.¹⁴⁹ This is due to the increased C-H bond enthalpy in cyclopropane (106 kcal mol⁻¹) compared to ethane (101 kcal mol⁻¹)¹⁵⁴ and is exemplified in development of Respiratory Syncytial Virus (RSV) fusion inhibitors. Development of benzimidazole based structures showed significant variation in microsomal clearance upon modification of *iso*-propyl **181** to cyclopropyl **182** (Figure 77).¹⁵⁵



181

Human Liver Microsomes $t_{1/2}$ 7.4 mins



182

Human Liver Microsomes $t_{1/2}$ 39 mins

Figure 77 - The influence of replacing an iso-propyl with a cyclopropyl on clearance in a series of RSV fusion inhibitors.

In summary, cyclopropyl rings are attractive motifs in drug discovery with benefits including increased potency, increased chemical and metabolic stability, increased solubility and reduced lipophilicity. Due to the interest in cyclopropyl rings as structures in natural products, drugs and intermediates in synthesis, a number of syntheses have been developed and a brief precis of these is given in the following section.

3.1.3 Synthesis of Cyclopropyl Rings

The general strategy for cyclopropane synthesis consists of disconnection of two cyclopropyl bonds to give alkene and carbene type synthons (Figure 78). An overview of a selection of methods for synthesis are given below.

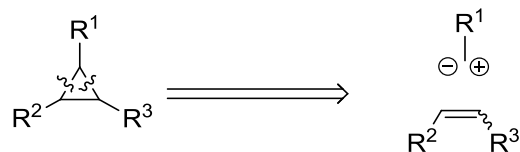
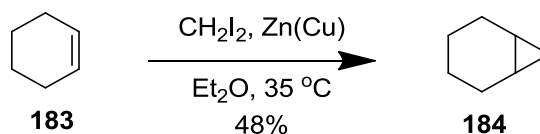


Figure 78 - General disconnection strategy for synthesis of cyclopropyl rings.

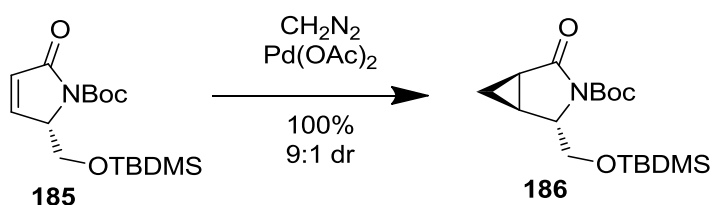
These include a Simmons-Smith cyclopropanation,¹⁵⁶ where an alkene is transformed into a cyclopropane using a zinc source in the presence of an alkyl dihalide species (Scheme 33). The alkyl dihalide undergoes oxidative addition to the zinc generating a zinc-carbenoid species which can undergo addition to the alkene. The reaction has been developed into diastereoselective¹⁵⁷ and catalytic enantioselective^{158,159} variants. However, the reaction is limited by the modularity of the process restricting the applicability for library synthesis.

Simmons-Smith:



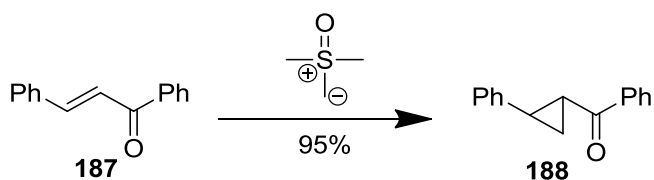
Scheme 33 - The original report of the Simmons-Smith Cyclopropanation.

An alternative method is metal-catalysed decomposition of diazo-compounds (Scheme 34).¹⁶⁰ In this reaction a diazo-compound is activated to form a metal-carbenoid complex, releasing nitrogen. The metal-carbenoid can then undergo addition to the alkene in a similar manner to the zinc-carbenoid species. However, the requirement for unstable diazonium species is a drawback of this procedure.



Scheme 34 – An example of a palladium catalysed cyclopropanation using diazomethane.

Corey-Chaykovsky cyclopropanation is another widely utilised cyclopropanation methodology (Scheme 35).^{161,162} Here, a sulfur ylide is added to an electron poor alkene and subsequent displacement of dimethyl sulfoxide yields a cyclopropane. However the requirement for an electron poor alkene limits the scope of the reaction to mainly carbonyl substituted alkenes.¹⁶³



Scheme 35 – The original report of the Corey- Chaykovsky Cyclopropanation.

Development of a synthesis of substituted cyclopropanes with a functional handle for ease of derivatisation was therefore sought. This would allow synthesis of a wide range of derivatives and lends itself to a modular approach for exploration of chemical space in the context of a medicinal chemistry lead optimisation effort. Access to a wide range of cyclopropyl rings with a functional handle would enable facile incorporation of cyclopropyl rings into drug-like molecules. Hence, a range of functional groups were considered for incorporation and boronic esters were selected for further study.

3.1.4 Synthetic Utility of Boronic Esters

The functional group of choice was a pinacol boronic ester; the synthetic utility of pinacol boronic esters and the range of transformations possible from this functional group are very well established (Figure 79).^{164,165}

Boronic ester functionality can be converted into alcohol functionality by use of basic hydrogen peroxide.¹⁶⁶ Amines can be synthesised by addition of lithiated methoxylamine,¹⁶⁷ while protodeborylation can be initiated by addition of aqueous fluoride.¹⁶⁸ Aryl boronic esters can also be halogenated by addition of electrophilic halide sources such as Selectfluor®¹⁶⁹ or *N*-halosuccinamides.¹⁷⁰

A wide range of cross-coupling reactions employ boronic esters as coupling partners, such as the Suzuki-Miyaura¹⁷¹⁻¹⁷³ or Chan-Evans-Lam¹⁷⁴⁻¹⁷⁶ couplings. Boronic esters are also reagents in the Petasis reaction, where an amine, a carbonyl compound and a boronic ester are reacted to form tertiary amine products.¹⁷⁷

A number of recent protocols have been developed for homologation of boronic ester functionality with many chiral variants existing.¹⁷⁸⁻¹⁸⁰

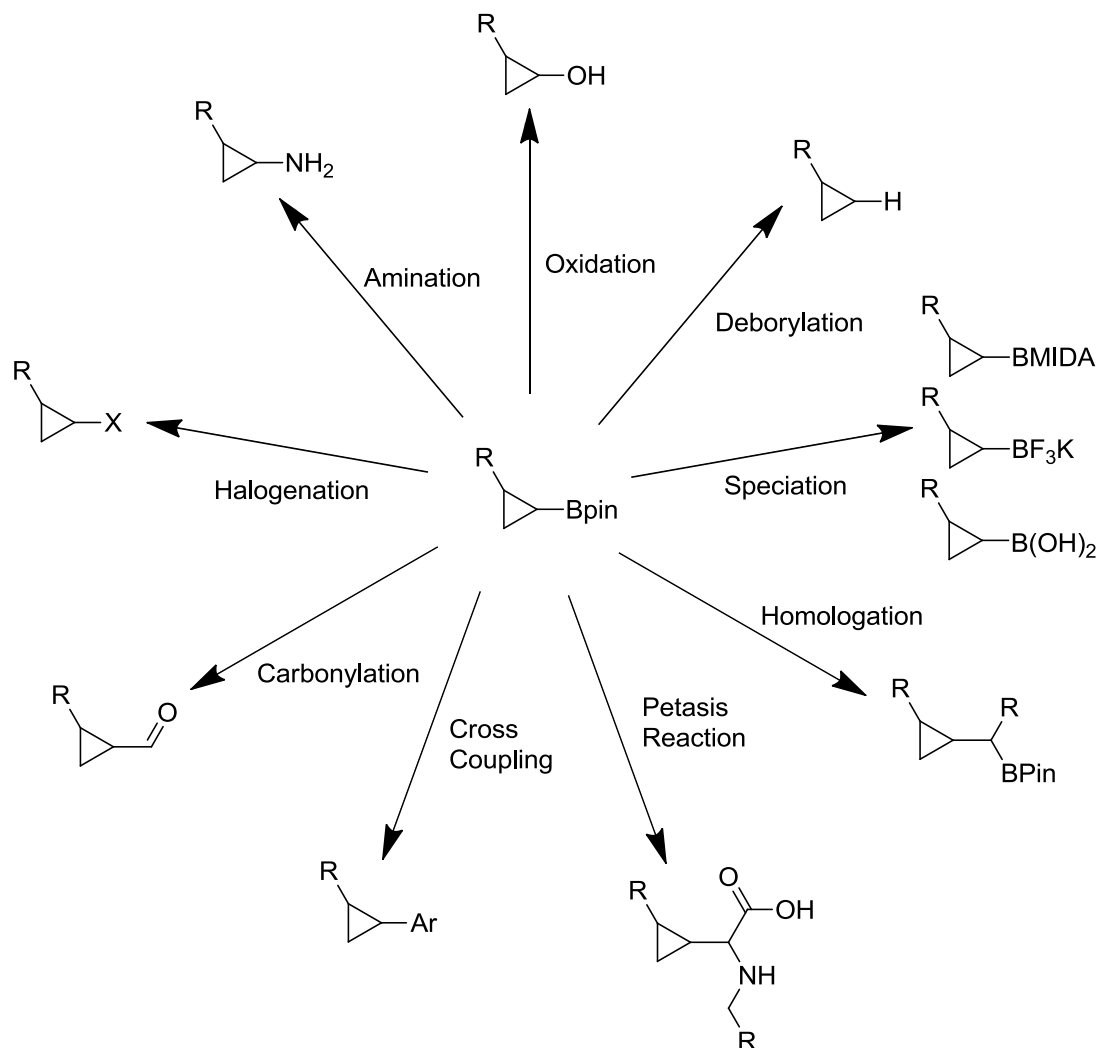


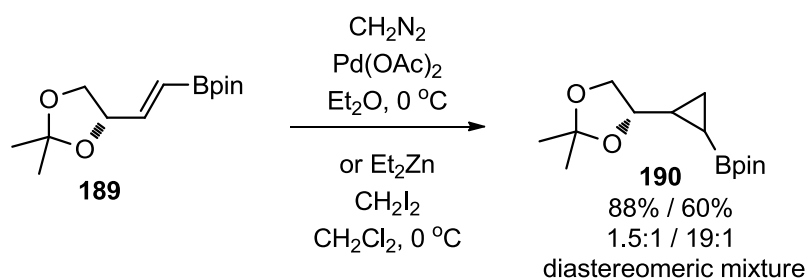
Figure 79 - A selection of possible reactions of cyclopropylboronic acid pinacol esters.

Based on all of the above, introduction of boronic ester functionality to cyclopropyl ring building blocks was an attractive strategy to access a diverse range of cyclopropyl ring containing structures and the syntheses of cyclopropylboronic esters have been explored further in this thesis.

3.1.5 Synthesis of Cyclopropylboronic Esters

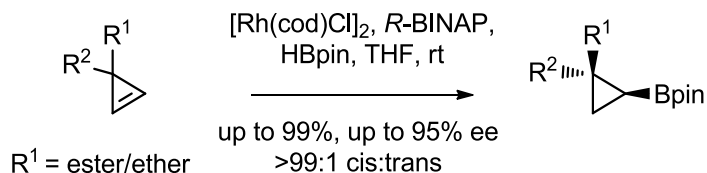
There are a small number of syntheses of cyclopropylboronic ester functionality in the literature.

Firstly, subjecting a vinyl pinacol boronic ester to a Simmons-Smith cyclopropanation or Pd-catalysed diazomethane addition (Scheme 36).¹⁸¹ This method highlights the stability of pinacol boronic ester functionality to organometallic reagents. However, there are few examples of this strategy and therefore other methods have been developed.



Scheme 36 - Synthesis of cyclopropyl boronic ester functionality by subjecting a vinylic boronic ester to cyclopropanation methodology.

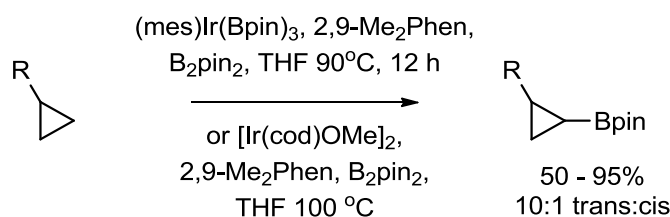
An alternative strategy involves subjecting a cyclopropene ring to a hydroboration.¹⁸² This method was further developed by Gevorgyan into an enantioselective variant, by using a chiral rhodium catalyst (Scheme 37).¹⁸³ However diastereoselectivity and enantioselectivity relies upon presence of an ester or ether directing group, which limits the applicability of the reaction to a narrow range of substrates. The requisite cyclopropene starting material also requires a multi-step synthesis involving cyclopropanation of acetylene derivatives and then multiple functional group interconversions.



Scheme 37 - Synthesis of cyclopropyl boronic ester functionality by hydroboration of cyclopropene functionality.

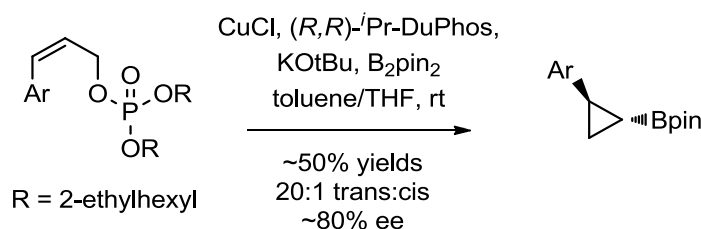
CONFIDENTIAL – PROPERTY OF GSK – DO NOT COPY

Hartwig *et al.* have developed a C-H activation borylation of cyclopropyl rings (Scheme 38).¹⁸⁴ The authors show that it is possible to selectively borylate cyclopropyl C-H bonds, with steric demands of the catalyst providing *trans* selectivity for the reaction. However, there are no examples with aryl substituents, presumably due to these groups borylating preferentially under the reaction conditions. Also, the reaction must be carried out under argon using glove box conditions, which limits the applicability within a medicinal chemistry setting. Also, optimal yields require use of the non-commercial (mesitylene)Ir(Bpin)₃, which requires a two-step synthesis,¹⁸⁵ again using glove box conditions.



Scheme 38 – C-H borylation of cyclopropyl rings developed by Hartwig.

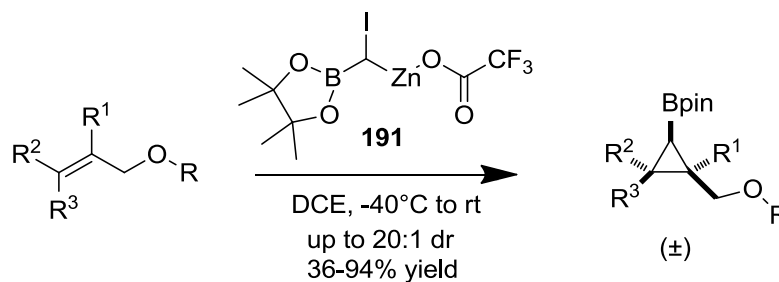
Conditions developed by Ito allow an asymmetric copper(I) catalysed borylation cyclisation (Scheme 39).¹⁸⁶ The proposed mechanism involves formation of a copper-Bpin species, which adds across the alkene in an enantioselective manner and the resulting organocopper species cyclises onto the phosphate leaving group yielding a cyclopropylboronic ester. The enantioselectivity of this methodology makes it particularly attractive, as well as the ability to construct the cyclopropyl ring and add the boron species in one reaction manifold. However, the complexity of the starting material required and the need for an aryl substituent are limitations for the utility of this reaction.



Scheme 39 – Asymmetric copper catalysed borylation-cyclisation developed by Ito.

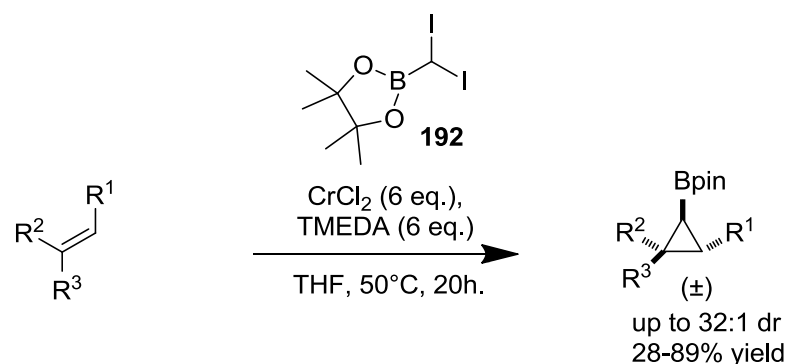
CONFIDENTIAL – PROPERTY OF GSK – DO NOT COPY

Charette *et al.* have developed a modified Simmons-Smith reagent to introduce a boron containing carbenoid to alkenes (Scheme 40).¹⁸⁷ The reaction enables synthesis of cyclopropyl rings substituted with up to three additional groups. Presence of an ether group is not necessary, however provides increased diastereomeric ratio and overall yield. The main problems with this reaction manifold are the requirement for a three-step synthesis of the zinc reagent. However, the reaction does form the cyclopropyl ring and introduce the boron species in one step. ±



Scheme 40 – Modified Simmons-Smith reaction developed by Charette.

Recently, a synthesis has been developed by Takai *et al.* using chromium to promote a borylcyclopropanation with diiodomethylene derivatives (Scheme 41).¹⁸⁸



Scheme 41 – Chromium-promoted cyclopropanation developed by Takai.

In this reaction methodology, diiodomethylboronate ester is converted into a chromium carbenoid, which facilitates the cyclopropanation. The reaction works well for both electron poor and electron rich alkenes. However, selectivity is derived from sterics meaning that high selectivities are only obtained with *Z*-alkenes and mono- or geminal- substituted alkenes give poor selectivity. The diiodomethylboronate ester reagent requires a three-step synthesis under cryogenic conditions, however, the

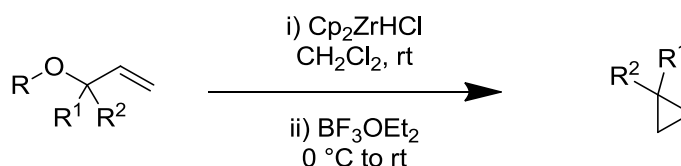
alkene starting materials are tractable. The reaction also requires a large excess of moderately expensive chromium(II) chloride.

In summary, there are a limited number of cyclopropylboronic ester syntheses present in the literature. However, current methods are restricted by scope, modularity, starting material tractability, reagent/catalyst availability, or a combination of these factors. Hence, there are opportunities to develop novel cyclopropyl boronic ester syntheses to address one or more of these problems.

Therefore, the aim of this work was to develop a novel synthesis of cyclopropylboronic esters, which would be practical to conduct as part of the PI3K δ drug discovery programme. Ideally, the synthesis would use commercial reagents, readily tractable starting materials, non-glove box conditions and be able to generate a range of interesting products for medicinal chemistry. It should then be facile to incorporate the products into the lactam series of PI3K δ inhibitors, as well as within other medicinal chemistry programmes to explore introduction of cyclopropyl rings into drug-like compounds.

3.1.6 Strategy for Novel Cyclopropylboronic Ester Synthesis

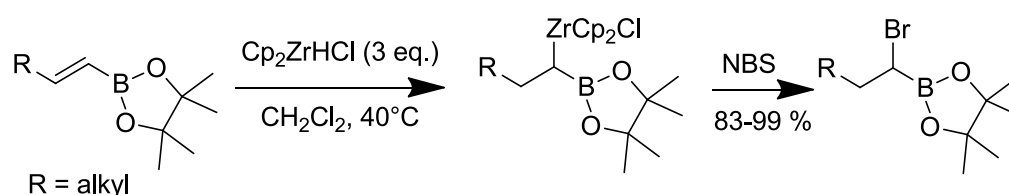
Initial work to develop a novel cyclopropyl boronic ester synthesis focused on the Szymoniak cyclopropanation (Scheme 42).¹⁸⁹



Scheme 42 – Cyclopropanation methodology developed by Szymoniak.

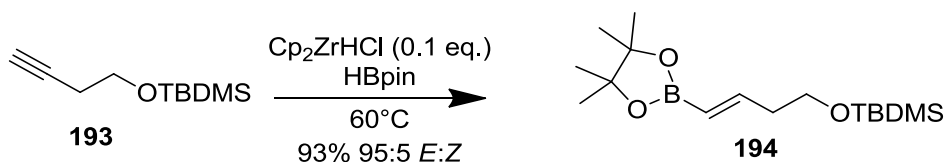
This method uses Schwartz's Reagent followed by the addition of a Lewis acid to mediate the cyclisation. It was anticipated that this methodology could be extended to synthesise boronic esters for a number of reasons.

Firstly, it has been shown that *gem*-borazirconocene complexes can be utilised in synthesis and, indeed can be isolated and characterised (Scheme 43).^{190,191}



Scheme 43 – Use of *gem*-borazirconocene complexes to synthesise α -haloboronic esters.

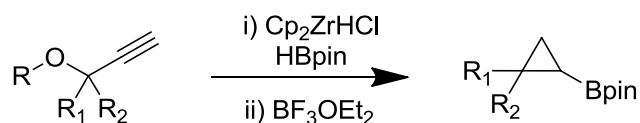
Srebnik *et al.*¹⁹⁰ report that a vinyl boronic ester can undergo hydrozirconation leading to an isolable and characterisable intermediate, which has been further reacted with *N*-bromosuccinimide to yield α -haloboronic esters. Whilst this work shows the potential for incorporating boronic esters into Schwartz's Reagent mediated processes, it also highlights the forcing conditions required for the hydrozirconation.



Scheme 44 – Preparation of vinyl boronic esters using a catalytic amount of Schwartz's Reagent.

CONFIDENTIAL – PROPERTY OF GSK – DO NOT COPY

Secondly, Srebnik *et al.*¹⁹² and Wang *et al.*¹⁹³ have shown that terminal alkynes can be converted into vinyl boronic esters by treatment with a catalytic amount of Schwartz's Reagent and pinacol borane (Scheme 44).

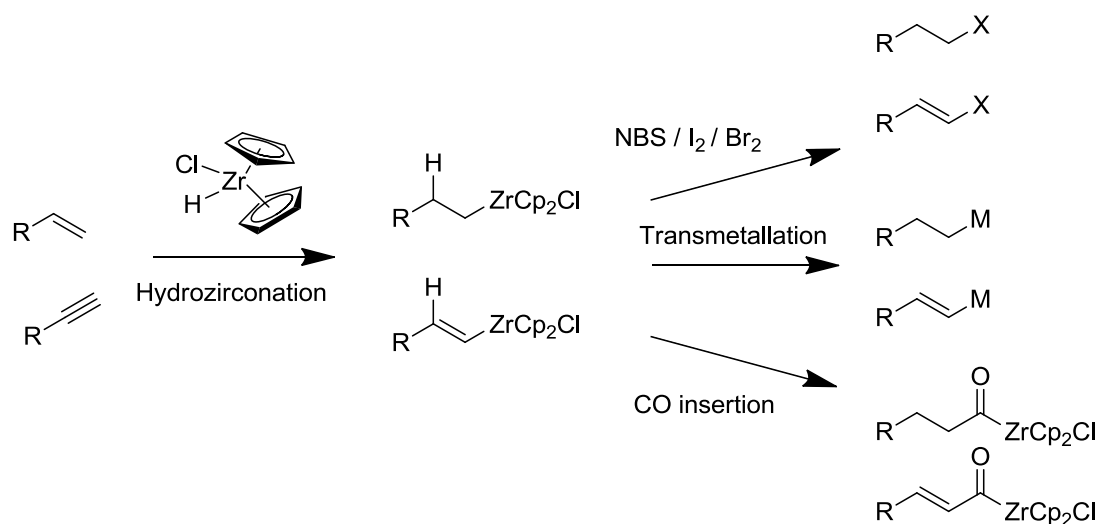


Scheme 45 – Hypothesised reaction to allow conversion of propargylic ethers into cyclopropyl boronic esters.

It was therefore proposed that an alkyne could undergo Schwartz's Reagent catalysed hydroboration to generate an intermediate vinyl boronic ester; which after subsequent hydrozirconation and Lewis acid mediated cyclisation would yield the desired cyclopropyl boronic ester (Scheme 45). This proposed reaction was therefore explored further.

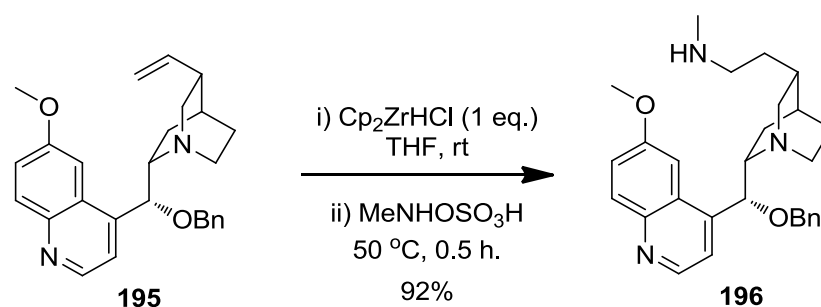
3.1.7 Use of Schwartz's Reagent in Synthesis

Use of Schwartz's Reagent is an established method for alkene and alkyne activation *via* a hydrozirconation to form an organozirconium species.¹⁹⁴ The resulting complex can then be transformed using various reactions (Scheme 46) such as addition to an electrophile¹⁹⁵⁻¹⁹⁷ or transmetalation.¹⁹⁸⁻²⁰⁰ This allows alkenes or alkynes to be considered as a precursor for alkyl or vinyl organometallics.



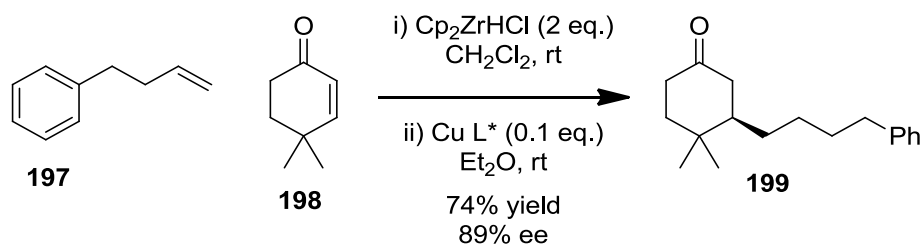
Scheme 46 – An illustration of the typical reactivity of Schwartz's Reagent.

This reactivity has been utilised in the development of a number of methodologies utilising Schwartz's Reagent. A recent example developed by Hartwig *et al.* employs an initial hydrozirconation, followed by addition of an electrophilic nitrogen reagent to facilitate an amination¹⁹⁷ and has been successfully applied to cinchona alkaloids (Scheme 47).



Scheme 47 – Methodology developed by Hartwig utilising Schwartz's Reagent to enable an anti-Markovnikov hydroamination.

Fletcher *et al.* have also developed chemistry with Schwartz's Reagent (Scheme 48). In this methodology, hydrozirconation is followed by transmetalation to a chiral copper species and addition into a Michael acceptor.²⁰⁰



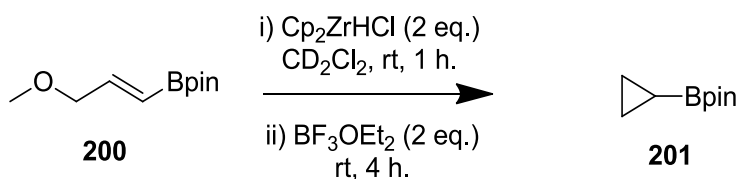
Scheme 48 – Methodology developed by Fletcher utilising Schwartz's Reagent to enable an enantioselective Michael addition.

With an established precedence of Schwartz's Reagent in the literature, it was thought that the reagent could be utilised for a novel synthesis of cyclopropylboronic esters.

3.2 Results and Discussion

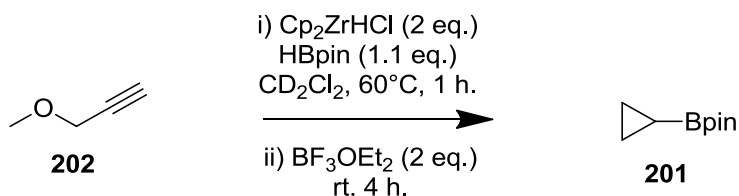
3.2.1 Optimisation of Reaction Conditions

Initial proof of concept studies were carried out using simple substrates to synthesise the commercially available cyclopropylboronic ester **201**. Reactions were run in deuterated solvent to allow facile analysis of reaction milieu. The crude NMR spectra were then compared to that of the product purchased from commercial suppliers. Initially, the reaction was explored starting with a vinyl boronic ester with the hope that the borylation step could be incorporated in future reactions.



Scheme 49 – Initial proof of concept experiment showing conversion of a vinyl boronic ester to a cyclopropyl boronic ester.

Conversion of vinyl boronic ester **200** to trace amounts of product **201** was achieved by utilising Szymoniak-type conditions (Scheme 49). Hence, the reaction manifold was then further extended to include the borylation step.



Scheme 50 – Proof of concept experiment showing conversion of a propargylic ether to a cyclopropyl boronic ester.

Conversion to product **201** was also observed when Schwartz's Reagent catalysed hydroboration was combined into a one-pot procedure from the appropriate alkyne **202** (Scheme 50). This showed the feasibility of this transformation and prompted an optimisation campaign to be undertaken.

CONFIDENTIAL – PROPERTY OF GSK – DO NOT COPY

Quantitative NMR was selected to quantify product formation, since the cyclopropyl protons should be distinct from other protons in the molecule. Conversion to product was analysed with reference to 1,4-bis(trimethylsilyl)benzene.

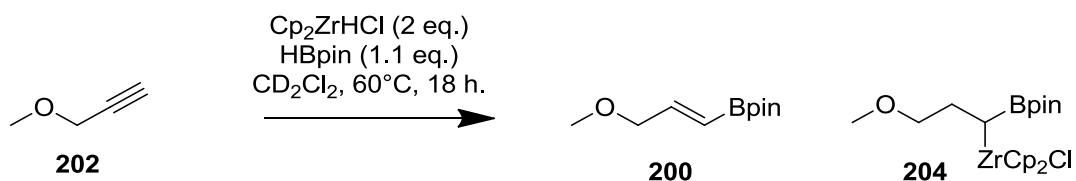


Figure 80 – Reaction conducted without addition of Lewis acid to probe conversion and selectivity of the first reaction step.

Initial analysis of the reaction mixture upon completion of the first hydroboration step showed a complex mixture with only a small proportion of peaks corresponding to expected reaction intermediates **200** and **204** (Figure 80). It was suggested that the remaining material could be made up of other species formed due to overreaction with Schwartz's Reagent (Figure 81). Indeed, double hydrozirconation products are proposed in the literature as intermediates in alkyl-zirconium rearrangements.²⁰¹

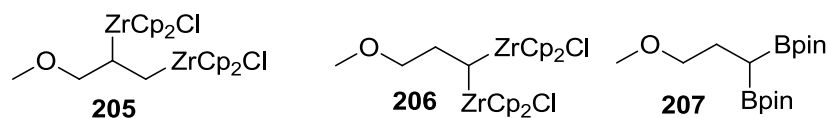


Figure 81 – Proposed off pathway intermediates caused by super stoichiometric Schwartz's Reagent.

It was thought that these overreaction products could be prevented by using the catalytic method described by Wang.¹⁹³ Full consumption of pinacol borane and low concentrations of Schwartz's Reagent could yield a higher conversion to intermediate **200**. Additional Schwartz's Reagent could then be added after completion of the hydroboration step to facilitate further hydrozirconation.

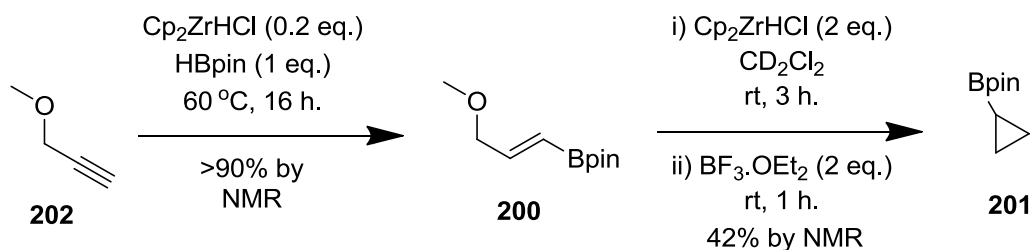
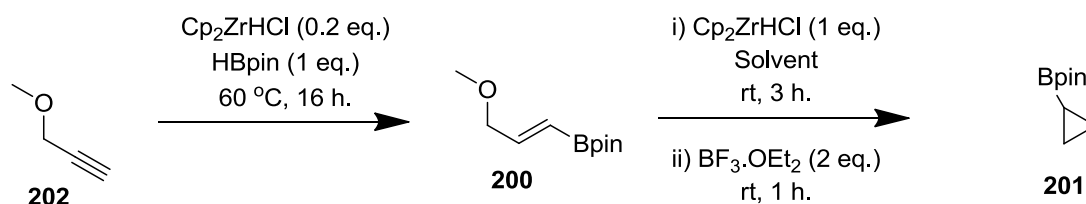


Figure 82 – Separation of initial step to minimise overreaction products with excess Schwartz’s Reagent.

The initial step was therefore hyphenated into a catalytic hydroboration step, followed by a stoichiometric hydrozirconation step (Figure 82). Analysis of an aliquot of the reaction mixture showed greater than 90% conversion to the expected vinyl boronic ester species **200**. When this material was advanced to the next steps of the reaction, a 42% conversion to the expected product **201** was observed. Therefore, subsequent work was focused on optimisation of the second hydrozirconation step and the Lewis acid cyclisation step.

The first parameter explored was solvent; since the first step is run neat in pinacol borane, any solvent could be added. Dichloromethane is the most common solvent for Schwartz’s Reagent mediated reactions in the literature and was hence selected. Tetrahydrofuran is also a common solvent in these processes and has been shown to have fast reaction times in hydrozirconation processes.²⁰² In addition, benzene is another solvent with precedence for use in hydrozirconation reactions, however was substituted for toluene and chlorobenzene in this study due to safety concerns associated with the use of benzene.²⁰³

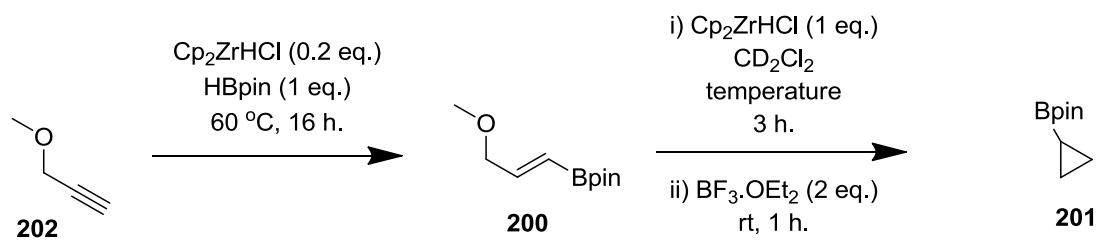


Entry	Solvent	% intermediate, 200	% product, 201
1	$\text{d}_2\text{-DCM}$	21	43
2	$\text{d}_8\text{-THF}$	0	0
3	$\text{d}_8\text{-Toluene}$	0	40
4	Chlorobenzene ^a	0	0

Table 25 – Solvent screening carried out on simplest cyclopropyl boronic ester synthesis reaction. ^aDeuterated solvent was not available, hence the solvent was evaporated and the residue redissolved in deuterated dichloromethane.

Analysis of NMR samples of the reactions (Table 25) showed that dichloromethane led to the highest conversion to expected product **201** and a significant quantity of on-pathway intermediate **200** remaining. THF (entry **2**) led to no formation of expected product **201** and this is hypothesised to be due to the Lewis basic oxygen of THF coordinating to the Lewis acidic boron trifluoride. Toluene (entry **3**) gave slightly reduced conversion to expected product, however no on pathway intermediates appeared to be remaining, indicating a poorer by-product profile. No product was observed in the chlorobenzene reaction (entry **4**), however the need to evaporate solvent (boiling point $131\text{ }^\circ\text{C}$)²⁰⁴ and the volatility of product **201** (boiling point $146\text{ }^\circ\text{C}$)²⁰⁵ may have led to product losses. Dichloromethane (entry **1**) was selected as it gave the highest conversion to product, whilst also containing intermediate **200** which could be converted to product with additional optimisation.

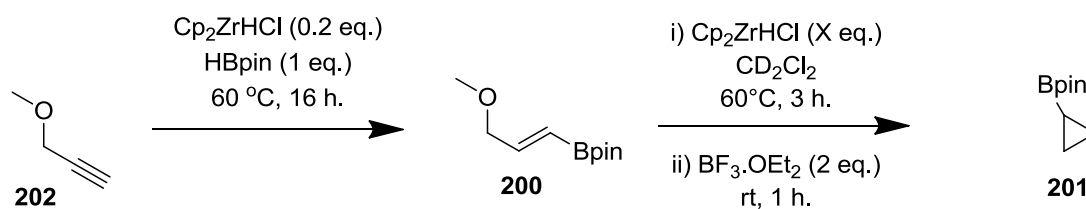
Optimisation was then carried out in an effort to increase conversion of intermediate **200** to product **201**. It was postulated that the steric bulk of pinacol boronic ester was hindering approach of Schwartz's Reagent to intermediate **200**. The initial hypothesis was to increase the temperature, a range from $0\text{ }^\circ\text{C}$ to $60\text{ }^\circ\text{C}$ was selected.



Entry	Temperature / $^\circ\text{C}$	% intermediate, 200	% product, 201
1	0	92	1
2	20	83	5
3	40	75	11
4	60	61	24

Table 26 – Temperature Screening for hydrozirconation step.

It was found that higher temperatures promoted formation of the desired cyclopropyl product **201**. However, $60\text{ }^\circ\text{C}$ (entry **4**) was the highest practical temperature for heating of dichloromethane in a sealed tube. Hence, an alternative strategy for increasing conversion to desired product **201**, exploring the stoichiometry of Schwartz's Reagent was investigated (Table 27).



Entry	Equivalents of Schwartz's Reagent	% intermediate, 200	% product, 201
1	1.0 ^a	75	1
2	1.0	66	3
3	1.3	46	19
4	1.5	36	27
5	1.7	30	36
6	2.0	23	39
7	3.0	4	50

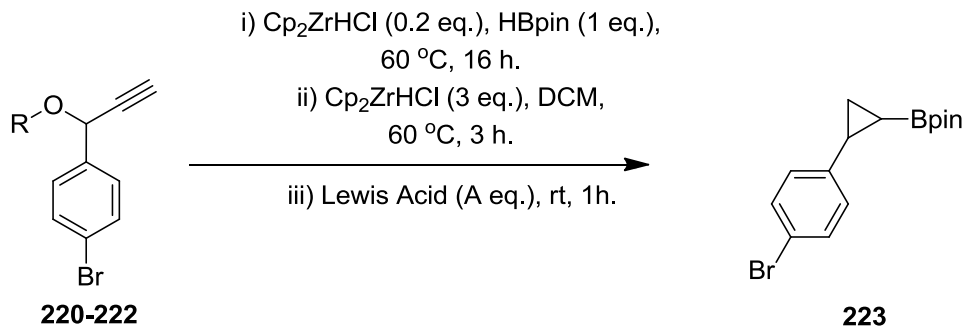
Table 27 – Equivalents of Schwartz's Reagent screening. ^aSchwartz's Reagent was synthesised according to literature procedure.²⁰⁶

The results of this study showed that increasing equivalents of Schwartz's Reagent led to increased conversion from intermediate **200** to product **201**. Accordingly, three equivalents (entry **7**) were selected as the best conditions tested. This is consistent with the observation by Srebnik, that multiple equivalents of Schwartz's Reagent are required to hydrozirconate a vinyl boronic ester.¹⁹¹ The number of equivalents was not increased further, since conditions using a vast excess of reagent were not thought to be synthetically valuable.

Next, the nature of the leaving group was explored. Leaving groups reported by Szymoniak¹⁸⁹ (OMe and OBn) as well as a number of others were selected and screened (Table 28).

CONFIDENTIAL – PROPERTY OF GSK – DO NOT COPY

to stabilise α -anions²⁰⁷ by accepting electron density into the silicon-carbon σ^* -orbital renders the silyloxy a competent leaving group. The successful methoxy, benzyloxy and silyloxy leaving groups were then applied to more complex systems **220-222** (Table 28).



Entry	R =	Product% (<i>cis:trans</i>)
1	Me	0
2	Bn	0
3	TBDMS	61 (1.7:1)

Table 29 – Application of methodology to bromophenyl derivative.

Application of the conditions optimised for the synthesis of cyclopropyl boronic ester **223**, showed that only the silyl ether leaving group (entry **3**) provided product in 61% yield. Surprisingly, methyl and benzyl ethers (entries **1** & **2**) were found to give no conversion to expected product. Results from this more complex substrate also gave the first indication of diastereoselectivity for the reaction with a slight preference for the *cis*-product **223** observed.

It was hypothesised that there could be several possible origins of this diastereomeric mixture (Figure 83).

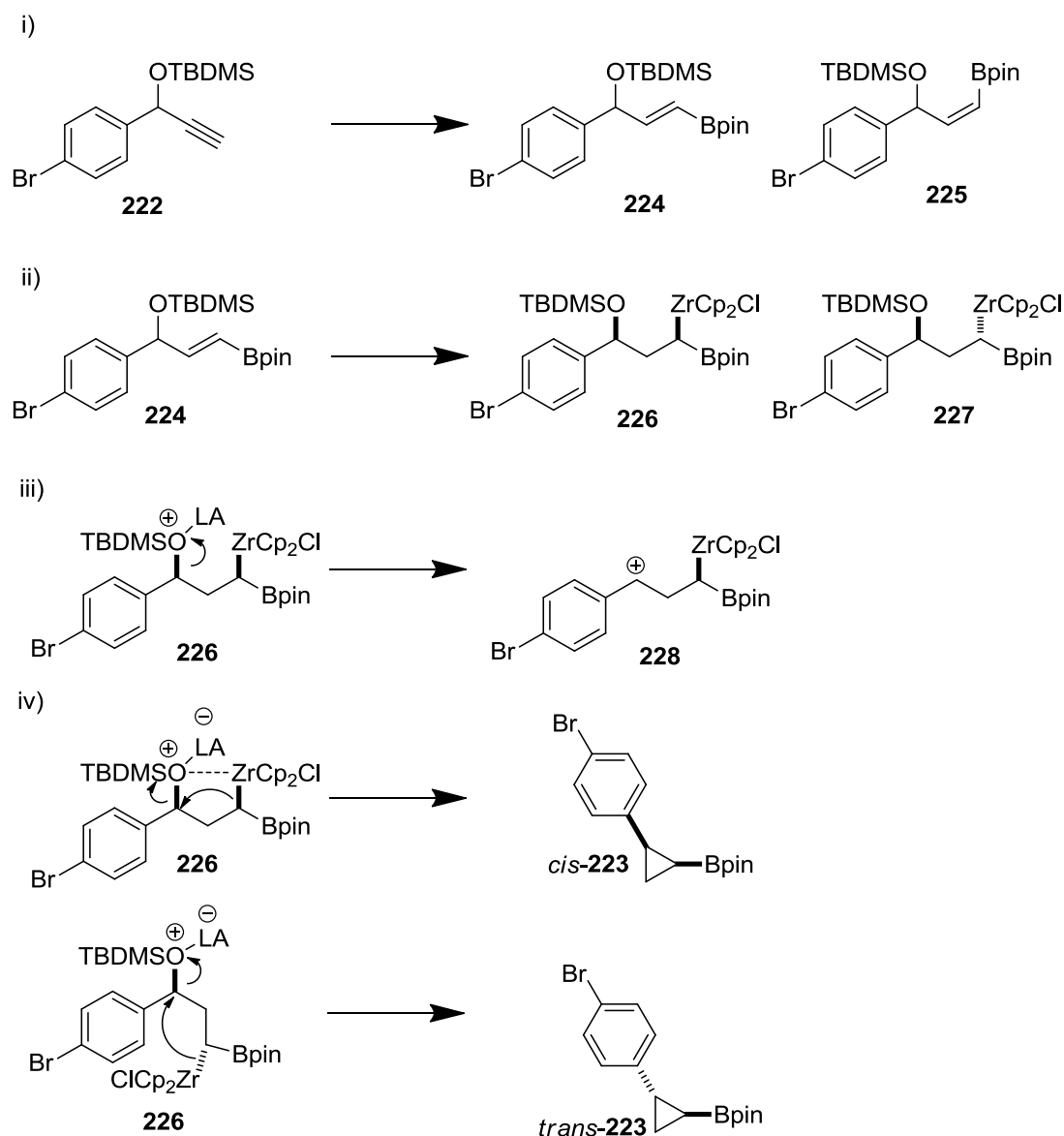
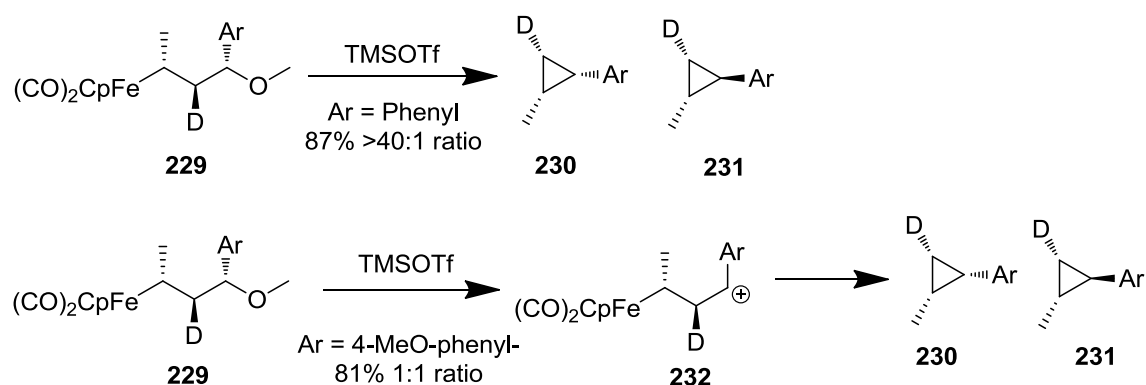


Figure 83 – Possible mechanisms for formation of diastereomeric mixtures of cyclopropyl products.

Firstly, it was possible that the Schwartz's Reagent catalysed hydroboration could be resulting in a mixture of *E*- and *Z*-alkenes **224** and **225** leading to a mixture of products (Figure 83i).

Secondly, hydrozirconation of intermediate **224** results in two possible diastereoisomers **226** and **227** (Figure 83ii). A lack of selectivity in this reaction would lead to a diastereomeric mixture, which could be leading to a mixture of diastereoisomers in the cyclopropyl product **223**.

Thirdly, it is possible that the cyclisation is proceeding *via* a carbocation intermediate in an S_N1-type process (Figure 83iii). This mechanism has been proposed in iron catalysed cyclopropanation reactions by Brookhart *et al.*²⁰⁸⁻²¹⁰ (Scheme 51). Here, it was shown that cyclisation of phenyl substituted compound **229** resulted in a single diastereoisomer of product **230**. However, presence of an electron rich anisole substituent causes loss of selectivity in the cyclisation step due to a proposed planar carbocation intermediate. Hence, in a zirconium-mediated reaction manifold this would render the diastereomeric mixture of the intermediates **226** and **227** inconsequential. This pathway is shown to be substrate dependent, with tertiary carbocations and electron-donating groups increasing the stability of the intermediate and is also hypothesised to be Lewis acid dependent, with stronger Lewis acids increasing the stability of the leaving group.



Scheme 51 – Iron mediated cyclopropanation reported by Brookhart in which a γ -carbocation is proposed to result in a cis/trans mixture of products for carbocation stabilising substituent.

Finally, there are two possible concerted cyclisations that could be envisaged (Figure 83iv). Syzmoniak proposes a co-ordinated mechanism with leaving group oxygen co-ordinating to both Lewis acid and zirconium.¹⁸⁹ However, the oxygen atom appears sterically encumbered in this mechanism and would possess a formal 2⁺ charge making this manifold unlikely. It was hypothesised that a backside-attack type mechanism may be more likely due to reduced steric crowding and better σ^* -orbital overlap.

Based on all of the above, a number of strategies were employed to explore which of the possible mechanisms was the most significant.

The hydroboration step is known to give high *E* selectivity in literature reactions¹⁹³ and in this case conversion to a single species with an *E*-alkene coupling pattern (alkene protons 5.71 and 6.59 ppm, $^3J_{H-H} = 17.9$ Hz) (Figure 84), which ruled out the possibility of issues with selectivity in this step.

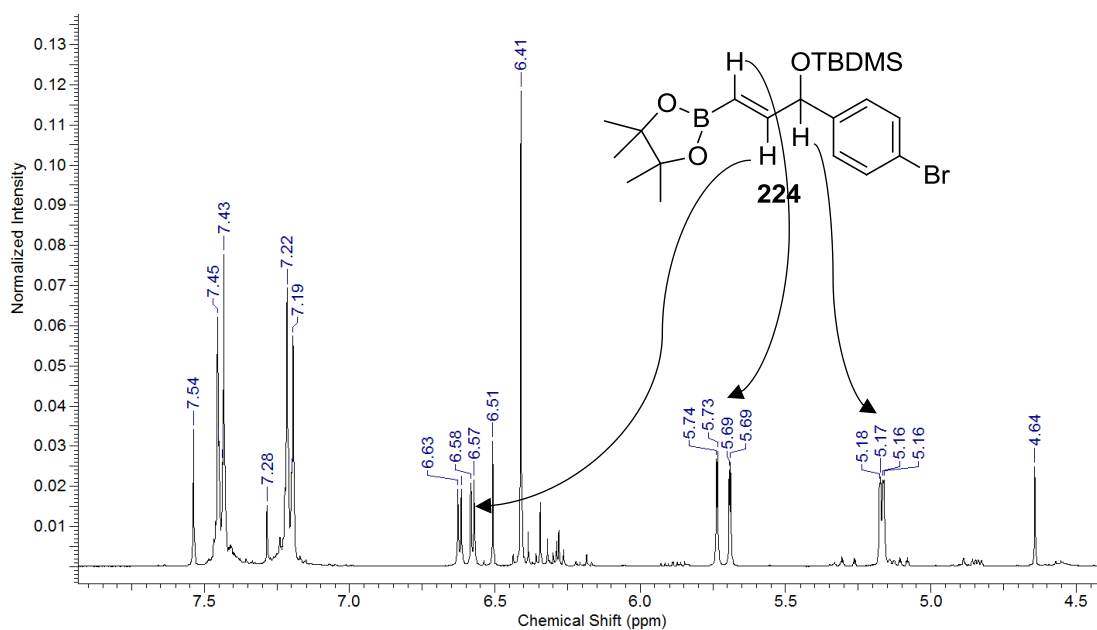
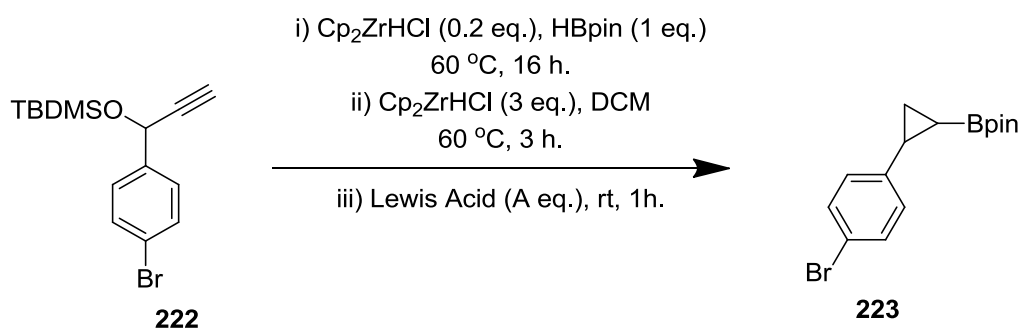


Figure 84 – Crude NMR spectrum of vinyl boronic ester intermediate, showing major component as the *E*-isomer.

Following on from this, a range of Lewis acids were screened to explore whether the Lewis acidity affected the *cis:trans* ratio (Table 30).

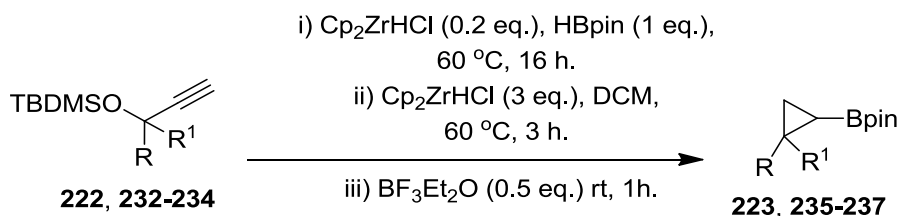


Entry	Lewis Acid	Equivalents	Conversion (<i>cis:trans</i>)
1	BF ₃ OEt ₂	2.0	61 (1.7:1)
2	BF ₃ OEt ₂	1.0	65 (1.6:1)
3	BF ₃ OEt ₂	0.5	73 (1.5:1)
4	BF ₃ OEt ₂	0.25	35 (1.6:1)
5	AlCl ₃	2.0	13 (1.6:1)
6	ZnCl ₂	2.0	0
7	TMSOTf	2.0	0
8	TiCl ₄	2.0	0

Table 30 – Screening of a range of Lewis acids.

Results showed that boron trifluoride diethyl etherate was significantly more productive than other Lewis acids screened (entries **1** to **4**). The only other Lewis acid to show any trace of product **223** was aluminium trichloride (entry **5**), however, for these two Lewis acids the *cis:trans* ratios were consistent under all conditions screened. It was hypothesised that the boronic ester product may be unstable to strongly Lewis acidic conditions, which has been shown in the literature, specifically for alkyl boronic esters.²¹¹ Therefore, compromise must be sought in the strength of the Lewis acid required to initiate cyclisation without further reaction with the product formed. Boron trifluoride appears to be optimal in this regard and further reduction in its stoichiometry led to increased amounts of product **223**, possibly due to reduced product degradation.

At this stage, the presence of electron donating or withdrawing groups on the substrate were explored. It was thought that this could affect the *cis:trans* ratio, by affecting the propensity for formation of a carbocation intermediate (Table 31).



Entry	R =	R ¹ =	XX, % Conversion (<i>cis:trans</i>)
1	4-Br-phenyl, 222	H	223 , 73 (1.5:1)
2	4-MeO-phenyl, 232	H	235 , 64 (0.9:1)
3	Phenyl, 233	Me	236 , 39 (0.7:1)
4	4-CF ₃ -phenyl, 234	H	237 , 66 (4.3:1)

Table 31 – The effect of electron-donating and withdrawing substituents on conversion and diastereomeric ratio.

Substrates containing carbocation stabilising groups (**232** and **233**) gave closer to equal mixtures of diastereomeric products. By contrast, a substrate containing a destabilising electron-withdrawing trifluoromethyl group **234** led to predominance of the *cis* product **237**. This indicates that there may be multiple reaction pathways leading to cyclopropyl products with carbocation stabilisation leading to product through a carbocation intermediate and other substrates proceeding through a stereospecific cyclisation.

Next, control over hydrozirconation of intermediate **224** was explored. It was not possible to obtain a clear proton NMR of the products **226** and **227** to examine the ratio of diastereoisomers. Hence, controlling the diastereoselectivity of this step was an area of further interest. According to the Houk model for asymmetric induction in acyclic alkenes,²¹² the size of groups affect the diastereoselectivity of a reaction (Figure 85).

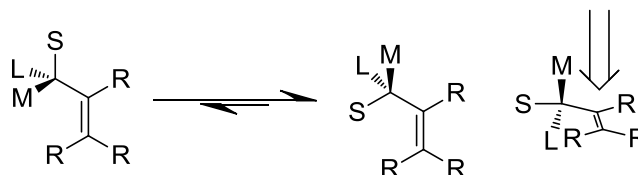
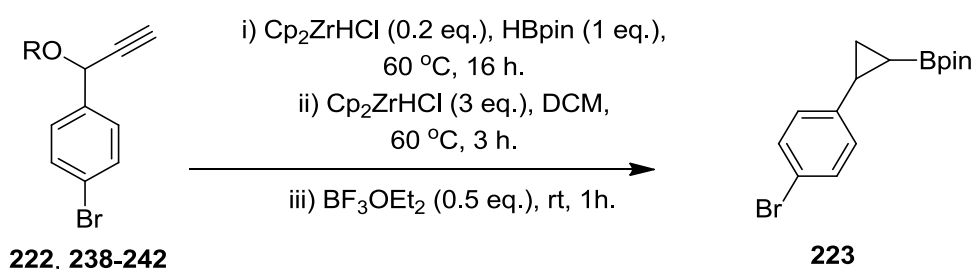


Figure 85 – The Houk model for asymmetric induction in acyclic alkenes.

CONFIDENTIAL – PROPERTY OF GSK – DO NOT COPY

The Houk model predicts that the lowest energy conformation for molecules with a chiral centre adjacent to an alkene. The most favourable conformation minimises allylic 1,2-strain by placing a group eclipsing the alkene. This leads to an allylic 1,3-strain and the most favourable conformation is therefore with the smallest group in this position. Reactions from this conformation are then more likely to occur from the face with the medium-sized group to avoid steric clashing with the large group.

Therefore, it was thought that the size of the silyl group may affect the side of approach for the hydrozirconation step. Hence, a range of propargylic silyl ether substrates were synthesised and subjected to the reaction conditions (Table 32).



Entry	Substrate, R =	<i>cis:trans</i>	223, Isolated / (NMR) Yield
1	238 , Si(OEt) ₃	0.4:1	44 / (48)
2	239 , SiEt ₃	0.6:1	(31)
3	222 , Si ^t BuMe ₂	1.2:1	73 / (76)
4	240 , Si ⁱ Pr ₃	1.5:1	(62)
5	241 , Si ^t BuPh ₂	1.1:1	(67)
6	242 , Si(SiMe ₃) ₃	3.8:1	21 / (26)

Table 32 – Exploration of effect of size of silyl group on diastereomeric ratio.

It was observed that varying the silyl group size does indeed affect the diastereomeric ratio, with the smallest triethoxysilyl group favouring the *trans*-product. Increasing sized groups led to a larger proportion of the *cis*-product and the largest tris(trimethylsilyl)silyl group favoured the *cis*-product.

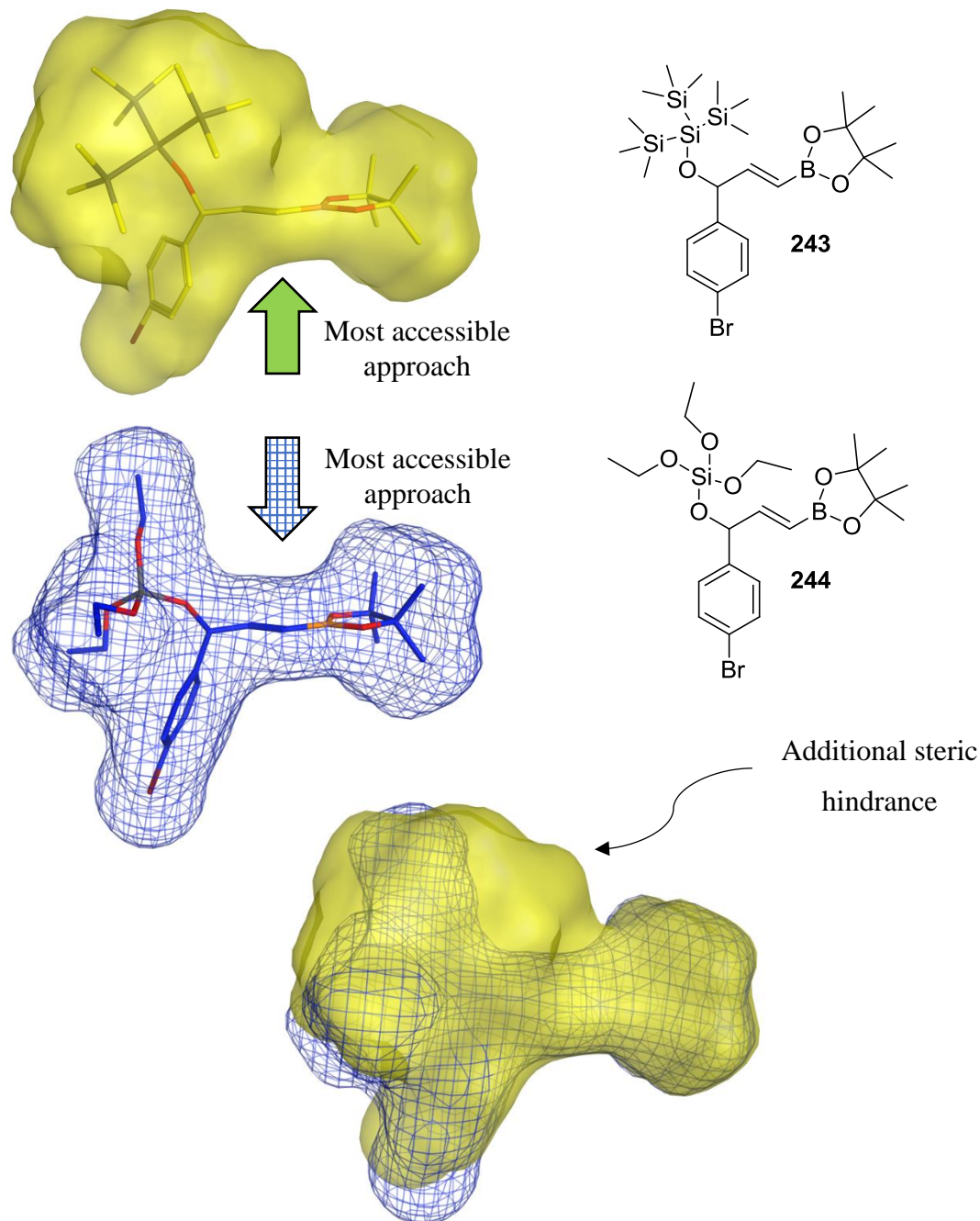


Figure 86 – Overlaid surfaces of energy minimised conformations of triethoxysilyl ether **244** (hatched blue) and tris(trimethylsilyl)silyl ether **243** (solid yellow) showing the change in steric hindrance at the top face of the vinyl boronic ester intermediates. Modelling was conducted in MOE using a LowModeMD method with Amber10:EHT force field.

By invoking the Houk model²¹² for asymmetric induction in acyclic alkenes and by considering the modelled structures of triethoxysilyl ether **244** and tris(trimethylsilyl)silyl ether **243** (Figure 86) it can be asserted that the larger group blocks the top face whereas the smaller group allows access to this face. This leads to the *anti*-diastereomer and the *syn*-diastereomer, respectively. These then cyclise to give the respective *cis* and *trans* products. This has implications for the reaction mechanism with *syn*-organozirconium intermediate only yielding *trans*-cyclopropyl product by virtue of an invertive cyclisation and a similar mechanism yielding *cis*-cyclopropyl product from *anti*-organozirconium intermediate (Figure 87).

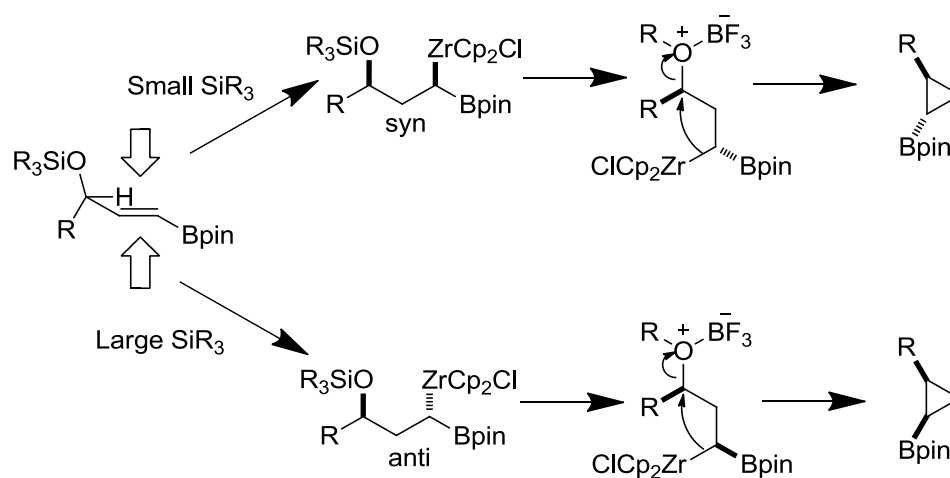
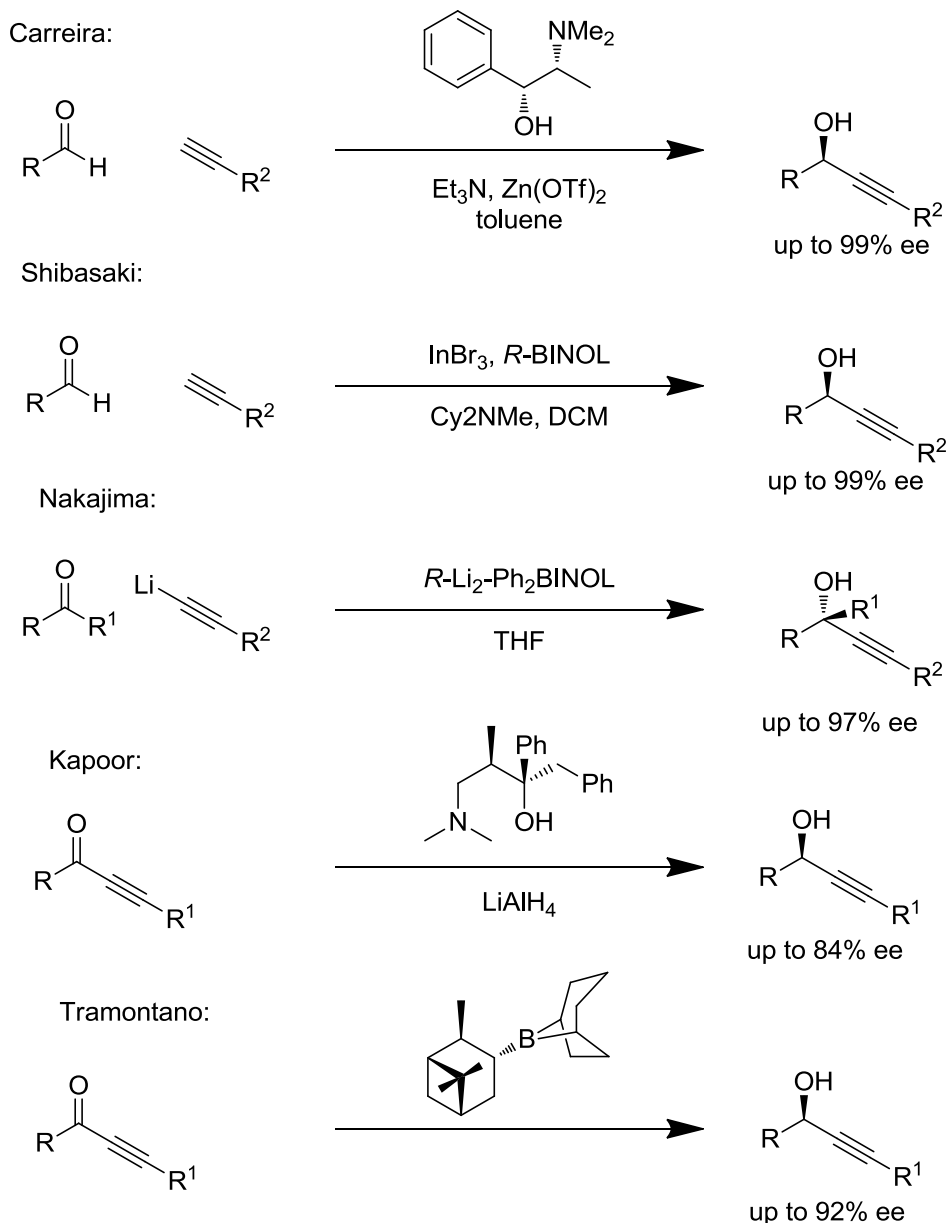


Figure 87 – Proposed mechanism for formation of *cis* and *trans* diastereoisomers and rationale for control by variation in size of silyl group.

Whilst these findings support the possibility of diastereomeric control, further optimisation of the reaction conditions for alternative leaving groups would be required. In the first instance, the high yielding conditions using *tert*-butyldimethyl silyl group were explored further.

Next, the mechanism for cyclisation was further explored by synthesis of enantioenriched substrates. Use of a known enantiomer of starting material would provide information on the stereospecificity and mechanism of the reaction.

Enantioenriched propargylic alcohols can be synthesised by numerous protocols including asymmetric addition of an alkyne to an aldehyde or ketone²¹³⁻²¹⁵ or *via* asymmetric reduction of a propargylic ketone (Scheme 52).^{216,217}



Scheme 52 – Methods for synthesis of enantioenriched propargylic alcohols.

A number of substrates were selected for study. Phenyl propargylic alcohol **245** is available commercially as either enantiomer. Analysis of further racemic propargylic alcohols *via* chiral HPLC showed that the enantiomers were readily separable and hence this method was successfully used for the preparation of the required amount of enantioenriched alcohols **246** and **247**.²¹⁸ Trifluorophenyl alcohol **248** was found to be unstable to separation conditions and hence was not explored further.

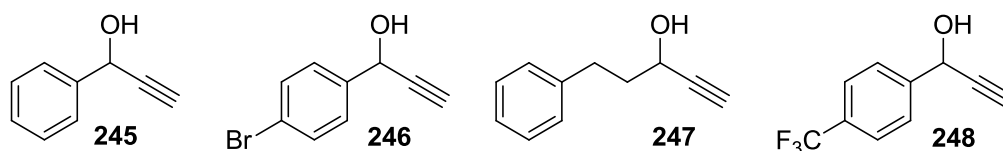


Figure 88 – Enantioenriched alcohols prepared for subsection to one-pot borylation-cyclisation conditions.

With the enantioenriched alcohols in hand, subsequent silyl protection yielded the desired starting materials, which were subjected to the optimised reaction conditions (Figure 89).

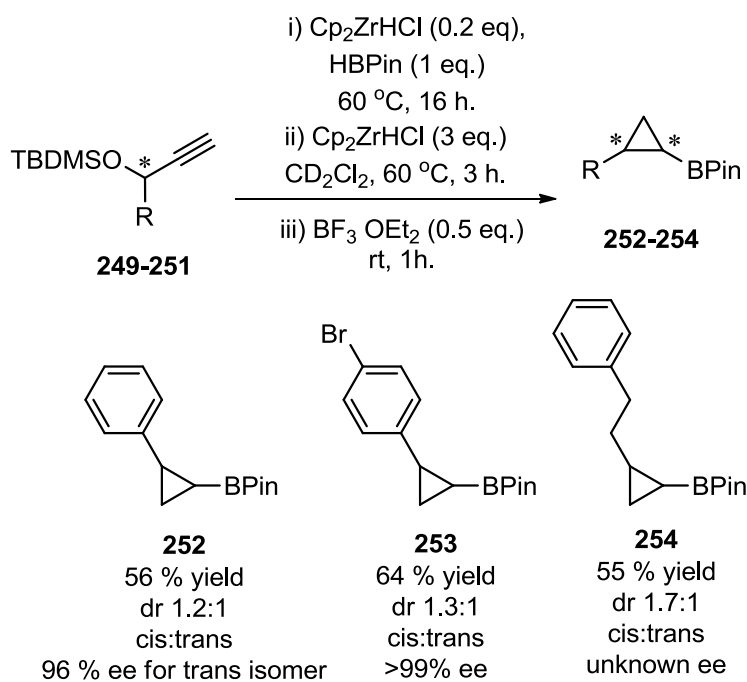


Figure 89 – Use of enantioenriched substrates to explore stereospecificity of the one-pot borylation-cyclisation process.

Analysis of products by chiral HPLC showed that racemisation had not occurred in the reaction for **252** and **253** (Figure 90). Analysis of racemic cyclopropyl boronic ester **223** shows presence of four peaks by chiral HPLC, indicating presence of a racemic mixture of diastereoisomers. However, analysis of the cyclopropyl boronic ester **253** derived from enantioenriched starting material (-)-**250** shows only two major peaks, indicating an enantioenriched mixture of diastereoisomers. This indicates that the cyclisation occurs *via* a single mechanism and is unlikely to occur *via* a carbocationic intermediate. For ethyl phenyl product **254**, the enantiomers could not be separated by chiral HPLC meaning the stereospecificity of the reaction could not be established. The observation that racemisation does not occur therefore enables use of this methodology for synthesis of enantioenriched cyclopropylboronic esters.

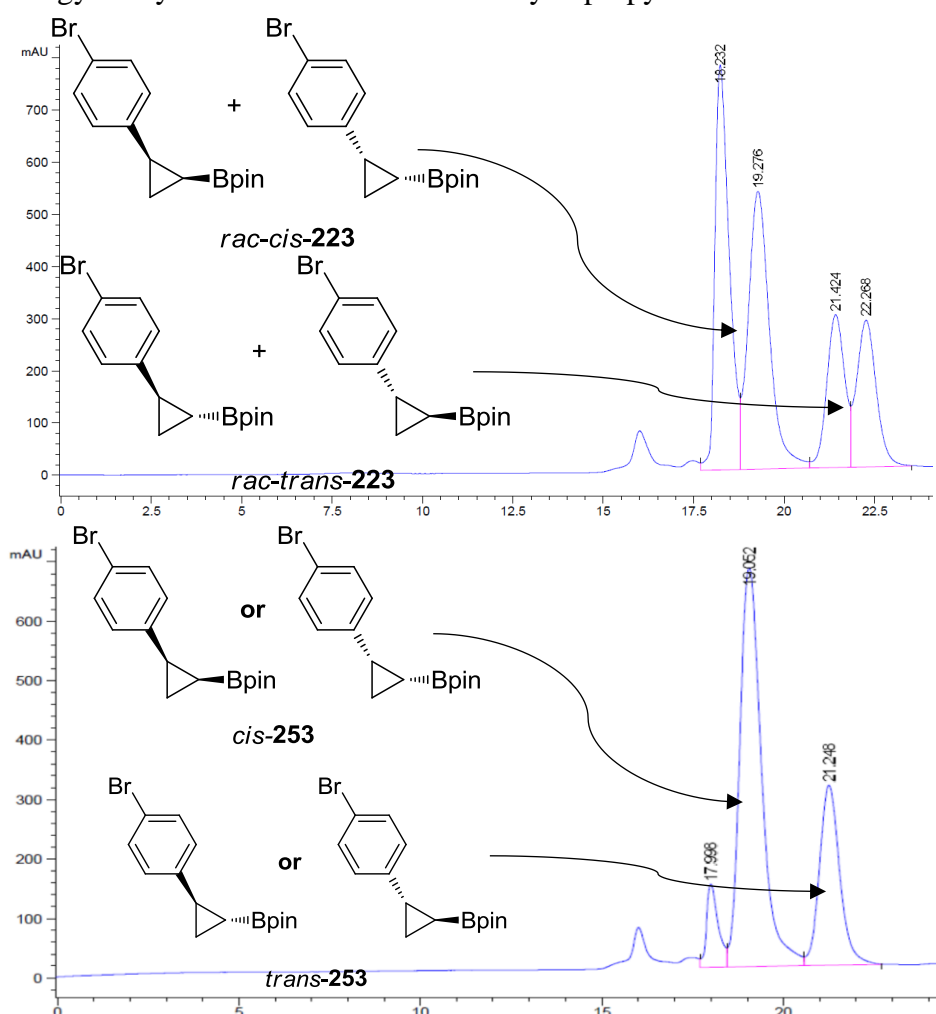


Figure 90 – Chiral HPLC analysis of products from racemic one-pot borylation-cyclopropanation (top) and from the same reaction using enantioenriched starting materials (bottom).

Further mechanistic knowledge was obtained through reaction of chiral starting material (*R*)-**249**. The cyclopropyl boronic ester formed in this case is a literature compound¹⁸⁶ which revealed that a stereospecific inversion had taken place. This supports the hypothesised ‘backside-attack’ type mechanism (Figure 91).

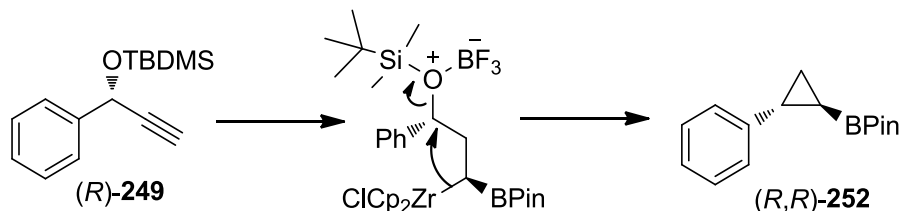
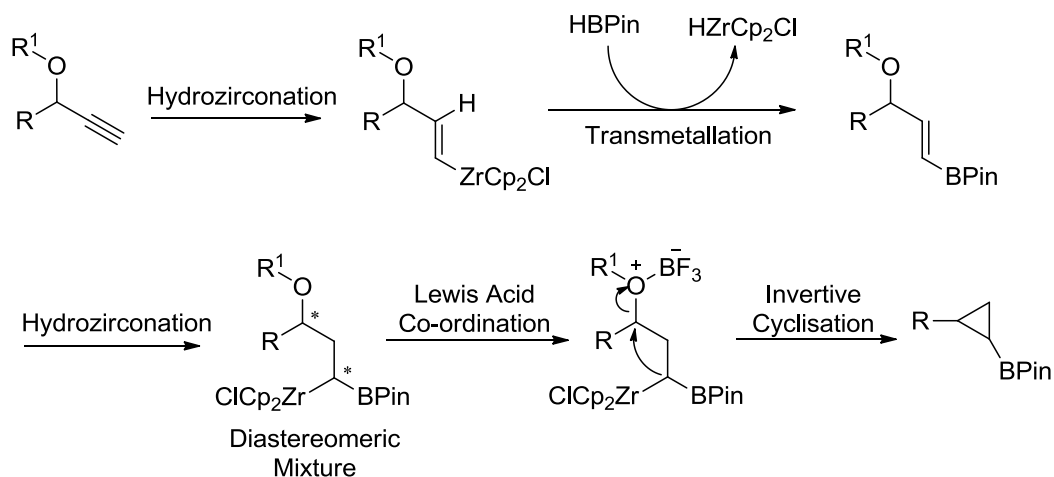


Figure 91 – Subjection of known enantiomer of starting material **249** to reaction conditions and proposed invertive mechanism to generate *R,R*-product **252**.

In summary, evidence shows that zirconium catalysed hydroboration generates selectively the *E*-vinyl boronic ester. Subsequent hydrozirconation of this species yields a diastereomeric mixture of *gem*-borazirconocene intermediates. It is then proposed that the reaction pathway divides between carbocation stabilising and non-carbocation stabilising substituents. For non-stabilising, it is proposed that a stereospecific invertive cyclisation occurs meaning diastereomeric ratio of cyclopropyl products reflects that of *gem*-borazirconocene intermediates. Whereas, for carbocation stabilising groups it is proposed that a non-diastereomeric carbocation forms, and cyclisation onto this cation yields an almost 1:1 mixture of diastereoisomers (Figure 92).

For R groups not able to stabilise a carbocation:



For R groups able to stabilise a carbocation:

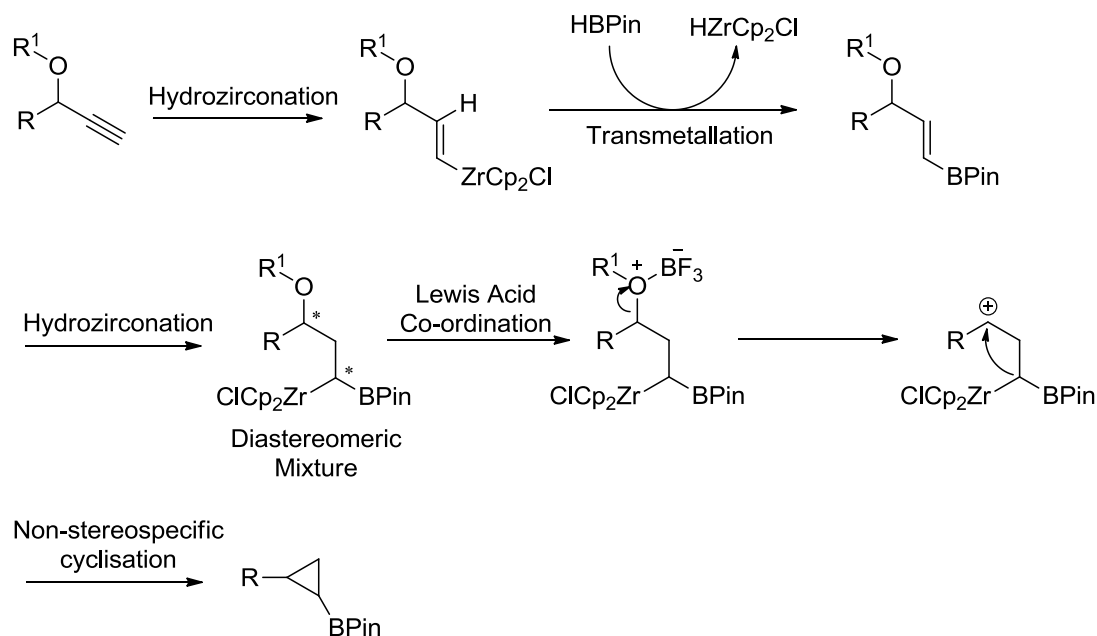
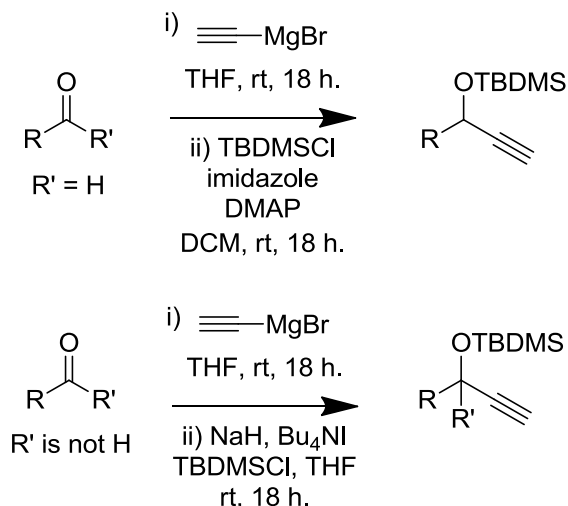


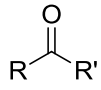
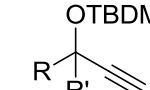
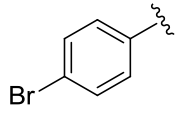
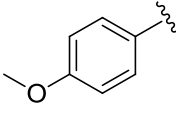
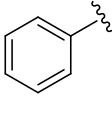
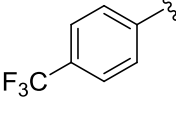
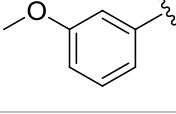
Figure 92 – Proposed mechanism for one-pot borylation-cyclisation methodology.

With optimised conditions and an understanding of the reaction mechanism in hand, the substrate scope for the reaction was then explored.

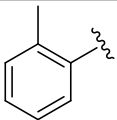
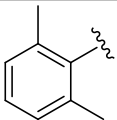
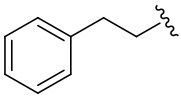
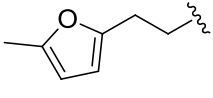
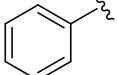
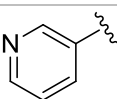
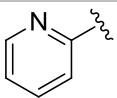
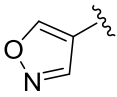
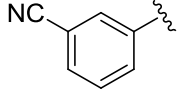
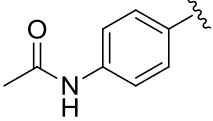
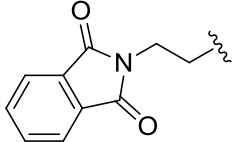
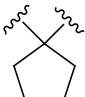
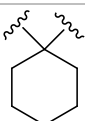
3.2.2 Substrate Scoping

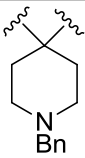
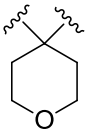
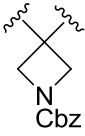
A variety of silyl ethers were selected containing a range of electron rich and electron poor benzylic ethers, aliphatic ethers and quaternary ethers. These were prepared by Grignard addition into commercially available aldehydes or ketones.²¹⁹ Secondary alcohols could then be protected using imidazole, dimethyl aminopyridine (DMAP) conditions.²²⁰ However, these conditions proved unproductive for tertiary alcohols and hence sodium hydride, tetra-*n*-butylammonium iodide conditions were used (Scheme 53).²²¹



R =	R' =			Yield /%
	H	255	222	72
	H	256	232	28
	H	N/A	271	54*
	H	257	234	43
	H	258	272	69

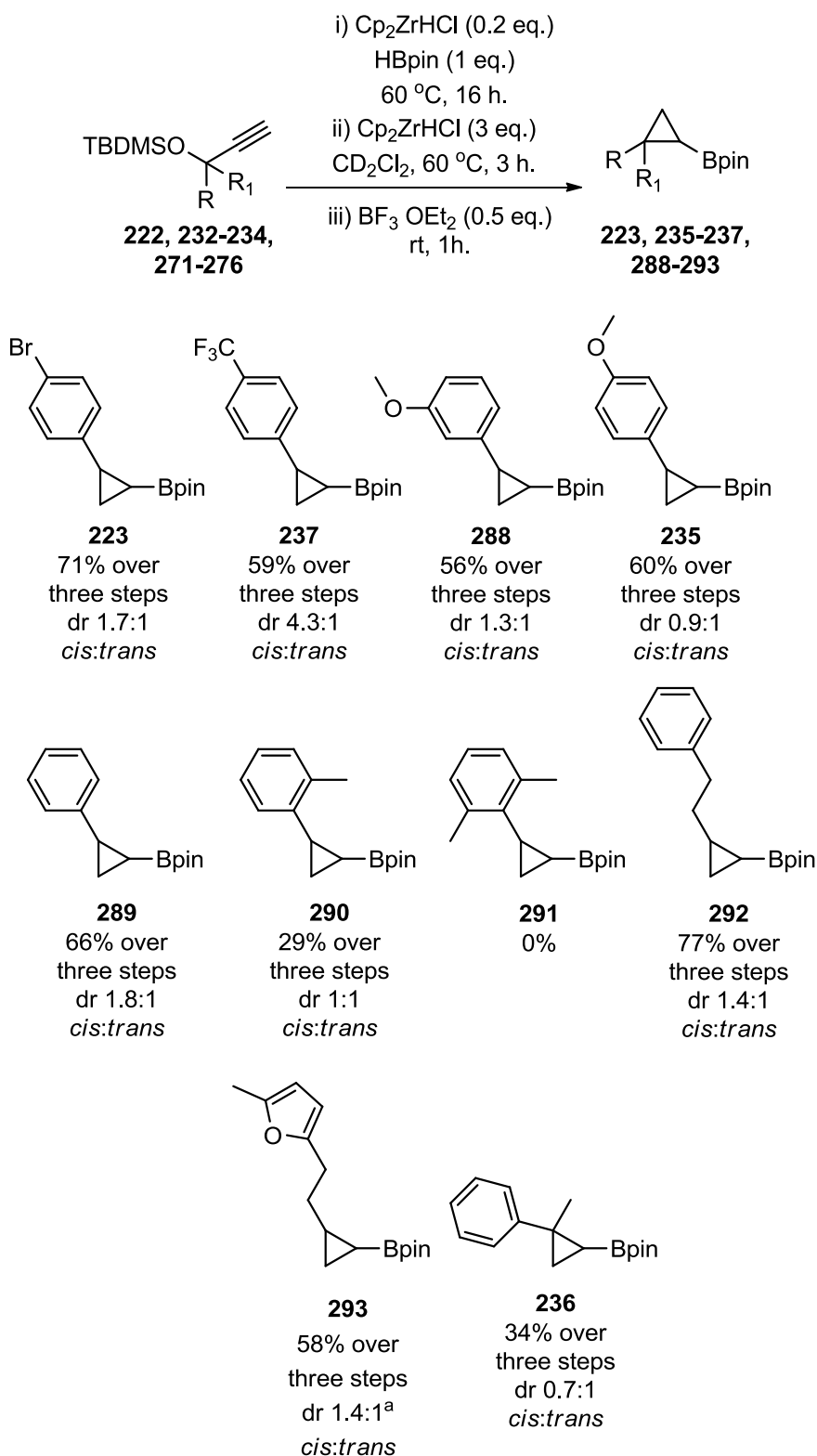
CONFIDENTIAL – PROPERTY OF GSK – DO NOT COPY

	H	259	273	34
	H	260	274	44
	H	261	275	48
	H	262	276	65
	Me	N/A	233	83*
	H	263	277	47
	H	264	278	62
	H	265	279	59
	H	266	280	33
	H	267	281	33
	H	268	282	58
		N/A	283	73*
		N/A	284	54*

	N/A	285	37*
	269	286	53
	270	287	41

Scheme 53 – Synthesis of substrates for one-pot borylation-cyclopropanation reaction.
 *Propargylic alcohols were commercially available and hence step i) was omitted and yields are quoted from alcohol.

Propargylic silyl ethers could be synthesised in moderate yield from a range of aldehydes and ketones. These silyl ether products were next subjected to the optimised reaction conditions to explore the scope of the one-pot borylation-cyclopropanation reaction (Scheme 54).



Scheme 54 – Substrate scope of one-pot borylation-cyclopropanation reaction.

^aIsomers were separable by normal phase chromatography.

CONFIDENTIAL – PROPERTY OF GSK – DO NOT COPY

A number of benzylic substituted propargylic ethers with electron-withdrawing and electron-donating groups were successfully converted into Bpin cyclopropyl monomers **223**, **235-237** & **288-293**. It was observed that the electronic properties of the aryl substituents influenced the diastereomeric ratio (cf. **237**, 4.3:1 and **235**, 0.9:1). It is thought that this is due to the electron-donating groups leading to an increased propensity for the carbocation type mechanism, meaning closer to 1:1 ratios were observed.

Comparison of ortho-substituted systems revealed a steric component to the reaction with a reduction in yield observed from phenyl **289** (66%) to *ortho*-tolyl **290** (30%) to 2,6-dimethylphenyl **291** (0%). From analysis of the reaction profile by crude NMR, it can be inferred that steric bulk appears to inhibit initial zirconium catalysed hydroboration step. Additionally, increasing the steric bulk of the aryl group leads to an increased proportion of *trans*-diastereomer. It is hypothesised that this is due to the bulk blocking the approach of the hydrozirconation to the aryl face of the alkene (Figure 93), leading to the *syn*-intermediate and the *trans*-product.

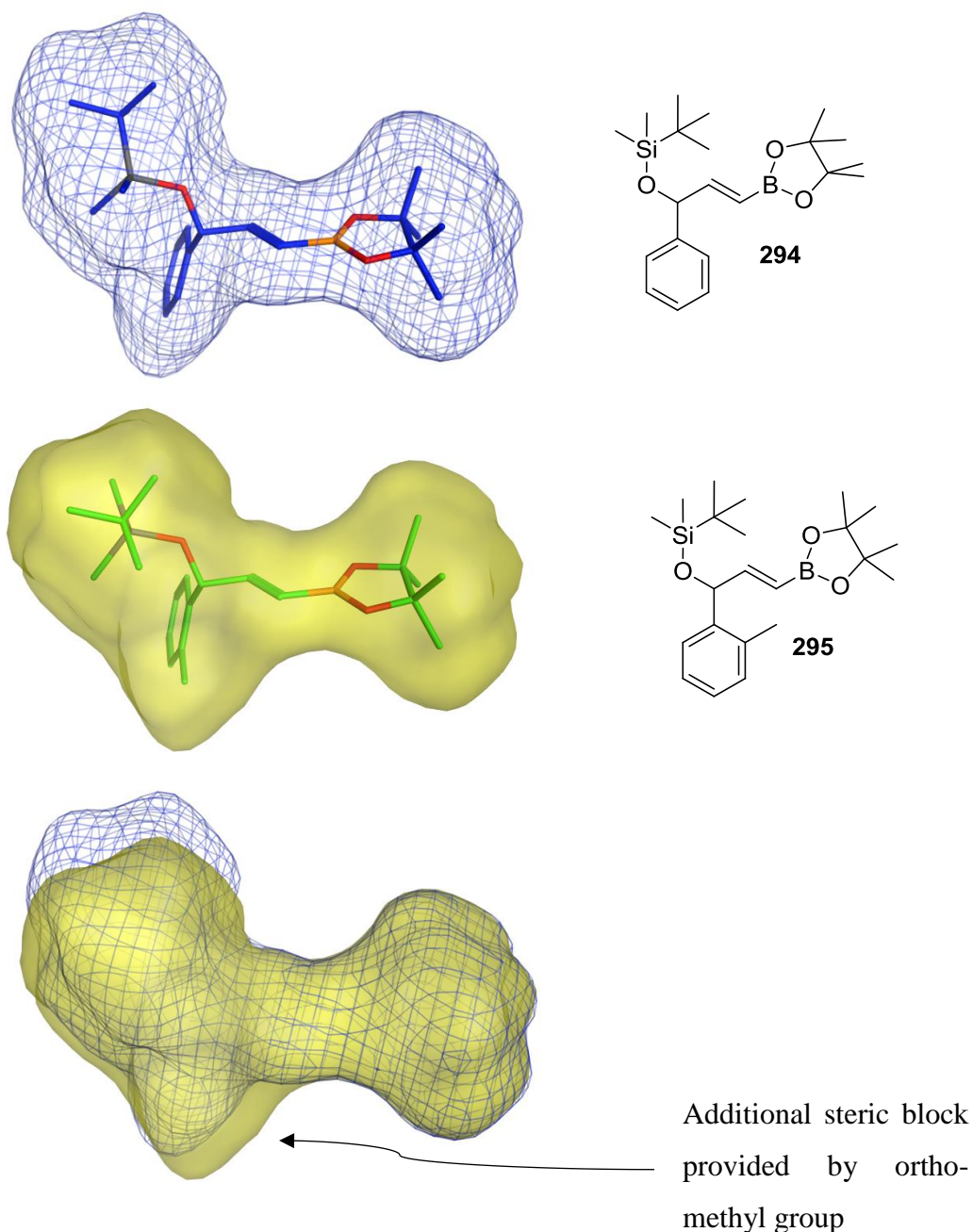
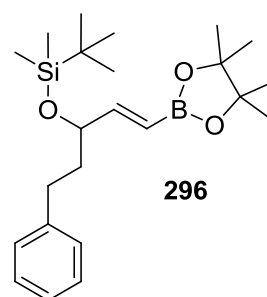
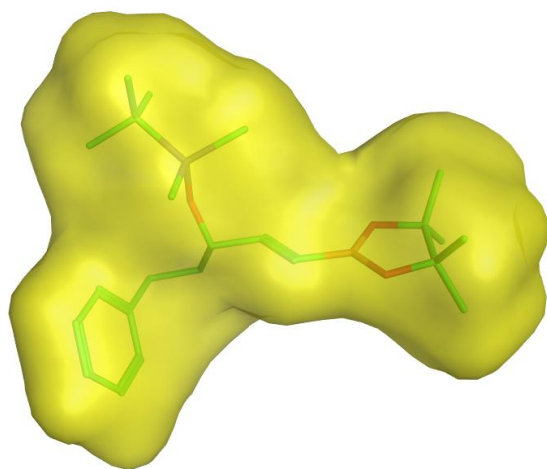
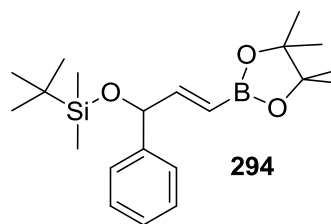
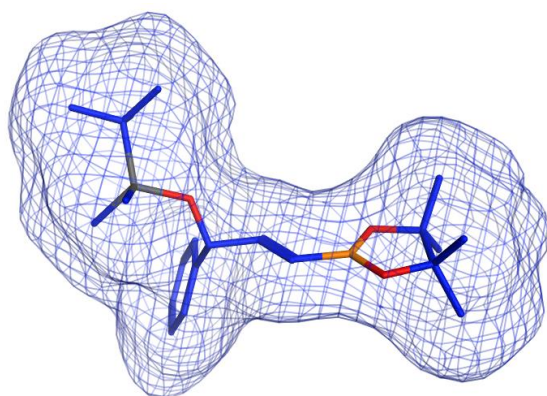


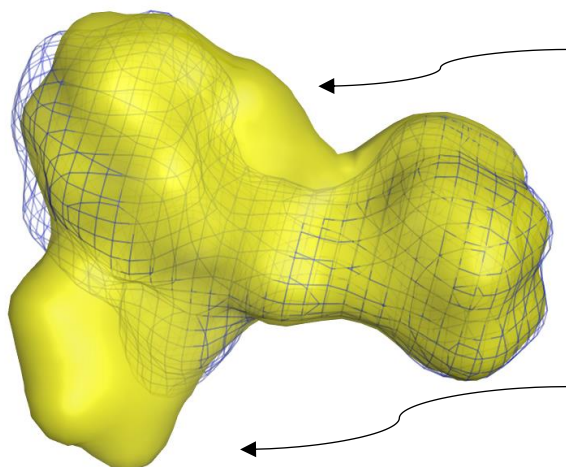
Figure 93 – Computationally modelled lowest energy conformations for phenyl vinyl boronic ester **294** (hatched blue) and *o*-tolyl vinyl boronic ester **295** (solid green) with increased steric bulk of *o*-tolyl group observed on the bottom face. Modelling was conducted in MOE using a LowModeMD method with Amber10:EHT force field.

The reaction was also found to proceed for aliphatic substituents ethyl phenyl **292** (59%) and ethyl furanyl **293** (67%). With these substrates, the ethyl chain is sterically smaller than the aryl group present in the other examples. However, this group is also more flexible and therefore the phenyl or furanyl portion could block approach to the

alkene. These opposing factors therefore make prediction difficult. In computationally modelled structures the ethyl group in **296** and phenyl group in **294** occupy a similar volume in this portion of the molecule. The increased bulk of the ethyl phenyl group closer to the silyl group leads to the silyl ether flipping, causing an increase in bulk on the upper face of the ethyl phenyl system (Figure 94). This would be expected to lead to an increased proportion of *cis*-diastereoisomer within the ethyl-phenyl system. However, the increased flexibility of the ethyl-phenyl system means that the phenyl portion of this compound can also orient to block the lower face for approach. Experimentally, it was found that the aliphatic substituted substrates are less *cis*-selective than the phenyl substrate. This means that approach from the lower face is less favoured in these systems, presumably due to steric blocking by the ethyl-phenyl group.



Additional steric block
due to change in silyl
ether conformation



Additional steric block
due to flexible ethyl
phenyl group

Figure 94 - Computationally modelled lowest energy conformations for phenyl vinyl boronic ester **294** and ethyl phenyl boronic ester **296** with change in silyl ether conformation in ethyl phenyl compound leading to increased steric bulk on the top face. Modelling was conducted in MOE using a LowModeMD method with Amber10:EHT force field.

CONFIDENTIAL – PROPERTY OF GSK – DO NOT COPY

With more challenging quaternary substituted centres, product formation was observed in slightly reduced yield, for example 2-methyl-2-phenyl **236** (35%). Modelling for this system shows a staggered conformation is favoured with the methyl-group rotating to avoid 1,3-diaxial interaction with vinylic proton. This greatly increases steric bulk on the top face and reduces steric bulk on the lower face, predicting the *cis*-diastereomer would be favoured (Figure 95). However, for this system, a ratio closer to 1:1 ratio was observed with slightly more of the *trans*-diastereoisomer. It is reasoned that this is due to increased propensity for the carbocation mechanism, with the stable tertiary carbocation in this system. Hence, the diastereomeric ratio of the associated intermediate is rendered insignificant.

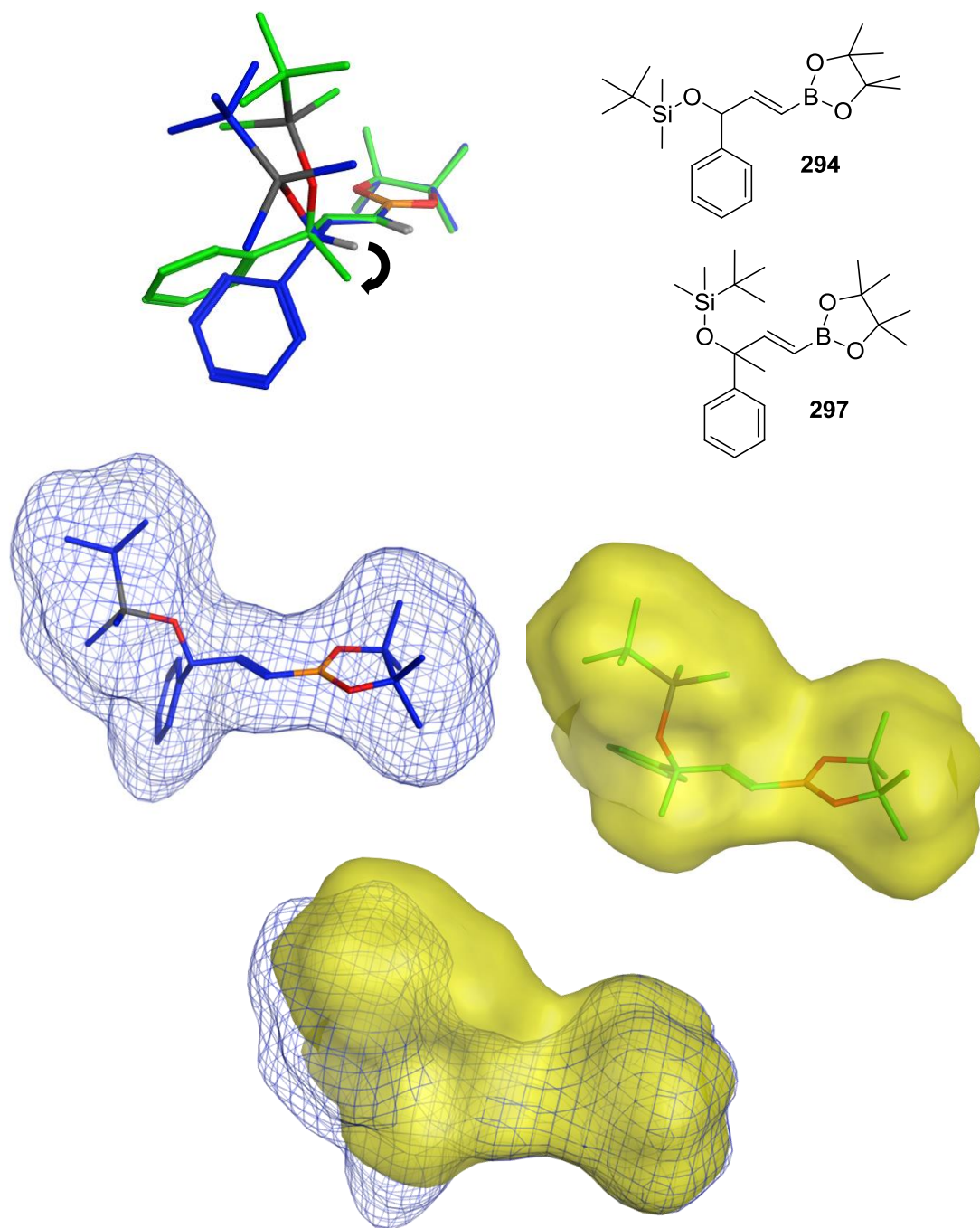


Figure 95 - Computationally modelled lowest energy conformations for phenyl vinyl boronic ester **294** and methyl phenyl boronic ester **297** showing changes in conformation upon replacing a hydrogen with a methyl group. Modelling was conducted in MOE using a LowModeMD method with Amber10:EHT force field.

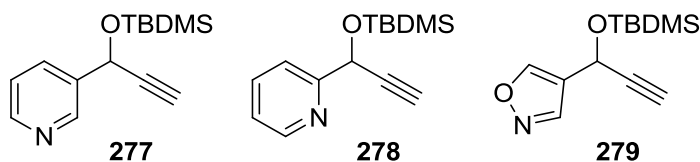


Figure 96 – Unsuccessful heterocyclic substrates screened in the reaction.

The reaction was found to be unproductive for heterocycle containing substrates **277-279**. Analysis of the reaction mixtures by crude NMR showed that zirconium-catalysed hydroboration was occurring, however complete consumption of this species and no cyclised product was observed by NMR. It was initially suggested that this was due to Lewis basic pyridine co-ordinating to the catalytic boron trifluoride Lewis acid, preventing leaving group activation. However, upon addition of two equivalents of Lewis acid to a reaction of 3-pyridyl substrate **277** a similar reaction profile was observed. There is no evidence in the literature for stability of a combination of pyridine-containing structures and super stoichiometric Schwartz's Reagent under high temperature conditions.

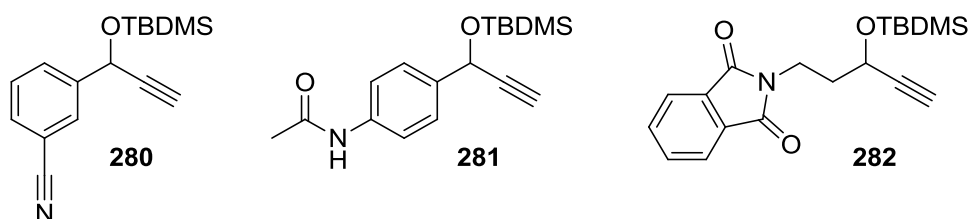
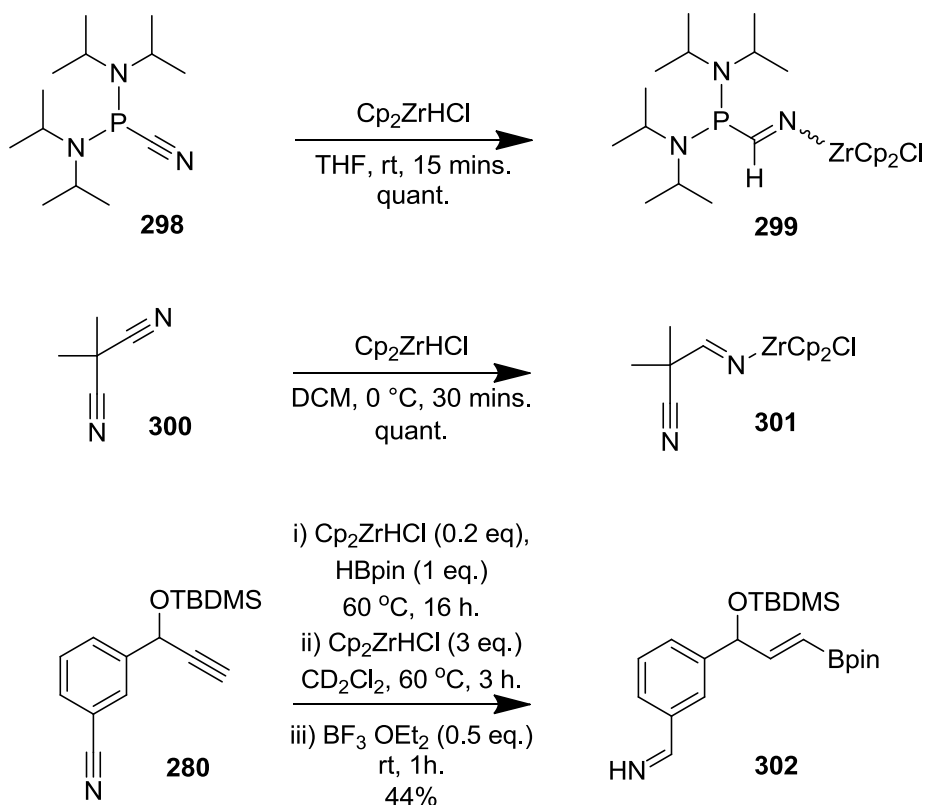


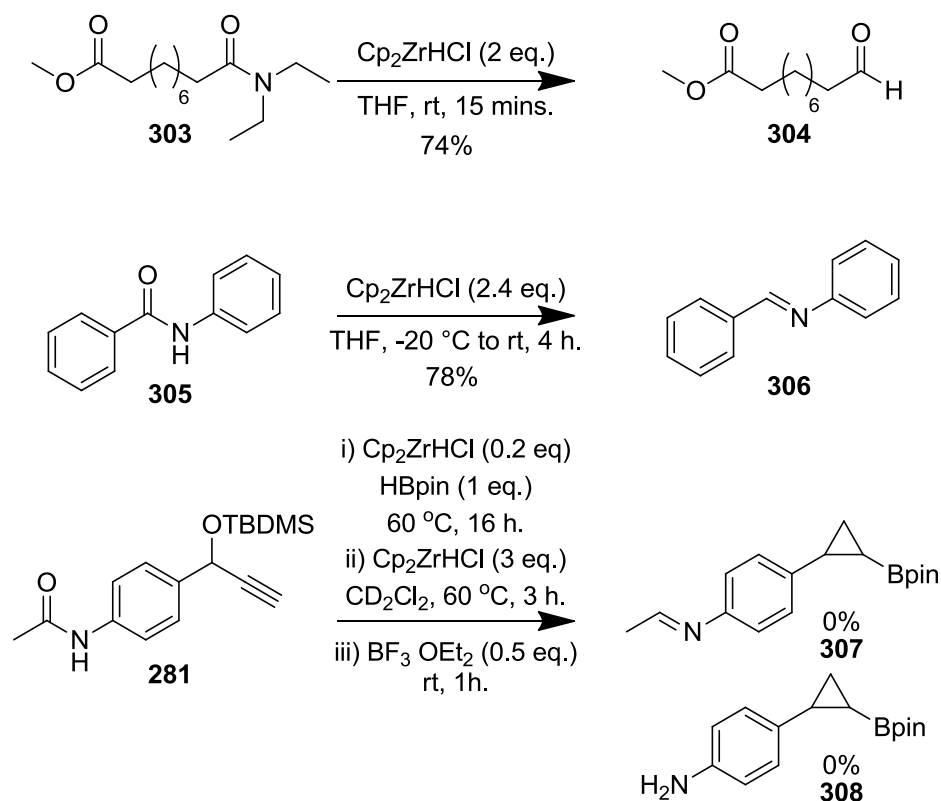
Figure 97 – Unsuccessful substrates containing electrophilic functionality.

The reaction was also found to be unproductive for substrates with electrophilic functionality such as nitriles, amides and phthalimides. Schwartz's Reagent is known to add across cyanophosphanes²²² and substituted malonitriles (Scheme 55).²²³ However aryl nitriles have been shown to be stable to some Schwartz's Reagent mediated processes.²²⁴ Subjecting nitrile **280** to the optimised reaction conditions resulted in only imine **302** being isolated. This imine could form from a Schwartz's reagent addition across the nitrile, which would be expected to remove one equivalent of Schwartz's reagent. However, it is not clear why this prevents subsequent hydrozirconation onto vinyl boronic ester and subsequent cyclisation.



Scheme 55 – Literature precedence for Schwartz’s Reagent reacting with nitriles and product isolated from subjection of nitrile **280** to one-pot borylation cyclopropanation conditions.

Schwartz’s Reagent is also known to reduce tertiary amides selectively in the presence of ester functionality to the corresponding aldehyde²²⁴ and secondary amides to the corresponding imine (Scheme 56).²²⁵ The secondary amide reduction is proposed to require two equivalents of Schwartz’s Reagent, one to act as a base in formation of a zirconium enolate and the second to carry out the reduction. It was therefore anticipated that subjection of amide **281** to optimised reaction conditions may lead to deacetylated amine product **308** or imine product **307**. However, no products could be isolated and a complex mixture was obtained. It is hypothesised that incomplete amide reduction is competitive with cyclisation and that three equivalents is not sufficient to force either reaction to completion. This results in possible partial reduction products, which may not have been identifiable in the complex mixture obtained.



Scheme 56 – Literature precedence for reduction of amides with Schwartz’s Reagent and result of subjecting amide **281** to reaction conditions.

It has been shown that phthalimides can be stable to Schwartz’s Reagent mediated processes.²²⁶⁻²²⁸ It was therefore thought that phthalimide **282** would be stable to reaction conditions and would lead to a boronic ester with orthogonally protected amine. However, despite conversion to intermediate vinyl boronic ester being observed, the phthalimide **282** was found to be unstable to three equivalents of Schwartz’s Reagent at 60 °C and a complex mixture was obtained with no identifiable cyclopropyl peaks by crude NMR.

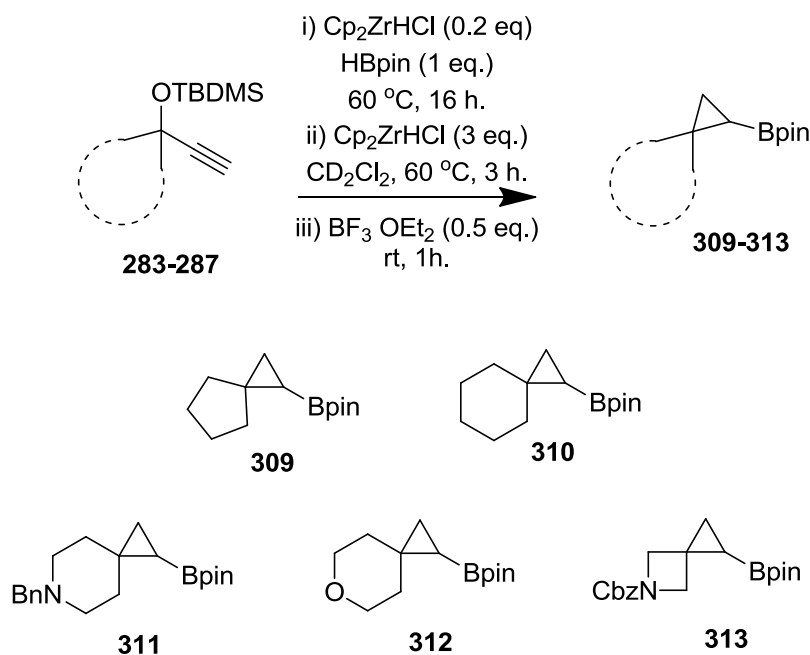
Due to the successful synthesis of quaternary cyclopropyl compound **236**, it was hypothesised that the scope of the reaction could be extended further to include spiro-fused cyclopropyl rings.

Spiro-fused rings are of particular interest within drug discovery due to the highly rigid three-dimensional character they possess.^{229,230} The structures have been introduced into molecules to modulate solubility,²²⁹ lipophilicity²³¹ and metabolic clearance.²³² Spirocyclic structures also introduce structural novelty leading to the possibility of

CONFIDENTIAL – PROPERTY OF GSK – DO NOT COPY

generating broad patents.²³³ Facile synthesis of modular spirocyclic building blocks would enable these areas of chemical space to be explored more widely in drug discovery.

Therefore, a number of substrates for this reaction were synthesised and subjected to optimised reaction conditions (Scheme 57).

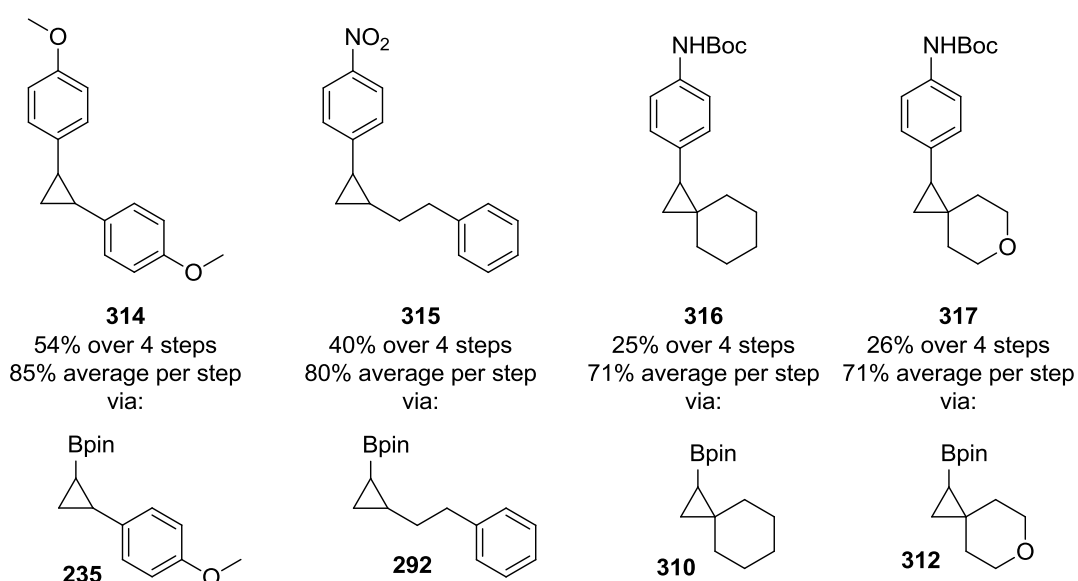
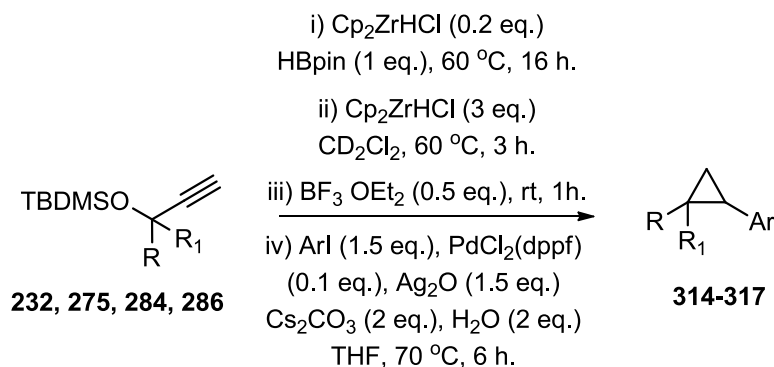


Scheme 57 – Attempts to synthesise spiro-cyclopropyl boronic esters.

Subjecting cyclopentyl **283**, cyclohexyl **284**, and tetrahydropyran **286** containing starting materials resulted in observation of cyclopropyl ring protons by crude NMR. However, clean products could not be isolated by normal phase or reverse phase chromatography due to the lipophilic nature of the products. Benzyl piperidine **285** was found to result in a complex mixture, which could be due to the basic amine present proving incompatible with the reaction. No product was observed with use of carboxybenzyl-azetidene **287**, possibly due to ring strain of 5-azaspiro[2.3]hexane ring system **313** and possibly due to reduction of the carbamate protecting group under forcing Schwartz's Reagent conditions.

To address the problems with isolation of these lipophilic spiro products it was decided to telescope the reaction into a Suzuki-Miyaura cross coupling (Scheme 58).²³⁴ This

also provided an opportunity to demonstrate the one-pot generation of a diverse range of products relevant to medicinal and agrochemical efforts.



Scheme 58 – Diversification of cyclopropylboronic ester products in a Suzuki-Miyaura cross-coupling.

Initial reactions focused on telescoping examples already preceded in the initial substrate scope into Suzuki-Miyaura cross coupling without isolation of the cyclopropyl boronic ester intermediates. Pleasingly, anisole **235** and ethyl phenyl **292** cyclopropyl boronic esters were synthesised under the standard conditions and were successfully coupled with both electron rich and electron poor aryl iodides, respectively. This generates a procedure for simple propargylic ether starting materials to be easily converted in one-pot to bis-substituted cyclopropyl rings. Next, the focus turned to synthesis of the more challenging spiro-cyclopropyl coupled products. Telescoping into Suzuki-Miyaura cross coupling allowed isolation of lead-like spiro-

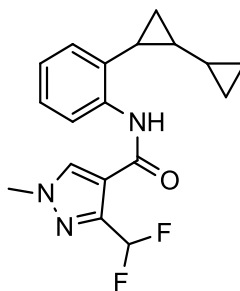
CONFIDENTIAL – PROPERTY OF GSK – DO NOT COPY

cyclohexyl **316** and spiro-tetrahydropyranyl **317** rings coupled to an aryl ring. Telescoping made isolation of these materials much more facile *via* reverse phase chromatography. These spiro compounds **310** and **312** represent highly complex building blocks which are of interest in bioactive compounds as they exhibit a significant degree of 3D character²²⁹ and conformationally constrained growth vectors for drug discovery.²³⁰

In summary, a method has been developed which allows conversion of synthetically tractable propargylic silyl ethers into complex cyclopropyl boronic esters, which could be subsequently transformed *via* Suzuki-Miyaura cross coupling.²³⁵ With this methodology now enabled, the next step was to explore the biological applications of the chemistry.

3.2.3 Synthesis of Sedaxane

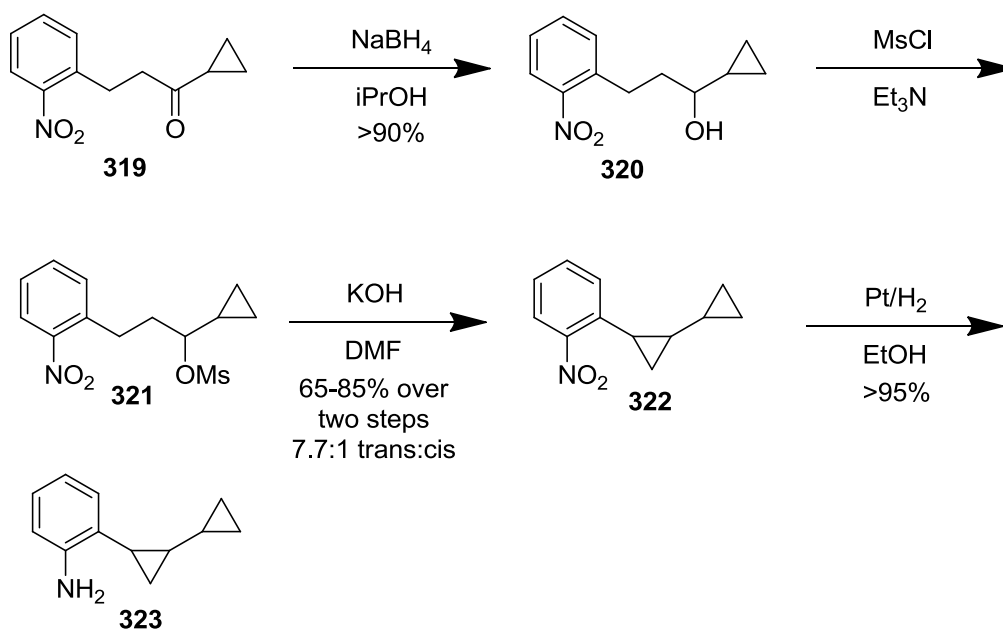
Sedaxane **318** is a succinate dehydrogenase inhibitor developed by Syngenta.²³⁶⁻²³⁸ The compound is used as a broad spectrum fungicide and is an active component of the marketed seed treatment Vibrance Duo. Seeds treated with Vibrance Duo result in faster establishment of roots and increased yield across a wide range of crops.²³⁸ The agrochemical is used as a mixture of cyclopropyl ring diastereoisomers, with the *trans*-diastereoisomer believed to be the active component.



Sedaxane
318

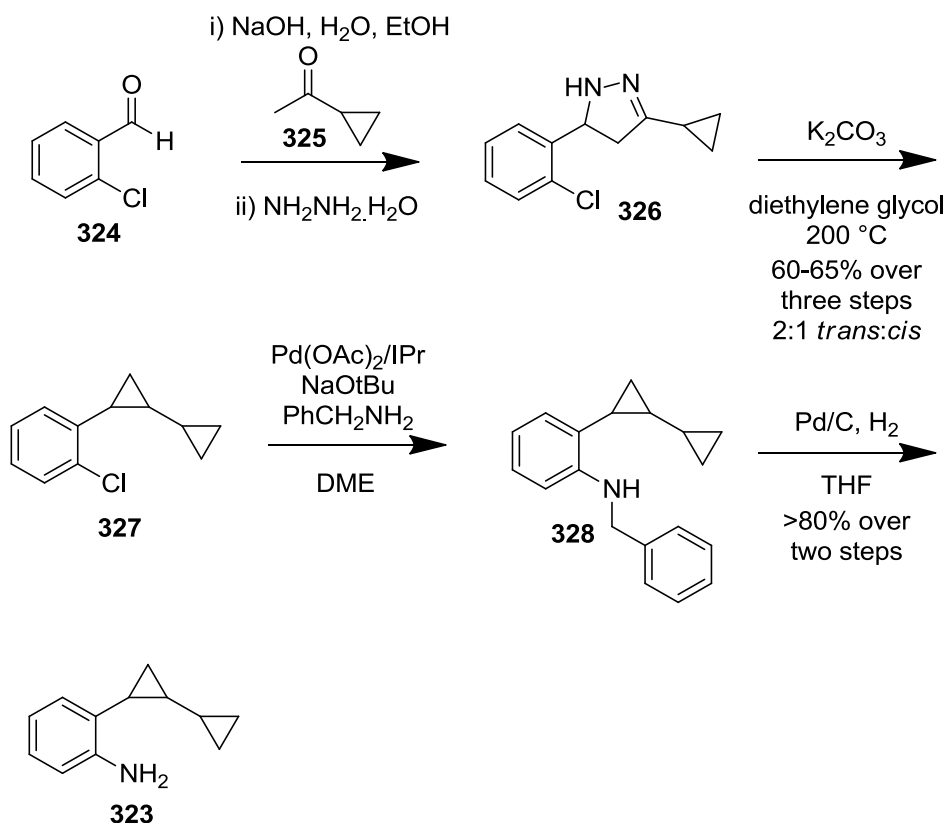
Figure 98 – The structure of Sedaxane, a broad-spectrum fungicide developed by Syngenta.

Synthesis of the *bis*-cyclopropyl aniline fragment **323** of the molecule has proved challenging; Syngenta has published two scale-up routes to this portion of the molecule (Scheme 59 and Scheme 60).



Scheme 59 – Syngenta synthesis of Sedaxane via a Nitro mediated benzyl deprotonation.

The first approach starts with nitrophenyl ketone **319**. Reduction of the ketone and subsequent mesylation gives intermediate compound **321**. The nitro- group then facilitates a benzyl deprotonation, which can cyclise onto the carbon bearing the mesylate leaving group to yield cyclopropyl ring product **322** with good *trans* selectivity. Hydrogenation then yields the key bis-cyclopropyl aniline fragment **323**. Whilst a reasonably efficient route, a robust synthesis of starting material **319** could not be developed and therefore the route was intractable.



Scheme 60 - Syngenta synthesis of Sedaxane via a Kizhner cyclisation.

An alternative route starts with an aldol reaction and hydrazine condensation to yield dihydropyrazole **326**. Under high temperature forcing conditions, this dihydropyrazole undergoes a Kizhner cyclisation^{239,240} to yield *bis*-cyclopropyl **327**. This can then be coupled to benzylamine under palladium catalysed conditions and the benzyl group removed under hydrogenolysis to yield *bis*-cyclopropyl aniline fragment **323**. The limitations of this route are the forcing conditions required for the cyclopropanation step. The route also introduces the cyclopropyl fragment early in the synthesis, meaning exploration of SAR in this region would require multistep syntheses.

It was reasoned that the newly developed borylation-cyclisation reaction could be used to synthesise the *bis*-cyclopropyl boronic ester component for an alternative synthesis of Sedaxane (Figure 99). There are only two methods to synthesise this boronic ester building block in the literature,²⁴¹⁻²⁴³ however both require multiple steps and multiple functional group interconversions to yield the product. Use of the nascent one-pot borylation-cyclisation methodology could enable facile access to this material.

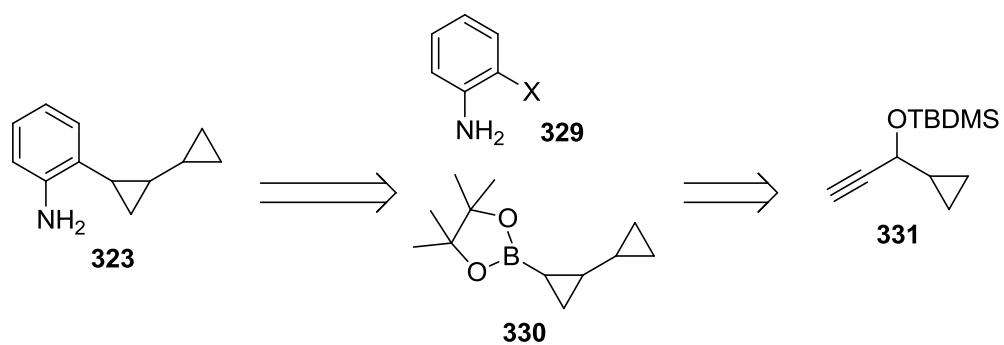
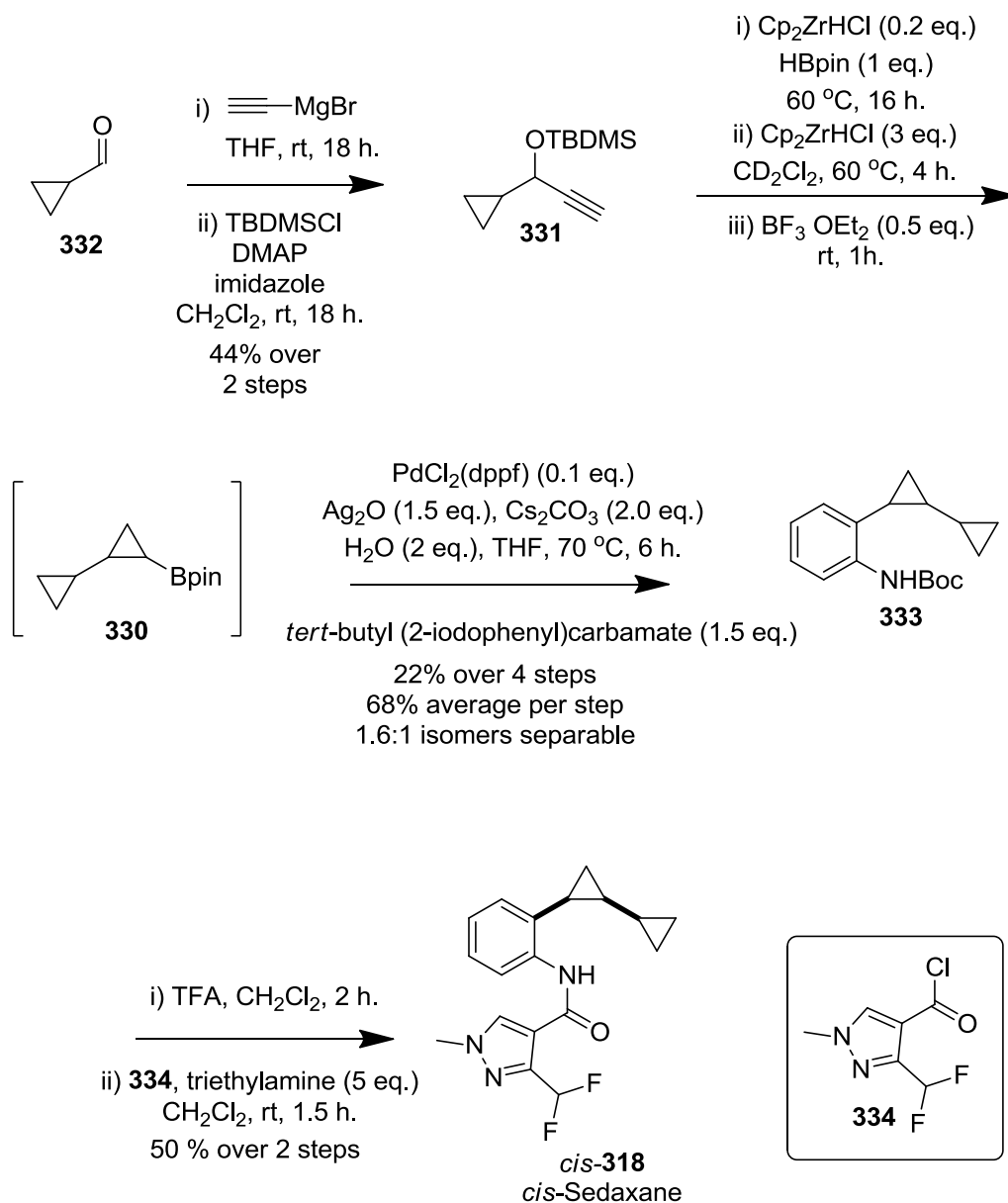


Figure 99 – Proposed synthesis of key fragment of Sedaxane.

This strategy was successfully employed, thus providing an alternative synthetic strategy for the synthesis of Sedaxane (Scheme 61).



Scheme 61 – The synthesis of Sedaxane via borylation-cyclisation methodology.

The synthesis commenced with readily available cyclopropyl aldehyde **332**, Grignard addition and silyl protection yielded substrate **331** for borylation-cyclisation in good yield. Application of the developed borylation-cyclisation protocol yielded bis-cyclopropyl boronic ester **330**, which was telescoped into the Suzuki-Miyaura cross coupling. This yielded protected *bis*-cyclopropyl aniline **333** in 18% yield over four steps, corresponding to an average of 65% per step, which is high considering the molecular complexity generated in the process. Boc-deprotection and amide coupling with acid chloride **334** ultimately yielded Sedaxane **318**.

CONFIDENTIAL – PROPERTY OF GSK – DO NOT COPY

The application of the borylation-cyclisation methodology identified a six-step synthesis, with an overall yield of 7%.²³⁵ Whilst this is slightly worse than the five transformations and >48% yield in Syngenta's preferred synthesis (Scheme 60), the route provides a more modular approach to the target. This would be of particular value in a discovery chemistry setting where it would be desirable to explore more diversity at this position.

3.2.4 Synthesis of PI3K δ Inhibitors

Returning to the PI3K δ template discussed previously, analogues of lactam compound **173** were sought. It was hypothesised that substitution of the cyclopropyl ring could provide novel growth vectors and improved properties for drug design.

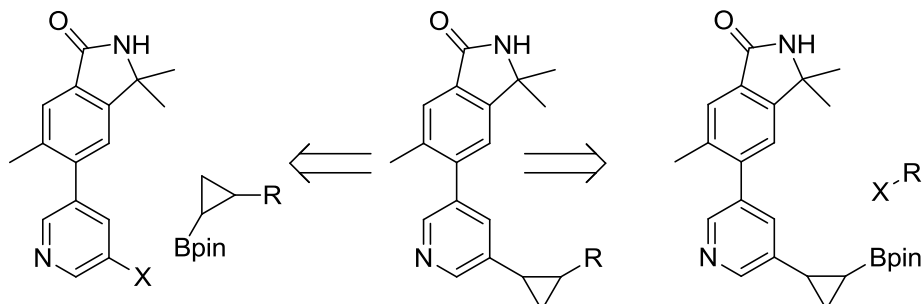
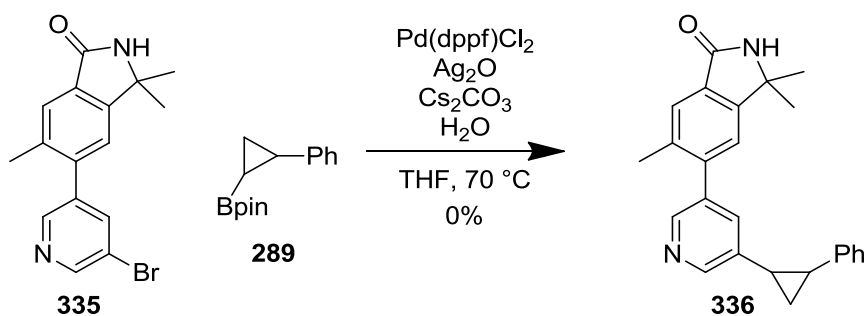


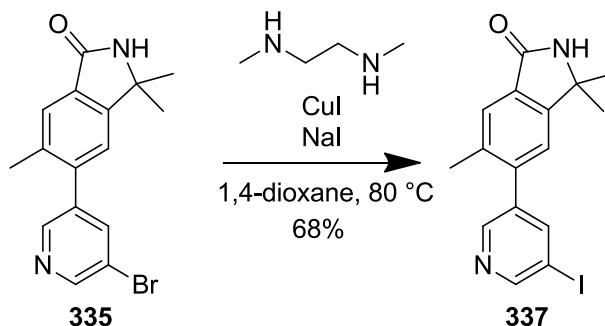
Figure 100 – Two possible Suzuki-Miyaura cross coupling disconnections for synthesis of lactam cyclopropyl analogues.

Two possible disconnection strategies were considered (Figure 100). The preferred strategy for modular synthetic design was to incorporate the cyclopropylboronic ester into the lactam portion of the molecule. This would then allow an array of aryl halides to be coupled to the same intermediate to generate multiple analogues for screening. However, previous substrate scoping of one-pot borylation-cyclopropanation methodology (Page 187) had already indicated it was unlikely to be productive for pyridine containing substrates. Hence, a disconnection strategy employing lactam halide and substituted cyclopropylboronic esters was used. This disconnection requires more synthetic steps, however allows incorporation of aliphatic as well as aryl R-groups. The lactam containing aryl bromide **335**, was a key building block already available within our laboratories.⁵⁶



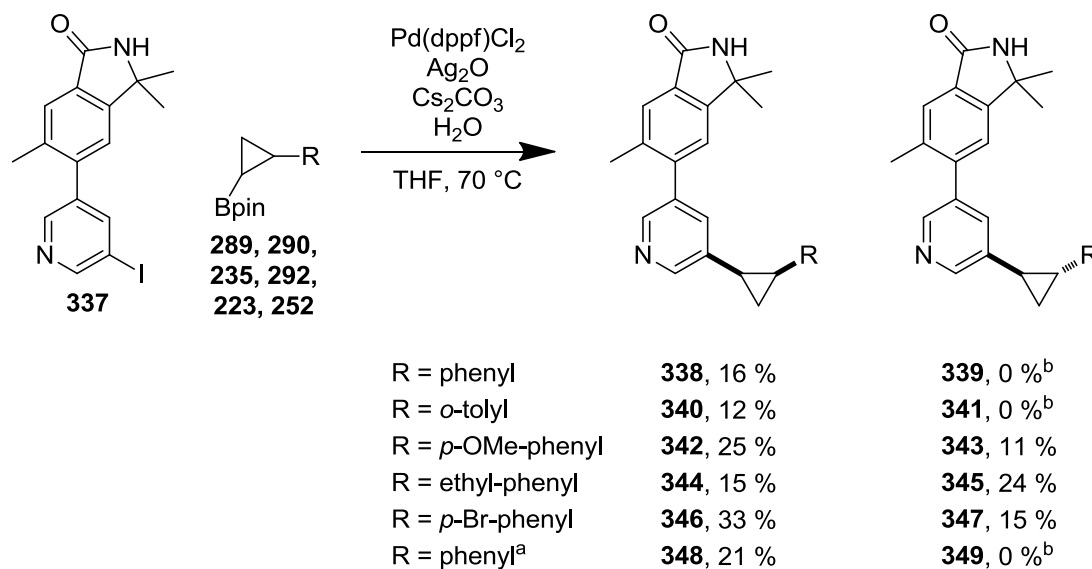
Scheme 62 – Unsuccessful Suzuki-Miyaura cross coupling reaction using lactam bromide.

Subjecting aryl bromide **335** to Suzuki-Miyaura cross coupling conditions²³⁴ showed no conversion to expected product (Scheme 62). It was hoped that aryl iodide **337** may have higher reactivity than aryl bromide **335**.²⁴⁴ Accordingly, an aromatic Finkelstein reaction²⁴⁵ was conducted.



Scheme 63 – Aromatic Finkelstein reaction to convert lactam bromide to lactam iodide.

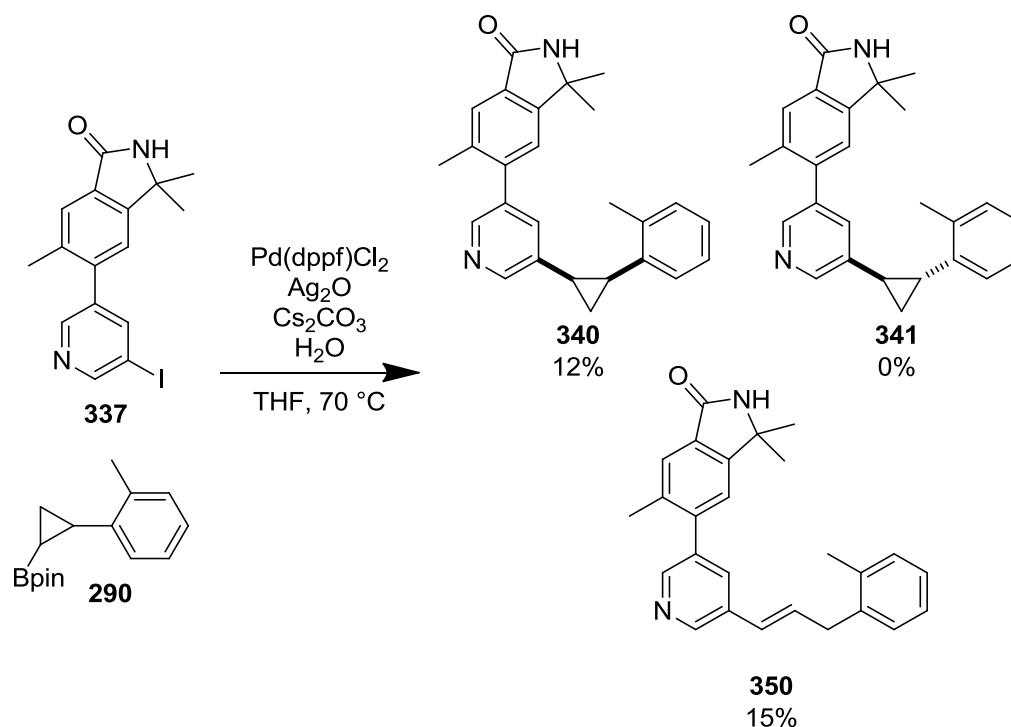
Subjecting aryl bromide **335** to copper catalysed halogen exchange conditions²⁴⁵ formed aryl iodide **337** in good yield (Scheme 63). Aryl iodide **337** was then subjected to Suzuki coupling conditions with a number of cyclopropylboronic esters prepared previously using the borylation-cyclisation methodology.



Scheme 64 – Suzuki-Miyaura cross-coupling reactions to explore substitution from cyclopropyl lactam. ^aEnantioenriched cyclopropylboronic ester was used. ^bAn alkene containing product was also isolated.

Pleasingly six cyclopropylboronic esters were coupled onto lactam iodide **337** using Suzuki-Miyaura coupling conditions²³⁴ in up to 48% combined yield of both diastereoisomers (Scheme 64). This yielded several substituted cyclopropyl analogues for biological profiling.

Trans-substituted cyclopropyl products could not be isolated in some cases and the reactions were found to yield only ring-opened alkene products and *cis*-substituted products (Scheme 65).



Scheme 65 – Products isolated from reaction of *ortho*-tolyl-cyclopropylboronic ester **290** with lactam iodide **337**.

Reaction of a diastereomeric mixture *ortho*-tolyl-cyclopropylboronic ester **290** with aryl iodide **337** yielded only *cis*-substituted product **340** and ring opened alkene product **350**. Analysis of the reaction mixture by LCMS showed two peaks with ionisation corresponding to product mass and matched the retention times of isolated products **340** and **350**. This indicates that *trans*-cyclopropane **341** is likely to decompose to ring opened alkene **350** under reaction conditions and not under work-up or purification conditions.

Mechanistically, it is proposed that the *cis*-cyclopropyl ring undergoes fast reductive elimination from palladium resulting in the cyclopropyl ring product. However, the *trans*-cyclopropyl ring has less steric bulk around the palladium centre and hence, this step may be slower. Therefore, an alternative pathway may be possible for the *trans* system, where either base mediated ring opening to give an aryl stabilised carbanion or a [1,3]-hydride shift to give vinylic palladium species, followed by reductive elimination could generate the ring opened products observed (Figure 101).

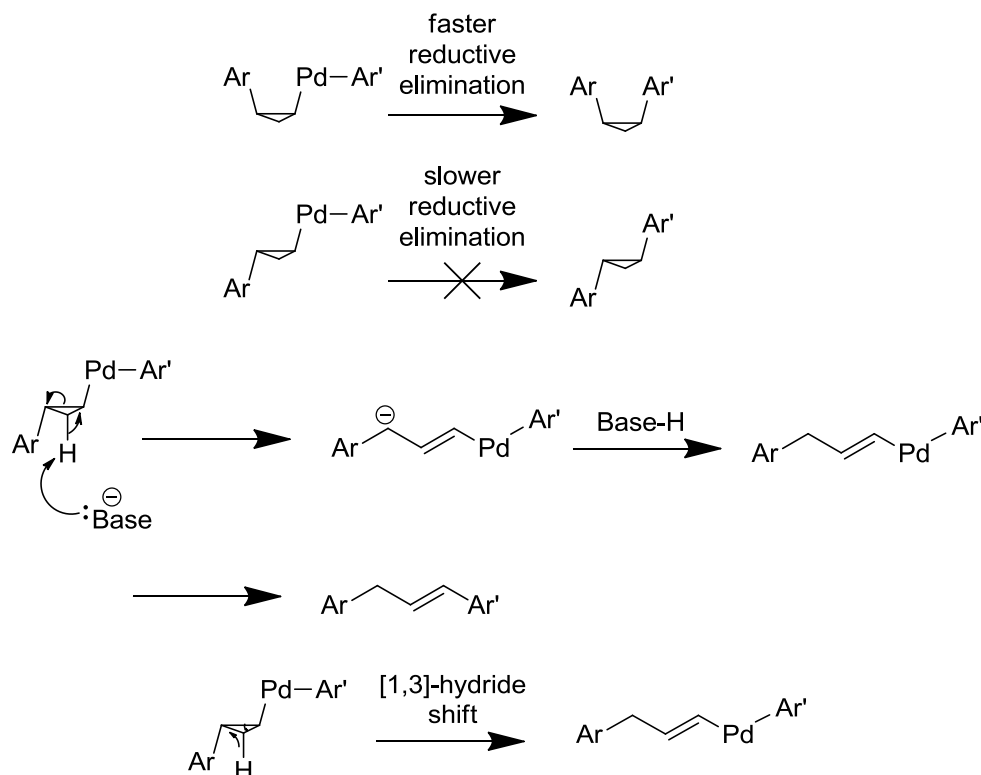
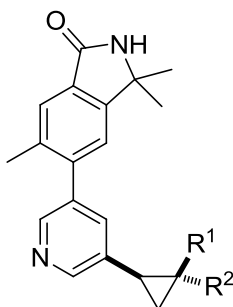


Figure 101 – Possible mechanism for formation of ring opened alkene species.

Despite the formation of a few ring opened alkene products, nine cyclopropyl containing analogues of cyclopropyl lactam **173** were synthesised. These molecules were then profiled in the available biological assays running in our laboratories.

***In vitro* PI3K α , PI3K β , PI3K γ and PI3K δ enzyme assay results for cyclopropyl lactam compounds**

	R ₁ =	R ₂ =	pIC ₅₀ PI3K				LE	Chrom logD pH 7.4
			δ	α	β	γ		
173	H	H	7.4	6.7	5.8	7.4	0.46	3.87
338	Ph	H	6.9*	6.6*	5.7*	6.9*	0.34	5.00
340	<i>o</i> -Me- C ₆ H ₄	H	7.3	6.7	5.1	7.2	0.34	5.89
342	<i>p</i> -OMe- C ₆ H ₄	H	6.8	5.7	5.3	7.1	0.30	4.96
343	H	<i>p</i> -OMe- C ₆ H ₄	7.5	6.8	5.6	7.3	0.33	5.15
344	C ₂ H ₄ -Ph	H	8.0	6.1	6.1	7.0	0.36	6.34
345	H	C ₂ H ₄ -Ph	7.5*	6.1*	5.2*	7.4*	0.34	6.29
346	<i>p</i> -Br- C ₆ H ₄	H	8.2	7.2	7.2	7.6	0.37	5.67
347	H	<i>p</i> -Br- C ₆ H ₄	7.3	6.6	5.5	7.2	0.33	6.39
348	Ph ^a	H	7.4	7.2	6.2	7.7	0.34	

Figure 102 – Biological data for compounds within the cyclopropyl lactam series. ^aenantioenriched cyclopropylboronic ester was used. All $n \geq 2$ unless otherwise indicated.* $n=1$

Biological profiling of analogues in the PI3K enzyme assays²⁴⁶ showed that substitution in both *cis* and *trans* orientations was tolerated. A small number of analogues (*cis*-4-Br-Ph **346** and *cis*-ethyl-Ph **344**) exhibited improved potency, with up to a 6-fold increase. *Cis*-ethyl-phenyl analogue **344** gave improved potency and improved selectivity over the other class I PI3K isoforms. However, all analogues

CONFIDENTIAL – PROPERTY OF GSK – DO NOT COPY

resulted in increased lipophilicity and potency increases which did not outweigh the additional molecular weight of the molecules; reflected in the lower ligand efficiencies.

However, since substitution is tolerated it may be advantageous to explore some less lipophilic analogues, such as heteroaromatic rings, or analogues containing functional groups known to interact strongly with tryptophan-760, such as saturated heterocyclic derivatives. However, further work is required to design and synthesise compounds of this type.

3.3 Summary and Conclusions

This methodology²³⁵ provides a modular approach, from simple, readily available starting materials to access complex three-dimensional cyclopropyl ring containing systems. A wide range of cyclopropylboronic esters, containing aliphatic, aromatic, quaternary and spiro substituents and be accessed *via* the reaction manifold. The method provides improvements upon literature procedures with regard to availability of reagents, scope of reaction and the modularity of the process. Hence, the reaction is a valuable addition to the available synthetic chemistry armamentarium.

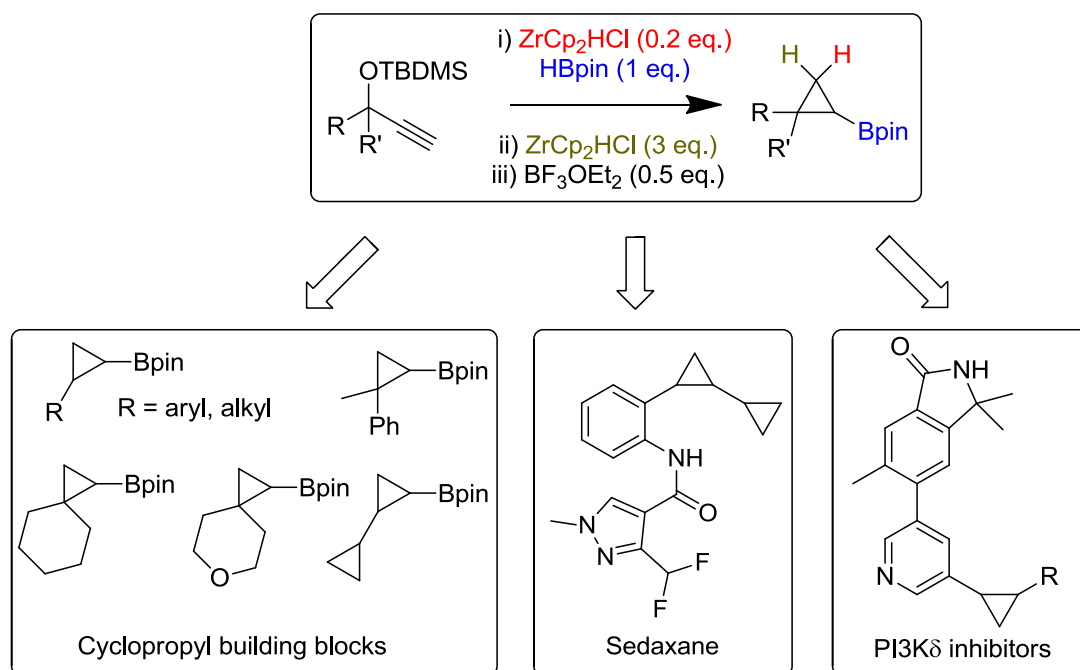


Figure 103 – Summary of methodology developed to enable a one-pot borylation-cyclopropanation and applications of the methodology.

This new approach also allows synthesis of biologically active agrochemical, Sedaxane **318**, *via* the concise synthesis of an interesting *bis*-cyclopropyl boronic ester motif. This route provides a useful alternative route to Sedaxane, providing further opportunities for analogue synthesis.

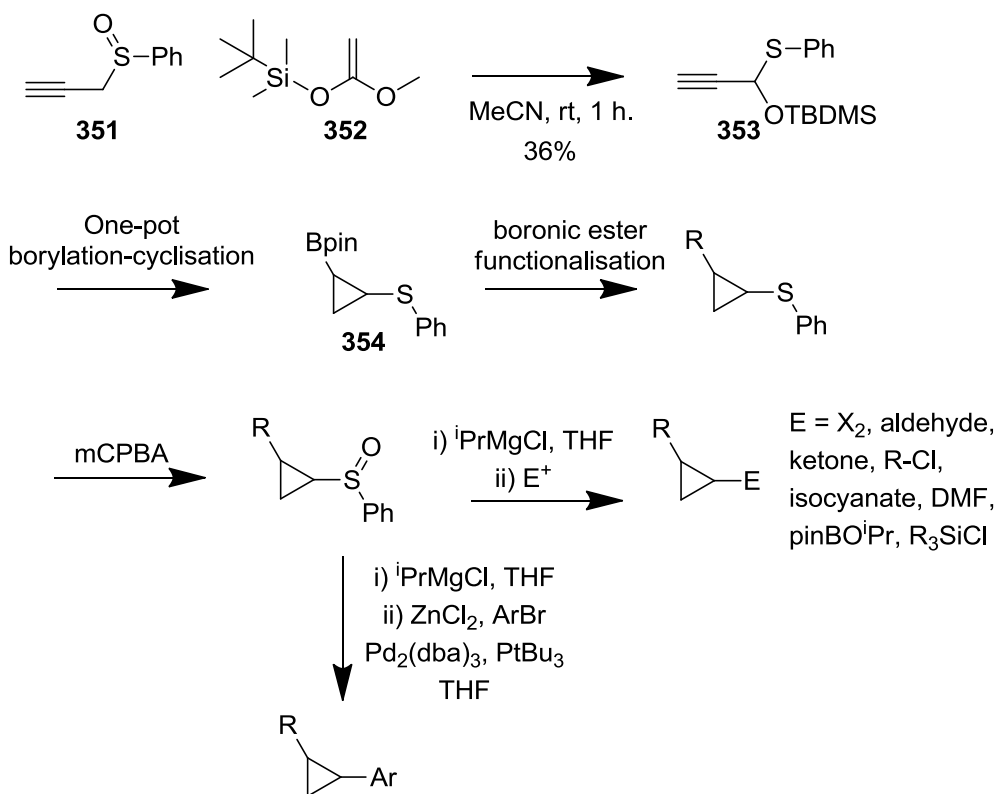
The methodology has also been applied to explore substitution from a cyclopropyl ring in a lead series of compounds to a target of interest to our laboratories, PI3Kδ. The work has shown that substitution is tolerated and can offer improvements in selectivity, however more optimisation is required to reach a candidate molecule.

3.4 Further Work

Re-optimisation of reaction conditions for the most selective silyl groups, as well as optimisation for the diastereomeric ratio may mean that a selective high yielding synthesis of cyclopropyl boronic esters could be developed. Optimisation of reaction conditions to favour *trans* cyclopropyl rings could be achieved using the small triethoxysilyl group and further optimisation could lead to high *cis* selectivity with the large tris(trimethyl)silyl group. It is possible that reducing the temperature for the hydrozirconation step may improve the selectivity leading to the kinetically favoured product in each case.

Further work is required to optimise the cyclopropyl lactam series of PI3K δ inhibitors. To further explore substitution of the cyclopropyl ring a number of more hydrophilic substituents should be tested. To explore this, it would be beneficial to have access to a cyclopropyl building block with orthogonal functionality to pinacol boronic ester.

Work from the Bull group has shown the synthetic utility of cyclopropyl phenyl sulfides.²⁴⁷ In addition to this, chemistry has been developed by Tamura to allow synthesis of the required starting materials (Scheme 66).²⁴⁸



Scheme 66 – Proposed synthesis and application of cyclopropyl boronic ester and sulfide functionality.

Tamura has shown that the required propargylic combined sulfide and silyl ether **353** can be synthesised *via* a Pummerer-type rearrangement.²⁴⁸ Subjecting this compound to one-pot borylation-cyclisation conditions could allow access to versatile intermediate **354**. It is proposed that cyclisation could occur selectively onto silyl ether, rather than phenyl sulfide, due to the stronger Lewis acid interaction between boron and oxygen. Intermediate **354** contains orthogonal boronic ester and sulfide functionality making a number of transformations possible and increasing the synthetic utility of the intermediate. The boronic ester functionality could be manipulated in a number of means discussed previously. Whilst Bull has shown that cyclopropyl sulfide functionality can be selectively oxidised to the corresponding sulfoxide. Treatment of this sulfoxide with a Grignard reagent yields a metallated cyclopropyl ring which could undergo reaction with a number of electrophiles to generate a wide range of functionality. The metallated intermediate could also undergo transmetallation to zinc enabling a Negishi cross-coupling reaction.

CONFIDENTIAL – PROPERTY OF GSK – DO NOT COPY

Access to compounds such as this would also negate the need for expansion of substrate scope of the one-pot borylation-cyclopropanation reaction, since functionality can be introduced selectively after the cyclopropanation has taken place.

Chapter 4. Conclusions

Two independent strategies have been explored to target the design and synthesis of small molecule PI3K δ inhibitors, which have led to a number of wider valuable findings.

Firstly, work to design and synthesise macrocyclic inhibitors has shown that macrocycles are tolerated within the PI3K δ binding site, adding to the literature supporting macrocyclic templates as attractive novel chemotypes for the inhibition of kinases and possibly other target classes.

The macrocycles have been compared to comparator acyclic compounds and the effect of macrocyclisation explored. In several instances macrocyclisation provided differentiation in biological or physicochemical properties, leading to the conclusion that a macrocyclisation approach could generate compounds in novel physicochemical, biochemical and intellectual property space.

Secondly, in design of PI3K δ inhibitors containing cyclopropyl rings, an opportunity for developing novel effective methodology to generate the requisite building blocks was explored. This resulted in a new reaction manifold which provides more facile reaction set up, more easy to synthesise starting materials and differentiated substrate scope to conditions available in the literature.

In summary, new knowledge has been added in the generation of a macrocyclisation case study and through conception and development of a new reaction manifold.

Chapter 5. Experimental

5.1 General Methods

All solvents were of analytical grade, purchased from Sigma Aldrich in anhydrous form. Unless otherwise stated reagents were purchased from regular suppliers, such as Sigma Aldrich or Fluorochem and used without further purification.

Thin layer chromatography (TLC) was carried out using plastic-backed precoated silica plates (particle size 0.2 mm). Spots were visualized by ultraviolet (UV) light ($\lambda_{\text{max}} = 254 \text{ nm}$ or 365 nm) and then stained with potassium permanganate solution followed by gentle heating.

Silica gel chromatography was carried out using the Teledyne ISCO CombiFlash[®] Rf+ apparatus with RediSep[®] silica cartridges or RediSep[®] C₁₈ reverse phase cartridges.

Chiral analytical and purification chromatography were conducted on an Agilent 1100 Series High-Performance Liquid Chromatography systems using the conditions detailed in individual experimentals.

Microwave reactions were carried out in a Biotage Initiator, using the conditions stated in each experimental.

Infrared spectra were recorded on a Perkin Elmer Spectrum One Fourier Transform spectrometer, with samples used neat. Only selected absorptions are reported and quoted in reciprocal centimetres (cm^{-1}).

¹H NMR were recorded on a Bruker AVI (400 MHz), Bruker Nano (400 MHz) or Bruker AVII+ (600 MHz) spectrometer. Chemical shifts (δ) are quoted in ppm relative to tetramethylsilane and are internally referenced to the residual solvent peak. Coupling constants (J) are given in Hz to the nearest 0.1 Hz (although are only accurate to +/- 0.5 Hz). The following abbreviations are used: s, singlet; d, doublet; t, triplet; q, quartet; dd, doublet doublet; m, multiplet; br., broad; app., apparent.

CONFIDENTIAL – PROPERTY OF GSK – DO NOT COPY

¹³C NMR were recorded on a Bruker AVI (400 MHz) or Bruker AVII+ (600 MHz) spectrometer. Chemical shifts (δ) are quoted in ppm relative to the residual solvent peak.

High resolution mass spectra were recorded using a Micromass Q-ToF Ultima hybrid quadrupole time-of-flight mass spectrometer equipped with a Z-spray (ESI) interface, over a mass range of 100-1100 Da, with a scan time of 0.9 s and an interscan delay of 0.1 s. Reserpine was used as the external mass calibrant ($[M+H]^+ = 609.2812$ Da). The Q-ToF Ultima mass spectrometer was operated in W reflection mode to give a resolution (FWHM) of 16000-20000. Ionisation was achieved with a spray voltage of 3.2 kV, a cone voltage of 100 V, with cone and desolvation gas flows of 10-20 and 600 L h⁻¹ respectively. The elemental composition was calculated using MassLynx v4.1 for the $[M+H]^+$.

LCMS Method A: The HPLC analysis was conducted on an Acquity UPLC BEH C₁₈ column (1.7 μ m, 2.1 mm x 50 mm) at 40 °C.

Solvent A = 0.1% v/v Formic Acid in water

Solvent B = 0.1% v/v Formic acid in acetonitrile

The gradient employed was:

Time (min)	Flow Rate (mL/min)	% A	% B
0	1	97	3
1.5	1	0	100
1.9	1	0	100
2	1	97	3

The UV detection was based on an averaged signal from wavelength of 210 nm to 350 nm and mass spectra were recorded on a mass spectrometer using alternate-scan positive and negative mode electrospray ionization.

CONFIDENTIAL – PROPERTY OF GSK – DO NOT COPY

LCMS Method B: The HPLC analysis was conducted on an Acquity UPLC BEH C₁₈ column (1.7 μm, 2.1 mm x 50 mm) at 40 °C.

Solvent A = 10 mM Ammonium Bicarbonate in water adjusted to pH 10 with ammonia solution

Solvent B = Acetonitrile

The gradient employed was:

Time (min)	Flow Rate (mL/min)	% A	% B
0	1	93	7
1.5	1	3	97
1.9	1	3	97
2	1	0	100

The UV detection was based on an averaged signal from wavelength of 210 nm to 350 nm and mass spectra were recorded on a mass spectrometer using alternate-scan positive and negative mode electrospray ionization.

Mass directed auto preparation (MDAP). Mass-directed automated purification was carried out using an H₂O_s ZQ MS using alternate-scan positive and negative electrospray and a summed UV wavelength of 210–350 nm. Two liquid phase methods were used:

Formic – Sunfire C18 column (100 mm x 19 mm, 5 μm packing diameter, 20 mL/min flow rate) or Sunfire C18 column (150 mm x 30 mm, 5 μm packing diameter, 40 mL/min flow rate). Gradient elution at ambient temperature with the mobile phases as (A) H₂O containing 0.1% volume/volume (v/v) formic acid and (B) acetonitrile containing 0.1% (v/v) formic acid.

High pH – Xbridge C18 column (100 mm x 19 mm, 5 μm packing diameter, 20 mL/min flow rate) or Xbridge C18 column (150 mm x 30 mm, 5 μm packing diameter, 40 mL/min flow rate). Gradient elution at ambient temperature with the mobile phases

CONFIDENTIAL – PROPERTY OF GSK – DO NOT COPY

as (A) 10 mM aqueous ammonium bicarbonate solution, adjusted to pH 10 with 0.88 M aqueous ammonia and (B) acetonitrile.

5.2 Experimental procedures

5.2.1 Procedures for Optimisation Screens

Sulfonamide Coupling Screen

To a solution of sulfonyl chloride (1 eq.) and base (1 eq.) in solvent (~0.2 M), was added amine (1 eq.). The mixture was then stirred at the specified temperature for the specified time. Reaction mixtures were then analysed by LCMS.

Buchwald-Hartwig Amination Screen

To catalyst (0.2 eq.), ligand (0.4 eq.), base (3 eq.) and amine (1 eq.) in a sealed degassed vial, was added a solution of aryl bromide (1 eq.) in 1,4-dioxane. The vial was then heated under microwave irradiation conditions to 140 °C for three hours. The reaction mixtures were then analysed by LCMS.

Lactam Coupling Screen

To a solution of amino acid (5 mg, 1 eq.) in solvent (0.1 mL), was added coupling agent (1 eq.) and additive if required (1 eq.). The mixtures were then stirred at the required temperature for 18 hours. The reaction mixtures were then analysed by LCMS.

Lactam Coupling Concentration Screen

A 0.25 mL portion of a solution of amino acid (40 mg, 1 eq.) in DMF (0.50 mL) was added to DMF (0.25 mL). Process was repeated six times to yield 8 solutions with two-fold difference in concentration between each solution. The same process was carried out to dilute down a solution of HATU (36 mg, 1 eq.) and DIPEA (33 µL, 1 eq.) in DMF (0.50 mL) to generate 8 solutions two-fold concentration difference. The corresponding mixtures were combined and the mixtures stirred for 18 hours. The reaction mixtures were then analysed by LCMS.

Lactam Reduction Reagents Screen

To a solution of lactam (5 mg, 1 eq.) in solvent (0.5 mL), was added reducing agent (1.1 eq.). The mixtures were then stirred at the required temperature for 6 hours. The reaction mixtures were then analysed by LCMS.

Lactam Reduction Temperature/Equivalents Screen

To a solution of lactam (5 mg, 1 eq.) in dry THF (0.5 mL) under anhydrous conditions, was added reducing agent (2-6 eq.). The reactions were then stirred at the required temperature for 6 hours and then analysed by LCMS.

Chloride Displacement Screen

To a solution of nucleophile (1-3 eq.) in solvent (1 mL), was added base (1.1 eq.) and the mixture was stirred at room temperature for 30 mins. Alkyl chloride (10 mg, 1 eq.) was then added and the mixture stirred for a further 6 hours. The reaction mixtures were then analysed by LCMS.

Ring Closing Metathesis Screen

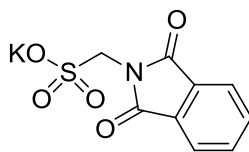
To a solution of catalyst (0.1 eq.) and additive (0.2 eq.) in solvent (0.2 mL), was added *N*-allyl-4-(5-(*N*-allylsulfamoyl)-6-methoxypyridin-3-yl)-3,4-dihydro-2*H*-benzo[*b*][1,4]oxazine-6-carboxamide (10 mg, 1 eq.). The reaction mixture was then stirred at reaction temperature for 2 hours, a sample was then analysed by LCMS.

Cyclopropanation Optimisation Screens

To Schwartz's Reagent (0.2 eq.) and 1,4-bis(trimethylsilyl)benzene (0.055 eq.), was added propargyl ether (1 eq.) and the mixture was stirred in a sealed microwave vial under an atmosphere of nitrogen for 30 mins at room temperature. Pinacol borane (1 eq.) was then added and the mixture stirred at 60 °C for 18 hours. Further Schwartz's Reagent (X eq.) and solvent (0.4 M reaction concentration) was then added and the mixture stirred at Y °C for a further Z hours. The reaction mixture was then cooled to room temperature, Lewis acid (A eq.) was added and the mixture stirred at room temperature for 1 hour. The crude reaction mixtures were then analysed by NMR.

5.2.2 Compound Synthesis and Characterisation – Benzoxazine Series

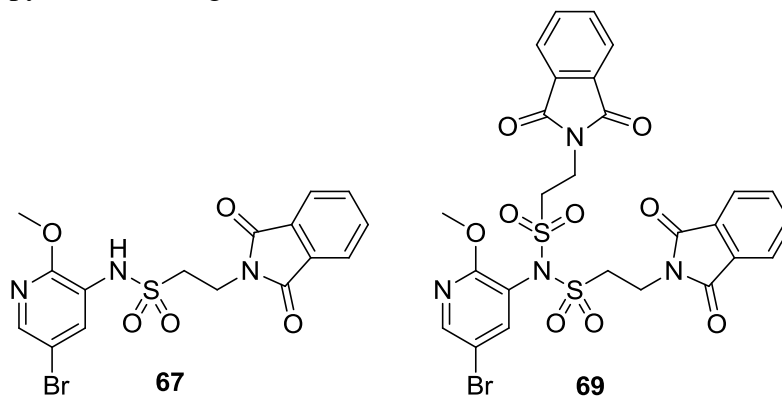
Potassium (1,3-dioxisoindolin-2-yl)methanesulfonate, 55



A suspension of aminomethanesulfonic acid (8.0 g, 72 mmol) and potassium acetate (7.8 g, 79 mmol) in acetic acid (30 mL) was refluxed for 10 minutes. Isobenzofuran-1,3-dione (11.7 g, 79 mmol) was then added and the resulting mixture was refluxed for 3 hours. The product was collected by filtration and washed with acetic acid (10 mL) and ethanol (10 mL) to give the title compound (14.0 g, 81% yield). $\nu_{\max}/\text{cm}^{-1}$ (neat) 1702, 1716, 1787; $^1\text{H NMR}$ (400 MHz, $\text{DMSO-}d_6$) δ 4.37 (s, 2H), 7.83-7.93 (m, 4H); $^{13}\text{C NMR}$ (101 MHz, $\text{DMSO-}d_6$) δ 53.9, 123.5, 132.1, 134.9, 166.7; LCMS (Method A): $[\text{M-K}]^-$ 240.1, R_t 0.64 min, 100% by UV; HRMS exact mass calculated for $[\text{M-K}]^-$ ($\text{C}_9\text{H}_6\text{NO}_5\text{S}$) requires m/z 239.9967, found 239.9967.

N-(5-Bromo-2-methoxypyridin-3-yl)-2-(1,3-dioxisoindolin-2-yl)methanesulfonamide, 69

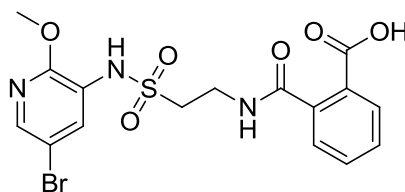
To a solution of 2-(1,3-dioxisoindolin-2-yl)ethane-1-sulfonyl chloride (2.0 g, 7.3 mmol) and pyridine (0.58 g, 7.3 mmol) in DCM (40 mL), was added 5-bromo-2-



methoxypyridin-3-amine (1.5 g, 7.3 mmol). The reaction mixture was then stirred at room temperature for 18 hours. The mixture was then diluted with water (50 mL) and extracted with DCM (3 x 50 mL). The organic portions were combined, dried over a hydrophobic frit and the solvent removed *in vacuo*. The sample was loaded preabsorbed on florisil and purified by column chromatography on silica using a 0-

50% ethyl acetate/cyclohexane gradient. The appropriate fractions were combined and concentrated *in vacuo* to give the title compound **67** as a white solid (920 mg, 29% yield) $\nu_{\max}/\text{cm}^{-1}$ (neat) 1708, 1767, 3284; $^1\text{H NMR}$ (400 MHz, CDCl_3) δ 3.48 (t, $J = 6.4$ Hz, 2H), 4.04 (s, 3H), 4.19 (t, $J = 6.1$ Hz, 2H), 7.77 (dd, $J = 5.5, 3.1$ Hz, 2H), 7.89 (dd, $J = 5.5, 3.1$ Hz, 2H), 7.93 (d, $J = 2.2$ Hz, 1H), 7.99 (d, $J = 2.3$ Hz, 1H); $^{13}\text{C NMR}$ (101 MHz, CDCl_3) δ 32.6, 48.9, 54.4, 112.0, 122.0, 123.6, 129.8, 131.8, 134.4, 142.6, 153.1, 168.0; LCMS (Method A): MH^+ 440, 442, Rt 1.09 min, 95% by UV; HRMS exact mass calculated for $[\text{M}+\text{H}]^+$ ($\text{C}_{16}\text{H}_{15}\text{BrN}_3\text{O}_5\text{S}$) requires m/z 439.9919, found 439.9919. Also isolated was the by-product **69** as a white solid (260 mg, 11% yield) $^1\text{H NMR}$ (400 MHz, CDCl_3) δ 4.05 (t, $J = 6.6$ Hz, 4H), 4.08 (s, 3H), 4.25-4.30 (m, 4H), 7.75 (dd, $J = 5.5, 3.1$ Hz, 4H), 7.87 (d, $J = 2.4$ Hz, 1H), 7.88 (dd, $J = 5.5, 3.1$ Hz, 4H), 8.30 (d, $J = 2.4$ Hz, 1H); LCMS (Method A): MH^+ 677, 679, Rt 1.25 min, 99% by UV.

2-((2-(*N*-(5-Bromo-2-methoxypyridin-3-yl)sulfamoyl)ethyl)carbamoyl)benzoic acid, 70

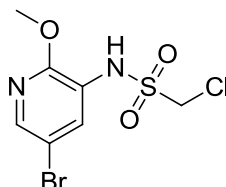


To a solution of *N*-(5-bromo-2-methoxypyridin-3-yl)-2-(1,3-dioxoisindolin-2-yl)-*N*-((2-(1,3-dioxoisindolin-2-yl)ethyl)sulfonyl)ethane-1-sulfonamide (250 mg, 0.4 mmol), methanol (3 mL) and THF (9 mL), was added 2M aqueous sodium hydroxide (5 mL, 10.0 mmol). The reaction mixture was then stirred at room temperature for 24 hours. The reaction mixture was then acidified with 2M hydrochloric acid to pH 2 and extracted with DCM (3 x 10 mL). The organic portions were combined, dried over a hydrophobic frit and the solvent removed *in vacuo* to yield 2-((2-(*N*-(5-bromo-2-methoxypyridin-3-yl)sulfamoyl)ethyl)carbamoyl)benzoic acid (180 mg, quantitative yield) as a white solid. $\nu_{\max}/\text{cm}^{-1}$ (neat) 1644, 1712, 3065 (broad); $^1\text{H NMR}$ (400 MHz, CDCl_3) δ 3.46-3.51 (m, 2H), 3.94 (s, 3H), 3.98 (app. q, $J = 5.9$ Hz, 2H), 6.75 (br. t, $J = 5.6, 5.6$ Hz, 1H), 7.13 (br. d, $J = 3.2$ Hz, 1H), 7.51 (dt, $J = 7.6, 1.0$ Hz, 1H), 7.56 (tt, $J = 7.6, 1.2$ Hz, 1H), 7.63 (tt, $J = 7.3, 1.0$ Hz, 1H), 7.90 (d, $J = 2.2$ Hz, 1H), 8.00 (d, $J = 2.2$ Hz, 1H), 8.06 (dt, $J = 7.6, 1.7$ Hz, 1H); $^{13}\text{C NMR}$ (101 MHz, $\text{DMSO}-d_6$) δ 34.5,

CONFIDENTIAL – PROPERTY OF GSK – DO NOT COPY

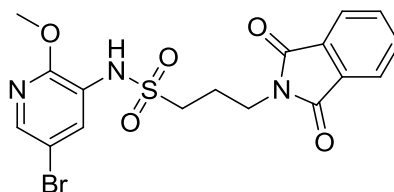
51.6, 55.4, 111.1, 123.0, 123.6, 128.0, 129.8, 130.7, 131.9, 133.9, 138.7, 143.1, 156.0, 168.1, 169.3; LCMS (Method A): MH^+ 458, 460, Rt 0.87 min, 90% by UV; HRMS exact mass calculated for $[M+H]^+$ ($C_{16}H_{17}BrN_3O_6S$) requires m/z 458.0021, found 458.0022.

***N*-(5-Bromo-2-methoxypyridin-3-yl)-1-chloromethanesulfonamide, 65**



To a solution of chloromethanesulfonyl chloride (0.73 g, 4.9 mmol) in DCM (25 mL), was added pyridine (0.40 mL, 4.9 mmol) and the reaction was stirred at room temperature for 20 mins. To this was added 5-bromo-2-methoxypyridin-3-amine (1.0 g, 4.9 mmol). The reaction mixture was then stirred at room temperature for 4 hours. The reaction was then quenched with water (25 mL) and extracted with DCM (3 x 20 mL). The organic portions were combined and the solvent removed *in vacuo*. The sample was loaded in DCM and purified by column chromatography on silica using a 0-50% ethyl acetate/cyclohexane gradient. The appropriate fractions were dried down *in vacuo* to yield *N*-(5-bromo-2-methoxypyridin-3-yl)-1-chloromethanesulfonamide (0.62 g, 40% yield) as a brown solid. ν_{max}/cm^{-1} (neat) 1582, 3255; 1H NMR (400 MHz, $DMSO-d_6$) δ 3.92 (s, 3H), 5.09 (s, 2H), 7.83 (d, $J = 2.20$ Hz, 1H), 8.15 (d, $J = 2.20$ Hz, 1H), 10.03 (br. s., 1H); ^{13}C NMR (101 MHz, $DMSO-d_6$) δ 54.5, 56.8, 110.9, 122.3, 135.5, 144.0, 156.7; LCMS (Method B): MH^+ 315, Rt 0.58 min, 81% by UV; HRMS exact mass calculated for $[M+H]^+$ ($C_7H_9BrClN_2O_3S$) requires m/z 314.9206, found 314.9205.

***N*-(5-Bromo-2-methoxypyridin-3-yl)-3-(1,3-dioxisoindolin-2-yl)propane-1-sulfonamide, 68**

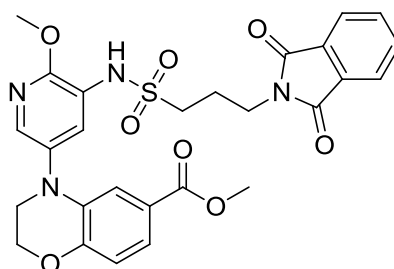


To a solution of pyridine (6.9 g, 87 mmol), 3-(1,3-dioxisoindolin-2-yl)propane-1-sulfonyl chloride (5.0 g, 17 mmol) in DCM (40 mL), was added 5-bromo-2-

CONFIDENTIAL – PROPERTY OF GSK – DO NOT COPY

methoxypyridin-3-amine (3.5 g, 17 mmol). The reaction mixture was then stirred at room temperature for 18 hours. The reaction was quenched with water (50 mL), and the organic phase separated and dried over a hydrophobic frit. The solvent was then removed *in vacuo*, the residue was loaded preabsorbed on florisil and purified by column chromatography on silica 80 g using a 0-100% ethyl acetate/cyclohexane gradient. The appropriate fractions were combined and concentrated *in vacuo* to give the title compound (2.3 g, 29% yield) as an off-white solid. $\nu_{\max}/\text{cm}^{-1}$ (neat) 1707, 1770, 3289; $^1\text{H NMR}$ (400 MHz, CDCl_3) δ 2.18-2.27 (m, 2H), 3.17-3.23 (m, 2H), 3.82 (t, $J = 6.6$ Hz, 2H), 4.01 (s, 3H), 6.71 (s, 1H), 7.76 (dd, $J = 5.5, 3.1$ Hz, 2H), 7.83-7.89 (m, 4H); $^{13}\text{C NMR}$ (101 MHz, $\text{DMSO-}d_6$) δ 23.1, 36.5, 50.6, 54.4, 111.0, 123.0, 123.5, 132.1, 134.1, 134.8, 143.0, 155.9, 168.4; LCMS (Method A): MH^+ 454, 456, R_t 1.09 min, 95% by UV; HRMS exact mass calculated for $[\text{M}+\text{H}]^+$ ($\text{C}_{17}\text{H}_{17}\text{BrN}_3\text{O}_5\text{S}$) requires m/z 454.0073, found 454.0071.

Methyl 4-(5-(3-(1,3-dioxoisindolin-2-yl)propylsulfonamido)-6-methoxypyridin-3-yl)-3,4-dihydro-2H-benzo[*b*][1,4]oxazine-6-carboxylate, 71

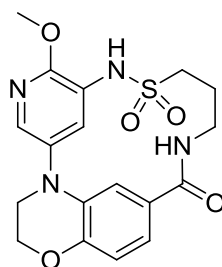


To caesium carbonate (4.3 g, 13 mmol), RuPhos Pd G2 (0.68 g, 0.9 mmol), methyl 3,4-dihydro-2H-benzo[*b*][1,4]oxazine-6-carboxylate (0.85 g, 4.4 mmol) and dicyclohexyl(2',6'-diisopropoxy-[1,1'-biphenyl]-2-yl)phosphane (0.82 g, 1.7 mmol) in a sealed degassed vial, was added a solution of *N*-(5-bromo-2-methoxypyridin-3-yl)-3-(1,3-dioxoisindolin-2-yl)propane-1-sulfonamide (2.0 g, 4.4 mmol) in dry 1,4-dioxane (15 mL). The reaction mixture was heated under microwave conditions to 140 °C for 3 hours. The reaction mixture was filtered through celite and washed with methanol (50 mL). The solvent was then removed *in vacuo*. The residue was dissolved in water (20 mL), extracted with ethyl acetate (20 mL) and washed with further ethyl acetate (20 mL). The solvent was then removed *in vacuo* and the residue was loaded preabsorbed on florisil and purified by column chromatography on silica using a 0-

CONFIDENTIAL – PROPERTY OF GSK – DO NOT COPY

100% ethyl acetate/cyclohexane gradient. This yielded the title compound (1.74 g, 70% yield) as a clear oil. $\nu_{\max}/\text{cm}^{-1}$ (neat) 1709, 1771, 2931; ^1H NMR (400 MHz, CDCl_3) δ 2.21-2.29 (m, 2H), 3.22-3.28 (m, 2H), 3.67-3.72 (m, 2H), 3.81 (s, 3H), 3.86 (t, $J = 6.7$ Hz, 2H), 4.05 (s, 3H), 4.38-4.42 (m, 2H), 6.76 (s, 1H), 6.91 (d, $J = 8.3$ Hz, 1H), 7.40 (d, $J = 2.0$ Hz, 1H), 7.47 (dd, $J = 8.3, 2.0$ Hz, 1H), 7.72-7.76 (m, 3H), 7.80-7.86 (m, 3H); ^{13}C NMR (151 MHz, CDCl_3) δ 23.3, 36.1, 48.6, 49.8, 51.8, 54.2, 64.7, 116.8, 117.0, 121.8, 122.2, 123.1, 123.4, 123.8, 131.9, 132.6, 134.2, 137.3, 137.5, 148.6, 150.9, 166.8, 168.1; LCMS (Method A): MH^+ 567, R_t 1.17 min, 90% by UV; HRMS exact mass calculated for $[\text{M}+\text{H}]^+$ ($\text{C}_{27}\text{H}_{27}\text{N}_4\text{O}_8\text{S}$) requires m/z 567.1551, found 567.1547.

9-Methoxy-2-oxa-12-thia-5,8,11,16-tetraazatetracyclo[16.2.2.16,(10),0(20,5)]tricoso-1(20),6(23),7,9,18,21-hexaen-17-one 12,12-dioxide, 77

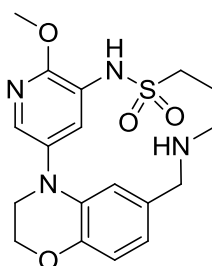


To a solution of methyl 4-(5-((3-(1,3-dioxoisoindolin-2-yl)propyl)sulfonamido)-6-methoxypyridin-3-yl)-3,4-dihydro-2H-benzo[b][1,4]oxazine-6-carboxylate (220 mg, 0.4 mmol) in ethanol (25 mL) and water (25 mL), was added lithium hydroxide (190 mg, 7.8 mmol). The reaction mixture was then heated at reflux for 4 days. The solvent was then removed *in vacuo*. The residue was loaded in water onto an isolute-103 cartridge. The cartridge was washed with water (50 mL), followed by methanol (50 mL). The methanol containing portion was then concentrated *in vacuo* to yield a white solid (124 mg). To a solution of white solid (50 mg, 0.12 mmol) in DMF (10 mL), was added HATU (45.0 mg, 0.12 mmol) and DIPEA (0.04 mL, 0.24 mmol). The reaction mixture was then stirred at room temperature for 3 days. The solvent was removed *in vacuo* and the residue was dissolved in DMSO and purified by mass directed HPLC on Sunfire C18 column using acetonitrile/water with a formic acid modifier. The solvent was removed *in vacuo* to give the title compound (2 mg, 4% yield) as an off-

CONFIDENTIAL – PROPERTY OF GSK – DO NOT COPY

white solid. $\nu_{\max}/\text{cm}^{-1}$ (neat) 1606, 1711, 2935; ^1H NMR (400 MHz, DMSO- d_6) δ 1.70 (quin, $J = 7.0$ Hz, 2H), 2.71 (t, $J = 7.5$ Hz, 2H), 3.28 (t, $J = 6.0$ Hz, 2H), 3.77-3.82 (m, 2H), 3.89 (s, 2H), 4.07 (s, 3H), 4.27-4.31 (m, 2H), 6.76 (dd, $J = 8.0, 1.8$ Hz, 1H), 6.86-6.91 (m, 1H), 6.89 (d, $J = 8.0$ Hz, 1H), 7.14 (dd, $J = 8.2, 2.1$ Hz, 1H), 7.20 (d, $J = 2.1$ Hz, 1H), 7.74 (d, $J = 2.7$ Hz, 1H), 8.25 (d, $J = 2.7$ Hz, 1H); ^{13}C NMR (101 MHz, CDCl_3) δ 21.1*, 37.6*, 45.8 $^\wedge$, 48.9*, 54.1, 65.0, 113.1, 117.7, 119.6*, 120.5*, 123.9 $^\wedge$, 129.4*, 131.4*, 134.3, 135.5*, 146.7*, 150.5*, 107.4*, *Peak not observed in 1D ^{13}C spectrum due to poor signal to noise ratio, coupling detected to this chemical shift in HMBC, $^\wedge$ Peak not observed in 1D ^{13}C spectrum, coupling detected to this chemical shift in HSQC; LCMS (Method A): MH^+ 405, Rt 0.81min, 98% by UV; HRMS exact mass calculated for $[\text{M}+\text{H}]^+$ ($\text{C}_{18}\text{H}_{21}\text{N}_4\text{O}_5\text{S}$) requires m/z 405.1232, found 405.1230.

9-Methoxy-2-oxa-12-thia-5,8,11,16-tetraazatetracyclo[16.2.2.16,(10),0(20,5)]tricoso-1(20),6(23),7,9,18,21-hexaene 12,12-dioxide, 78

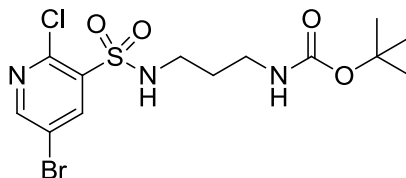


To a solution of 26-methoxy-13,14-dihydro-12H-4-thia-3,8-diaza-1(4,6)-benzo[*b*][1,4]oxazina-2(3,5)-pyridinacyclononaphan-9-one 4,4-dioxide (2.0 mg, 0.005 mmol) in THF (0.5 mL) was added 2M DIBAL-H in THF (0.015 mL, 0.030 mmol). the mixture was then stirred at room temperature for 6 hours. The reaction was then quenched with 1M aqueous potassium sodium tartrate (1 mL) and extracted with DCM (1 mL). The solvent was then removed *in vacuo*. The residue was dissolved in DMSO and purified by mass directed HPLC on an Xbridge column using acetonitrile:water with an ammonium carbonate modifier. The solvent was removed *in vacuo* to give the title compound (1.2 mg, 62%) as a clear oil. $\nu_{\max}/\text{cm}^{-1}$ (neat) 1508, 1586, 2939; ^1H NMR (400 MHz, MeOD) δ 1.70 (quin, $J = 7.0$ Hz, 2H), 2.71 (t, $J = 7.5$ Hz, 2H), 3.28 (t, $J = 6.0$ Hz, 2H), 3.77-3.82 (m, 2H), 3.89 (s, 2H), 4.07 (s, 3H), 4.27-4.31 (m, 2H), 6.76 (dd, $J = 8.0, 1.8$ Hz, 1H), 6.86-6.91 (m, 1H), 6.89 (d, $J = 8.0$

CONFIDENTIAL – PROPERTY OF GSK – DO NOT COPY

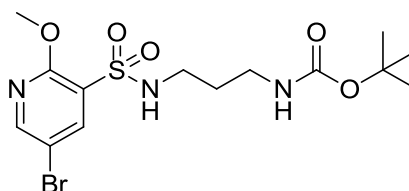
Hz, 1H), 8.09 (d, $J = 2.6$ Hz, 1H), 8.29 (d, $J = 2.5$ Hz, 1H); LCMS (Method A): MH^+ 391, Rt 0.42 min, 92% by UV; HRMS exact mass calculated for $[M+H]^+$ ($C_{18}H_{23}N_4O_4S$) requires m/z 391.1440, found 391.1437. Not enough material remained after biological testing to obtain a ^{13}C NMR spectrum.

***Tert*-butyl (3-(5-bromo-2-chloropyridine-3-sulfonamido)propyl)carbamate, 84**



To a solution of 5-bromo-2-chloropyridine-3-sulfonyl chloride (2.5 g, 8.6 mmol) in 1,4-dioxane (20 mL), was added neat pyridine (1 mL, 12.9 mmol). The reaction mixture was stirred at room temperature for 20 mins. To the reaction mixture, was then added a solution of *tert*-butyl (3-aminopropyl)carbamate (1.95 g, 11.2 mmol) in 1,4-dioxane (15 mL) in four aliquots over a one hour period. The reaction was then stirred at room temperature for 16 hours. The solvent was removed *in vacuo* and the residue dissolved in water (30 mL) and extracted with ethyl acetate (30 mL). The aqueous layer was washed with further ethyl acetate (30 mL) and the organic layers were combined and dried through a hydrophobic frit. The solvent was then removed *in vacuo* to yield the title compound (3.22 g, 87%) as an off white solid; ν_{max}/cm^{-1} (neat) 1689, 2901, 2972; 1H NMR (400 MHz, DMSO- d_6) δ 1.36 (s, 9H), 1.44-1.66 (m, 2H), 2.89 (t, $J = 5.9$ Hz, 2H), 2.91 (t, $J = 5.9$ Hz, 2H), 6.73 (br. s., 1H), 8.24 (br. s., 1H), 8.44 (d, $J = 2.3$ Hz, 1H), 8.83 (d, $J = 2.3$ Hz, 1H); ^{13}C NMR (101 MHz, DMSO- d_6) δ 28.7, 30.4, 37.7, 40.9, 78.0, 119.6, 136.7, 141.9, 146.0, 153.8, 156.0; LCMS (Method A): $[M-H]^-$ 426, 428, Rt 1.13 min, 92% by UV; HRMS exact mass calculated for $[M+H]^+$ ($C_{13}H_{20}BrClN_3O_4S$) requires m/z 428.0041, found 428.0052.

***Tert*-butyl (3-(5-bromo-2-methoxypyridine-3-sulfonamido)propyl)carbamate, 85**

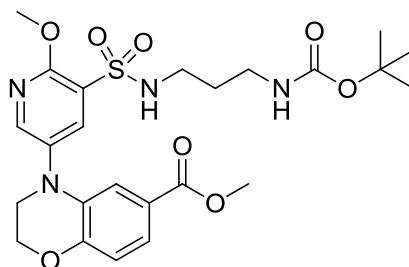


To sodium methoxide (3 x 0.94 g, 17.4 mmol) and *tert*-butyl (3-(5-bromo-2-chloropyridine-3-sulfonamido)propyl)carbamate (3 x 1.0 g, 2.3 mmol), was added

CONFIDENTIAL – PROPERTY OF GSK – DO NOT COPY

methanol (3 x 16 mL). Each reaction vial was sealed and heated under microwave irradiation to 120 °C for 1 hour. After cooling the reaction vials were combined and quenched with water (50 mL). The mixture was then extracted with ethyl acetate (20 mL), however partitioning was not observed, so brine (20 mL) was added, and partitioning was still not observed. The mixture was then extracted with DCM (2 x 25 mL) and the organic layers combined. These layers were then dried on a hydrophobic frit and the solvent removed *in vacuo* yielding the title compound (2.79 g, 94%) as an off white solid. $\nu_{\max}/\text{cm}^{-1}$ (neat) 1682, 3305; $^1\text{H NMR}$ (400 MHz, DMSO-*d*6) δ 1.36 (s, 9H), 1.43-1.56 (m, 2H), 2.81-2.92 (m, 4H), 4.00 (s, 3H), 6.73 (br. s., 1H), 7.69 (s, 1H), 8.16 (d, $J = 2.4$ Hz, 1H), 8.55 (d, $J = 2.4$ Hz, 1H); $^{13}\text{C NMR}$ (101 MHz, DMSO-*d*6) δ 28.7, 30.3, 37.7, 41.0, 55.0, 79.6, 111.0, 125.1, 141.1, 151.8, 156.1, 158.7; LCMS (Method A): $[\text{M}-\text{H}]^-$ 422, 424, Rt 1.12 min, 95% by UV; HRMS exact mass calculated for $[\text{M}+\text{H}]^+$ ($\text{C}_{14}\text{H}_{23}\text{BrN}_3\text{O}_5\text{S}$) requires m/z 424.0536, found 424.0535.

Methyl 4-(5-(*N*-(3-((*tert*-butoxycarbonyl)amino)propyl)sulfamoyl)-6-methoxy-pyridin-3-yl)-3,4-dihydro-2*H*-benzo[*b*][1,4]oxazine-6-carboxylate, 86

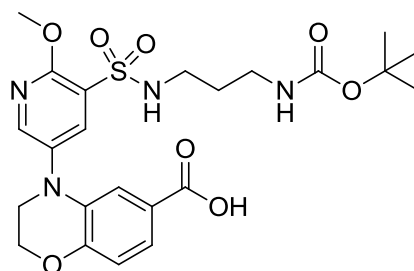


To *tert*-butyl (3-(5-bromo-2-methoxypyridine-3-sulfonamido)propyl)carbamate (2 x 1.25 g, 3.0 mmol), methyl 3,4-dihydro-2*H*-benzo[*b*][1,4]oxazine-6-carboxylate (2 x 0.57 g, 3.0 mmol), dicyclohexyl(2',6'-diisopropoxy-[1,1'-biphenyl]-2-yl)phosphine (2 x 0.14 g, 0.30 mmol), chloro(2-dicyclohexylphosphino-2',6'-diisopropoxy-1,1'-biphenyl)[2-(2'-amino-1,1'-biphenyl)]palladium(II), (2 x 0.23 g, 0.30 mmol) and caesium carbonate (2 x 2.88 g, 8.8 mmol) was added 1,4-dioxane (2 x 14 mL). Each reaction vial was sealed and heated under microwave irradiation to 120 °C for 2 hours. After cooling the reaction vials were combined, filtered through celite, washed with DCM (10 mL) and the solvent removed *in vacuo*. The residue was then dissolved in water (20 mL), extracted with ethyl acetate (20 mL) and washed with further ethyl acetate (20 mL). The organic layers were then combined, dried over a hydrophobic frit

CONFIDENTIAL – PROPERTY OF GSK – DO NOT COPY

and the solvent removed *in vacuo*. The residue was then loaded, preabsorbed on florisil, and purified by column chromatography on ethyl acetate/cyclohexane gradient. The appropriate fractions were combined and concentrated *in vacuo* to give the title compound (2.66 g, 84%) as a brown oil which solidified on standing. $\nu_{\max}/\text{cm}^{-1}$ (neat) 1693, 2901, 2988; $^1\text{H NMR}$ (400 MHz, $\text{DMSO-}d_6$) δ 1.38 (s, 9H), 1.50 (quin, $J = 6.7$ Hz, 2H), 2.79-2.95 (m, 4H), 3.73 (s, 3H), 3.74 (t, $J = 4.4$ Hz, 2H), 4.04 (s, 3H), 4.39 (t, $J = 4.3$ Hz, 2H), 6.72 (br. s., 1H), 6.95 (d, $J = 8.3$ Hz, 1H), 7.14 (d, $J = 2.0$ Hz, 1H), 7.36 (dd, $J = 8.3, 2.0$ Hz, 1H), 7.61 (br. s., 1H), 8.02 (d, $J = 2.8$ Hz, 1H), 8.41 (d, $J = 2.8$ Hz, 1H); $^{13}\text{C NMR}$ (101 MHz, $\text{DMSO-}d_6$) δ 21.2, 28.7, 30.4, 37.8, 40.9, 48.3, 52.3, 54.8, 65.1, 78.0, 115.6, 117.4, 121.9, 122.6, 124.1, 133.4, 136.1, 136.5, 147.9, 148.9, 156.6, 166.3, 170.8; LCMS (Method A): MH^+ 537, R_t 1.20 min, 83% by UV; HRMS exact mass calculated for $[\text{M}+\text{H}]^+$ ($\text{C}_{24}\text{H}_{33}\text{N}_4\text{O}_8\text{S}$) requires m/z 537.2014, found 537.1996.

4-(5-(*N*-(3-((*Tert*-butoxycarbonyl)amino)propyl)sulfamoyl)-6-methoxypyridin-3-yl)-3,4-dihydro-2*H*-benzo[*b*][1,4]oxazine-6-carboxylic acid, 87

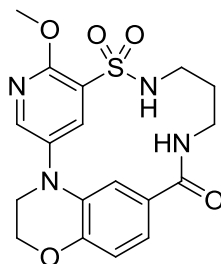


To a solution of methyl 4-(5-(*N*-(3-((*tert*-butoxycarbonyl)amino)propyl)sulfamoyl)-6-methoxypyridin-3-yl)-3,4-dihydro-2*H*-benzo[*b*][1,4]oxazine-6-carboxylate (2.60 g, 4.85 mmol) in THF (12 mL) and water (12 mL), stirred at room temperature, was added lithium hydroxide (0.70 g, 29.1 mmol). The reaction mixture was stirred at room temperature for 48 hours. The reaction mixture was then acidified with 2M hydrochloric acid to pH 4. The mixture was extracted with DCM (20 mL), dried over a hydrophobic frit, and the solvent removed *in vacuo*. This yielded the title compound (1.63 g, 64%) as an off white solid. $\nu_{\max}/\text{cm}^{-1}$ (neat): 3380 (broad), 1697; $^1\text{H NMR}$ (400 MHz, $\text{DMSO-}d_6$) δ 1.36 (s, 9H), 1.50 (quin, $J = 6.9$ Hz, 2H), 2.78-2.95 (m, 4H), 3.73 (t, $J = 4.3$ Hz, 2H), 4.03 (s, 3H), 4.38 (t, $J = 4.2$ Hz, 2H), 6.72 (br. s., 1H), 6.92 (d, $J = 8.3$ Hz, 1H), 7.14 (d, $J = 2.0$ Hz, 1H), 7.34 (dd, $J = 8.3, 2.0$ Hz, 1H), 7.60 (t, J

CONFIDENTIAL – PROPERTY OF GSK – DO NOT COPY

= 5.8 Hz, 1H), 8.01 (d, $J = 2.8$ Hz, 1H), 8.40 (d, $J = 2.5$ Hz, 1H), 12.50 (br. s., 1H); ^{13}C NMR (126 MHz, DMSO- d_6) δ 28.7, 30.4, 37.7, 40.9, 48.2, 54.8, 65.1, 78.1, 115.8, 117.3, 122.1, 123.8, 123.9, 133.1, 136.1, 136.5, 147.9, 148.6, 156.1, 156.5, 167.4; LCMS (Method A): MH⁻ 521, Rt 1.06 min, 96% by UV; HRMS exact mass calculated for [M+H]⁺ (C₂₃H₃₁N₄O₈S) requires m/z 523.1857, found 523.1853.

9-Methoxy-2-oxa-11-thia-5,8,12,16-tetraazatetracyclo[16.2.2.16,(10),0(20,5)]tricoso-1(20),6(23),7,9,18,21-hexaen-17-one 11,11-dioxide, 88

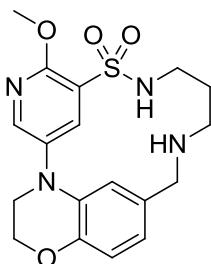


To a solution of 4-(5-(*N*-(3-((*tert*-butoxycarbonyl)amino)propyl)sulfamoyl)-6-methoxypyridin-3-yl)-3,4-dihydro-2*H*-benzo[*b*][1,4]oxazine-6-carboxylic acid (100 mg, 0.19 mmol) in DCM (2 mL), was added trifluoroacetic acid (0.1 mL, 1.3 mmol). The reaction mixture was then stirred at room temperature for 18 hours. Further trifluoroacetic acid (0.14 mL, 1.8 mmol) was then added and the reaction mixture stirred at room temperature for a further 5 hours. The solvent was removed *in vacuo*. The residue was dissolved in THF (20 mL) and HATU (90 mg, 0.24 mmol) and *N,N*-diisopropylethylamine (0.061 mL, 0.47 mmol) was added. The reaction was then stirred at room temperature for 16 hours. The solvent was then removed *in vacuo*, the residue dissolved in water (5 mL), extracted with ethyl acetate (2 x 5 mL). The organic layers were combined, dried over a hydrophobic frit and the solvent removed *in vacuo*. The sample was dissolved in DMSO and purified by mass directed HPLC using formic acid modifier. The appropriate fractions were concentrated *in vacuo* to give the title compound (24 mg, 25%) as an off white solid. $\nu_{\text{max}}/\text{cm}^{-1}$ (neat) 1655; ^1H NMR (400 MHz, DMSO- d_6) δ 1.60 (br. s., 2H), 2.76 (br. s., 2H), 3.13 (br. s, 2H), 3.84 (t, $J = 4.0$ Hz, 2H), 4.02 (s, 3H), 4.42 (t, $J = 4.0$ Hz, 2H), 6.86 (d, $J = 8.1$ Hz, 1H), 7.01 (d, $J = 7.8$ Hz, 1H), 7.25 (br. s., 1H), 7.71-7.86 (m, 2H), 8.17 (d, $J = 2.8$ Hz, 1H), 8.39 (d, $J = 2.8$ Hz, 1H); ^{13}C NMR (101 MHz, DMSO- d_6) 30.0, 36.4, 40.4, 48.7, 54.3, 65.0, 115.4,

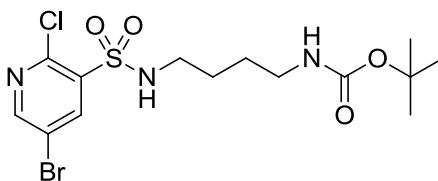
CONFIDENTIAL – PROPERTY OF GSK – DO NOT COPY

115.4, 117.0, 119.5, 128.4, 131.3, 135.4, 138.4, 146.0, 146.5, 155.7, 168.0; LCMS (Method A): MH^+ 405, Rt 0.74 min, 100% by UV; HRMS exact mass calculated for $[M+H]^+$ ($C_{18}H_{21}N_4O_5S$) requires m/z 405.1227, found 405.1239.

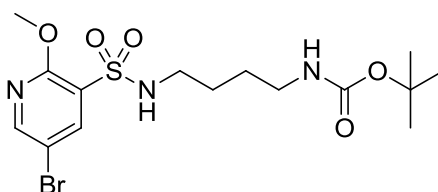
9-Methoxy-2-oxa-11-thia-5,8,12,16-tetraazatetracyclo[16.2.2.16,(10),0(20,5)]tricoso-1(20),6(23),7,9,18,21-hexaene-11,11-dioxide, 80



To a solution of 9-methoxy-2-oxa-11-thia-5,8,12,16-tetraazatetracyclo[16.2.2.16,(10),0(20,5)]tricoso-1(20),6(23),7,9,18,21-hexaen-17-one 11,11-dioxide (100 mg, 0.25 mmol) in 2-methyltetrahydrofuran (1 mL), was added 1M borane tetrahydrofuran complex (0.50 mL, 0.50 mmol). The mixture was then stirred at 60 °C for 18 hours. The reaction mixture was then diluted with water (2 mL) and extracted with DCM (3 x 2 mL). The organic portions were combined, dried over a hydrophobic frit and the solvent was then removed *in vacuo*. The sample was dissolved in DMSO (1 mL) and purified by mass directed HPLC using an ammonium carbonate modifier. The solvent was removed *in vacuo* to give the title compound (17 mg, 18%) as a white solid. ν_{max}/cm^{-1} (neat), 3296 (weak); 1H NMR (400 MHz, $CDCl_3$) δ 1.65 (quin, $J = 6.6$ Hz, 2H), 2.58 (t, $J = 6.4$ Hz, 2H), 3.24 (t, $J = 6.6$ Hz, 2H), 3.74 (s, 2H), 3.75-3.80 (m, 2H), 4.12 (s, 3H), 4.29-4.36 (m, 2H), 6.62 (dd, $J = 8.1, 1.9$ Hz, 1H), 6.83 (d, $J = 8.1$ Hz, 1H), 6.97 (d, $J = 1.8$ Hz, 1H), 8.17 (d, $J = 2.8$ Hz, 1H), 8.22 (d, $J = 2.8$ Hz, 1H); ^{13}C NMR (101 MHz, $CDCl_3$) δ 30.3, 42.1, 46.2, 49.3, 52.5, 54.6, 64.2, 115.6, 117.1, 120.7, 122.8, 131.6, 133.1, 134.2, 137.8, 144.5, 145.1, 156.1; LCMS (Method B): MH^+ 391, Rt 0.87 min, 100% by UV; HRMS exact mass calculated for $[M+H]^+$ ($C_{18}H_{23}N_4O_4S$) requires m/z : 391.1435, found: 391.1445.

***Tert*-butyl (4-(5-bromo-2-chloropyridine-3-sulfonamido)butyl)carbamate, 95**

To a solution of 5-bromo-2-chloropyridine-3-sulfonyl chloride (3.0 g, 10.3 mmol) and *tert*-butyl (4-aminobutyl)carbamate (2.56 mL, 13.4 mmol) in 1,4-dioxane (50 mL), was added pyridine (1.25 mL, 15.5 mmol). The mixture was stirred at room temperature for 18 hours. The solvent was then removed *in vacuo* and the residue dissolved in ethyl acetate (50 mL). The organic layer was washed with water (50 mL) and the aqueous layer extracted with further ethyl acetate (50 mL). The organic portions were then combined, dried over a hydrophobic frit and the solvent removed *in vacuo*. The sample was loaded in DCM and purified by column chromatography on silica using a 0-100% ethyl acetate:cyclohexane gradient. The appropriate fractions were combined and concentrated *in vacuo* to give the title compound (2.67 g, 59%) as a colourless oil which solidified on standing. $\nu_{\max}/\text{cm}^{-1}$ (neat) 1686, 2933, 2977; ^1H NMR (400 MHz, DMSO- d_6) δ 1.31-1.40 (m, 13H), 2.82-2.93 (m, 2H), 6.73 (t, $J = 5.3$ Hz, 1H), 8.27 (s, 1H), 8.44 (d, $J = 2.5$ Hz, 1H), 8.82 (d, $J = 2.5$ Hz, 1H); ^{13}C NMR (101 MHz, DMSO- d_6) δ 27.0, 27.1, 28.7, 42.8, 55.3, 77.8, 119.5, 136.9, 141.8, 146.0, 153.7, 156.0; LCMS (Method A): MH^+ 440, 442, Rt 1.12 min, 100% by UV; HRMS exact mass calculated for $[\text{M}+\text{H}]^+$ ($\text{C}_{14}\text{H}_{22}\text{BrClN}_3\text{O}_4\text{S}$) requires m/z 442.0197, found 442.0186.

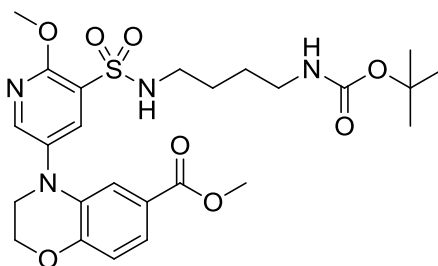
***Tert*-butyl (4-(5-bromo-2-methoxypyridine-3-sulfonamido)butyl)carbamate, 96**

To solid sodium methoxide (2 x 0.94 g, 17.4 mmol) and *tert*-butyl (4-(5-bromo-2-chloropyridine-3-sulfonamido)butyl)carbamate (2 x 1.0 g, 2.3 mmol) was added methanol (2 x 16 mL) The vials were then sealed and heated in under microwave irradiation to 120 °C for 2 hours. The reaction mixtures were combined and quenched with water (30 mL). The mixture was then extracted with ethyl acetate (2 x 30 mL)

CONFIDENTIAL – PROPERTY OF GSK – DO NOT COPY

and the organic portions combined, dried over a hydrophobic frit and the solvent removed *in vacuo*. The sample was loaded in DCM and purified by column chromatography on silica using a 0-100% ethyl acetate/cyclohexane gradient. The appropriate fractions were combined and concentrated *in vacuo* to give the title compound (1.67 g, 84%) as a colourless oil. $\nu_{\max}/\text{cm}^{-1}$ (neat): 1689; $^1\text{H NMR}$ (400 MHz, $\text{DMSO-}d_6$) δ 1.30-1.35 (m, 4H), 1.37 (s, 9H), 2.81-2.88 (m, 4H), 4.00 (s, 3H), 6.72 (t, $J = 5.1$ Hz, 1H), 7.72 (s, 1H), 8.16 (d, $J = 2.5$ Hz, 1H), 8.55 (d, $J = 2.5$ Hz, 1H); $^{13}\text{C NMR}$ (101 MHz, $\text{DMSO-}d_6$) δ 27.1, 27.2, 28.7, 42.8, 55.0, 77.8, 111.0, 125.3, 141.1, 151.7, 156.0, 158.7, (4° *tert*-butyl carbon not observed); LCMS (Method A): MH^- 436, 438, Rt 1.14 min, 100% by UV; HRMS exact mass calculated for $[\text{M}+\text{H}]^+$ ($\text{C}_{15}\text{H}_{25}\text{BrN}_3\text{O}_5\text{S}$) requires m/z : 438.0693, found 438.0701.

Methyl 4-(5-(*N*-(4-((*tert*-butoxycarbonyl)amino)butyl)sulfamoyl)-6-methoxypyridin-3-yl)-3,4-dihydro-2*H*-benzo[*b*][1,4]oxazine-6-carboxylate, 97

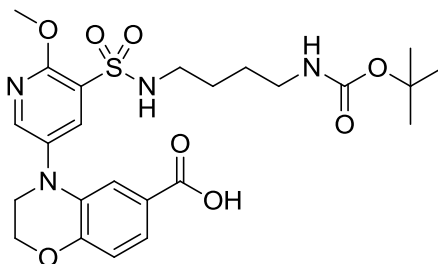


To solid *tert*-butyl (4-(5-bromo-2-methoxypyridine-3-sulfonamido)butyl)carbamate (2 x 0.80 g, 1.83 mmol), methyl 3,4-dihydro-2*H*-benzo[*b*][1,4]oxazine-6-carboxylate (2 x 0.35 g, 1.83 mmol), caesium carbonate (2 x 0.89 g, 2.74 mmol) and RuPhos Pd G2 (2 x 0.142 g, 0.183 mmol), was added 1,4-dioxane (2 x 12 mL). The reaction vessels were sealed and heated in under microwave irradiation to 130 °C for 3 hours. The reaction mixtures were then combined, filtered through celite and washed with DCM (30 mL). The solvent was then removed *in vacuo*. The sample was loaded in DCM and purified by column chromatography on silica using a 0-100% ethyl acetate/cyclohexane gradient. The appropriate fractions were combined and concentrated *in vacuo* to give the title compound (1.75 g, 87%) as a yellow oil. $\nu_{\max}/\text{cm}^{-1}$ (neat) 1699; $^1\text{H NMR}$ (400 MHz, $\text{DMSO-}d_6$) δ 1.32-1.39 (m, 13H), 2.78-2.94 (m, 4H), 3.72 (s, 3H), 3.74 (t, $J = 4.3$ Hz, 2H), 4.03 (s, 3H), 4.39 (t, $J = 4.3$ Hz, 2H), 6.71 (t, $J = 5.6$ Hz, 1H), 6.95 (d, $J = 8.3$ Hz, 1H), 7.13 (d, $J = 2.0$ Hz, 1H), 7.36 (dd, $J =$

CONFIDENTIAL – PROPERTY OF GSK – DO NOT COPY

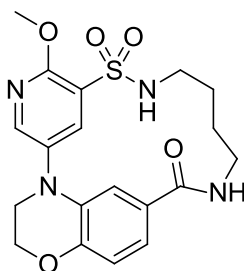
8.3, 2.0 Hz, 1H), 7.66 (br. s., 1H), 8.02 (d, $J = 2.7$ Hz, 1H), 8.40 (d, $J = 2.8$ Hz, 1H); ^{13}C NMR (101 MHz, DMSO- d_6) 27.1, 27.2, 28.7, 42.9, 48.3, 52.3, 60.2, 65.1, 77.8, 115.5, 117.4, 117.5, 121.9, 122.7, 124.1, 133.4, 136.2, 136.5, 148.0, 148.9, 156.6, 166.3, LCMS (Method A): MH^- 549, Rt 1.23 min, 92% by UV; HRMS exact mass calculated for $[\text{M}+\text{H}]^+$ ($\text{C}_{25}\text{H}_{35}\text{N}_4\text{O}_8\text{S}$) requires m/z : 551.2170, found 551.2159.

4-(5-(*N*-(4-((*tert*-butoxycarbonyl)amino)butyl)sulfamoyl)-6-methoxypyridin-3-yl)-3,4-dihydro-2*H*-benzo[*b*][1,4]oxazine-6-carboxylic acid, 98



To a solution of methyl 4-(5-(*N*-(4-((*tert*-butoxycarbonyl)amino)butyl)sulfamoyl)-6-methoxypyridin-3-yl)-3,4-dihydro-2*H*-benzo[*b*][1,4]oxazine-6-carboxylate (1.65 g, 3.0 mmol) in THF (10 mL) and water (10 mL), was added lithium hydroxide (0.43 g, 18.0 mmol). The reaction mixture was then stirred at room temperature for 3 days. The reaction mixture was then acidified to pH 4 using aqueous 2M hydrochloric acid. The mixture was extracted with DCM (30 mL) and dried over a hydrophobic frit. The solvent was then removed *in vacuo* to yield the title compound (1.43 g, 89%) as a clear oil. $\nu_{\text{max}}/\text{cm}^{-1}$ (neat) 1683, 1740; ^1H NMR (400 MHz, DMSO- d_6) δ 1.30-1.40 (m, 13H), 2.78-2.93 (m, 4H), 3.72 (t, $J = 4.3$ Hz, 2H), 4.02 (s, 3H), 4.32-4.40 (m, 2H), 6.75 (t, $J = 5.3$ Hz, 1H), 6.87 (d, $J = 8.3$ Hz, 1H), 7.14 (d, $J = 2.0$ Hz, 1H), 7.32 (dd, $J = 8.3, 2.0$ Hz, 1H), 7.63 (t, $J = 5.8$ Hz, 1H), 8.00 (d, $J = 2.8$ Hz, 1H), 8.38 (d, $J = 2.8$ Hz, 1H); ^{13}C NMR (101 MHz, DMSO- d_6) δ 27.1, 27.2, 28.7, 42.8, 42.9, 48.4, 54.4, 65.0, 77.8, 116.0, 117.0, 122.1, 124.0, 132.9, 136.0, 136.7, 147.8, 148.1, 151.4, 156.0, 156.5, 167.7; LCMS (Method A): MH^- 535, Rt 1.08 min, 92% by UV; HRMS exact mass calculated for $[\text{M}+\text{H}]^+$ ($\text{C}_{24}\text{H}_{33}\text{N}_4\text{O}_8\text{S}$) requires m/z : 537.2014, found 537.1996.

9-Methoxy-2-oxa-11-thia-5,8,12,17-tetraazatetracyclo[17.2.2.16,10,0(20,5)]tetracos-1(21),6(24),7,9,19,22-hexaen-18-one 11,11-dioxide, 99

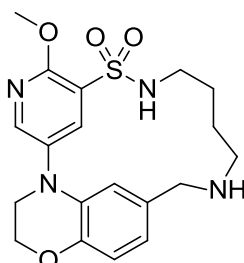


To a solution of 4-(5-(*N*-(4-((*tert*-butoxycarbonyl)amino)butyl)sulfamoyl)-6-methoxypyridin-3-yl)-3,4-dihydro-2*H*-benzo[*b*][1,4]oxazine-6-carboxylic acid (1.0 g, 1.9 mmol) in DCM (20 mL), was added trifluoroacetic acid (2.30 mL, 29.8 mmol) and the reaction mixture was stirred at room temperature for 18 hours. The solvent was then removed *in vacuo*. The residue was then dissolved in *N,N*-dimethylformamide (50 mL) to this was added HATU (700 mg, 1.8 mmol) and DIPEA (0.64 mL, 3.7 mmol) The reaction mixture was then stirred at room temperature for 48 hours. The reaction mixture was then diluted with saturated aqueous sodium hydrogen carbonate (50 mL) and extracted with ethyl acetate (3 x 30 mL). The organic portions were then combined, dried over a hydrophobic frit and the solvent removed *in vacuo* to yield crude product (680 mg). Two samples (2 x 90 mg) were dissolved in DMSO (2 x 1 mL) and purified by mass directed HPLC on Xbridge column using acetonitrile/water with an ammonium carbonate modifier. The solvent was removed *in vacuo* to give the title compound (13 mg, 2%) as an off white solid. The remaining crude product was loaded in DMSO and purified by column chromatography on C₁₈ reverse phase using a 0-100 water:acetonitrile gradient. The appropriate fractions from reverse phase purification were combined and concentrated *in vacuo* to give the title compound (200 mg, 26%) as an off-white solid. $\nu_{\max}/\text{cm}^{-1}$ (neat) 1715, 3269, 3310; ¹H NMR (400 MHz, DMSO-*d*₆) δ 1.33-1.47 (m, 4H), 2.87 (br. s., 2H), 3.06-3.15 (m, 2H), 3.80 (t, *J* = 4.3 Hz, 2H), 4.03 (s, 3H), 4.42 (t, *J* = 4.3 Hz, 2H), 6.85 (d, *J* = 8.2 Hz, 1H), 7.03 (d, *J* = 1.9 Hz, 1H), 7.07 (dd, *J* = 8.2, 1.9 Hz, 1H), 7.69 (br. s., 1H), 7.95 (t, *J* = 5.6 Hz, 1H), 8.04 (d, *J* = 2.8 Hz, 1H), 8.38 (d, *J* = 2.7 Hz, 1H); ¹³C NMR (126 MHz, DMSO-*d*₆) δ 26.3, 27.8, 40.9, 44.5, 47.6, 54.7, 65.3, 114.0, 117.1, 119.7, 123.2, 128.4, 132.6, 136.0, 137.6, 146.7, 147.2, 156.4, 166.9, LCMS (Method A): [M-H]⁻ 535, Rt 1.08 min, 92%

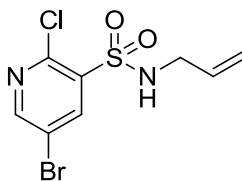
CONFIDENTIAL – PROPERTY OF GSK – DO NOT COPY

by UV; HRMS exact mass calculated for $[M+H]^+$ ($C_{19}H_{22}N_4O_5S$) requires m/z 418.1310, found 418.1313.

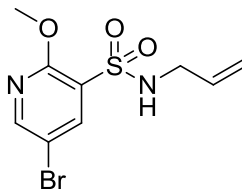
9-Methoxy-2-oxa-11-thia-5,8,12,17-tetraazatetracyclo[17.2.2.16,10,0(20,5)]tetracos-1(21),6(24),7,9,19,22-hexaen-18-one 11,11-dioxide, 81



To a solution of 9-methoxy-2-oxa-11-thia-5,8,12,17-tetraazatetracyclo[17.2.2.16,10,0(20,5)]tetracos-1(21),6(24),7,9,19,22-hexaen-18-one 11,11-dioxide (40 mg, 0.09 mmol) in THF (1.5 mL), stirred at 0 °C, was added diisobutylaluminum hydride (1 M in THF, 0.35 mL, 0.35 mmol) The reaction mixture was then allowed to warm to room temperature and was stirred for a further 18 hours. The reaction was cooled to 0 °C and quenched with water (1.5 mL). The reaction mixture was then extracted with ethyl acetate (3 x 5 mL), the organic portions combined, dried over a hydrophobic frit and the solvent removed *in vacuo*. The sample was dissolved in DMSO (1 mL) and purified by mass directed HPLC on Xbridge column using acetonitrile/water with an ammonium carbonate modifier. The solvent was removed *in vacuo* to give the title compound (6 mg, 16%). 1H NMR (400 MHz, $CDCl_3$) δ 1.32-1.41 (m, 2H), 1.46-1.55 (m, 2H), 2.54 (t, $J = 5.8$ Hz, 2H), 3.09-3.19 (m, 2H), 3.61 (s, 2H), 3.71 (t, $J = 4.3$ Hz, 2H), 4.16 (s, 3H), 4.43 (t, $J = 4.5$ Hz, 2H), 4.99 (br. s., 1H), 6.54 (dd, $J = 7.8, 1.8$ Hz, 1H), 6.57 (d, $J = 1.8$ Hz, 1H), 6.78 (d, $J = 7.8$ Hz, 1H), 8.10-8.29 (m, 2H); LCMS (Method A): MH^- 405, R_t 0.99 min, 99% by UV; Not enough sample remained after biological testing to obtain complete characterisation.

***N*-Allyl-5-bromo-2-chloropyridine-3-sulfonamide, 103**

To a solution of 5-bromo-2-chloropyridine-3-sulfonyl chloride (5.0 g, 17 mmol), in 1,4-dioxane (80 mL), was added pyridine (2.0 mL, 26 mmol). The reaction mixture was stirred at room temperature for 30 mins. To this, was then added prop-2-en-1-amine (1.7 mL, 22 mmol), in four charges over one hour. The reaction was stirred at room temperature for 18 hours, the solvent was removed *in vacuo*, and the residue dissolved in water (50 mL). This was then extracted with ethyl acetate (50 mL) and the aqueous layer washed with further ethyl acetate (50 mL). The organic layers were combined, dried over a hydrophobic frit and the solvent removed *in vacuo*. The sample was loaded preabsorbed on florisil and purified by column chromatography on silica using a 0-100% ethyl acetate/cyclohexane gradient. The appropriate fractions were combined and concentrated *in vacuo* to give the title compound (3.4 g, 64%) as a white solid. $\nu_{\max}/\text{cm}^{-1}$ (neat) 2901, 2988, 3296; ^1H NMR (400 MHz, DMSO- d_6) δ 3.61 (dt, $J = 5.6, 1.5$ Hz, 2H), 5.01 (dq, $J = 10.3, 1.4$ Hz, 1H), 5.13 (dq, $J = 17.1, 1.6$ Hz, 1H), 5.62-5.79 (m, 1H), 8.44 (d, $J = 2.4$ Hz, 1H), 8.53 (br. s, 1H), 8.82 (d, $J = 2.4$ Hz, 1H); ^{13}C NMR (101 MHz, DMSO- d_6) δ 44.8, 116.7, 119.0, 133.9, 136.6, 141.4, 145.5, 153.3; LCMS (Method A): MH^+ 313, 315, Rt 0.97 min, 100% by UV; HRMS exact mass calculated for $[\text{M}+\text{H}]^+$ ($\text{C}_8\text{H}_9\text{BrClN}_2\text{O}_2\text{S}$) requires m/z 310.9251, found 310.9261.

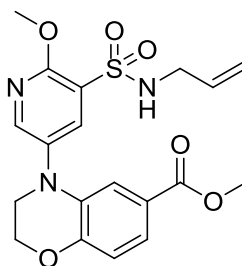
***N*-Allyl-5-bromo-2-methoxyppyridine-3-sulfonamide, 104**

To solid sodium methoxide (3 x 1.04 g, 19.3 mmol) and *N*-allyl-5-bromo-2-chloropyridine-3-sulfonamide (3 x 0.75 g, 2.4 mmol), was added methanol (3 x 12 mL). The vials were sealed and heated under microwave irradiation conditions to 120 °C for 2 hours. The reaction mixtures were then combined and quenched with water

CONFIDENTIAL – PROPERTY OF GSK – DO NOT COPY

(20 mL). The solution was then extracted with ethyl acetate (20 mL); brine (20 mL) was added to aid separation. The aqueous layer was then washed with further ethyl acetate (3 x 20 mL). The organic layers were combined, dried over a hydrophobic frit and the solvent removed *in vacuo* to yield the title compound (1.90 g, 86%) as a white solid. $\nu_{\max}/\text{cm}^{-1}$ (neat) 3351; $^1\text{H NMR}$ (400 MHz, $\text{DMSO-}d_6$) δ 3.55 (dt, $J = 5.5, 1.5$ Hz, 2H), 3.99 (s, 3H), 4.97 (dq, $J = 10.2, 1.4$ Hz, 1H), 5.09 (dq, $J = 17.2, 1.7$ Hz, 1H), 5.60-5.72 (m, 1H), 8.15 (d, $J = 2.5$ Hz, 1H), 8.51 (br. s, 1H), 8.53 (d, $J = 2.6$ Hz, 1H); $^{13}\text{C NMR}$ (101 MHz, $\text{DMSO-}d_6$) δ 45.6, 55.0, 110.9, 116.5, 135.0, 141.0, 151.6, 158.7, 166.9; LCMS (Method A): MH^+ 309, 311, R_t 1.00 min, 98% by UV; HRMS exact mass calculated for $[\text{M}+\text{H}]^+$ ($\text{C}_9\text{H}_{12}\text{BrN}_2\text{O}_3\text{S}$) requires m/z 306.9752, found 306.9742.

Methyl-4-(5-(*N*-allylsulfamoyl)-6-methoxypyridin-3-yl)-3,4-dihydro-2*H*-benzo[*b*][1,4]oxazine-6-carboxylate, 105

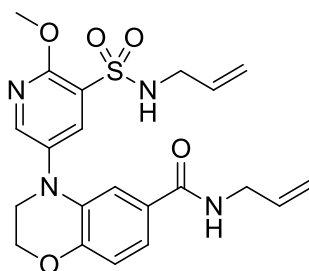


To solid *N*-allyl-5-bromo-2-methoxypyridine-3-sulfonamide (2 x 0.95 g, 3.1 mmol), methyl 3,4-dihydro-2*H*-benzo[*b*][1,4]oxazine-6-carboxylate (2 x 0.60 g, 3.1 mmol), dicyclohexyl(2',6'-diisopropoxy-[1,1'-biphenyl]-2-yl)phosphine (2 x 0.14 g, 0.31 mmol), RuPhos Pd G2 (2 x 0.24 g, 0.31 mmol) and caesium carbonate (2 x 3.0 g, 9.3 mmol), was added 1,4-dioxane (2 x 15 mL). The vials were sealed and heated under microwave irradiation to 120 °C for 2 hours. The reaction mixtures were then combined, filtered through celite, washed with DCM (20 mL) and the solvent removed *in vacuo*. The residue was then dissolved in water (20 mL) and extracted with ethyl acetate (20 mL), washed with further ethyl acetate (20 mL) and dried over a hydrophobic frit. The residue was then loaded in DCM and purified by column chromatography on silica using a 0-50% ethyl acetate/cyclohexane gradient. The appropriate fractions were combined and concentrated *in vacuo* to give the title compound (1.35 g, 52%) as an off-white solid. $\nu_{\max}/\text{cm}^{-1}$ (neat) 1715, 3379; $^1\text{H NMR}$ (400 MHz, $\text{DMSO-}d_6$) δ 3.56 (d, $J = 5.8$ Hz, 2H), 3.72 (s, 3H), 3.73 (t, $J = 4.0$ Hz,

CONFIDENTIAL – PROPERTY OF GSK – DO NOT COPY

2H), 4.03 (s, 3H), 4.39 (t, $J = 3.9$ Hz, 2H), 4.98 (dq, $J = 10.4, 1.5$ Hz, 1H), 5.09 (dq, $J = 17.2, 1.5$ Hz, 1H), 5.58-5.76 (m, 1H), 6.95 (d, $J = 8.3$ Hz, 1H), 7.11 (d, $J = 2.0$ Hz, 1H), 7.36 (dd, $J = 8.3, 2.0$ Hz, 1H), 7.90 (br. s., 1H), 8.01 (d, $J = 2.5$ Hz, 1H), 8.39 (d, $J = 2.5$ Hz, 1H); ^{13}C NMR (101 MHz, DMSO- d_6) δ 45.5, 48.4, 52.3, 54.8, 65.1, 115.5, 116.8, 117.4, 121.8, 122.7, 124.5, 133.5, 134.7, 136.3, 136.4, 148.2, 148.9, 156.7, 166.3 LCMS (Method A): MH^+ 420, Rt 1.12 min, 92% by UV; HRMS exact mass calculated for $[\text{M}+\text{H}]^+$ ($\text{C}_{19}\text{H}_{22}\text{N}_3\text{O}_6\text{S}$) requires m/z 420.1224, found 420.1224.

***N*-Allyl-4-(5-(*N*-allylsulfamoyl)-6-methoxypyridin-3-yl)-3,4-dihydro-2*H*-benzo[*b*][1,4]oxazine-6-carboxamide, 106**

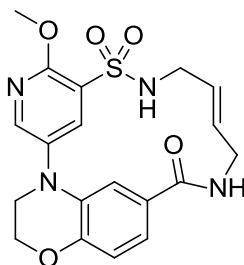


To a solution of methyl 4-(5-(*N*-allylsulfamoyl)-6-methoxypyridin-3-yl)-3,4-dihydro-2*H*-benzo[*b*][1,4]oxazine-6-carboxylate (1.0 g, 2.4 mmol) in 2-methyltetrahydrofuran (50 mL) was added potassium trimethylsilanolate (0.61 g, 4.8 mmol) and the mixture was then stirred at 80 °C for 24 hours. The solvent was removed *in vacuo* and the residue added to a solution of DIPEA (0.65 mL, 3.7 mmol) and HATU (0.94 g, 2.5 mmol) in *N,N*-dimethylformamide (10 mL). The mixture was stirred at room temperature for 30 mins, then prop-2-en-1-amine (0.37 mL, 4.9 mmol) was added and the mixture stirred at room temperature for 18 hours. The reaction mixture was then diluted with saturated aqueous sodium hydrogen carbonate (20 mL) and extracted with ethyl acetate (20 mL). The aqueous layer was washed with further ethyl acetate (20 mL), the organic layers combined, dried over a hydrophobic frit and the solvent removed *in vacuo*. The sample was loaded preabsorbed on florisil and purified by column chromatography on silica using a 0-100% ethyl acetate/cyclohexane gradient. The appropriate fractions were combined and concentrated *in vacuo* to give the title compound (490 mg, 44%) as a yellow oil. $\nu_{\text{max}}/\text{cm}^{-1}$ (oil) 1638, 3300; ^1H NMR (400 MHz, DMSO- d_6) δ 3.55 (br. s., 2H), 3.71 (t, $J = 4.5$ Hz, 2H), 3.80 (tt, $J = 5.3, 1.5$ Hz, 2H), 4.02 (s, 3H), 4.33 (t, $J = 3.8$ Hz, 2H), 4.96-5.15 (m, 4H), 5.60-5.72 (m, 1H), 5.76-

CONFIDENTIAL – PROPERTY OF GSK – DO NOT COPY

5.88 (m, 1H), 6.89 (d, $J = 8.3$ Hz, 1H), 7.15 (d, $J = 2.0$ Hz, 1H), 7.30 (dd, $J = 8.3, 2.0$ Hz, 1H), 7.85 (br. s., 1H), 7.96 (d, $J = 2.7$ Hz, 1H)(overlap with DMF), 8.07 (br. s., 1H), 8.37 (d, $J = 2.8$ Hz, 1H); ^{13}C NMR (101 MHz, DMSO- d_6) δ 38.7, 41.9, 45.6, 48.8, 64.8, 114.9, 115.4, 116.8, 116.9, 119.6, 124.4, 127.6, 132.9, 134.8, 136.0, 136.0, 137.0, 147.3, 147.9, 156.5, 165.9 LCMS (Method A): MH^+ 445, Rt 0.97 min, 96% by UV; HRMS exact mass calculated for $[\text{M}+\text{H}]^+$ ($\text{C}_{21}\text{H}_{25}\text{N}_4\text{O}_5\text{S}$) requires m/z 445.1540, found 445.1544.

9-Methoxy-2-oxa-11-thia-5,8,12,17-tetraazatetracyclo[17.2.2.16,10,0(20,5)]tetracos-1(21),6(24),7,9,14(E),19,22-heptaen-18-one 11,11-dioxide, 102

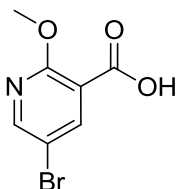


To a solution of *N*-allyl-4-(5-(*N*-allylsulfamoyl)-6-methoxypyridin-3-yl)-3,4-dihydro-2*H*-benzo[*b*][1,4]oxazine-6-carboxamide (50 mg, 0.11 mmol) in DCM (4 mL), was added Hoveyda-Grubbs 1st generation catalyst (7 mg, 0.011 mmol). The reaction mixture was then stirred at 40 °C for 4 hours. Further Hoveyda-Grubbs 1st generation catalyst (7 mg, 0.011 mmol) was added and the reaction mixture was stirred at 40 °C for a further 18 hours. Further Hoveyda-Grubbs 1st generation (7 mg, 0.011 mmol) was added and the reaction mixture stirred at 40 °C for a further 24 hours. The reaction mixture was then filtered through celite, washed with DCM (20 mL) and the solvent removed *in vacuo*. The sample was dissolved in DMSO (1 mL) and purified by mass directed HPLC with an ammonium carbonate modifier. The solvent was removed *in vacuo* to give the title compound (5 mg, 11%) as an off white solid. $\nu_{\text{max}}/\text{cm}^{-1}$ (neat) 1643, 1607; ^1H NMR (600 MHz, CDCl_3) δ 3.79 (t, $J = 4.0$ Hz, 2H), 3.89-4.04 (m, 4H), 4.17 (s, 3H), 4.52 (t, $J = 4.4$ Hz, 2H), 5.26 (t, $J = 5.2$ Hz, 1H), 5.52 (dt, $J = 15.4, 6.6$ Hz, 1H), 5.65 (t, $J = 5.9$ Hz, 1H), 5.72 (d, $J = 15.4$ Hz, 1H), 6.68 (br. s., 1H), 6.95 (d, $J = 8.1$ Hz, 1H), 7.30 (d, $J = 8.1$ Hz, 1H), 8.21 (d, $J = 2.9$ Hz, 1H), 8.25 (br. s., 1H); ^{13}C NMR (151 MHz, CDCl_3) δ 39.0, 45.8, 47.2, 55.0, 65.4, 112.0, 116.3, 117.8, 120.6,

CONFIDENTIAL – PROPERTY OF GSK – DO NOT COPY

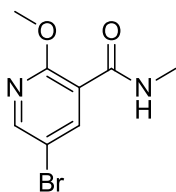
124.6, 127.9, 130.6, 133.0, 135.4, 136.8, 146.8, 147.0, 156.8, 167.7 LCMS (Method A): MH^+ 417, Rt 0.80 min, 87% by UV; HRMS exact mass calculated for $[M+H]^+$ ($C_{19}H_{20}N_4O_5S$) requires m/z : 417.1227, found: 417.1217.

5-Bromo-2-methoxynicotinic acid, 131²⁴⁹



To a solution of methyl 5-bromo-2-methoxynicotinate (5.0 g, 20 mmol) in THF (50 mL) and water (50 mL), was added lithium hydroxide (1.17 g, 48.8 mmol). The mixture was then stirred at room temperature for 18 hours. The reaction mixture was then extracted with DCM (50 mL). The organic phase was then dried over a hydrophobic frit and the solvent removed *in vacuo*. This yielded the title compound (3.8 g, 80%) as a white solid. ν_{max}/cm^{-1} (neat) 3366 (broad), 1680, 1647; 1H NMR (400 MHz, $DMSO-d_6$) δ 3.92 (s, 3H), 8.20 (d, $J = 2.5$ Hz, 1H), 8.47 (d, $J = 2.5$ Hz, 1H), 13.24 (br. s., 1H); ^{13}C NMR (101 MHz, $DMSO-d_6$) δ 54.5, 111.0, 117.7, 142.7, 150.7, 160.8, 165.2, LCMS (Method A): MH^+ 232. 234, Rt 0.79 min, 100% by UV; HRMS exact mass calculated for $[M+H]^+$ ($C_7H_7BrNO_3$) requires m/z : 231.9604, found: 231.9613.

5-Bromo-2-methoxy-*N*-methylnicotinamide, 132²⁵⁰

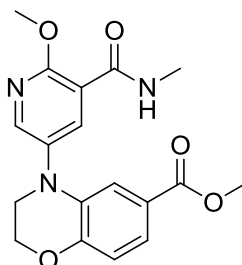


To a solution of 5-bromo-2-methoxynicotinic acid (1.0 g, 4.3 mmol) in *N,N*-Dimethylformamide (20 mL) was added HATU (1.6 g, 4.3 mmol) and DIPEA (2.3 mL, 12.9 mmol) The reaction mixture was then stirred at room temperature for 30 mins. To the reaction mixture, was then added methylamine (40 wt% aqueous) (0.82 mL, 9.5 mmol) and the reaction mixture was stirred for a further 18 hours. The reaction was then diluted with saturated aqueous sodium hydrogen carbonate (20 mL) and extracted with ethyl acetate (3 x 20 mL). The organic portions were then combined

CONFIDENTIAL – PROPERTY OF GSK – DO NOT COPY

and were washed with 5% aqueous lithium chloride (30 mL). The organic portion was then dried over a hydrophobic frit and the solvent removed *in vacuo*. This yielded the title compound (732 mg, 69%) as an off white solid. $\nu_{\max}/\text{cm}^{-1}$ (neat) 3371, 1646; ^1H NMR (400 MHz, DMSO- d_6) δ 2.81 (d, $J = 4.8$ Hz, 3H), 3.96 (s, 3H), 8.21 (d, $J = 2.5$ Hz, 1H), 8.29 (br. s., 1H), 8.42 (d, $J = 2.5$ Hz, 1H); ^{13}C NMR (101 MHz, DMSO- d_6) δ 26.9, 54.7, 111.8, 119.9, 142.0, 149.5, 159.7, 163.2; LCMS (Method B): MH^+ 245, 247, Rt 0.84 min, 94% by UV; HRMS exact mass calculated for $[\text{M}+\text{H}]^+$ ($\text{C}_8\text{H}_{10}\text{BrN}_2\text{O}_2$) requires m/z : 244.9920, found: 244.9925.

Methyl 4-(6-methoxy-5-(methylcarbamoyl)pyridin-3-yl)-3,4-dihydro-2H-benzo[*b*][1,4]oxazine-6-carboxylate, 133

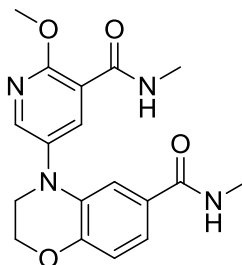


To methyl 3,4-dihydro-2H-benzo[*b*][1,4]oxazine-6-carboxylate (550 mg, 2.9 mmol) caesium carbonate (1861 mg, 5.7 mmol) and RuPhos Pd G2 (220 mg, 0.29 mmol) was added a solution of 5-bromo-2-methoxy-*N*-methylnicotinamide (700 mg, 2.9 mmol) in 1,4-dioxane (17 mL). The vial was sealed and heated under microwave irradiation to 130 °C for 3 hours. The reaction mixture was then filtered through celite and washed with DCM (30 mL). The solvent was then removed *in vacuo* and the sample was loaded in DCM and purified by column chromatography on silica using a 0-100% ethyl acetate/cyclohexane gradient. The appropriate fractions were combined and concentrated *in vacuo* to give the title compound (780 mg, 76%) as a white solid. $\nu_{\max}/\text{cm}^{-1}$ (neat): 3390, 1702, 1660; ^1H NMR (400 MHz, DMSO- d_6) δ 2.83 (d, $J = 4.8$ Hz, 3H), 3.70 (t, $J = 4.3$ Hz, 2H), 3.72 (s, 3H), 4.02 (s, 3H), 4.38 (t, $J = 4.3$ Hz, 2H), 6.93 (d, $J = 8.3$ Hz, 1H), 7.10 (d, $J = 2.0$ Hz, 1H), 7.34 (dd, $J = 8.3, 2.0$ Hz, 1H), 8.08 (d, $J = 2.8$ Hz, 1H), 8.30 (d, $J = 2.8$ Hz, 1H), 8.32 (t, $J = 4.0$ Hz, 1H); ^{13}C NMR (101 MHz, DMSO- d_6) δ 26.9, 48.5, 52.3, 54.5, 65.1, 115.6, 117.3, 118.5, 121.6, 122.7, 133.8, 137.1, 137.3, 146.3, 148.8, 157.9, 163.8, 166.4; LCMS (Method B): MH^+ 358,

CONFIDENTIAL – PROPERTY OF GSK – DO NOT COPY

Rt 1.01 min, 100% by UV; HRMS exact mass calculated for $[M+H]^+$ ($C_{18}H_{20}N_3O_5$) requires m/z : 358.1398, found: 358.1400.

4-(6-Methoxy-5-(methylcarbamoyl)pyridin-3-yl)-N-methyl-3,4-dihydro-2H-benzo[*b*][1,4]oxazine-6-carboxamide, 134

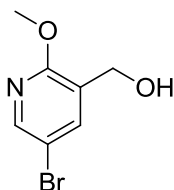


To a solution of methyl 4-(6-methoxy-5-(methylcarbamoyl)pyridin-3-yl)-3,4-dihydro-2H-benzo[*b*][1,4]oxazine-6-carboxylate (700 mg, 2.0 mmol) and THF (10 mL) was added lithium hydroxide (280 mg, 12 mmol) The mixture was then stirred at room temperature for 4 days. The reaction mixture was acidified with 2M aqueous hydrochloric acid to pH 3 and extracted with DCM. The organic phase was then dried over a hydrophobic frit and the solvent removed *in vacuo* to yield an off white solid (642 mg) which was dissolved in *N,N*-dimethylformamide (7 mL) and HATU (660 mg, 1.8 mmol) and DIPEA (0.9 mL, 5.0 mmol) were added. The reaction mixture was stirred at room temperature for 30 minutes. To the reaction mixture, was then added methylamine (40 wt% aqueous) (0.33 mL, 3.8 mmol) and the reaction mixture stirred at room temperature for a further 18 hours. The reaction mixture was diluted with saturated aqueous sodium hydrogen carbonate (10 mL) and extracted with ethyl acetate (2 x 10 mL). The organic portions were combined, dried over a hydrophobic frit and the solvent removed *in vacuo*. A portion (90 mg) was dissolved in DMSO and purified by mass directed HPLC with an ammonium carbonate modifier. The solvent was removed *in vacuo* to give the title compound (46 mg, 7%) as a white solid. The remaining solid (340 mg) was loaded in DCM and purified by column chromatography on silica using a 0-100% ethyl acetate/cyclohexane gradient. The appropriate fractions were combined and concentrated *in vacuo* to give the title compound (156 mg, 25%) as a white solid. Analytical data provided for larger batch. $\nu_{\max}/\text{cm}^{-1}$ (neat) 1642; ^1H NMR (400 MHz, DMSO- d_6) δ 2.83 (d, $J = 4.8$ Hz, 3H), 3.70 (t, $J = 4.3$ Hz, 2H), 3.72 (s, 3H), 4.02 (s, 3H), 4.38 (t, $J = 4.3$ Hz, 2H), 6.93 (d, $J = 8.3$ Hz, 1H), 7.10 (d, $J =$

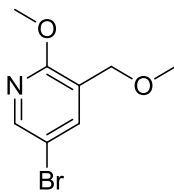
CONFIDENTIAL – PROPERTY OF GSK – DO NOT COPY

2.0 Hz, 1H), 7.34 (dd, $J = 8.3, 2.0$ Hz, 1H), 8.08 (d, $J = 2.8$ Hz, 1H), 8.30 (d, $J = 2.8$ Hz, 1H), 8.32 (t, $J = 4.0$ Hz, 1H); ^{13}C NMR (101 MHz, DMSO- d_6) δ 26.6, 26.9, 48.9, 55.4, 64.8, 114.7, 116.8, 118.2, 119.1, 127.8, 133.3, 137.1, 137.7, 146.1, 147.1, 157.6, 163.9, 166.6; LCMS (Method B): MH^+ 357, Rt 0.78 min, 95% by UV; HRMS exact mass calculated for $[\text{M}+\text{H}]^+$ ($\text{C}_{18}\text{H}_{21}\text{N}_4\text{O}_4$) requires m/z : 357.1557, found: 357.1562.

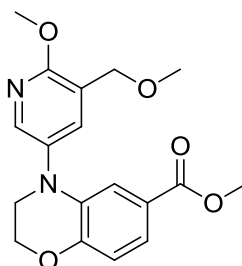
(5-Bromo-2-methoxypyridin-3-yl)methanol,²⁵¹ 136



To (5-bromo-2-chloropyridin-3-yl)methanol (1.0 g, 4.5 mmol) and sodium methoxide (1.94 g, 36.0 mmol) was added methanol (18 mL) The vial was sealed and heated under microwave irradiation to 120 °C for 2 hours. After cooling the reaction was quenched with water (10 mL), extracted with ethyl acetate (20 mL) and washed with further ethyl acetate (20 mL). The organic layers were then combined, dried over a hydrophobic frit and the solvent removed *in vacuo*. The sample was loaded preabsorbed on florisil and purified by column chromatography on silica using a 0-50% ethyl acetate/cyclohexane gradient. The appropriate fractions were combined and concentrated *in vacuo* to give the title compound (746 mg, 76%) as a white solid. $\nu_{\text{max}}/\text{cm}^{-1}$ (neat): 3287 (broad), 1588, 1571; ^1H NMR (400 MHz, DMSO- d_6) δ 3.30 (s, 3H) 4.45 (dt, $J = 5.6, 1.0$ Hz, 2H) 5.34 (t, $J = 5.6$ Hz, 1H) 7.82 (dt, $J = 2.5, 1.0$ Hz, 1H) 8.16 (d, $J = 2.4$ Hz, 1H); ^{13}C NMR (101 MHz, DMSO- d_6) δ 54.0, 57.4, 111.9, 127.8, 137.9, 145.0, 159.6; LCMS (Method A): MH^+ 220, 222, Rt 0.78 min, 95% by UV; HRMS exact mass calculated for $[\text{M}+\text{H}]^+$ ($\text{C}_7\text{H}_9\text{BrNO}_2$) requires m/z : 217.9811, found: 217.9817.

5-Bromo-2-methoxy-3-(methoxymethyl)pyridine, 137

To a solution of (5-bromo-2-methoxypyridin-3-yl)methanol (100 mg, 0.46 mmol) in THF (5 mL) was added sodium hydride (28 mg, 0.69 mmol). The reaction mixture was then stirred at room temperature for 30 mins. To the reaction mixture was then added methyl iodide (0.034 mL, 0.55 mmol) and the mixture stirred for 24 hours. The reaction mixture was then poured into ice cold water (10 mL), extracted with ethyl acetate (2 x 20 mL) and the organic portions combined. The organic portions were then dried over a hydrophobic frit and the solvent removed *in vacuo* to yield the title compound (44 mg, 41%) $\nu_{\max}/\text{cm}^{-1}$ (neat): 2925, 1584, 1572; $^1\text{H NMR}$ (400 MHz, DMSO- d_6) δ 3.35 (s, 3H), 3.89 (s, 3H), 4.37 (s, 2H), 7.81 (d, $J = 2.5$ Hz, 1H), 8.23 (d, $J = 2.5$ Hz, 1H); $^{13}\text{C NMR}$ (101 MHz, DMSO- d_6) δ 54.1, 58.6, 67.9, 111.7, 123.7, 139.1, 146.1, 160.1; LCMS (Method A): MH^+ 232, 234, R_t 1.10 min, 100% by UV; HRMS exact mass calculated for $[\text{M}+\text{H}]^+$ ($\text{C}_8\text{H}_{11}\text{BrNO}_2$) requires m/z : 231.9968, found: 231.9969.

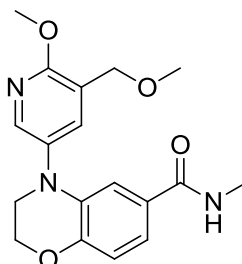
Methyl 4-(6-methoxy-5-(methoxymethyl)pyridin-3-yl)-3,4-dihydro-2H-benzo[*b*][1,4]oxazine-6-carboxylate, 138

To methyl 3,4-dihydro-2H-benzo[*b*][1,4]oxazine-6-carboxylate (220 mg, 1.1 mmol), caesium carbonate (730 mg, 2.2 mmol) and RuPhos Pd G2 (87 mg, 0.11 mmol) was added a solution of 5-bromo-2-methoxy-3-(methoxymethyl)pyridine (260 mg, 1.1 mmol) in 1,4-dioxane (4 mL). The reaction vessel was sealed and heated under microwave irradiation to 130 °C for 3 hours. The reaction mixture was then filtered through celite, washed with DCM (20 mL) and the solvent removed *in vacuo*. The

CONFIDENTIAL – PROPERTY OF GSK – DO NOT COPY

sample was loaded in DCM and purified by column chromatography on silica using a 0-100% ethyl acetate/cyclohexane gradient. The appropriate fractions were combined and concentrated *in vacuo* to give the title compound (175 mg, 45%) as a colourless solid. $\nu_{\max}/\text{cm}^{-1}$ (neat): 1703; $^1\text{H NMR}$ (400 MHz, $\text{DMSO-}d_6$) δ 3.35 (s, 3H), 3.68 (t, $J = 4.3$ Hz, 2H), 3.71 (s, 3H), 3.93 (s, 3H), 4.38 (t, $J = 4.3$ Hz, 2H), 4.41 (s, 2H), 6.91 (d, $J = 8.3$ Hz, 1H), 7.08 (d, $J = 2.0$ Hz, 1H), 7.31 (dd, $J = 8.3, 2.0$ Hz, 1H), 7.65 (d, $J = 2.8$ Hz, 1H), 8.09 (d, $J = 2.8$ Hz, 1H); $^{13}\text{C NMR}$ (101 MHz, $\text{DMSO-}d_6$) δ 26.8, 48.6, 52.2, 58.4, 65.2, 68.3, 115.3, 117.2, 121.2, 122.2, 122.6, 134.4, 134.8, 136.7, 142.8, 148.7, 158.5 168.8; LCMS (Method B): MH^+ 345, R_t 1.19 min, 100% by UV; HRMS exact mass calculated for $[\text{M}+\text{H}]^+$ ($\text{C}_{18}\text{H}_{21}\text{N}_2\text{O}_5$) requires m/z : 345.1445, found: 345.1452.

4-(6-Methoxy-5-(methoxymethyl)pyridin-3-yl)-*N*-methyl-3,4-dihydro-2*H*-benzo[*b*][1,4]oxazine-6-carboxamide, 139

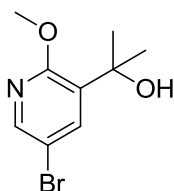


To a solution of methyl 4-(6-methoxy-5-(methoxymethyl)pyridin-3-yl)-3,4-dihydro-2*H*-benzo[*b*][1,4]oxazine-6-carboxylate (160 mg, 0.47 mmol) in water (2 mL) and THF (2 mL) was added lithium hydroxide (67 mg, 2.8 mmol). The mixture was then stirred at room temperature for 7 days. The reaction mixture was acidified with 2M aqueous hydrochloric acid to pH 3, and extracted with DCM (10 mL). The organic portion was then dried over a hydrophobic frit and solvent removed *in vacuo* to yield a white solid (102 mg). To this, was added HATU (116 mg, 0.30 mmol) and DIPEA (0.14 mL, 0.90 mmol) in *N,N*-dimethylformamide (1 mL) and the reaction mixture was stirred for 30 mins. Methylamine (40 wt% aqueous) (0.029 mL, 0.33 mmol) was then added and the mixture stirred for 18 hours. The reaction mixture was diluted with 5% aqueous lithium chloride solution (2 mL) and extracted with ethyl acetate (3 x 2 mL). The organic portions were combined, dried over a hydrophobic frit and the solvent removed *in vacuo*. The sample was dissolved in DMSO (1 mL) and purified by mass

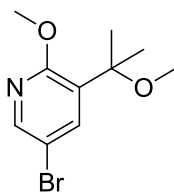
CONFIDENTIAL – PROPERTY OF GSK – DO NOT COPY

directed HPLC on using acetonitrile/water with an ammonium carbonate modifier. The solvent was removed *in vacuo* to give the title compound (65 mg, 40%) as an off white solid. $\nu_{\max}/\text{cm}^{-1}$ (neat) 3330 (broad), 1635; $^1\text{H NMR}$ (400 MHz, CDCl_3) δ 2.91 (d, $J = 4.8$ Hz, 3H), 3.47 (s, 3H), 3.67 (t, $J = 4.3$ Hz, 2H), 4.00 (s, 3H), 4.38 (t, $J = 4.3$ Hz, 2H), 4.46 (s, 2H), 5.94 (br. s., 1H), 6.87 (d, $J = 8.3$ Hz, 1H), 7.02 (d, $J = 2.0$ Hz, 1H), 7.08 (dd, $J = 8.3, 2.0$ Hz, 1H), 7.60 (d, $J = 2.5$ Hz, 1H), 8.01 (d, $J = 2.6$ Hz, 1H); $^{13}\text{C NMR}$ (101 MHz, CDCl_3) δ 26.7, 49.2, 53.6, 58.8, 64.7, 68.7, 114.2, 116.7, 118.0, 122.5, 127.9, 134.0, 134.3, 136.8, 142.7, 147.0, 158.6, 167.9 LCMS (Method B): MH^+ 344, Rt 0.91 min, 100% by UV; HRMS exact mass calculated for $[\text{M}+\text{H}]^+$ ($\text{C}_{18}\text{H}_{22}\text{N}_3\text{O}_4$) requires m/z : 344.1605, found: 344.1610.

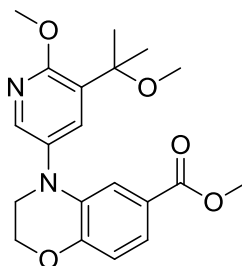
2-(5-Bromo-2-methoxypyridin-3-yl)propan-2-ol, 140



To a solution of methyl 5-bromo-2-methoxynicotinate (1.0 g, 4.0 mmol) in 2-methyltetrahydrofuran (15 mL) cooled to 0 °C was added methylmagnesium bromide (3.4 M in THF) (2.6 mL, 8.9 mmol). This was then stirred at room temperature for 18 hours. The reaction mixture was cooled to 0 °C and quenched with 1M aqueous hydrochloric acid (5 mL). The reaction mixture was extracted with ethyl acetate (3 x 10 mL), the organic portions combined, dried over a hydrophobic frit and the solvent removed *in vacuo*. This afforded the title compound (980 mg, 98%) as an off white solid. $\nu_{\max}/\text{cm}^{-1}$ (neat): 3439 (broad); $^1\text{H NMR}$ (400 MHz, $\text{DMSO}-d_6$) δ 1.47 (s, 6H), 3.89 (s, 3H), 7.98 (d, $J = 2.5$ Hz, 1H), 8.15 (d, $J = 2.5$ Hz, 1H); $^{13}\text{C NMR}$ (101 MHz, $\text{DMSO}-d_6$) δ 29.0, 54.0, 69.9, 112.0, 134.8, 137.6, 145.0, 159.3 LCMS (Method A): MH^+ 246, 248, Rt 1.00 min, 88% by UV; HRMS exact mass calculated for $[\text{M}+\text{H}]^+$ ($\text{C}_9\text{H}_{13}\text{BrNO}_2$) requires m/z : 246.0124, found: 246.0126.

5-Bromo-2-methoxy-3-(2-methoxypropan-2-yl)pyridine, 141

To a solution of 2-(5-bromo-2-methoxy-3-(2-methoxypropan-2-yl)pyridin-3-yl)propan-2-ol (300 mg, 1.2 mmol) in THF (5 mL) was added sodium hydride (73 mg, 1.8 mmol) and the mixture was stirred for 30 minutes. To the reaction, was then added methyl iodide (0.091 mL, 1.5 mmol) and the mixture stirred for a further 4 hours. The reaction was then poured into ice cold water (5 mL) and extracted with ethyl acetate (3 x 10 mL). The organic portions were combined, dried over a hydrophobic frit and the solvent removed *in vacuo* to yield 5-bromo-2-methoxy-3-(2-methoxypropan-2-yl)pyridine (194 mg, 61%) as a clear oil. $\nu_{\max}/\text{cm}^{-1}$ (oil) 2926, 1561; $^1\text{H NMR}$ (400 MHz, $\text{DMSO-}d_6$) δ 1.48 (s, 6H), 3.16 (s, 3H), 3.89 (s, 3H), 7.80 (d, $J = 2.5$ Hz, 1H), 8.20 (d, $J = 2.5$ Hz, 1H); $^{13}\text{C NMR}$ (101 MHz, $\text{DMSO-}d_6$) δ 25.2, 50.1, 54.1, 75.4, 111.9, 131.1, 138.2, 145.6, 159.8 LCMS (Method A): MH^+ 260, 262, R_t 1.27 min, 96% by UV; HRMS exact mass calculated for $[\text{M}+\text{H}]^+$ ($\text{C}_{10}\text{H}_{15}\text{BrNO}_2$) requires m/z :260.0281, found: 260.0284.

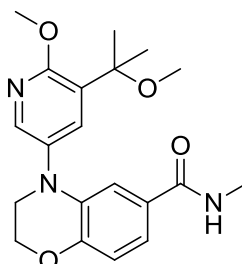
Methyl 4-(6-methoxy-5-(2-methoxypropan-2-yl)pyridin-3-yl)-3,4-dihydro-2H-benzo[*b*] [1,4]oxazine-6-carboxylate, 142

To solid methyl 3,4-dihydro-2H-benzo[*b*][1,4]oxazine-6-carboxylate (134 mg, 0.69 mmol) dicyclohexyl(2',6'-diisopropoxy-[1,1'-biphenyl]-2-yl)phosphine (129 mg, 0.28 mmol) caesium carbonate (680 mg, 2.1 mmol) and $\text{Pd}_2(\text{dba})_3$ (127 mg, 0.14 mmol), was added a solution of 5-bromo-2-methoxy-3-(2-methoxypropan-2-yl)pyridine (180 mg, 0.69 mmol) in 1,4-dioxane (4 mL). The vial was sealed and heated under microwave irradiation to 130 °C for 3 hours. The reaction mixture was then filtered through celite, washed with DCM (20 mL) and the solvent removed *in vacuo*. The

CONFIDENTIAL – PROPERTY OF GSK – DO NOT COPY

sample was loaded in DCM and purified by column chromatography on silica using a 0-100% ethyl acetate/cyclohexane gradient. The appropriate fractions were combined and concentrated *in vacuo* to give the title compound (116 mg, 45%) as a colourless glass. $\nu_{\max}/\text{cm}^{-1}$ (neat): 1713; $^1\text{H NMR}$ (400 MHz, $\text{DMSO-}d_6$) δ 1.52 (s, 6H), 3.14 (s, 3H), 3.71 (t, $J = 4.5$ Hz, 2H), 3.70 (s, 3H), 3.93 (s, 3H), 4.39 (t, $J = 4.5$ Hz, 2H), 6.92 (d, $J = 8.3$ Hz, 1H), 7.17 (d, $J = 2.0$ Hz, 1H), 7.31 (dd, $J = 8.3, 2.0$ Hz, 1H), 7.66 (d, $J = 2.5$ Hz, 1H), 8.06 (d, $J = 2.5$ Hz, 1H); $^{13}\text{C NMR}$ (101 MHz, $\text{DMSO-}d_6$) δ 25.9, 48.3, 50.2, 52.2, 53.9, 65.2, 75.7, 115.2, 117.2, 121.2, 122.6, 129.2, 133.7, 134.0, 136.6, 141.5, 148.7, 158.1, 166.4; LCMS (Method B): MH^+ 373, R_t 1.30 min, 93% by UV; HRMS exact mass calculated for $[\text{M}+\text{H}]^+$ ($\text{C}_{20}\text{H}_{25}\text{BrN}_2\text{O}_5$) requires m/z : 373.1758, found: 373.1755.

4-(6-Methoxy-5-(2-methoxypropan-2-yl)pyridin-3-yl)-*N*-methyl-3,4-dihydro-2H-benzo[*b*][1,4]oxazine-6-carboxamide, 143

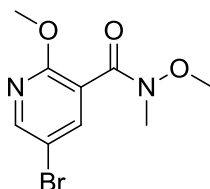


To a solution of methyl 4-(6-methoxy-5-(2-methoxypropan-2-yl)pyridin-3-yl)-3,4-dihydro-2H-benzo[*b*][1,4]oxazine-6-carboxylate (110 mg, 0.30 mmol) in water (2 mL) and THF (2 mL) was added lithium hydroxide (42 mg, 1.8 mmol). The mixture was then stirred at room temperature for 7 days. The reaction mixture was acidified with 2M aqueous hydrochloric acid to pH 3, and extracted with DCM (10 mL). The organic portion was then dried over a hydrophobic frit and solvent removed *in vacuo* to yield a clear glass. This was then dissolved in *N,N*-dimethylformamide (1 mL), HATU (53 mg, 0.14 mmol) and DIPEA (0.073 mL, 0.42 mmol) were added and the reaction mixture was stirred for 30 mins. Methylamine (40 wt% aqueous) (0.027 mL, 0.31 mmol) was then added and the mixture stirred for 18 hours. The reaction mixture was diluted with 5% aqueous lithium chloride solution (2 mL) and extracted with ethyl acetate (3 x 2 mL). The organic portions were then combined, dried over a hydrophobic frit and the solvent removed *in vacuo*. The samples were dissolved in DMSO (1 mL)

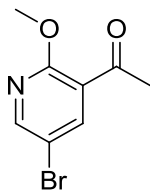
CONFIDENTIAL – PROPERTY OF GSK – DO NOT COPY

and purified by mass directed HPLC using acetonitrile/water with an ammonium carbonate modifier. The solvent was removed *in vacuo* to give the title compound (17 mg, 16%) as a clear glass. $\nu_{\max}/\text{cm}^{-1}$ (neat): 3320, 1631; $^1\text{H NMR}$ (400 MHz, CDCl_3) 1.60 (s, 6H), 2.92 (d, $J = 4.8$ Hz, 3H), 3.26 (s, 3H), 3.69 (t, $J = 4.5$ Hz, 2H), 4.00 (s, 3H), 4.39 (t, $J = 4.3$ Hz, 2H), 6.88 (d, $J = 8.3$ Hz, 1H), 7.06 (dd, $J = 8.3, 2.0$ Hz, 1H), 7.12 (d, $J = 2.0$ Hz, 1H), 7.68 (d, $J = 2.8$ Hz, 1H), 7.99 (d, $J = 2.8$ Hz, 1H); $^{13}\text{C NMR}$ (101 MHz, CDCl_3) δ 25.5, 26.7, 49.1, 50.4, 53.4, 64.7, 75.9, 114.3, 116.7, 117.7, 127.8, 129.8, 133.6, 133.9, 136.7, 141.6, 147.0, 158.4, 167.9; LCMS (Method B): MH⁺ 370, Rt 1.02 min, 93% by UV; HRMS exact mass calculated for $[\text{M}+\text{H}]^+$ ($\text{C}_{20}\text{H}_{26}\text{N}_3\text{O}_4$) requires m/z : 372.1917, found: 372.1913.

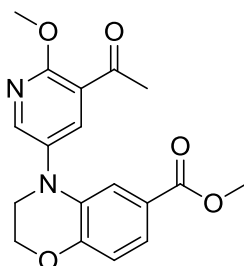
5-Bromo-*N*,2-dimethoxy-*N*-methylnicotinamide, 144²⁵²



To a solution of 5-bromo-2-methoxynicotinic acid (500 mg, 2.2 mmol) in *N,N*-dimethylformamide (20 mL), was added HATU (820 mg, 2.2 mmol) and DIPEA (0.84 mL, 6.5 mmol). The mixture was stirred at room temperature for 30 mins. To the mixture was then added *N,O*-dimethylhydroxylamine hydrochloride (210 mg, 2.2 mmol) and the reaction was stirred for a further 18 hours. The solution was diluted with saturated aqueous sodium hydrogen carbonate (20 mL) and extracted with ethyl acetate (2 x 20 mL). The organic portions were combined and the solvent removed *in vacuo*. The sample was loaded in DCM and purified by column chromatography on silica using a 0-100% ethyl acetate/cyclohexane gradient. The appropriate fractions were combined and concentrated *in vacuo* to give the title compound (480 mg, 81%) as an off-white solid. $\nu_{\max}/\text{cm}^{-1}$ (neat) 1641; $^1\text{H NMR}$ (400 MHz, $\text{DMSO}-d_6$) δ 3.23 (br. s., 3H), 3.51 (br. s., 3H), 3.90 (s, 3H), 8.01 (d, $J = 2.5$ Hz, 1H), 8.37 (d, $J = 2.5$ Hz, 1H); $^{13}\text{C NMR}$ (101 MHz, $\text{DMSO}-d_6$) δ 32.1, 54.4, 61.5, 111.3, 121.8, 139.1, 148.2, 158.7, 165.2, LCMS (Method B): MH⁺ 275, 277, Rt 0.86 min, 94% by UV; HRMS exact mass calculated for $[\text{M}+\text{H}]^+$ ($\text{C}_9\text{H}_{12}\text{BrN}_2\text{O}_3$) requires m/z : 275.0026, found: 275.0036.

1-(5-Bromo-2-methoxypyridin-3-yl)ethanone, 145²⁵²

To a solution of 5-bromo-*N*,2-dimethoxy-*N*-methylnicotinamide (1.5 g, 5.5 mmol) in 2-methyltetrahydrofuran (30 mL), cooled to 0 °C, was added methylmagnesium bromide (2.4 mL, 8.2 mmol). The reaction mixture was then allowed to warm to room temperature and was stirred for 4 hours. The reaction mixture was cooled to 0 °C and quenched by dropwise addition of 1M aqueous hydrochloric acid (3 mL). The organic phase was separated and the aqueous phase extracted with further ethyl acetate (5 mL). The organic phases were then combined, dried over a hydrophobic frit and the solvent removed *in vacuo* to yield the title compound (1.15 g, 92%) as a yellow solid. $\nu_{\max}/\text{cm}^{-1}$ (neat) 1674; $^1\text{H NMR}$ (400 MHz, DMSO- d_6) δ 2.57 (s, 3H), 3.98 (s, 3H), 8.13 (d, $J = 2.5$ Hz, 1H), 8.50 (d, $J = 2.5$ Hz, 1H); $^{13}\text{C NMR}$ (101 MHz, DMSO- d_6) δ 31.2, 54.8, 111.9, 123.4, 141.6, 151.3, 160.7, 196.8 LCMS (Method A): MH+ 230, 232, Rt 1.03 min, 100% by UV; HRMS exact mass calculated for $[\text{M}+\text{H}]^+$ ($\text{C}_8\text{H}_9\text{BrNO}_2$) requires m/z : 229.9811, found: 229.9809.

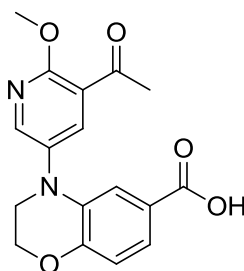
Methyl 4-(5-acetyl-6-methoxypyridin-3-yl)-3,4-dihydro-2H-benzo[*b*][1,4]oxazine-6-carboxylate, 146

To solid 1-(5-bromo-2-methoxypyridin-3-yl)ethanone (1.0 g, 4.4 mmol) methyl 3,4-dihydro-2H-benzo[*b*][1,4]oxazine-6-carboxylate (0.84 g, 4.4 mmol) caesium carbonate (2.83 g, 8.6 mmol) and RuPhos Pd G2 (0.34 g, 0.44 mmol) was added 1,4-dioxane (16 mL). The reaction vessel was sealed and heated under microwave irradiation conditions to 130 °C for 3 hours. After cooling, the reaction mixture was filtered through celite, washed with DCM (30 mL) and the solvent removed *in vacuo*.

CONFIDENTIAL – PROPERTY OF GSK – DO NOT COPY

The sample was loaded in DCM and purified by column chromatography on silica using a 0-100% TBME/cyclohexane gradient. The appropriate fractions were combined and concentrated *in vacuo* to give the title compound (610 mg, 41%) as a yellow gum. $\nu_{\max}/\text{cm}^{-1}$ (neat) 1671, 1715; $^1\text{H NMR}$ (400 MHz, $\text{DMSO-}d_6$) δ 2.60 (s, 3H), 3.72 (s, 3H), 3.71 (t, $J = 4.5$ Hz, 2H), 4.04 (s, 3H), 4.38 (t, $J = 4.3$ Hz, 2H), 6.94 (d, $J = 8.3$ Hz, 1H), 7.11 (d, $J = 2.0$ Hz, 1H), 7.34 (dd, $J = 8.3, 2.0$ Hz, 1H), 7.99 (d, $J = 2.8$ Hz, 1H), 8.40 (d, $J = 2.8$ Hz, 1H) $^{13}\text{C NMR}$, (101 MHz, $\text{DMSO-}d_6$) δ 31.4, 48.4, 52.3, 54.6, 65.1, 115.6, 117.3, 121.6, 122.2, 122.7, 133.7, 136.5, 137.0, 148.3, 148.8, 159.1, 166.4, 197.4; LCMS (Method B): MH^+ 343, R_t 1.16 min, 97% by UV; HRMS exact mass calculated for $[\text{M}+\text{H}]^+$ ($\text{C}_{18}\text{H}_{19}\text{N}_2\text{O}_5$) requires m/z : 343.1289, found: 343.1289.

4-(5-Acetyl-6-methoxypyridin-3-yl)-3,4-dihydro-2H-benzo[*b*][1,4]oxazine-6-carboxylic acid, 147

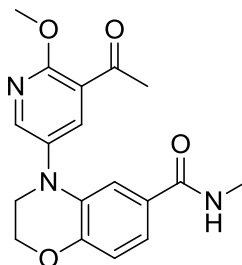


To a solution of methyl 4-(5-acetyl-6-methoxypyridin-3-yl)-3,4-dihydro-2H-benzo[*b*][1,4]oxazine-6-carboxylate (600 mg, 1.8 mmol) in THF (5 mL) and water (5 mL) was added lithium hydroxide (250 mg, 11 mmol) The mixture was then stirred at room temperature for 5 days. The reaction was acidified with 2M aqueous hydrochloric acid to pH 3. The mixture was extracted with DCM (40 mL), the organic portion dried over a hydrophobic frit and the solvent removed *in vacuo* to yield the title compound (560 mg, 97% yield) as a yellow gum. $\nu_{\max}/\text{cm}^{-1}$ (neat): 3455 (broad), 1633; $^1\text{H NMR}$ (400 MHz, $\text{DMSO-}d_6$) δ 2.60 (s, 3H), 3.70 (t, $J = 4.5$ Hz, 2H), 4.03 (s, 3H), 4.37 (t, $J = 4.3$ Hz, 2H), 6.91 (d, $J = 8.3$ Hz, 1H), 7.11 (d, $J = 2.0$ Hz, 1H), 7.32 (dd, $J = 8.3, 2.0$ Hz, 1H), 7.99 (d, $J = 2.8$ Hz, 1H), 8.40 (d, $J = 2.8$ Hz, 1H), 12.49 (br. s., 1H) $^{13}\text{C NMR}$ (101 MHz, $\text{DMSO-}d_6$) δ 31.4, 48.3, 54.6, 65.1, 115.8, 117.1, 121.8, 122.2, 123.8, 133.6, 136.5, 137.1, 148.3, 148.5, 159.1, 167.4, 197.4; LCMS (Method

CONFIDENTIAL – PROPERTY OF GSK – DO NOT COPY

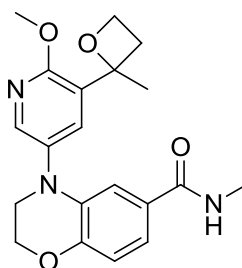
A): MH⁺ 329, Rt 0.94 min, 94% by UV; HRMS exact mass calculated for [M+H]⁺ (C₁₇H₁₇N₂O₅) requires *m/z*: 329.1132, found: 329.1134.

4-(5-Acetyl-6-methoxypyridin-3-yl)-*N*-methyl-3,4-dihydro-2*H*-benzo[*b*][1,4]oxazine-6-carboxamide, 148



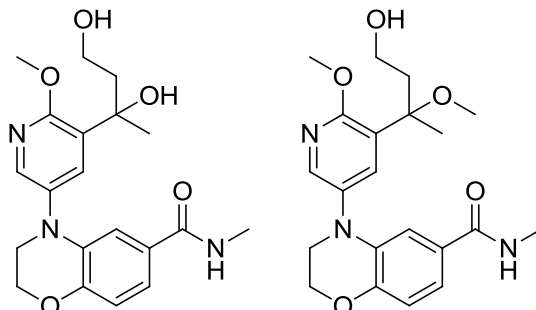
To a solution of 4-(5-acetyl-6-methoxypyridin-3-yl)-3,4-dihydro-2*H*-benzo[*b*][1,4]oxazine-6-carboxylic acid (550 mg, 1.7 mmol) in *N,N*-dimethylformamide (10 mL) was added HATU (640 mg, 1.7 mmol) and DIPEA (0.87 mL, 5.0 mmol). The mixture was then stirred at room temperature for 30 mins. To the reaction mixture, was then added methylamine (40 wt% aqueous) (0.32 mL, 3.7 mmol). The reaction mixture was then stirred at room temperature for a further 18 hours. The reaction mixture was then diluted with saturated aqueous sodium hydrogen carbonate (10 mL) and extracted with ethyl acetate (2 x 10 mL). The combined organic portions were then dried over a hydrophobic frit and the solvent removed *in vacuo*. The sample was loaded in DCM and purified by column chromatography on silica using a 0-100% ethyl acetate/cyclohexane gradient. The appropriate fractions were combined and concentrated *in vacuo* to give the title compound (290 mg, 51%) as a yellow oil which solidified on standing. $\nu_{\max}/\text{cm}^{-1}$ (neat): 3396, 1705, 1660; ¹H NMR (400 MHz, DMSO-*d*₆) δ 2.60 (s, 3H), 2.68 (d, *J* = 4.3 Hz, 3H), 3.69 (t, *J* = 4.3 Hz, 2H), 4.03 (s, 3H), 4.32 (t, *J* = 4.3 Hz, 2H), 6.87 (d, *J* = 8.3 Hz, 1H), 7.08 (d, *J* = 2.0 Hz, 1H), 7.22 (dd, *J* = 8.3, 2.0 Hz, 1H), 7.95 (d, *J* = 2.8 Hz, 1H), 8.11 (q, *J* = 4.5 Hz, 1H), 8.37 (d, *J* = 2.8 Hz, 1H); ¹³C NMR (101 MHz, DMSO-*d*₆) δ 31.4, 38.7, 48.8, 54.5, 64.8, 114.6, 116.8, 119.2, 122.1, 127.8, 133.2, 136.3, 137.6, 147.1, 148.2, 158.9, 166.6, 197.4; LCMS (Method B): MH⁺ 342, Rt 0.89 min, 99% by UV; HRMS exact mass calculated for [M+H]⁺ (C₁₈H₂₀N₃O₄) requires *m/z*: 342.1448, found: 342.1451.

4-(6-Methoxy-5-(2-methyloxetan-2-yl)pyridin-3-yl)-N-methyl-3,4-dihydro-2H-benzo[*b*][1,4]oxazine-6-carboxamide, 149

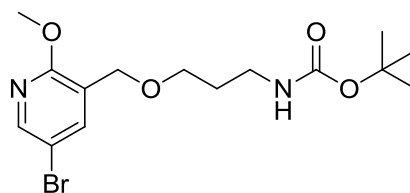


To solid trimethylsulfoxonium iodide (260 mg, 1.2 mmol) and potassium *tert*-butoxide (130 mg, 1.2 mmol) was added *t*-butanol (2 mL) and the mixture was stirred at 50 °C for 30 mins. To the reaction mixture, was then added a solution of 4-(5-acetyl-6-methoxypyridin-3-yl)-*N*-methyl-3,4-dihydro-2H-benzo[*b*][1,4]oxazine-6-carboxamide (100 mg, 0.3 mmol) in *t*-butanol (1 mL). The reaction mixture was then stirred at 50 °C for 5 days. The solvent was removed *in vacuo* and the residue dissolved in water (5 mL). This was then extracted with ethyl acetate (2 x10 mL), the organic portions combined, dried over a hydrophobic frit and the solvent removed *in vacuo*. The residue was dissolved in DMSO (2 mL) and purified by Mass Directed HPLC using acetonitrile/water with an ammonium carbonate modifier. The solvent was removed *in vacuo* to give the title compound (35 mg, 32%) as a white solid. $\nu_{\max}/\text{cm}^{-1}$ (neat): 3330, 1632; $^1\text{H NMR}$ (400 MHz, DMSO- d_6) δ 1.64 (s, 3H), 2.60-2.66 (m, 1H), 2.68 (d, $J = 4.5$ Hz, 3H), 2.75-2.83 (m, 1H), 3.69 (t, $J = 4.5$ Hz, 2H), 3.92 (s, 3H), 4.33 (t, $J = 4.4$ Hz, 2H), 4.34-4.39 (m, 1H), 4.50 (dt, $J = 8.6, 6.1$ Hz, 1H), 6.85 (d, $J = 8.1$ Hz, 1H), 7.18 (d, $J = 2.0$ Hz, 1H), 7.20 (dd, $J = 8.1, 2.0$ Hz, 1H), 7.67 (d, $J = 2.8$ Hz, 1H), 8.04 (d, $J = 2.8$ Hz, 1H), 8.12 (q, $J = 4.5$ Hz, 1H); $^{13}\text{C NMR}$ (101 MHz, DMSO- d_6) δ 26.6, 28.5, 34.2, 40.7, 48.8, 53.9, 64.9, 84.5, 114.6, 116.7, 118.7, 127.7, 130.8, 130.9, 133.4, 137.3, 141.4, 147.0, 156.3, 166.7; LCMS (Method B): MH^+ 370, Rt 0.96 min, 100% by UV; HRMS exact mass calculated for $[\text{M}+\text{H}]^+$ ($\text{C}_{20}\text{H}_{24}\text{N}_3\text{O}_4$) requires m/z : 370.1761, found: 370.1764.

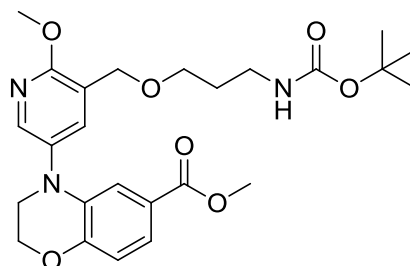
4-(5-(2,4-Dihydroxybutan-2-yl)-6-methoxy-pyridin-3-yl)-*N*-methyl-3,4-dihydro-2*H*-benzo[*b*][1,4]oxazine-6-carboxamide, 151 & 4-(5-(4-Hydroxy-2-methoxybutan-2-yl)-6-methoxy-pyridin-3-yl)-*N*-methyl-3,4-dihydro-2*H*-benzo[*b*][1,4]oxazine-6-carboxamide, 152



To a solution of 4-(6-methoxy-5-(2-methyloxetan-2-yl)pyridin-3-yl)-*N*-methyl-3,4-dihydro-2*H*-benzo[*b*][1,4]oxazine-6-carboxamide (10 mg, 0.027 mmol) in dimethyl sulfoxide (1 mL) was added 2M aqueous hydrochloric acid (5 μ l, 0.165 mmol). After 5 minutes, the sample was purified by mass directed HPLC using acetonitrile/water with a formic acid modifier. The solvent was removed *in vacuo* to give the title compounds **151** (3 mg, 29%) and **152** (5 mg, 46%). **151**: ^1H NMR (400 MHz, CDCl_3) δ 1.63 (s, 3H), 2.10-2.27 (m, 2H), 2.93 (d, $J = 4.8$ Hz, 3H), 3.68-3.77 (m, 2H), 3.78-3.93 (m, 2H), 4.03 (s, 3H), 4.32-4.45 (m, 2H), 6.15 (br. s., 1H), 6.86 (d, $J = 8.6$ Hz, 1H), 6.89 (dd, $J = 8.6, 2.0$ Hz, 1H), 7.16 (d, $J = 2.0$ Hz, 1H), 7.94 (d, $J = 2.8$ Hz, 1H), 8.17 (d, $J = 2.8$ Hz, 1H); LCMS (Method A): MH^+ 388, Rt 0.81 min, 83% by UV; **152**: ^1H NMR (400 MHz, CDCl_3) δ 1.73 (s, 3H), 2.15-2.29 (m, 2H), 2.87 (d, $J = 4.53$ Hz, 3H), 3.32 (s, 3H), 3.46 (m, 1H), 3.59-3.73 (m, 2H), 3.73-3.80 (m, 1H), 3.99 (s, 3H), 4.37-4.48 (m, 2H), 6.58 (br. s., 1H), 6.90 (d, $J = 8.31$ Hz, 1H), 6.95 (d, $J = 2.30$ Hz, 1H), 7.19 (dd, $J = 8.31, 2.27$ Hz, 1H), 7.77 (d, $J = 2.60$ Hz, 1H), 7.99 (d, $J = 2.52$ Hz, 1H); ^{13}C NMR (101 MHz, CDCl_3) δ 22.3, 26.6, 39.3, 48.7, 50.3, 53.6, 59.9, 64.9, 79.9, 113.1, 116.9, 118.9, 126.9, 128.0, 133.5, 134.5, 136.4, 141.4, 146.8, 157.9, 168.1; LCMS (Method A): MH^+ 402, Rt 0.87 min, 94% by UV.

***Tert*-butyl (3-((5-bromo-2-methoxypyridin-3-yl)methoxy)propyl)carbamate, 155**

To a solution of (5-bromo-2-methoxypyridin-3-yl)methanol (1.5 g, 6.9 mmol) in THF (50 mL), was added sodium hydride (0.42 g, 10.3 mmol). The reaction mixture was then stirred at room temperature for 30 mins. To the reaction mixture was then added *tert*-butyl (3-bromopropyl)carbamate (1.97 g, 8.3 mmol) and the mixture stirred for 16 hours. The reaction mixture was then quenched with water (25 mL), extracted with ethyl acetate (2 x 30 mL) and the organic portions combined. The organic portions were then dried over a hydrophobic frit and the solvent removed *in vacuo*. The sample was loaded preabsorbed on florisil and purified by column chromatography on silica using a 0-25% ethyl acetate:cyclohexane gradient. The appropriate fractions were combined and concentrated *in vacuo* to give the title compound (1.68 g, 65% yield) as a white crystalline solid. $\nu_{\max}/\text{cm}^{-1}$ (neat) 1518, 1678, 3370; ^1H NMR (400 MHz, CDCl_3) δ 1.46 (s, 9H), 1.85 (quin, $J = 6.2$ Hz, 2H), 3.29 (q, $J = 6.1$ Hz, 2H), 3.63 (t, $J = 5.9$ Hz, 2H), 3.96 (s, 3H), 4.46 (s, 2H), 4.84 (br. s, 1H), 7.71-7.78 (m, 1H), 8.13 (d, $J = 2.7$ Hz, 1H); ^{13}C NMR (101 MHz, CDCl_3) δ 26.9, 28.4, 29.8, 38.6, 53.7, 66.8, 69.5, 111.9, 123.2, 138.6, 145.9, 156.0, 159.8; LCMS (Method B): $[\text{M}+\text{H}]^+$ 277, 279, Rt 1.29 min, 95% by UV; HRMS exact mass calculated for $[\text{M}+\text{Na}]^+$ ($\text{C}_{15}\text{H}_{23}\text{BrN}_2\text{NaO}_4$) requires m/z 397.0742, found 397.0737.

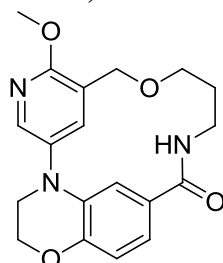
Methyl 4-(5-((3-((*tert*-butoxycarbonyl)amino)propoxy)methyl)-6-methoxypyridin-3-yl)-3,4-dihydro-2H-benzo[*b*][1,4]oxazine-6-carboxylate, 156

To methyl 3,4-dihydro-2H-benzo[*b*][1,4]oxazine-6-carboxylate (360 mg, 1.9 mmol), caesium carbonate (1.2 g, 3.7 mmol) and RuPhos Pd G2 (145 mg, 0.19 mmol), was added a solution of *tert*-butyl (3-((5-bromo-2-methoxypyridin-3-

CONFIDENTIAL – PROPERTY OF GSK – DO NOT COPY

yl)methoxy)propyl)carbamate (700 mg, 1.9 mmol) in 1,4-dioxane (15 mL). The reaction vessel was sealed and heated under microwave irradiation conditions to 130 °C for 3 hours. The reaction mixture was then filtered through celite, and was washed with DCM (30 mL). The solvent was then removed *in vacuo*. The sample was loaded in DCM and purified by column chromatography on silica using a 0-100% ethyl acetate:cyclohexane gradient. The appropriate fractions were combined and concentrated *in vacuo* to give the title compound (300 mg, 33%) as a clear oil. $\nu_{\max}/\text{cm}^{-1}$ (neat) 1581, 1607, 1705; $^1\text{H NMR}$ (400 MHz, CDCl_3) δ 1.45 (s, 9H), 1.83 (quin, $J = 6.4$ Hz, 2H), 3.25 (q, $J = 6.0$ Hz, 2H), 3.63 (t, $J = 6.0$ Hz, 2H), 3.67-3.72 (m, 2H), 3.81 (s, 3H), 4.02 (s, 3H), 4.39-4.44 (m, 2H), 4.51 (s, 2H), 6.90 (d, $J = 8.3$ Hz, 1H), 7.30 (d, $J = 2.0$ Hz, 1H), 7.45 (dd, $J = 8.3, 2.0$ Hz, 1H), 7.60 (d, $J = 2.8$ Hz, 1H), 8.01 (d, $J = 2.8$ Hz, 1H); $^{13}\text{C NMR}$ (101 MHz, CDCl_3) δ 26.9, 28.4, 29.8, 38.5*, 49.0, 51.8, 53.7, 64.8, 67.1, 69.2, 116.6, 116.8, 121.7, 122.4, 123.1, 133.5, 134.1, 136.8, 142.2, 148.5, 156.0, 158.6, 166.9, *Peak not observed in 1D ^{13}C spectrum, coupling detected to this chemical shift in HMBC.; LCMS (Method B): $[\text{M}-\text{H}]^-$ 486, R_t 1.34 min, 87% by UV; HRMS exact mass calculated for $[\text{M}+\text{Na}]^+$ ($\text{C}_{25}\text{H}_{33}\text{N}_3\text{NaO}_7$) requires m/z 510.2216, found 510.2216.

9-Methoxy-2,12-dioxa-5,8,16-triazatetracyclo[16.2.2.16,(10),0(20,5)]tricosan-1(20),6(23),7,9,18,21-hexaen-17-one, 157

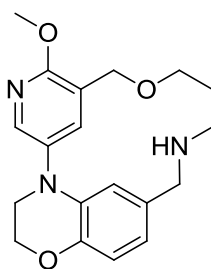


To a solution of methyl 4-(5-((3-((*tert*-butoxycarbonyl)amino)propoxy)methyl)-6-methoxypyridin-3-yl)-3,4-dihydro-2*H*-benzo[*b*][1,4]oxazine-6-carboxylate (0.3 g, 0.62 mmol) in water (5 mL) and THF (5 mL), was added lithium hydroxide (0.09 g, 3.7 mmol). The mixture was then stirred at room temperature for 4 days. The reaction mixture was then acidified to pH 3 using 2M aqueous hydrochloric acid and extracted with DCM (30 mL). The organic portion was then dried over a hydrophobic frit and the solvent removed *in vacuo* to yield a white solid (256 mg). To this was added DCM (5 mL) and trifluoroacetic acid (0.78 mL, 10.1 mmol) and the reaction mixture was

CONFIDENTIAL – PROPERTY OF GSK – DO NOT COPY

stirred at room temperature for 18 hours. The solvent was removed *in vacuo* to yield an orange oil (230 mg). This was dissolved in DMF (100 mL), HATU (360 mg, 0.94 mmol) and DIPEA (0.33 mL, 1.9 mmol) were added. The reaction mixture was then stirred at room temperature for 2 hours. The solvent was removed *in vacuo* and the residue was then dissolved in ethyl acetate (10 mL) and washed with 5% aqueous lithium chloride (3 x 10 mL). The organic portions were then dried over a hydrophobic frit and the solvent removed *in vacuo*. The samples were dissolved in DMSO and purified by mass directed HPLC on Xbridge column using acetonitrile:water with an ammonium carbonate modifier. The appropriate fractions were combined and concentrated *in vacuo* to give the title compound (65 mg, 16%) as a white solid. $\nu_{\max}/\text{cm}^{-1}$ (neat) 1653, 1701; $^1\text{H NMR}$ (400 MHz, CDCl_3) δ 1.89-1.98 (m, 2H), 3.50-3.58 (m, 2H), 3.84 (t, $J = 4.2$ Hz, 2H), 3.88 (t, $J = 4.9$ Hz, 2H), 4.01 (s, 3H), 4.37-4.48 (m, 2H), 4.53 (s, 2H), 6.90 (d, $J = 8.2$ Hz, 1H), 7.31 (dd, $J = 8.2, 2.0$ Hz, 1H), 7.40 (s, 1H), 7.90 (d, $J = 2.8$ Hz, 1H), 8.15 (d, $J = 2.8$ Hz, 1H); $^{13}\text{C NMR}$ (101 MHz, CDCl_3) δ 29.1*, 40.6*, 46.6, 53.8, 64.8, 66.6, 72.5*, 113.9, 117.3, 119.8, 121.0*, 128.2*, 130.8*, 133.9*, 136.1*, 137.4*, 147.3, 156.7*, 162.5*, *Peak not observed in 1D ^{13}C spectrum, coupling detected to this chemical shift in HMBC.; LCMS (Method B): MH^+ 356, Rt 0.99 min, 100% by UV; HRMS exact mass calculated for $[\text{M}+\text{H}]^+$ ($\text{C}_{19}\text{H}_{22}\text{N}_3\text{O}_4$) requires m/z 356.1010, found 356.1005.

9-Methoxy-2,12-dioxa-5,8,16-triazatetracyclo[16.2.2.16,(10),0(20,5)]tricosan-1(20),6(23),7,9,18,21-hexaene, 158

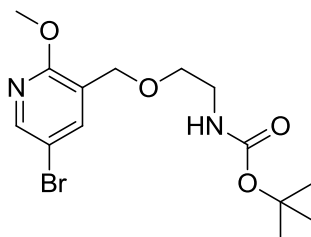


To 26-methoxy-13,14-dihydro-12*H*-4-oxa-8-aza-1(4,6)-benzo[*b*][1,4]oxazina-2(3,5)-pyridinacyclonaphan-9-one (50 mg, 0.14 mmol) in THF (5 mL) at 0 °C under nitrogen, was added 2M lithium aluminium hydride in THF (0.14 mL, 0.28 mmol) dropwise. The reaction mixture was then allowed to warm to room temperature and was stirred for 4 hours. The reaction mixture was then heated to 60 °C overnight. The

CONFIDENTIAL – PROPERTY OF GSK – DO NOT COPY

reaction was then quenched with water (5 mL) and the volume was reduced *in vacuo*. The residual solvent was then extracted with DCM (2 x 10 mL), dried over a hydrophobic frit and the solvent removed *in vacuo*. The sample was then dissolved in DMSO and purified by mass directed HPLC on Xbridge column using acetonitrile:water with an ammonium carbonate modifier. The solvent was removed *in vacuo* to give the title compound (12 mg, 25%) as a brown glass. $\nu_{\max}/\text{cm}^{-1}$ (neat) 1587, 1683, 2863, 2917; $^1\text{H NMR}$ (400 MHz, CDCl_3) δ 1.77-1.80 (m, 2H), 2.60-2.67 (m, 2H), 3.54-3.60 (m, 2H), 3.75-3.80 (m, 2H), 3.82 (s, 2H), 3.96 (s, 3H), 4.27-4.31 (m, 2H), 4.55 (s, 2H), 6.58 (dd, $J = 8.1, 1.5$ Hz, 1H), 6.82 (d, $J = 8.1$ Hz, 1H), 7.19 (d, $J = 1.5$ Hz, 1H), 7.89 (d, $J = 2.8$ Hz, 1H), 7.93 (d, $J = 2.8$ Hz, 1H); $^{13}\text{C NMR}$ (101 MHz, CDCl_3) δ 31.1, 43.9, 49.5, 52.2, 53.4, 64.2, 65.6, 67.2, 114.9, 116.8, 119.9, 121.7, 130.8, 131.7, 132.0, 138.4, 138.5, 144.2, 157.1; LCMS (Method B): MH^+ 342, Rt 1.09 min, 100% by UV; HRMS exact mass calculated for $[\text{M}+\text{H}]^+$ ($\text{C}_{19}\text{H}_{24}\text{N}_3\text{O}_3$) requires m/z 342.1818, found 342.1815.

***Tert*-butyl (2-((5-bromo-2-methoxypyridin-3-yl)methoxy)ethyl)carbamate, 160**



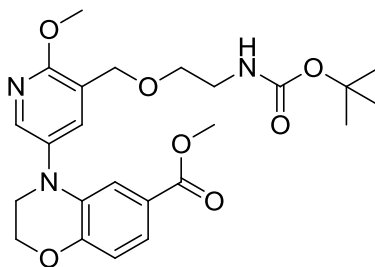
Under nitrogen, triphenylphosphine (3.6 g, 13.8 mmol) in DCM (20 mL) was added dropwise to a stirred solution of (5-bromo-2-methoxypyridin-3-yl)methanol (2.0 g, 9.2 mmol) and carbon tetrabromide (4.6 g, 13.8 mmol) in DCM (20 mL) at 0 °C and left to stir for one hour. The reaction mixture was then warmed to room temperature and left to stir for a further 16 hours. The solvent was removed *in vacuo* and the sample was loaded in DCM and purified by column chromatography on silica using a 0-22% ethyl acetate/cyclohexane gradient. The appropriate fractions were combined and the solvent removed *in vacuo* to afford a white solid (1.04 g).

To *tert*-butyl (2-hydroxyethyl)carbamate (275 mg, 1.1 mmol) in THF (10 mL), was added sodium hydride (85 mg, 2.1 mmol). The mixture was then stirred at room temperature for 30 mins. To the reaction mixture was then added a portion of the white

CONFIDENTIAL – PROPERTY OF GSK – DO NOT COPY

solid (400 mg, 1.4 mmol) and the mixture stirred for a further 2 hours. The reaction mixture was then poured into ice cold water (10 mL), extracted with ethyl acetate (2 x 20 mL) and the organic portions combined. The organic portions were then dried over a hydrophobic frit and the solvent removed *in vacuo*. The sample was loaded in DCM and purified by column chromatography on silica using a 0-25% ethyl acetate:cyclohexane gradient. The appropriate fractions were combined and concentrated *in vacuo* to give the title compound (450 mg, 35%) as a white solid. $\nu_{\max}/\text{cm}^{-1}$ (neat) 1688, 3365; $^1\text{H NMR}$ (400 MHz, CDCl_3) δ 1.48 (s, 9H), 3.40 (q, $J = 5.1$ Hz, 2H), 3.63 (t, $J = 5.1$ Hz, 2H), 3.96 (s, 3H), 4.48 (s, 2H), 4.92 (br. s, 1H), 7.75 (d, $J = 2.4$ Hz, 1H), 8.14 (d, $J = 2.4$ Hz, 1H); $^{13}\text{C NMR}$ (101 MHz, CDCl_3) δ 28.4, 40.2*, 53.7, 66.8, 70.2, 79.5*, 111.8, 123.0, 138.8, 146.0, 155.7*, 159.9, *Peak not observed in 1D ^{13}C spectrum, coupling detected to this chemical shift in HMBC.; LCMS (Method B): MH^+ 361, R_t 1.25 min, 100% by UV; HRMS exact mass calculated for $[\text{M}+\text{Na}]^+$ ($\text{C}_{14}\text{H}_{21}\text{BrN}_2\text{NaO}_4$) requires m/z 383.0583, found 383.0579.

Methyl 4-(5-((2-((*tert*-butoxycarbonyl)amino)ethoxy)methyl)-6-methoxypyridin-3-yl)-3,4-dihydro-2H-benzo[*b*][1,4]oxazine-6-carboxylate, 164

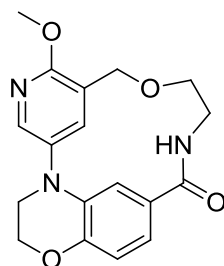


To methyl 3,4-dihydro-2H-benzo[*b*][1,4]oxazine-6-carboxylate (209 mg, 1.1 mmol), caesium carbonate (700 mg, 2.2 mmol) and RuPhos Pd G2 (84 mg, 0.11 mmol), was added a solution of *tert*-butyl (2-((5-bromo-2-methoxypyridin-3-yl)methoxy)ethyl)carbamate (390 mg, 1.1 mmol) in 1,4-dioxane (15 mL). The reaction vessel was sealed and heated under microwave irradiation conditions to 130 °C for 3 hours. The reaction mixture was then filtered through celite, and was washed with DCM (30 mL). The solvent was removed *in vacuo* and the sample loaded in DCM and purified by column chromatography on silica using a 0-100% ethyl acetate:cyclohexane gradient. The appropriate fractions were combined and concentrated *in vacuo* to give the title compound (404 mg, 79%) as a clear oil. $\nu_{\max}/\text{cm}^{-1}$ (neat) 1581, 1608, 1706; $^1\text{H NMR}$ (400 MHz, CDCl_3) δ 1.45 (s, 9H), 3.38 (q, $J = 4.8$

CONFIDENTIAL – PROPERTY OF GSK – DO NOT COPY

Hz, 2H), 3.63 (t, $J = 5.3$ Hz, 2H), 3.67-3.72 (m, 2H), 3.82 (s, 3H), 4.02 (s, 3H), 4.38-4.45 (m, 2H), 4.53 (s, 2H), 6.90 (d, $J = 8.6$ Hz, 1H), 7.30 (d, $J = 2.0$ Hz, 1H), 7.45 (dd, $J = 8.3, 2.0$ Hz, 1H), 7.60 (d, $J = 2.7$ Hz, 1H), 8.02 (d, $J = 2.7$ Hz, 1H); ^{13}C NMR (101 MHz, CDCl_3) δ 28.4, 48.9, 51.8, 53.7, 60.5, 64.8, 65.6, 67.2, 70.0, 116.5, 116.8, 121.7, 122.0, 123.1, 133.5, 134.3, 136.7, 142.4, 148.5, 158.7, 163.5, 166.9; LCMS (Method A): MH^+ 474, R_t 1.28 min, 92% by UV; HRMS exact mass calculated for $[\text{M}+\text{Na}]^+$ ($\text{C}_{24}\text{H}_{31}\text{N}_3\text{NaO}_7$) requires m/z 496.2060, found 496.2060.

9-Methoxy-2,12-dioxa-5,8,15-triazatetracyclo[15.2.2.16,(10),0(20,5)]docosa-6,8,10(22),17,19,20-hexaen-16-one, 165



To a solution of methyl 4-(5-((2-((*tert*-butoxycarbonyl)amino)ethoxy)methyl)-6-methoxypyridin-3-yl)-3,4-dihydro-2*H*-benzo[*b*][1,4]oxazine-6-carboxylate (0.5 g, 1.1 mmol) in water (5 mL) and THF (5 mL), was added lithium hydroxide (0.15 g, 6.3 mmol). The mixture was then stirred at 50 °C for 3 days. The reaction mixture was acidified to pH 3 using 2M aqueous hydrochloric acid and extracted with DCM (30 mL). The organic portion was then dried over a hydrophobic frit and the solvent removed *in vacuo* to yield a white solid (498 mg). To this was added, DCM (5 mL) and trifluoroacetic acid (1.3 mL, 17 mmol) and the reaction mixture was stirred at room temperature for 18 hours. The solvent was then removed *in vacuo* to yield an off-white solid (403 mg). To a solution of the above off-white solid (400 mg) in DMF (500 mL), was added HATU (423 mg, 1.1 mmol) and DIPEA (0.4 mL, 2.2 mmol). The reaction mixture was then stirred at room temperature for 2 hours. The solvent was then removed *in vacuo*, the residue was then dissolved in ethyl acetate (10 mL) and washed with 5% aqueous lithium chloride (3 x 10 mL). The organic portion was then dried over a hydrophobic frit and the solvent removed *in vacuo*. The samples were dissolved in DMSO and purified by mass directed HPLC on Xbridge column using acetonitrile:water with an ammonium carbonate modifier. The appropriate fractions were combined and the solvent removed *in vacuo* to yield the title compound (5 mg,

CONFIDENTIAL – PROPERTY OF GSK – DO NOT COPY

1%) as a white solid. $\nu_{\text{max}}/\text{cm}^{-1}$ (neat) 1580, 1648; $^1\text{H NMR}$ (400 MHz CDCl_3) δ 3.48-3.55 (m, 4H), 3.82-3.87 (m, 2H), 4.06 (s, 3H), 4.41-4.46 (m, 2H), 4.63 (s, 2H), 5.60 (br. s., 1H), 6.98 (d, $J = 8.8$ Hz, 1H), 7.05-7.13 (m, 2H), 7.91 (d, $J = 2.9$ Hz, 1H), 8.06 (d, $J = 2.4$ Hz, 1H); LCMS (Method A): MH^+ 342, Rt 0.87 min, 97% by UV; HRMS exact mass calculated for $[\text{M}+\text{H}]^+$ ($\text{C}_{18}\text{H}_{20}\text{N}_3\text{O}_4$) requires m/z 342.1453, found 342.1452. Not enough sample remained after biological testing to obtain a $^{13}\text{C NMR}$.

5.2.3 Compound Synthesis and Characterisation – Lactam Series

Relative stereochemistry of cyclopropyl rings. Relative configuration of literature compounds were assigned by comparison to literature assignment. Novel compounds were assigned by consideration of $^3J_{\text{H-H}}$ coupling constants in the cyclopropyl ring.

For the tertiary substituted cyclopropyl C-H:

Cis diastereoisomer is expected to have two couplings in the range 7-11 Hz ($^3J_{\text{H-H}}$ to two *cis* protons) and one coupling in the range 5-7Hz ($^3J_{\text{H-H}}$ to one *trans* proton) and *trans* diastereoisomer is expected to have one coupling in the range 7-11 Hz ($^3J_{\text{H-H}}$ to one *cis* proton) and two couplings in the range 5-7Hz ($^3J_{\text{H-H}}$ to two *trans* protons). For example, compound **254** *cis* - -0.03 (td, $J = 9.2, 6.8$ Hz, 1H), *trans* - -0.35 (dt, $J = 9.4, 5.8$ Hz, 1H).

Compound **315** was assigned in the same manner, however a proton on the secondary cyclopropane centre was selected due to signal overlap of the other peaks. For the *cis* diastereoisomer three couplings in the range 5-7Hz ($^3J_{\text{H-H}}$ to two *trans* protons and $^2J_{\text{H-H}}$ to one geminal protons) and zero in the range 7-11 Hz ($^3J_{\text{H-H}}$ to zero *cis* protons) are expected and for the *trans* diastereoisomer one coupling in the range 7-11 Hz ($^3J_{\text{H-H}}$ to one *cis* proton) and two couplings in the range 5-7Hz ($^3J_{\text{H-H}}$ to two *trans* protons) are expected. This supports the assignment *cis* - 0.83 (q, $J = 5.6$ Hz, 1H), *trans* - 1.04 (dt, $J = 8.6, 5.0$ Hz, 1H).

General Procedure A - Synthesis of Secondary Propargylic Silyl Ethers

- i) To ethynylmagnesium bromide (1.5 eq., 0.5 M in THF), was added a solution of aldehyde (1 eq.) in THF (0.2 M reaction concentration). The mixture was then stirred at room temperature for 18 hours. The reaction was then quenched with saturated aqueous ammonium chloride, and extracted with DCM. The organic portion was dried over a hydrophobic frit and the solvent removed *in vacuo* to give the product which was used crude.
- ii) To propargylic alcohol (1 eq.), imidazole (1.4 eq.) and DMAP (1.4 eq.), was added a solution of silyl chloride (1.2 eq.) in DCM (to make 0.2 M reaction concentration). The mixture was then stirred at room temperature for 18 hours.

CONFIDENTIAL – PROPERTY OF GSK – DO NOT COPY

The reaction was then diluted with water and extracted with DCM. The organic portions were combined, dried over a hydrophobic frit and the solvent removed *in vacuo*. The sample was purified by column chromatography on silica using a 0-50% ethyl acetate/cyclohexane gradient. The appropriate fractions were combined and concentrated *in vacuo* to give the required products.

General Procedure B - Synthesis of Tertiary Propargylic Silyl Ethers

- i) To ethynylmagnesium bromide (1.5 eq., 0.5 M in THF), was added a solution of ketone (1 eq.) in THF (0.2 M reaction concentration). The mixture was then stirred at room temperature for 18 hours. The reaction was then quenched with saturated aqueous ammonium chloride, and extracted with DCM (1 reaction volume). The organic portion was dried over a hydrophobic frit and the solvent removed *in vacuo* to give the product which was used crude.
- ii) To a suspension of sodium hydride (1 eq.) in THF (0.2 M) was added propargylic alcohol (1 eq.) in THF (0.2 M) and the mixture was stirred at room temperature for 30 mins. *Tert*-butyldimethylsilyl chloride (1.2 eq.) and tetrabutylammonium iodide (0.2 eq.) were then added and the mixture stirred for a further 18 hours. The mixture was then diluted with water and extracted with DCM. The organic portions were combined, dried over a hydrophobic frit and the solvent removed *in vacuo*. The sample was purified by column chromatography on silica using a 0-50% ethyl acetate/cyclohexane gradient. The appropriate fractions were combined and concentrated *in vacuo* to give the required products.

General Procedure C - One-Pot Borylation-Cyclopropanation

To Schwartz's Reagent (0.2 eq.), was added silyl propargyl ether (1 eq.) and the mixture was stirred in a sealed microwave vial under an atmosphere of nitrogen for 30 mins at room temperature. Pinacol borane (1 eq.) was then added and the mixture stirred at 60 °C for 18 hours. Further Schwartz's Reagent (3 eq.) and DCM-d₂ (0.4 M reaction concentration) was then added and the mixture stirred at 60 °C for a further 3 hours. The reaction mixture was then cooled to room temperature, boron trifluoride diethyl etherate complex (0.5 eq.) was added and the mixture stirred at room

CONFIDENTIAL – PROPERTY OF GSK – DO NOT COPY

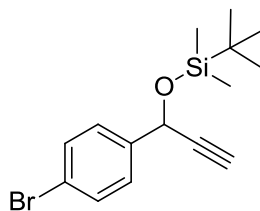
temperature for 1 hour. The solvent was then removed *in vacuo* and the residue purified by column chromatography on silica using a 0-5% ethyl acetate/cyclohexane gradient. The appropriate fractions were combined and concentrated *in vacuo* to give the required products.

General Procedure D - One-Pot Borylation-Cyclopropanation Followed by Suzuki Coupling

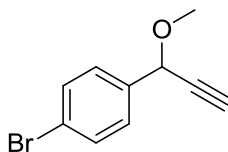
To Schwartz's Reagent (0.2 eq.), was added silyl propargyl ether (1 eq.) and the mixture was stirred for 30 mins at room temperature. Pinacol borane (1 eq.) was then added and the mixture stirred in a sealed microwave vial under an atmosphere of nitrogen at 60 °C for 18 hours. Further Schwartz's Reagent (3 eq.) and DCM was then added and the mixture stirred at 60 °C for a further 3 hours. The reaction mixture was then cooled to room temperature and boron trifluoride diethyl etherate complex (0.5 eq.) was added and the mixture stirred at room temperature for 1 hour. The solvent was then removed *in vacuo* and the residue dissolved in DCM and filtered through a plug of silica. The solvent was then removed *in vacuo*. Silver(I) oxide (1.5 eq.), caesium carbonate (2 eq.), aryl iodide (1.5 eq.), [1,1'-Bis(diphenylphosphino)ferrocene]palladium(II) dichloride complex with DCM (0.1 eq.) and water (2 eq.) were then added and the mixture dissolved in THF. The mixture was then stirred at 70 °C for 18 hours. The solvent was removed *in vacuo*, the residue dissolved in water and extracted with DCM. The solvent was then removed *in vacuo* and the residue purified by chromatography, detailed in individual experimental.

General Procedure E - Lactam Series Suzuki Coupling

To degassed 5-(5-iodopyridin-3-yl)-3,3,6-trimethylisoindolin-1-one (1.0 eq.), PdCl₂(dppf)-CH₂Cl₂ adduct (0.1 eq.), silver oxide (1.5 eq.) and caesium carbonate (2.0 eq.), was added 2-(2-(4-methoxyphenyl)cyclopropyl)-4,4,5,5-tetramethyl-1,3,2-dioxaborolane (1.0 eq.) and water (2.0 eq.) in THF (1 mL). The mixture was then heated in a sealed tube for 18 hours at 70 °C. The solvent was then removed *in vacuo*, the residue dissolved in water (1 mL), extracted with DCM (1 mL) and the DCM removed *in vacuo*. The residue was dissolved in DMSO and purified by mass directed HPLC on Xbridge column using acetonitrile:water with an ammonium carbonate modifier. The solvent was removed *in vacuo* to give the required products.

((1-(4-Bromophenyl)prop-2-yn-1-yl)oxy)(tert-butyl)dimethylsilane, 222

Prepared following the general procedure A (scale: step i) 4-bromobenzaldehyde, 5.0 g; step ii) 1-(4-bromophenyl)prop-2-yn-1-ol (portion of crude product from step i), 2.0 g). Isolated yield: 2.30 g, 72% (from aldehyde), clear oil. $\nu_{\max}/\text{cm}^{-1}$ (neat) 1677, 1584; ^1H NMR (400 MHz, DMSO- d_6) δ 0.10 (s, 3H), 0.16 (s, 3H), 0.89 (s, 9H), 3.62 (d, $J = 2.0$ Hz, 1H), 5.60 (d, $J = 2.0$ Hz, 1H), 7.40 (d, $J = 8.3$ Hz, 2H), 7.59 (d, $J = 8.3$ Hz, 2H); ^{13}C NMR (101 MHz, DMSO- d_6) δ -4.5, -4.2, 18.3, 26.1, 63.8, 77.3, 84.8, 121.4, 128.8, 131.8, 141.3; LCMS (Method A): MH^+ mass not observed, R_t 1.63 min, 100% by UV; HRMS exact mass calculated for $[\text{M}+\text{H}]^+$ ($\text{C}_{15}\text{H}_{22}\text{BrOSi}$) requires m/z 325.0618, found 325.0615.

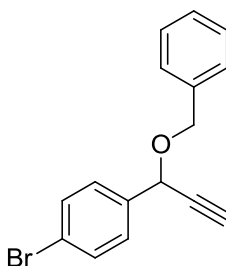
1-Bromo-4-(1-methoxyprop-2-yn-1-yl)benzene, 220

1-(4-bromophenyl)prop-2-yn-1-ol was prepared following general procedure Ai (scale: 4-bromobenzaldehyde, 2.5 g). Then, to a suspension of sodium hydride (95 mg, 2.4 mmol) in THF (10 mL), was added 1-(4-bromophenyl)prop-2-yn-1-ol (500 mg, 2.4 mmol) in THF (10 mL). The mixture was then stirred for 1 hour at room temperature. Methyl iodide (0.30 mL, 4.7 mmol) was then added and the mixture stirred for a further 3 hours. The reaction mixture was then diluted with water (10 mL) and extracted with DCM (20 mL). The organic portion was dried over a hydrophobic frit and the solvent removed *in vacuo*. The sample was loaded in DMSO and purified by column chromatography on C_{18} -silica using a 0-100% water, acetonitrile gradient to yield 1-bromo-4-(1-methoxyprop-2-yn-1-yl)benzene (86 mg, 0.382 mmol, 16.13% yield). $\nu_{\max}/\text{cm}^{-1}$ (neat) 1584, 1681, 2922; ^1H NMR (400 MHz, CDCl_3) δ 3.36 (s, 3H), 5.27 (s, 1H), 5.89 (s, 1H), 6.94-7.00 (m, 2H), 7.13-7.21 (m, 2H); ^{13}C NMR (101 MHz, CDCl_3) δ ppm 50.8, 63.7, 75.0, 83.1, 122.5, 128.3, 131.7, 139.1; LCMS (Method A):

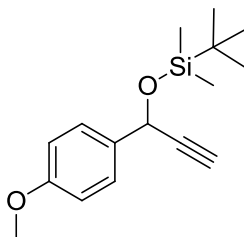
CONFIDENTIAL – PROPERTY OF GSK – DO NOT COPY

mass not observed, Rt 1.55 min, 75% by UV; HRMS no mass corresponding to derivatives of the title compound could be observed.

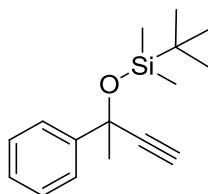
1-(1-(Benzyloxy)prop-2-yn-1-yl)-4-bromobenzene, 221



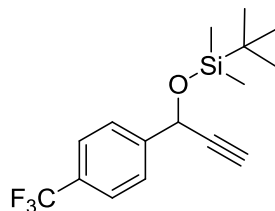
1-(4-bromophenyl)prop-2-yn-1-ol was prepared following general procedure Ai (scale: 4-bromobenzaldehyde, 1.85 g). Then, to a suspension of sodium hydride (0.095 g, 2.4 mmol) in THF (10 mL), was added 1-(4-bromophenyl)prop-2-yn-1-ol (0.5 g, 2.4 mmol) in THF (10 mL). The mixture was then stirred for 1 hour at 0 °C. Benzyl bromide (0.282 mL, 2.4 mmol) was then added and the mixture stirred for a further 3 hours. The reaction mixture was then diluted with water (10 mL) and extracted with DCM (20 mL). The organic portion was dried over a hydrophobic frit and the solvent removed *in vacuo*. The sample was loaded in DMSO and purified by column chromatography on C₁₈-silica using a 0-100% water, acetonitrile gradient. This yielded the title compound (130 mg, 0.432 mmol, 18% yield). $\nu_{\max}/\text{cm}^{-1}$ (neat) 1587, 2120, 3281; ¹H NMR (400 MHz, CDCl₃) δ 2.72 (d, J = 2.3 Hz, 1H), 4.68 (d, J = 11.9 Hz, 1H), 4.77 (d, J = 11.9 Hz, 1H), 5.20 (d, J = 2.3 Hz, 1H), 7.30-7.42 (m, 5H), 7.44 (d, J = 8.3 Hz, 2H), 7.51-7.58 (m, 2H); ¹³C NMR (101 MHz, CDCl₃) δ 63.5, 65.2, 74.9, 83.2, 122.4, 126.9, 127.6, 128.2, 128.5, 131.6, 139.2, 140.8; LCMS (Method A): mass not observed, Rt 1.42 min, 100% by UV; HRMS no mass corresponding to derivatives of the title compound could be observed.

Tert-butyl((1-(4-methoxyphenyl)prop-2-yn-1-yl)oxy)dimethylsilane, 232²⁵³

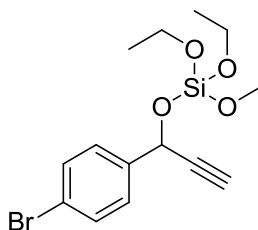
Prepared following the general procedure A (scale: step i) 4-methoxybenzaldehyde, 1.0 g; step ii) 1-(4-methoxyphenyl)prop-2-yn-1-ol (portion of crude product from step i), 100 mg). Isolated yield: 43 mg, 28% (from aldehyde), clear oil. $\nu_{\text{max}}/\text{cm}^{-1}$ (neat) 2956, 2933, 2864, 1611, 1511; $^1\text{H NMR}$ (400 MHz, CDCl_3) δ 0.16 (s, 3H), 0.20 (s, 3H), 0.96 (s, 9H), 2.58 (d, $J = 2.0$ Hz, 1H), 3.83 (s, 3H), 5.47 (d, $J = 2.0$ Hz, 1H), 6.89-6.94 (m, 2H), 7.41-7.47 (m, 2H); $^{13}\text{C NMR}$ (101 MHz, CDCl_3) δ -4.9, -4.5, 18.3, 25.8, 55.3, 64.3, 73.5, 85.0, 113.7, 127.3, 133.7, 159.3; HRMS exact mass calculated for $[\text{M}+\text{H}]^+$ ($\text{C}_{16}\text{H}_{24}\text{O}_2\text{Si}$) requires m/z 276.1546, found 276.1542.

Tert-butyldimethyl((2-phenylbut-3-yn-2-yl)oxy)silane, 233²⁵⁴

Prepared following the general procedure B omitting step i) (scale: 2-phenylbut-3-yn-2-ol, 250 mg). Isolated yield: 370 mg, 83% (from propargylic alcohol), clear oil. $\nu_{\text{max}}/\text{cm}^{-1}$ (neat) 3315, 2959, 2930, 2859, 1475; $^1\text{H NMR}$ (400 MHz, CDCl_3) δ 0.07 (s, 3H), 0.25 (s, 3H), 0.96 (s, 9H), 1.76 (s, 3H), 2.69 (s, 1H), 7.25-7.31 (m, 1H), 7.33-7.39 (m, 2H), 7.63-7.68 (m, 2H); $^{13}\text{C NMR}$ (101 MHz, CDCl_3) δ -3.3, -2.9, 18.3, 25.9, 35.6, 70.9, 74.0, 87.7, 125.0, 127.2, 127.9, 146.6; LCMS (Method A): MH^+ mass not observed, R_t 1.71 min, 100% by UV; HRMS exact mass calculated for $[\text{M}+\text{H}]^+$ ($\text{C}_{16}\text{H}_{24}\text{OSi}$) requires m/z 260.1596, found 260.1599.

Tert-butyldimethyl((1-(4-(trifluoromethyl)phenyl)prop-2-yn-1-yl)oxy)silane, 234

Prepared following the general procedure A (scale: step i) 4-(trifluoromethyl)benzaldehyde, 250 mg; step ii) 1-(4-(trifluoromethyl)phenyl)prop-2-yn-1-ol (portion of crude product from step i), 150 mg). Isolated yield: 160 mg, 43% (from aldehyde), clear oil. $\nu_{\max}/\text{cm}^{-1}$ (neat) 1692, 1584; $^1\text{H NMR}$ (400 MHz, CDCl_3) δ 0.19 (s, 3H), 0.23 (s, 3H), 0.97 (s, 9H), 2.60 (d, $J = 2.3$ Hz, 1H), 5.55 (d, $J = 2.2$ Hz, 1H), 7.64 (app. s, 4H); $^{13}\text{C NMR}$ (101 MHz, CDCl_3) δ -5.0, -4.6, 18.3, 25.7, 64.1, 74.3, 84.0, 124.1 (q, $J = 272.0$ Hz), 125.4 (q, $J = 4.0$ Hz), 126.3, 130.0 (q, $J = 32.8$ Hz), 145.2; $^{19}\text{F NMR}$ (376 MHz, CDCl_3) δ -62.54 (s, 3F); LCMS (Method B): MH^+ mass not observed, Rt 1.62 min, 100% by UV; HRMS exact mass calculated for $[\text{M}+\text{H}]^+$ ($\text{C}_{16}\text{H}_{21}\text{F}_3\text{OSi}$) requires m/z 314.1314, found 314.1315.

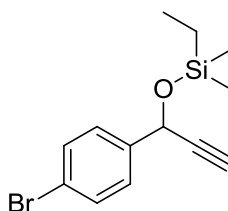
1-(4-Bromophenyl)prop-2-yn-1-yl triethyl orthosilicate, 238

To ethynylmagnesium bromide (40 mL, 20.3 mmol), was added a solution of 4-bromobenzaldehyde (2.50 g, 13.5 mmol) in THF (20 mL). The mixture was then stirred at room temperature for 18 hours. The reaction mixture was then quenched with saturated aqueous ammonium chloride (10 mL), and extracted with DCM (3 x 20 mL). The organic portions were combined, dried over a hydrophobic frit and the solvent removed *in vacuo* to give an oil which solidified to a brown solid (2.52 g, 87%). To a portion of brown solid (250 mg) and dry pyridine (0.11 mL, 1.42 mmol) in dry DCM (10 mL), was added chlorotriethoxysilane (0.28 mL, 1.42 mmol). The mixture was then stirred at room temperature for 18 hours and the solvent was removed *in vacuo*.

CONFIDENTIAL – PROPERTY OF GSK – DO NOT COPY

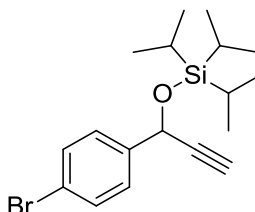
The sample was loaded in DCM and purified by column chromatography on silica using a 0-50% ethyl acetate/cyclohexane gradient. The appropriate fractions were combined and concentrated *in vacuo* to give the title compound (345 mg, 69%, 58% over two steps) as a colourless oil. $\nu_{\max}/\text{cm}^{-1}$ (neat) 3291, 1674, 1585; $^1\text{H NMR}$ (400 MHz, CDCl_3) δ 1.25 (t, $J = 6.9$ Hz, 9H), 2.63 (d, $J = 2.3$ Hz, 1H), 3.87 (app. qd, $J = 7.0, 2.0$ Hz, 6H), 5.68 (d, $J = 2.3$ Hz, 1H), 7.44 (app. dt, $J = 8.6, 2.0$ Hz, 2H), 7.52 (app. dt, $J = 8.6, 2.0$ Hz, 2H); $^{13}\text{C NMR}$ (101 MHz, CDCl_3) δ 18.0, 59.5, 64.4, 74.2, 83.0, 122.1, 128.2, 131.5, 139.4; LCMS (Method B): MH^+ mass not observed, Rt 1.48 min, 77% by UV; HRMS exact mass calculated for $[\text{M}+\text{H}]^+$ ($\text{C}_{15}\text{H}_{22}\text{BrO}_4\text{Si}$) requires m/z 373.0465, found 373.0468.

((1-(4-Bromophenyl)prop-2-yn-1-yl)oxy)triethylsilane, 239



Prepared following the general procedure A (scale: step i) 4-bromobenzaldehyde, 5.0 g; step ii) 4-bromophenylprop-2-yn-1-ol (portion of crude product from step i), 250 mg). Isolated yield: 240 mg, 53% (from aldehyde), clear oil. $\nu_{\max}/\text{cm}^{-1}$ (neat) 2955, 1675, 1585; $^1\text{H NMR}$ (400 MHz, CDCl_3) δ 0.68-0.75 (m, 6H), 1.00 (t, $J = 7.9$ Hz, 9H), 2.58 (d, $J = 2.3$ Hz, 1H), 5.45 (d, $J = 2.3$ Hz, 1H), 7.38-7.42 (m, 2H), 7.48-7.53 (m, 2H); $^{13}\text{C NMR}$ (101 MHz, CDCl_3) δ 4.8, 6.7, 63.8, 73.9, 84.1, 121.8, 127.8, 131.5, 140.5; LCMS (Method A): MH^+ mass not observed, Rt 1.64 min, 100% by UV; HRMS exact mass calculated for $[\text{M}+\text{H}]^+$ ($\text{C}_{15}\text{H}_{22}\text{BrOSi}$) requires m/z 325.0618, found 325.0622.

((1-(4-Bromophenyl)prop-2-yn-1-yl)oxy)triisopropylsilane, 240

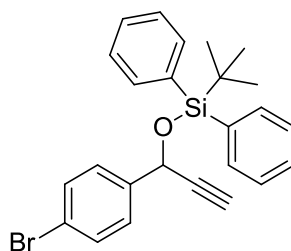


Prepared following the general procedure A (scale: step i) 4-bromobenzaldehyde, 5.0 g; step ii) 4-bromophenylprop-2-yn-1-ol (portion of crude product from step i), 250

CONFIDENTIAL – PROPERTY OF GSK – DO NOT COPY

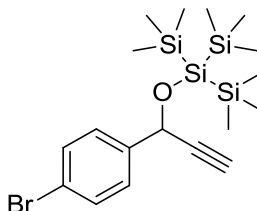
mg). Isolated yield: 256 mg, 38% (from aldehyde), clear oil. $\nu_{\max}/\text{cm}^{-1}$ (neat) 3090, 2943, 2668, 2549, 1673, 1585; ^1H NMR (400 MHz, CDCl_3) δ 1.09 (d, $J = 7.1$ Hz, 9H), 1.13 (d, $J = 6.8$ Hz, 9H), 1.16-1.27 (m, 3H), 2.56 (d, $J = 2.0$ Hz, 1H), 5.53 (d, $J = 2.0$ Hz, 1H), 7.40 (d, $J = 8.3$ Hz, 2H), 7.51 (d, $J = 8.3$ Hz, 2H); ^{13}C NMR (101 MHz, CDCl_3) δ 12.2, 18.0, 64.1, 73.7, 84.6, 121.6, 127.6, 131.5, 141.0; LCMS (Method A): MH^+ mass not observed, Rt 1.78 min, 100% by UV; HRMS exact mass calculated for $[\text{M}+\text{H}]^+$ ($\text{C}_{18}\text{H}_{27}\text{BrOSi}$) requires m/z 366.1015, found 366.1019.

((1-(4-Bromophenyl)prop-2-yn-1-yl)oxy)(tert-butyl)diphenylsilane, 241



Prepared following the general procedure A (scale: step i) 4-bromobenzaldehyde, 5.0 g; step ii) 4-bromophenylprop-2-yn-1-ol (portion of crude product from step i), 250 mg). Isolated yield: 490 mg, 79% (from aldehyde), clear oil. $\nu_{\max}/\text{cm}^{-1}$ (neat) 3287, 2857, 1484, 1426; ^1H NMR (400 MHz, CDCl_3) δ 1.11 (s, 9H), 2.50 (d, $J = 2.3$ Hz, 1H), 5.33 (d, $J = 2.3$ Hz, 1H), 7.24-7.28 (m, 2H), 7.31-7.36 (m, 2H), 7.39-7.50 (m, 6H), 7.58 (dd, $J = 8.0, 1.4$ Hz, 2H), 7.79 (dd, $J = 8.0, 1.5$ Hz, 2H); ^{13}C NMR (101 MHz, CDCl_3) δ 19.3, 26.8, 65.1, 74.4, 83.9, 121.8, 127.6, 127.6, 128.1, 129.9, 131.5, 132.8, 132.9, 135.8, 136.0, 140.4; LCMS (Method A): MH^+ mass not observed, Rt 1.74 min, 100% by UV; HRMS exact mass calculated for $[\text{M}+\text{H}]^+$ ($\text{C}_{25}\text{H}_{26}\text{BrOSi}$) requires m/z 449.0931, found 449.0928.

2-(((1-(4-Bromophenyl)prop-2-yn-1-yl)oxy)-1,1,1,3,3,3-hexamethyl-2-(trimethylsilyl)trisilane, 242

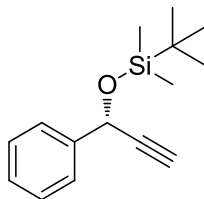


Prepared following the general procedure A (scale: step i) 4-bromobenzaldehyde, 5.0 g; step ii) 4-bromophenylprop-2-yn-1-ol (portion of crude product from step i), 250

CONFIDENTIAL – PROPERTY OF GSK – DO NOT COPY

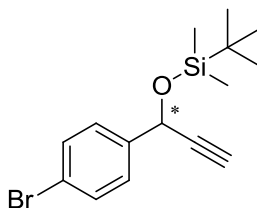
mg). Isolated yield: 254 mg, 40% (from aldehyde), clear oil. $\nu_{\max}/\text{cm}^{-1}$ (neat) 3308, 2949, 1485; $^1\text{H NMR}$ (400 MHz, CDCl_3) δ 0.23 (s, 27H), 2.58 (d, $J = 2.3$ Hz, 1H), 5.14 (d, $J = 2.3$ Hz, 1H), 7.33 (d, $J = 8.3$ Hz, 2H), 7.49 (d, $J = 8.3$ Hz, 2H); $^{13}\text{C NMR}$ (101 MHz, CDCl_3) δ 0.4, 67.9, 74.5, 84.6, 121.6, 127.4, 131.4, 140.8; LCMS (Method A): MH^+ mass not observed, R_t 2.01 min, 95% by UV; HRMS exact mass calculated for $[\text{M}+\text{H}]^+$ ($\text{C}_{18}\text{H}_{33}\text{BrOSi}_4$) requires m/z 456.0792, found 456.0800.

(R)-Tert-butyldimethyl((1-phenylprop-2-yn-1-yl)oxy)silane,²⁵⁵ 249



(R)-1-Phenylprop-2-yn-1-ol was subjected to general procedure Aii) (scale: (R)-1-phenylprop-2-yn-1-ol, 250 mg). Isolated yield: 368 mg, 79%. $\nu_{\max}/\text{cm}^{-1}$ (neat) 1682, 1584; $^1\text{H NMR}$ (400 MHz, CDCl_3) δ 0.17 (s, 3H), 0.21 (s, 3H), 0.95-0.98 (m, 9H), 2.58 (d, $J = 2.0$ Hz, 1H), 5.52 (d, $J = 2.1$ Hz, 1H), 7.29-7.42 (m, 3H), 7.47-7.56 (m, 2H); $^{13}\text{C NMR}$ (101 MHz, CDCl_3) δ -5.0, -4.6, 18.3, 25.8, 64.6, 73.6, 84.8, 126.0, 127.8, 128.3, 141.4; LCMS (Method A): MH^+ mass not observed, R_t 1.54 min, 94% by UV; HRMS exact mass calculated for $[\text{M}+\text{H}]^+$ ($\text{C}_{15}\text{H}_{22}\text{OSi}$) requires m/z 246.1440, found 246.1444. $[\alpha]_{\text{D}}^{25} = -14.2$ (c 2.00, CHCl_3).

(-)-((1-(4-Bromophenyl)prop-2-yn-1-yl)oxy)(tert-butyl)dimethylsilane, 250

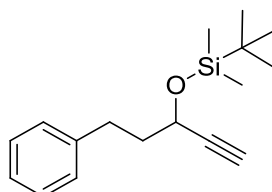


Propargylic alcohol was prepared following general procedure Ai) (scale: 4-bromobenzaldehyde, 2.5 g). Enantiomers were separated at this stage by chiral chromatography (Whelk O1 250 mm x 20 mm, heptane:ethanol 50:1, 20 mL min^{-1}). This yielded: **Enantiomer 1**: $t_R = 12.439$ mins, 295 mg, >99% ee, **Enantiomer 2**: $t_R = 14.189$ mins, 332 mg, >99% ee. Enantiomer 1 (100 mg) was then subjected to general procedure Aii). Isolated yield, 111 mg, 19% yield (from aldehyde). $\nu_{\max}/\text{cm}^{-1}$ (neat) 1682, 1584; $^1\text{H NMR}$ (400 MHz, CDCl_3) δ 0.17 (s, 3H), 0.20 (s, 3H), 0.96 (s, 9H),

CONFIDENTIAL – PROPERTY OF GSK – DO NOT COPY

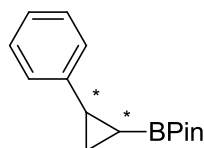
2.58 (d, $J = 2.1$ Hz, 1H), 5.45 (d, $J = 2.1$ Hz, 1H), 7.39 (d, $J = 8.5$ Hz, 2H), 7.51 (d, $J = 8.6$ Hz, 2H); ^{13}C NMR (101 MHz, CDCl_3) δ -5.0, -4.6, 18.3, 25.7, 64.1, 74.0, 84.2, 121.7, 127.7, 131.5, 140.5; LCMS (Method B): MH^+ mass not observed, R_t 1.66 min, 100% by UV; HRMS exact mass calculated for $[\text{M}+\text{H}]^+$ ($\text{C}_{15}\text{H}_{22}\text{OSi}$) requires m/z 246.1440, found 246.1444. $[\alpha]_{\text{D}}^{25} = -18.6$ (c 0.50, CHCl_3).

(+)-Tert-butyldimethyl((5-phenylpent-1-yn-3-yl)oxy)silane, 251



Propargylic alcohol was prepared following general procedure Ai) (scale: 3-phenylpropanal, 1.0 g). Enantiomers were separated at this stage by chiral chromatography (Chiralcel OD-H 250 mm x 30 mm, heptane:propan-2-ol 19:1, 42.5 mL min⁻¹). This yielded: **Enantiomer 1**: $t_R = 14.523$ mins, 223 mg, 98%ee, **Enantiomer 2**: $t_R = 17.603$ mins, 174 mg, 97%ee. Enantiomer 1 (100 mg) was then subjected to general procedure Aii). Isolated yield, 104 mg, 11% yield (from aldehyde). $\nu_{\text{max}}/\text{cm}^{-1}$ (neat) 3309, 2954, 2929, 2857; ^1H NMR (400 MHz, CDCl_3) δ 0.14 (s, 3H), 0.17 (s, 3H), 0.92-0.95 (m, 9H), 2.03 (dt, $J = 8.5, 6.9$ Hz, 2H), 2.45 (d, $J = 2.0$ Hz, 1H), 2.80 (td, $J = 7.9, 4.2$ Hz, 2H), 4.41 (td, $J = 6.3, 2.1$ Hz, 1H), 7.19-7.25 (m, 3H), 7.26-7.38 (m, 2H); ^{13}C NMR (101 MHz, CDCl_3) δ -5.0, -4.5, 18.2, 25.8, 31.3, 40.2, 62.2, 72.4, 85.3, 125.9, 128.4, 128.4, 141.6; HRMS no mass corresponding to derivatives of the title compound could be observed. $[\alpha]_{\text{D}}^{25} = +26.2$ (c 0.50, CHCl_3)

4,4,5,5-Tetramethyl-2-(2-phenylcyclopropyl)-1,3,2-dioxaborolane, 252¹⁸⁶

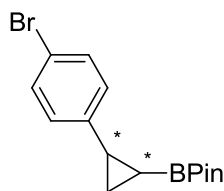


Prepared following the general procedure C (scale: (*R*)-tert-butyldimethyl((1-phenylprop-2-yn-1-yl)oxy)silane, 100 mg). Isolated yield: 56 mg, 57% (as a 1.2:1 *cis:trans* mixture), clear oil. Diastereomeric ratio was calculated by comparing ^1H NMR integrals of the following peaks: *cis* - 2.38 (ddd, $J = 10.1, 7.8, 6.1$ Hz, 1H), *trans*

CONFIDENTIAL – PROPERTY OF GSK – DO NOT COPY

- 2.14 (dt, $J = 8.1, 5.4$ Hz, 1H) **Cis**: *ee* could not be determined due to co-elution of enantiomers, ^1H NMR (400 MHz, CDCl_3) δ 0.48 (ddd, $J = 10.1, 9.3, 7.3$ Hz, 1H), 0.92 (s, 6H), 1.05 (s, 6H), 1.13 (ddd, $J = 9.2, 8.0, 4.3$ Hz, 1H), 2.38 (ddd, $J = 10.1, 7.8, 6.1$ Hz, 1H), 7.05-7.41 (m, 5H), in agreement with literature sample¹⁸⁶ except peak at 1.28 ppm could not be observed due to overlap with *trans*-isomer; **Trans**: 96% *ee*, ^1H NMR (400 MHz, CDCl_3) δ 0.34 (ddd, $J = 9.8, 6.8, 5.4$ Hz, 1H), 1.03 (ddd, $J = 9.8, 5.4, 3.7$ Hz, 1H), 1.13 (ddd, $J = 9.2, 8.0, 4.3$ Hz, 1H), 1.27 (s, 6H), 1.28 (s, 6H), 2.14 (dt, $J = 8.1, 5.4$ Hz, 1H), 7.07-7.35 (m, 5H); **Mixture**: $\nu_{\text{max}}/\text{cm}^{-1}$ (neat) 2974, 1491; HRMS exact mass calculated for $[\text{M}+\text{H}]^+$ ($\text{C}_{15}\text{H}_{22}\text{BO}_2$) requires m/z 245.1707, found 245.1700. Chiral Analytical HPLC (5 cm Chiracel OD-3, hexane, 0.3 mL min^{-1} , 40°C): **cis-14a** $t_{\text{R}} = 5.01$ mins (co-eluting enantiomers), **(1*S*,2*S*)-14a** $t_{\text{R}} = 6.13$ mins, **(1*R*,2*R*)-14a** $t_{\text{R}} = 6.75$ mins. Enantiomers were assigned by comparison with literature.¹⁸⁶

2-(2-(4-Bromophenyl)cyclopropyl)-4,4,5,5-tetramethyl-1,3,2-dioxaborolane, 253

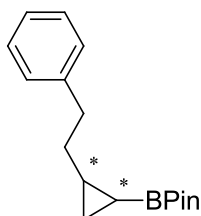


Prepared following the general procedure C (scale: (-)-((1-(4-Bromophenyl)prop-2-yn-1-yl)oxy)(*tert*-butyl)dimethylsilane, 125 mg). Isolated yield: 88 mg, 71% (as a 1.7:1.0 *cis:trans* mixture), clear oil. Diastereomeric ratio was calculated by comparing ^1H NMR integrals of the following peaks: *cis* - 2.35 (ddd, $J = 10.1, 7.8, 6.1$ Hz, 1H), *trans* - 2.06 (dt, $J = 8.2, 5.4$ Hz, 1H); **Cis**: >95% *ee*, ^1H NMR (400 MHz, CDCl_3) δ 0.44 (ddd, $J = 10.1, 9.3, 7.3$ Hz, 1H), 0.88 (s, 6H), 1.01 (s, 6H), 1.10 (ddd, $J = 9.3, 8.0, 4.2$ Hz, 1H), 1.28 (ddd, $J = 7.1, 6.1, 4.2$ Hz, 1H), 2.35 (ddd, $J = 10.1, 7.8, 6.1$ Hz, 1H), 7.17 (d, $J = 8.3$ Hz, 2H), 7.37 (d, $J = 8.3$ Hz, 2H); **Trans**: >99% *ee*, ^1H NMR (400 MHz, CDCl_3) δ 0.36 (ddd, $J = 9.9, 6.9, 5.4$ Hz, 1H), 0.96 (ddd, $J = 9.8, 5.4, 3.7$ Hz, 1H), 1.16 (ddd, $J = 8.2, 7.0, 3.7$ Hz, 1H), 1.24 (s, 6H), 1.25 (s, 6H), 2.06 (dt, $J = 8.2, 5.4$ Hz, 1H), 6.97 (d, $J = 8.3$ Hz, 2H), 7.36 (d, $J = 8.3$ Hz, 2H); **Mixture**: $\nu_{\text{max}}/\text{cm}^{-1}$ (neat) 2976, 1491; ^{13}C NMR (101 MHz, CDCl_3) δ 9.2, 14.9, 21.3, 21.4, 24.4, 24.7, 24.7, 24.8, 83.0, 83.3, 119.0, 119.3, 127.5, 130.6, 130.6, 131.2, 139.9, 142.5, the carbon directly attached to the boron atom was not detected, likely due to quadropolar relaxation.²⁵⁶

CONFIDENTIAL – PROPERTY OF GSK – DO NOT COPY

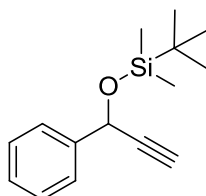
HRMS exact mass calculated for $[M+H]^+$ ($C_{15}H_{21}BBrO_2$) requires m/z 323.0813, found 323.0810. Chiral Analytical HPLC (25 cm Chiralpak AD-H, heptane:isopropanol, 50:1, 0.2 mL min⁻¹, 40 °C): **rac-7** *cis* t_R = 18.32 mins, 19.28 mins, *trans* t_R = 21.42 mins, 22.27 mins, **14b** *cis* t_R = 19.05 mins, *trans* t_R = 21.24 mins.

4,4,5,5-Tetramethyl-2-(2-phenethylcyclopropyl)-1,3,2-dioxaborolane, 254



Prepared following the general procedure C (scale: (+)-*Tert*-butyldimethyl((5-phenylpent-1-yn-3-yl)oxy)silane, 100 mg). Isolated yield: 59 mg, 59% (as a 1.5:1.0 *cis:trans* mixture), clear oil. Diastereomeric ratio was calculated by comparing ¹H NMR integrals of the following peaks: *cis* - -0.03 (td, J = 9.2, 6.8 Hz, 1H), *trans* - -0.35 (dt, J = 9.4, 5.8 Hz, 1H); *Cis*: ¹H NMR (400 MHz, CDCl₃) δ -0.03 (td, J = 9.2, 6.8 Hz, 1H), 0.41-0.48 (m, 1H), 0.82 (ddd, J = 9.2, 7.9, 3.4 Hz, 1H), 1.10 (dqt, J = 14.8, 7.5, 1.8 Hz, 1H), 1.26 (s, 6H), 1.27 (s, 6H), 1.75-1.80 (m, 2H), 2.67-2.81 (m, 2H), 7.13-7.34 (m, 5H); *Trans*: ¹H NMR (400 MHz, CDCl₃) δ -0.35 (dt, J = 9.4, 5.8 Hz, 1H), 0.41-0.48 (m, 1H), 0.71 (ddd, J = 7.7, 6.1, 3.4 Hz, 1H), 0.95-1.01 (m, 1H), 1.24 (s, 6H), 1.25 (s, 6H), 1.77 (m, 2H), 2.67-2.81 (m, 2H), 7.13-7.34 (m, 5H); **Mixture**: ν_{max}/cm^{-1} (neat) 2976, 2928, 2855; ¹³C NMR (101 MHz, CDCl₃) δ 11.0, 11.4, 18.0, 18.1, 24.7, 24.7, 24.7, 25.1, 32.6, 36.0, 36.4, 37.3, 82.8, 82.9, 125.5, 125.6, 128.1, 128.2, 128.4, 128.5, 142.5, 142.7 the carbon directly attached to the boron atom was not detected, likely due to quadropolar relaxation.²⁵⁶

***Tert*-butyldimethyl((1-phenylprop-2-yn-1-yl)oxy)silane,²⁵⁷ 271**

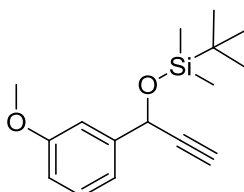


Prepared following the general procedure A omitting step i) (scale: 1-phenylprop-2-yn-1-ol, 1.0 g). Isolated yield: 1.02 g, 54% (from propargylic alcohol), yellow oil. ν_{max}/cm^{-1} (neat) 1682, 1584; ¹H NMR (400 MHz, CDCl₃) δ 0.17 (s, 3H), 0.21 (s, 3H),

CONFIDENTIAL – PROPERTY OF GSK – DO NOT COPY

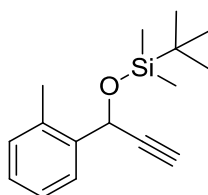
0.97 (s, 9H), 2.57 (d, $J = 2.0$ Hz, 1H), 5.52 (d, $J = 2.3$ Hz, 1H), 7.31-7.54 (m, 5H); ^{13}C NMR (101 MHz, CDCl_3) δ -4.9, -4.6, 18.3, 26.9, 64.6, 73.6, 84.8, 126.0, 127.8, 128.3, 141.4; LCMS (Method B): MH^+ mass not observed, R_t 1.57 min, 61% by UV (degradation under aqueous conditions); HRMS exact mass calculated for $[\text{M}+\text{H}]^+$ ($\text{C}_{15}\text{H}_{22}\text{OSi}$) requires m/z 246.1440, found 246.1444.

***Tert*-butyl((1-(3-methoxyphenyl)prop-2-yn-1-yl)oxy)dimethylsilane, 272**



Prepared following the general procedure A (scale: step i) 3-methoxybenzaldehyde, 250 mg; step ii) 1-(3-methoxyphenyl)prop-2-yn-1-ol (portion of crude product from step i), 150 mg). Isolated yield: 176 mg, 69% (from aldehyde), clear oil. $\nu_{\text{max}}/\text{cm}^{-1}$ (neat) 3288, 2954, 2930, 1691, 1599, 1585, 1487); ^1H NMR (400 MHz, CDCl_3) δ 0.17 (s, 3H), 0.21 (s, 3H), 0.97 (s, 9H), 2.57 (d, $J = 2.0$ Hz, 1H), 3.84 (s, 3H), 5.49 (d, $J = 2.0$ Hz, 1H), 6.86 (ddd, $J = 8.0, 2.4, 1.1$ Hz, 1H), 7.07-7.12 (m, 2H), 7.29 (t, $J = 8.0$ Hz, 1H); ^{13}C NMR (101 MHz, CDCl_3) δ -5.0, -4.6, 18.3, 25.8, 55.2, 64.5, 73.6, 84.7, 111.4, 113.5, 118.3, 129.3, 143.0, 159.7; LCMS (Method A): MH^+ mass not observed, R_t 1.57 min, 92% by UV; HRMS exact mass calculated for $[\text{M}+\text{H}]^+$ ($\text{C}_{16}\text{H}_{24}\text{O}_2\text{Si}$) requires m/z 276.1546, found 276.1534.

***Tert*-butyldimethyl((1-(*o*-tolyl)prop-2-yn-1-yl)oxy)silane, 273**

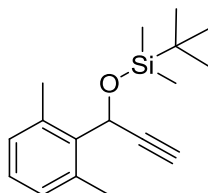


Prepared following the general procedure A (scale: step i) 2-methylbenzaldehyde, 250 mg; step ii) 1-(*o*-tolyl)prop-2-yn-1-ol (portion of crude product from step i), 300 mg). Isolated yield: 303 mg, 34% (from aldehyde), clear oil. $\nu_{\text{max}}/\text{cm}^{-1}$ (neat) 2954, 2928, 2889, 2855, 1474, 1403; ^1H NMR (400 MHz, CDCl_3) δ 0.14 (s, 3H), 0.19 (s, 3H), 0.95 (s, 9H), 2.45 (s, 3H), 2.52 (d, $J = 2.3$ Hz, 1H), 5.57 (d, $J = 2.3$ Hz, 1H), 7.13-7.27 (m, 3H), 7.51-7.62 (m, 1H); ^{13}C NMR (101 MHz, CDCl_3) δ -5.0, -4.6, 18.3, 19.0, 25.8,

CONFIDENTIAL – PROPERTY OF GSK – DO NOT COPY

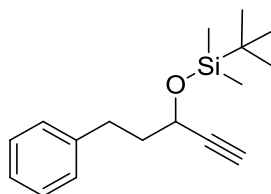
62.9, 73.2, 84.2, 126.0, 126.1, 127.7, 130.5, 135.0, 139.3; LCMS (Method A): MH^+ mass not observed, Rt 1.60 min, 82% by UV; HRMS exact mass calculated for $[M+H]^+$ ($C_{16}H_{24}OSi$) requires m/z 260.1596, found 260.1599.

***Tert*-butyl((1-(2,6-dimethylphenyl)prop-2-yn-1-yl)oxy)dimethylsilane, 274**

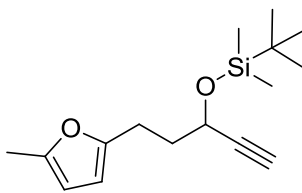


Prepared following the general procedure A (scale: step i) 2,6-dimethylbenzaldehyde, 250 mg; step ii) 1-(2,6-dimethylphenyl)prop-2-yn-1-ol (portion of crude product from step i), 250 mg). Isolated yield: 210 mg, 44% (from aldehyde), clear oil. ν_{max}/cm^{-1} (neat) 3309, 2956, 2928, 2857, 1474; 1H NMR (400 MHz, $CDCl_3$) δ 0.05 (s, 3H), 0.21 (s, 3H), 0.92 (s, 9H), 2.47 (d, $J = 2.4$ Hz, 1H), 2.52 (s, 6H), 5.87 (d, $J = 2.4$ Hz, 1H), 6.96-7.05 (m, 2H), 7.07-7.13 (m, 1H); ^{13}C NMR (101 MHz, $CDCl_3$) δ -5.0, -4.8, 18.1, 20.3, 25.7, 60.8, 72.5, 84.1, 127.6, 129.0, 129.7, 137.2; LCMS (Method A): MH^+ mass not observed, Rt 1.64 min, 69% by UV; HRMS exact mass calculated for $[M+H]^+$ ($C_{17}H_{26}OSi$) requires m/z 274.1753, found 274.1756.

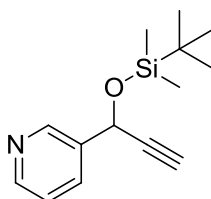
***Tert*-butyldimethyl((5-phenylpent-1-yn-3-yl)oxy)silane,²⁵⁸ 275**



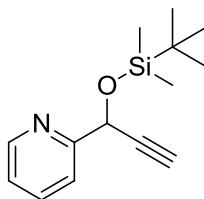
Prepared following the general procedure A (scale: step i) 3-phenylpropanal, 2 g; step ii) 5-phenylpent-1-yn-3-ol (portion of crude product from step i), 1.4 g). Isolated yield: 1.85 g, 48% (from aldehyde), clear oil. ν_{max}/cm^{-1} (neat) 2952, 2928; 1H NMR (400 MHz, CD_2Cl_2) δ 0.12 (s, 3H), 0.14 (s, 3H), 0.92 (s, 9H), 1.96-2.00 (m, 2H), 2.48 (br. s., 1H), 2.71-2.83 (m, 2H), 4.40 (br. s., 1H), 7.14-7.32 (m, 5H); ^{13}C NMR (101 MHz, CD_2Cl_2) δ -7.2, -6.7, 16.2, 23.6, 29.4, 38.4, 60.3, 70.3, 83.4, 123.9, 126.4, 126.5, 139.9; LCMS (Method A): MH^+ mass not observed, Rt 1.65 min, 85% by UV; HRMS exact mass calculated for $[M+H]^+$ ($C_{17}H_{26}OSi$) requires m/z 274.1753, found 274.1755.

***Tert*-butyldimethyl((5-(5-methylfuran-2-yl)pent-1-yn-3-yl)oxy)silane, 276**

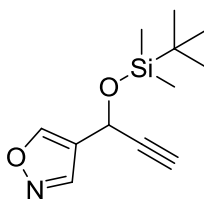
Prepared following the general procedure A (scale: step i) 3-(5-methylfuran-2-yl)propanal, 500 mg; step ii) 5-(5-methylfuran-2-yl)pent-1-yn-3-ol (portion of crude product from step i), 200 mg). Isolated yield: 287 mg, 65% (from aldehyde), clear oil. $\nu_{\text{max}}/\text{cm}^{-1}$ (neat) 3309, 2954, 2929, 2857, 1571; ^1H NMR (400 MHz, CDCl_3) δ 0.13 (s, 3H), 0.16 (s, 3H), 0.94 (s, 9H), 1.99-2.06 (m, 2H), 2.27 (s, 3H), 2.42 (d, $J = 2.2$ Hz, 1H), 2.75 (t, $J = 7.3$ Hz, 2H), 4.42 (td, $J = 6.4, 2.2$ Hz, 1H), 5.86 (dd, $J = 2.9, 0.7$ Hz, 1H), 5.89 (d, $J = 2.9$ Hz, 1H); ^{13}C NMR (101 MHz, CDCl_3) δ -5.1, -4.6, 13.5, 18.2, 23.7, 25.8, 36.9, 61.9, 72.3, 85.2, 105.6, 105.8, 150.4, 153.4; LCMS (Method A): $[\text{M}-\text{H}]^-$ 277, Rt 1.64 min, 97% by UV; HRMS exact mass calculated for $[\text{M}+\text{H}]^+$ ($\text{C}_{16}\text{H}_{26}\text{O}_2\text{Si}$) requires m/z 278.1702, found 278.1701.

***3*-(1-((*Tert*-butyldimethylsilyl)oxy)prop-2-yn-1-yl)pyridine, 277**

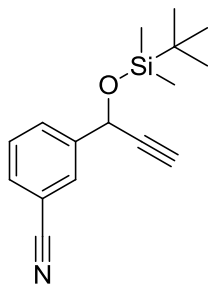
Prepared following the general procedure A (scale: step i) nicotinaldehyde, 500 mg; step ii) 1-(pyridin-3-yl)prop-2-yn-1-ol (portion of crude product from step i), 150 mg). Isolated yield: 187 mg, 47% (from aldehyde), clear oil. $\nu_{\text{max}}/\text{cm}^{-1}$ (neat) 3071, 1696, 1583; ^1H NMR (400 MHz, CDCl_3) δ 0.19 (s, 3H), 0.23 (s, 3H), 0.96 (s, 9H), 2.63 (d, $J = 2.3$ Hz, 1H), 5.55 (d, $J = 2.3$ Hz, 1H), 7.34 (dd, $J = 8.1, 5.1$ Hz, 1H), 7.87 (dt, $J = 8.1, 1.8$ Hz, 1H), 8.58 (dd, $J = 5.0, 1.8$ Hz, 1H), 8.75 (d, $J = 1.8$ Hz, 1H); ^{13}C NMR (101 MHz, CDCl_3) δ -5.0, -4.5, 18.2, 25.7, 62.7, 74.6, 83.5, 123.4, 134.0, 137.0, 147.6, 148.8; LCMS (Method A): MH^+ 248, Rt 1.32 min, 96% by UV; HRMS exact mass calculated for $[\text{M}+\text{H}]^+$ ($\text{C}_{14}\text{H}_{21}\text{NOSi}$) requires m/z 248.1470, found 248.1463.

2-(1-((*Tert*-butyldimethylsilyl)oxy)prop-2-yn-1-yl)pyridine,²⁵⁹ 278

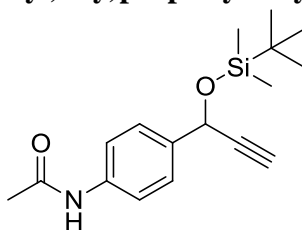
Prepared following the general procedure A (scale: step i) picolinaldehyde, 500 mg; step ii) 1-(pyridin-2-yl)prop-2-yn-1-ol (portion of crude product from step i), 150 mg). Isolated yield: 234 mg, 62% (from aldehyde), clear oil. $\nu_{\max}/\text{cm}^{-1}$ (neat) 1712, 2924; ^1H NMR (400 MHz, CDCl_3) δ 0.18 (s, 3H), 0.24 (s, 3H), 0.97 (s, 9H), 2.56 (d, $J = 2.3$ Hz, 1H), 5.59 (d, $J = 2.3$ Hz, 1H), 7.24 (ddd, $J = 7.3, 4.8, 1.0$ Hz, 1H), 7.66 (d, $J = 8.1$ Hz, 1H), 7.76 (td, $J = 7.7, 1.6$ Hz, 1H), 8.59 (dq, $J = 4.8, 1.0$ Hz, 1H); ^{13}C NMR (101 MHz, CDCl_3) δ -5.1, -4.6, 18.3, 25.8, 66.2, 73.6, 84.0, 120.0, 120.0, 122.8, 137.2, 148.7, 160.3; LCMS (Method A): MH^+ 248, Rt 1.36 min, 88% by UV; HRMS exact mass calculated for $[\text{M}+\text{H}]^+$ ($\text{C}_{14}\text{H}_{21}\text{NOSi}$) requires 248.1470 m/z , found 248.1469.

4-(1-((*Tert*-butyldimethylsilyl)oxy)prop-2-yn-1-yl)isoxazole, 279

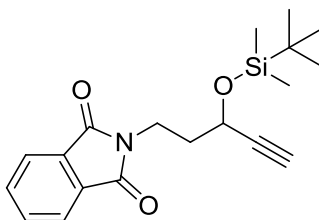
Prepared following the general procedure A (scale: step i) isoxazole-4-carbaldehyde, 250 mg; step ii) 1-(isoxazol-4-yl)prop-2-yn-1-ol (portion of crude product from step i), 150 mg). Isolated yield: 170 mg, 59% (from aldehyde), clear oil. $\nu_{\max}/\text{cm}^{-1}$ (neat) 1649, 2957; ^1H NMR (400 MHz, CDCl_3) δ 0.20 (s, 3H), 0.21 (s, 3H), 0.95 (s, 9H), 2.60 (d, $J = 2.3$ Hz, 1H), 5.50 (dd, $J = 2.3, 0.8$ Hz, 1H), 8.32 (s, 1H), 8.43 (d, $J = 0.8$ Hz, 1H); ^{13}C NMR (101 MHz, CDCl_3) δ -5.0, -4.5, 18.2, 25.6, 55.9, 73.6, 82.7, 148.4, 154.9; LCMS (Method A): MH^+ mass not observed, Rt 1.34 min, 100% by UV;

3-(1-((*Tert*-butyldimethylsilyl)oxy)prop-2-yn-1-yl)benzotrile, 280

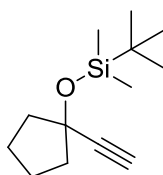
Prepared following the general procedure A (scale: step i) 3-formylbenzotrile, 250 mg; step ii) 3-(1-hydroxyprop-2-yn-1-yl)benzotrile (portion of crude product from step i), 150 mg). Isolated yield: 134 mg, 33% (from aldehyde), clear oil. $\nu_{\max}/\text{cm}^{-1}$ (neat) 1683, 2233, 2956; $^1\text{H NMR}$ (400 MHz, CDCl_3) δ 0.23 (s, 3H), 0.20 (s, 3H), 0.97 (s, 9H), 2.63 (d, $J = 2.2$ Hz, 1H), 5.52 (d, $J = 2.2$ Hz, 1H), 7.49 (t, $J = 7.8$ Hz, 1H), 7.62 (dt, $J = 7.8, 1.2$ Hz, 1H), 7.75 (dt, $J = 7.8, 1.8$ Hz, 1H), 7.83 (t, $J = 1.8$ Hz, 1H); $^{13}\text{C NMR}$ (101 MHz, CDCl_3) δ -5.0, -4.5, 18.3, 25.7, 63.7, 74.7, 83.5, 112.5, 118.7, 129.2, 129.7, 130.4, 131.5, 142.9; LCMS (Method A): MH^+ mass not observed, Rt 1.52 min, 90% by UV;

***N*-(4-(1-((*Tert*-butyldimethylsilyl)oxy)prop-2-yn-1-yl)phenyl)acetamide, 281**

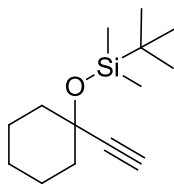
Prepared following the general procedure A (scale: step i) *N*-(4-formylphenyl)acetamide, 250 mg; step ii) *N*-(4-(1-hydroxyprop-2-yn-1-yl)phenyl)acetamide (portion of crude product from step i), 150 mg). Isolated yield: 146 mg, 33% (from aldehyde), clear oil. $\nu_{\max}/\text{cm}^{-1}$ (neat) 1669, 2862, 2930, 3265 (broad); $^1\text{H NMR}$ (400 MHz, CDCl_3) δ 0.16 (s, 3H), 0.19 (s, 3H), 0.95 (s, 9H), 2.19 (s, 3H), 2.57 (d, $J = 1.8$ Hz, 1H), 5.47 (d, $J = 1.8$ Hz, 1H), 7.22 (br. s., 1H), 7.46 (d, $J = 8.3$ Hz, 2H), 7.51 (d, $J = 8.3$ Hz, 2H); $^{13}\text{C NMR}$ (101 MHz, CDCl_3) δ -4.9, -4.6, 18.3, 24.6, 25.8, 57.3, 64.2, 73.7, 84.6, 119.7, 126.8, 137.3, 137.4, 168.1; LCMS (Method A): MH^+ 304, Rt 1.31 min, 70% by UV; No sample remained after subsequent steps in synthetic sequence, so HRMS could not be recorded.

2-(3-((*Tert*-butyldimethylsilyl)oxy)pent-4-yn-1-yl)isoindoline-1,3-dione, 282

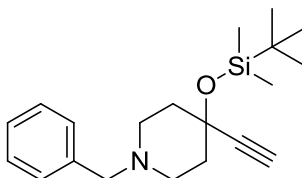
Prepared following the general procedure A (scale: step i) 3-(1,3-dioxoisoindolin-2-yl)propanal, 250 mg; step ii) 2-(3-hydroxypent-4-yn-1-yl)isoindoline-1,3-dione (portion of crude product from step i), 250 mg). Isolated yield: 243 mg, 58% (from aldehyde), clear oil. $\nu_{\max}/\text{cm}^{-1}$ (neat) 1709, 1767, 2929, 2956, 3265; ^1H NMR (400 MHz, CDCl_3) δ 0.15 (s, 3H), 0.16 (s, 3H), 0.93 (s, 9H), 2.05-2.17 (m, 2H), 2.41 (d, $J = 2.3$ Hz, 1H), 3.90 (t, $J = 7.2$ Hz, 2H), 4.52 (td, $J = 5.9, 2.3$ Hz, 1H), 7.73 (dd, $J = 5.6, 3.0$ Hz, 2H), 7.86 (dd, $J = 5.6, 3.0$ Hz, 2H); ^{13}C NMR (101 MHz, CDCl_3) δ -5.2, -4.6, 18.1, 25.7, 34.3, 36.8, 60.7, 72.9, 84.4, 123.1, 132.3, 133.8, 168.2; LCMS (Method A): MH^+ 344, Rt 1.49 min, 100% by UV; HRMS exact mass calculated for $[\text{M}+\text{H}]^+$ ($\text{C}_{19}\text{H}_{26}\text{NO}_3\text{Si}$) requires m/z 344.1682, found 344.1678.

***Tert*-butyl((1-ethynylcyclopentyl)oxy)dimethylsilane, 283**

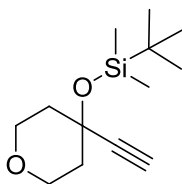
Prepared following the general procedure B omitting step i) (scale: 1-ethynylcyclopentanol, 500 mg). Isolated yield: 745 mg, 73% (from propargylic alcohol), clear oil. $\nu_{\max}/\text{cm}^{-1}$ (neat) 1461, 2853, 2921, 2955; ^1H NMR (400 MHz, CDCl_3) δ 0.20 (s, 6H), 0.89 (s, 9H), 1.68-1.83 (m, 4H), 1.89-1.96 (m, 4H), 2.47 (s, 1H); ^{13}C NMR (101 MHz, CDCl_3) δ -3.3, 18.0, 23.0, 25.7, 43.4, 71.6, 75.2, 88.3; LCMS and HRMS could not be recorded due to lack of UV chromophore.

Tert-butyl((1-ethynylcyclohexyl)oxy)dimethylsilane,²⁶⁰ 284

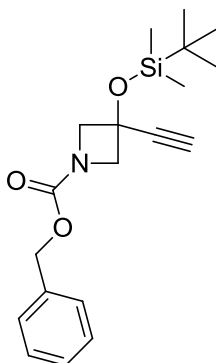
Prepared following the general procedure B omitting step i) (scale: 1-ethynylcyclohexanol, 500 mg). Isolated yield: 514 mg, 54% (from propargylic alcohol), clear oil. $\nu_{\max}/\text{cm}^{-1}$ (neat) 1461, 2853, 2921, 2955; ^1H NMR (400 MHz, CDCl_3) δ 0.20 (s, 6H), 0.91 (s, 9H), 1.27-1.39 (m, 2H), 1.50-1.59 (m, 2H), 1.61-1.72 (m, 4H), 1.78-1.86 (m, 2H), 2.47 (s, 1H); ^{13}C NMR (101 MHz, CDCl_3) δ -2.9, 18.1, 22.7, 25.3, 25.8, 41.0, 69.1, 72.7, 88.5; LCMS and HRMS could not be recorded due to lack of UV chromophore.

1-Benzyl-4-((tert-butyl dimethylsilyl)oxy)-4-ethynylpiperidine, 285

Prepared following the general procedure B omitting step i) (scale: 1-benzyl-4-ethynylpiperidin-4-ol, 250 mg). Isolated yield: 143 mg, 37% (from propargylic alcohol), clear oil. $\nu_{\max}/\text{cm}^{-1}$ (neat) 2928, 2954, 3307; ^1H NMR (400 MHz, CDCl_3) δ 0.19 (s, 6H), 0.90 (s, 9H), 1.85 (dd, $J = 7.5, 3.7$ Hz, 2H), 1.89-2.01 (m, 2H), 2.39-2.53 (m, 2H), 2.50 (s, 1H), 2.55-2.65 (m, 2H), 3.53 (s, 2H), 7.24-7.37 (m, 5H); ^{13}C NMR (101 MHz, CDCl_3) δ -2.9, 18.2, 25.8, 40.3, 49.7, 63.0, 67.3*, 73.2, 87.5*, 126.9, 128.2, 129.1, 139.1*, *Peak not observed in 1D ^{13}C spectrum, coupling detected to this chemical shift in HMBC; LCMS (Method A): MH^+ 330, Rt 1.73 min, 97% by UV; HRMS exact mass calculated for $[\text{M}+\text{H}]^+$ ($\text{C}_{20}\text{H}_{32}\text{NOSi}$) requires m/z 330.2253, found 330.2253.

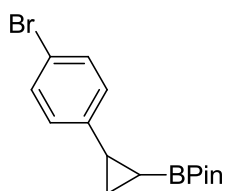
***Tert*-butyl((4-ethynyltetrahydro-2*H*-pyran-4-yl)oxy)dimethylsilane, 286²⁶⁰**

Prepared following the general procedure B (scale: step i) dihydro-2*H*-pyran-4(3*H*)-one, 1.0 g; step ii) 4-ethynyltetrahydro-2*H*-pyran-4-ol (portion of crude product from step i), 800 mg). Isolated yield: 970 mg, 53% (from ketone), clear oil. $\nu_{\text{max}}/\text{cm}^{-1}$ (neat) 3211, 2954, 2924, 2870, 2854; ^1H NMR (400 MHz, CDCl_3) δ 0.21 (s, 6H), 0.92 (s, 9H), 1.73-1.86 (m, 2H), 1.87-1.98 (m, 2H), 2.55 (s, 1H), 3.69 (ddd, $J = 11.3, 7.6, 3.3$ Hz, 2H), 3.86 (ddd, $J = 11.3, 6.8, 3.8$ Hz, 2H); ^{13}C NMR (101 MHz, CDCl_3) δ -3.4, 17.6, 25.3, 40.5, 63.8, 65.8, 73.1, 86.6; LCMS and HRMS could not be recorded due to lack of UV chromophore.

Benzyl 3-((*tert*-butyldimethylsilyl)oxy)-3-ethynylazetidide-1-carboxylate, 287

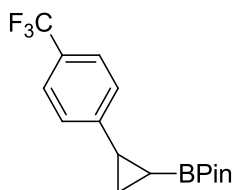
Prepared following the general procedure B (scale: step i) benzyl 3-oxoazetidide-1-carboxylate, 250 mg; step ii) benzyl 3-ethynyl-3-hydroxyazetidide-1-carboxylate (portion of crude product from step i), 190 mg). Isolated yield: 175 mg, 41% (from ketone), clear oil. $\nu_{\text{max}}/\text{cm}^{-1}$ (neat) 3288, 2953, 2930, 1709; ^1H NMR (400 MHz, CDCl_3) δ 0.18 (s, 6H), 0.92 (s, 9H), 2.67 (s, 1H), 4.07 (d, $J = 9.6$ Hz, 2H), 4.28 (d, $J = 9.6$ Hz, 2H), 5.14 (s, 2H), 7.31-7.39 (m, 5H); ^{13}C NMR (101 MHz, CDCl_3) δ -3.8, 17.7, 25.5, 63.0, 65.6, 66.9, 74.4, 84.5, 128.0, 128.1, 128.5, 136.5, 156.3; LCMS (Method A): MH^+ mass not observed, Rt 1.54 min, 95% by UV; HRMS exact mass calculated for $[\text{M}+\text{H}]^+$ ($\text{C}_{19}\text{H}_{28}\text{NO}_3\text{Si}$) requires m/z 346.1833, found 346.1821.

2-(2-(4-Bromophenyl)cyclopropyl)-4,4,5,5-tetramethyl-1,3,2-dioxaborolane,
223¹⁸⁶



Prepared following the general procedure C (scale: ((1-(4-bromophenyl)prop-2-yn-1-yl)oxy)(*tert*-butyl)dimethylsilane, 125 mg). Isolated yield: 88 mg, 71% (as a 1.7:1.0 *cis:trans* mixture), clear oil. Diastereomeric ratio was calculated by comparing ¹H NMR integrals of the following peaks: *cis* - 2.30 (ddd, *J* = 10.1, 7.8, 6.1 Hz, 1H), *trans* - 2.08 (dt, *J* = 8.2, 5.4 Hz, 1H); *Cis*: ¹H NMR (400 MHz, CDCl₃) δ 0.48 (ddd, *J* = 10.1, 9.3, 7.3 Hz, 1H), 0.94 (s, 6H), 1.06 (s, 6H), 1.10 (ddd, *J* = 9.3, 8.0, 4.2 Hz, 1H), 1.28 (ddd, *J* = 7.1, 6.1, 4.2 Hz, 1H), 2.30 (ddd, *J* = 10.1, 7.8, 6.1 Hz, 1H), 7.17 (d, *J* = 8.3 Hz, 2H), 7.37 (d, *J* = 8.3 Hz, 2H); *Trans*: ¹H NMR (400 MHz, CDCl₃) δ 0.27 (ddd, *J* = 9.9, 6.9, 5.4 Hz, 1H), 0.96 (ddd, *J* = 9.8, 5.4, 3.7 Hz, 1H), 1.16 (ddd, *J* = 8.2, 7.0, 3.7 Hz, 1H), 1.24 (s, 6H), 1.25 (s, 6H), 2.08 (dt, *J* = 8.2, 5.4 Hz, 1H), 6.97 (d, *J* = 8.3 Hz, 2H), 7.36 (d, *J* = 8.3 Hz, 2H); **Mixture**: $\nu_{\max}/\text{cm}^{-1}$ (neat) 2976, 1491; ¹³C NMR (101 MHz, CDCl₃) δ 9.2, 14.9, 21.3, 21.4, 24.4, 24.7, 24.7, 24.8, 83.0, 83.3, 119.0, 119.3, 127.5, 130.6, 130.6, 131.2, 139.9, 142.5, the carbon directly attached to the boron atom was not detected, likely due to quadropolar relaxation.²⁵⁶; HRMS exact mass calculated for [M+H]⁺ (C₁₅H₂₁BBro₂) requires *m/z* 323.0813, found 323.0810.

4,4,5,5-Tetramethyl-2-(2-(4-(trifluoromethyl)phenyl)cyclopropyl)-1,3,2-
dioxaborolane, 237¹⁸⁶

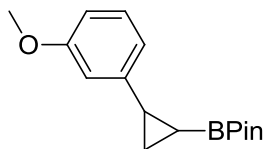


Prepared following the general procedure C (scale: *tert*-butyldimethyl((1-(4-(trifluoromethyl)phenyl)prop-2-yn-1-yl)oxy)silane, 100 mg). Isolated yield: 59 mg, 59% (as a 4.3:1.0 *cis:trans* mixture), clear oil. Diastereomeric ratio was calculated by comparing ¹H NMR integrals of the following peaks: *cis* - 2.40 (dt, *J* = 9.8, 7.1 Hz, 1H), *trans* - 2.17 (dt, *J* = 8.1, 5.4 Hz, 1H); *Cis*: ¹H NMR (400 MHz, CDCl₃) δ 0.54 (td, *J* = 9.7, 7.3 Hz, 1H), 0.90 (s, 6H), 1.04 (s, 6H), 1.20 (ddd, *J* = 9.3, 7.8, 4.3 Hz, 1H),

CONFIDENTIAL – PROPERTY OF GSK – DO NOT COPY

1.34 (ddd, $J = 7.1, 6.1, 4.3$ Hz, 1H), 2.40 (dt, $J = 9.8, 7.1$ Hz, 1H), 7.40 (d, $J = 8.2$ Hz, 2H), 7.49 (d, $J = 8.2$ Hz, 2H); ^{19}F NMR (376 MHz, CDCl_3) δ -62.31 (s, 3F); **Trans**: ^1H NMR (400 MHz, CDCl_3) δ 0.37 (ddd, $J = 9.9, 6.8, 5.6$ Hz, 1H), 1.07 (dd, $J = 5.1, 4.0$ Hz, 1H), 1.27 (s, 6H), 1.28 (s, 6H), 2.17 (dt, $J = 8.1, 5.4$ Hz, 1H), 7.18 (d, $J = 8.3$ Hz, 2H), 7.50 (d, $J = 8.3$ Hz, 2H) (other peaks not resolvable due to overlap with *cis* isomer); ^{19}F NMR (376 MHz, CDCl_3) δ -62.27 (s, 3F); **Mixture**: $\nu_{\text{max}}/\text{cm}^{-1}$ (neat) 2980, 1617; ^{13}C NMR (101 MHz, CDCl_3) δ 9.3, 15.4, 21.7, 24.3, 24.7, 24.8, 24.8, 26.9, 83.4, 124.5 (q, $J = 4$ Hz), 124.5 (q, $J = 271.6$ Hz), 125.1 (q, $J = 4$ Hz), 128.3 (q, $J = 32.8$ Hz), 129.1, 129.3, 147.8, 145.2, two expected quartets not observed., the carbon directly attached to the boron atom was not detected, likely due to quadropolar relaxation.²⁵⁶; HRMS exact mass calculated for $[\text{M}+\text{H}]^+$ ($\text{C}_{16}\text{H}_{21}\text{BF}_3\text{O}_2$) requires m/z 313.1587, found 313.1594.

2-(2-(3-Methoxyphenyl)cyclopropyl)-4,4,5,5-tetramethyl-1,3,2-dioxaborolane, 288²⁶¹

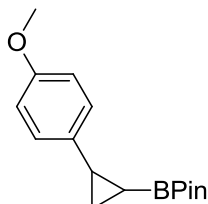


Prepared following the general procedure C (scale: *tert*-butyl((1-(3-methoxyphenyl)prop-2-yn-1-yl)oxy)dimethylsilane, 100 mg). Isolated yield: 55 mg, 56% (as a 1.3:1.0 *cis:trans* mixture), clear oil. Diastereomeric ratio was calculated by comparing ^1H NMR integrals of the following peaks: *cis* - 0.46 (td, $J = 9.7, 7.3$ Hz, 1H), *trans* - 0.33 (ddd, $J = 9.9, 6.6, 5.6$ Hz, 1H); **Cis**: ^1H NMR (400 MHz, CDCl_3) δ 0.46 (td, $J = 9.7, 7.3$ Hz, 1H), 0.94 (s, 6H), 1.06 (s, 6H), 1.12 (ddd, $J = 9.3, 8.3, 4.7$ Hz, 1H), 1.28-1.31 (m, 1H), 2.35 (ddd, $J = 10.1, 8.1, 6.3$ Hz, 1H), 3.81 (s, 3H), 6.64-6.73 (m, 3H), 7.14 (t, $J = 7.8$ Hz, 1H); **Trans**: ^1H NMR (400 MHz, CDCl_3) δ 0.33 (ddd, $J = 9.9, 6.6, 5.6$ Hz, 1H), 1.02 (ddd, $J = 9.8, 5.2, 3.7$ Hz, 1H), 1.17 (ddd, $J = 8.2, 6.8, 3.7$ Hz, 1H), 1.26 (s, 6H), 1.27 (s, 6H), 2.11 (dt, $J = 8.1, 5.4$ Hz, 1H), 3.80 (s, 3H), 6.83-6.92 (m, 3H), 7.17 (t, $J = 7.8$ Hz, 1H); **Mixture**: $\nu_{\text{max}}/\text{cm}^{-1}$ (neat) 2960, 2939, 2870; ^{13}C NMR (101 MHz, CDCl_3) δ 9.1, 15.0, 21.8, 21.9, 24.4, 24.7, 24.8, 24.8, 55.1, 55.1, 82.9, 83.2, 111.0, 111.5, 111.6, 112.0, 114.1, 114.2, 118.1, 118.2, 121.3, 121.4, 128.6, 129.2, the carbon directly attached to the boron atom was not detected, likely

CONFIDENTIAL – PROPERTY OF GSK – DO NOT COPY

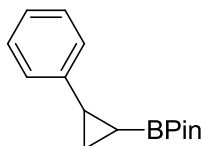
due to quadrupolar relaxation.²⁵⁶; HRMS exact mass calculated for $[M+H]^+$ ($C_{16}H_{24}BO_3$) requires m/z 275.1813, found 275.1805.

2-(2-(4-Methoxyphenyl)cyclopropyl)-4,4,5,5-tetramethyl-1,3,2-dioxaborolane,^{186,261,262} 235^{186,258,259}



Prepared following the general procedure C (scale: *tert*-butyl((1-(4-methoxyphenyl)-113-prop-2-yn-1-yl)oxy)dimethylsilane, 100 mg). Isolated yield: 60 mg, 60% (as a 0.9:1 *cis:trans* mixture), clear oil. Diastereomeric ratio was calculated by comparing 1H NMR integrals of the following peaks: *cis* - 0.41 (td, $J = 9.7, 7.2$ Hz, 1H), *trans* - 0.24 (dt, $J = 9.4, 5.8$ Hz, 1H); ***Cis***: 1H NMR (400 MHz, $CDCl_3$) δ 0.41 (td, $J = 9.7, 7.2$ Hz, 1H), 0.93 (s, 6H), 1.06 (s, 6H), 1.07-1.16 (m, 1H), 1.20-1.24 (m, 1H), 2.29-2.33 (m, 1H), 3.79 (s, 3H), 6.76-6.86 (m, 2H), 7.17-7.24 (m, 2H); ***Trans***: 1H NMR (400 MHz, $CDCl_3$) δ 0.24 (dt, $J = 9.4, 5.8$ Hz, 1H), 0.94-0.99 (m, 1H), 1.07-1.16 (m, 1H), 1.26 (s, 6H), 1.27 (s, 6H), 2.09 (dt, $J = 8.1, 5.4$ Hz, 1H), 3.79 (s, 3H), 6.76-6.86 (m, 2H), 6.96-7.07 (m, 2H); **Mixture**: ν_{max}/cm^{-1} (neat) 2958, 2934; ^{13}C NMR (101 MHz, $CDCl_3$) δ 9.0, 14.5, 21.0, 21.2, 24.4, 24.7, 24.7, 24.8, 55.3, 55.4, 82.9, 83.1, 113.2, 113.8, 126.8, 129.8, 133.0, 135.3, 157.7, 157.9, the carbon directly attached to the boron atom was not detected, likely due to quadrupolar relaxation.²⁵⁶; HRMS exact mass calculated for $[M+H]^+$ ($C_{16}H_{24}BO_3$) requires m/z 275.1813, found 275.1819.

4,4,5,5-Tetramethyl-2-(2-phenylcyclopropyl)-1,3,2-dioxaborolane, 289^{186,263}

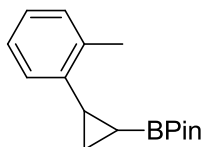


Prepared following the general procedure C (scale: *tert*-butyldimethyl((1-phenylprop-2-yn-1-yl)oxy)silane, 250 mg). Isolated yield: 163 mg, 66% (as a 1.8:1 *cis:trans* mixture), clear oil. Diastereomeric ratio was calculated by comparing 1H NMR integrals of the following peaks: *cis* - 2.38 (ddd, $J = 10.1, 7.8, 6.1$ Hz, 1H), *trans* - 2.14 (dt, $J = 8.1, 5.4$ Hz, 1H); ***Cis***: 1H NMR (400 MHz, $CDCl_3$) δ 0.48 (ddd, $J = 10.1,$

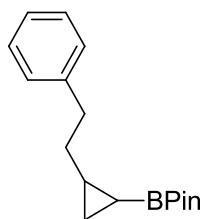
CONFIDENTIAL – PROPERTY OF GSK – DO NOT COPY

9.3, 7.3 Hz, 1H), 0.92 (s, 6H), 1.05 (s, 6H), 1.13 (ddd, $J = 9.2, 8.0, 4.3$ Hz, 1H), 2.38 (ddd, $J = 10.1, 7.8, 6.1$ Hz, 1H), 7.05-7.41 (m, 5H), in agreement with literature sample¹⁸⁶ except peak at 1.28 ppm could not be observed due to overlap with *trans*-isomer; **Trans**: ¹H NMR (400 MHz, CDCl₃) δ 0.34 (ddd, $J = 9.8, 6.8, 5.4$ Hz, 1H), 1.03 (ddd, $J = 9.8, 5.4, 3.7$ Hz, 1H), 1.13 (ddd, $J = 9.2, 8.0, 4.3$ Hz, 1H), 1.27 (s, 6H), 1.28 (s, 6H), 2.14 (dt, $J = 8.1, 5.4$ Hz, 1H), 7.07-7.35 (m, 5H); **Mixture**: $\nu_{\max}/\text{cm}^{-1}$ (neat) 2974, 1491; ¹³C NMR (101 MHz, CDCl₃) δ 8.9, 15.0, 21.7, 21.9, 24.4, 24.7, 24.7, 24.8, 82.9, 83.1, 125.5, 125.7, 127.6, 128.1, 128.2, 128.8, 140.8, 143.4, the carbon directly attached to the boron atom was not detected, likely due to quadropolar relaxation.²⁵⁶; HRMS exact mass calculated for [M+H]⁺ (C₁₅H₂₂BO₂) requires m/z 245.1707, found 245.1700.

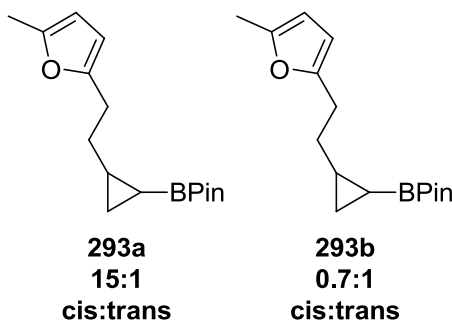
4,4,5,5-Tetramethyl-2-(2-(*o*-tolyl)cyclopropyl)-1,3,2-dioxaborolane, 290²⁶²



Prepared following the general procedure C (scale: *tert*-butyldimethyl((1-(*o*-tolyl)prop-2-yn-1-yl)oxy)silane, 100 mg). Isolated yield: 29 mg, 29% (as a 1:1 *cis:trans* mixture), clear oil. Diastereomeric ratio was calculated by comparing ¹H NMR integrals of the following peaks: *cis* - 0.55 (td, $J = 9.7, 6.8$ Hz, 1H), *trans* - 0.19 (dt, $J = 9.5, 6.2$ Hz, 1H); **Cis**: ¹H NMR (400 MHz, CDCl₃) δ 0.55 (td, $J = 9.7, 6.8$ Hz, 1H), 0.82 (s, 6H), 1.02 (s, 6H), 1.11-1.22 (m, 1H), 1.33-1.39 (m, 1H), 2.25 (dt, $J = 9.9, 6.9$ Hz, 1H), 2.45 (s, 3H), 6.96-7.27 (m, 4H); **Trans**: ¹H NMR (400 MHz, CDCl₃) δ 0.19 (dt, $J = 9.5, 6.2$ Hz, 1H), 1.06 (ddd, $J = 9.3, 5.6, 3.4$ Hz, 1H), 1.11-1.22 (m, 1H), 1.29 (s, 12H), 2.14 (dt, $J = 7.8, 5.9$ Hz, 1H), 2.44 (s, 3H), 6.96-7.27 (m, 4H); **Mixture**: $\nu_{\max}/\text{cm}^{-1}$ (neat) 2950, 2926, 1708; ¹³C NMR (101 MHz, CDCl₃) δ 8.5, 12.2, 19.5, 19.6, 20.3, 20.5, 24.2, 24.6, 24.7, 24.7, 24.8, 24.9, 82.7, 83.1, 125.1, 125.4, 125.8, 125.8, 125.9, 128.2, 129.1, 129.5, 137.9, 138.7, 138.9, 140.9, the carbon directly attached to the boron atom was not detected, likely due to quadropolar relaxation.²⁵⁶; HRMS exact mass calculated for [M+H]⁺ (C₁₆H₂₄BO₂) requires m/z 259.1869, found 259.1874.

4,4,5,5-Tetramethyl-2-(2-(phenethylcyclopropyl)-1,3,2-dioxaborolane, 292

Prepared following the general procedure C (scale: *tert*-butyldimethyl((5-phenylpent-1-yn-3-yl)oxy)silane), 100 mg). Isolated yield: 76 mg, 77% (as a 1.4:1 *cis:trans* mixture), clear oil. Diastereomeric ratio was calculated by comparing ^1H NMR integrals of the following peaks: *cis* - -0.03 (td, $J = 9.2, 6.8$ Hz, 1H), *trans* - -0.35 (dt, $J = 9.4, 5.8$ Hz, 1H); ***Cis***: ^1H NMR (400 MHz, CDCl_3) δ -0.03 (td, $J = 9.2, 6.8$ Hz, 1H), 0.41-0.48 (m, 1H), 0.82 (ddd, $J = 9.2, 7.9, 3.4$ Hz, 1H), 1.10 (dq, $J = 14.8, 7.5, 1.8$ Hz, 1H), 1.26 (s, 6H), 1.27 (s, 6H), 1.75-1.79 (m, 2H), 2.67-2.81 (m, 2H), 7.13-7.34 (m, 5H); ***Trans***: ^1H NMR (400 MHz, CDCl_3) δ -0.35 (dt, $J = 9.4, 5.8$ Hz, 1H), 0.41-0.48 (m, 1H), 0.71 (ddd, $J = 7.7, 6.1, 3.4$ Hz, 1H), 0.95-1.01 (m, 1H), 1.24 (s, 6H), 1.25 (s, 6H), 1.77 (m, 2H), 2.67-2.81 (m, 2H), 7.13-7.34 (m, 5H); **Mixture**: $\nu_{\text{max}}/\text{cm}^{-1}$ (neat) 2976, 2928, 2855; ^{13}C NMR (101 MHz, CDCl_3) δ 11.0, 11.4, 18.0, 18.1, 24.7, 24.7, 24.7, 25.1, 32.6, 36.0, 36.4, 37.3, 82.8, 82.9, 125.5, 125.6, 128.1, 128.2, 128.4, 128.5, 142.5, 142.7, the carbon directly attached to the boron atom was not detected, likely due to quadrupolar relaxation.²⁵⁶; HRMS exact mass calculated for $[\text{M}+\text{H}]^+$ ($\text{C}_{17}\text{H}_{26}\text{BO}_2$) requires m/z 273.2026, found 273.2031.

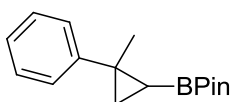
4,4,5,5-Tetramethyl-2-(2-(2-(5-methylfuran-2-yl)ethyl)cyclopropyl)-1,3,2-dioxaborolane, 293

Prepared following the general procedure C (scale: *tert*-butyldimethyl((5-(5-methylfuran-2-yl)pent-1-yn-3-yl)oxy)silane, 100 mg). Overall yield: 58 mg, 58% (1.4:1, *cis:trans*). Two product fractions were isolated **293a** and **293b**. Diastereomeric

CONFIDENTIAL – PROPERTY OF GSK – DO NOT COPY

ratio was calculated by comparing ^1H NMR integrals of the following peaks: *cis* - - 0.04 (td, $J = 9.3, 6.8$ Hz, 1H), *trans* - -0.35 (dt, $J = 9.4, 5.7$ Hz, 1H); **293a**: Isolated yield: 17 mg, 17% (as a 15:1 *cis:trans* mixture), clear oil, $\nu_{\text{max}}/\text{cm}^{-1}$ (neat) 2978, 2923, 1570; ^1H NMR (400 MHz, CDCl_3) δ -0.04 (td, $J = 9.3, 6.8$ Hz, 1H), 0.45 (td, $J = 6.1, 3.4$ Hz, 1H), 0.81 (ddd, $J = 9.0, 7.8, 3.4$ Hz, 1H), 1.07-1.17 (m, 1H), 1.25 (s, 6H), 1.26 (s, 6H), 1.65-1.75 (m, 1H), 1.75-1.85 (m, 1H), 2.26 (s, 3H), 2.66 (t, $J = 7.8$ Hz, 2H), 5.82-5.87 (m, 2H); ^{13}C NMR (101 MHz, CDCl_3) δ 10.9, 13.5, 18.0, 24.6, 25.1, 28.6, 29.7, 82.9, 105.1, 105.7, 149.9, 154.6 the carbon directly attached to the boron atom was not detected, likely due to quadropolar relaxation.²⁵⁶ HRMS exact mass calculated for $[\text{M}+\text{H}]^+$ ($\text{C}_{16}\text{H}_{26}\text{BO}_3$) requires m/z 277.1970, found 277.1966. **293b**: Isolated yield: 39 mg, 39% (as a 0.7:1, *cis:trans* mixture), clear oil. *Cis*: ^1H NMR (400 MHz, CDCl_3) δ -0.04 (td, $J = 9.3, 6.8$ Hz, 1H), 0.45 (td, $J = 6.1, 3.4$ Hz, 1H), 0.81 (ddd, $J = 9.0, 7.8, 3.4$ Hz, 1H), 1.07-1.17 (m, 1H), 1.25 (s, 6H), 1.26 (s, 6H), 1.65-1.75 (m, 1H), 1.75-1.85 (m, 1H), 2.26 (s, 3H), 2.66 (t, $J = 7.8$ Hz, 2H), 5.82-5.87 (m, 2H); ^{13}C NMR (101 MHz, CDCl_3) δ 10.9, 13.5, 18.0, 24.6, 25.1, 28.6, 29.7, 82.9, 105.1, 105.7, 149.9, 154.6, the carbon directly attached to the boron atom was not detected, likely due to quadropolar relaxation.²⁵⁶; *Trans*: ^1H NMR (400 MHz, CDCl_3) δ -0.35 (dt, $J = 9.4, 5.7$ Hz, 1H), 0.70 (ddd, $J = 7.6, 6.1, 3.4$ Hz, 1H), 0.95-1.05 (m, 1H), 1.23 (s, 12H), 1.28-1.31 (m, 1H), 1.51-1.66 (m, 2H), 2.26 (s, 3H), 2.67 (q, $J = 8.0$ Hz, 2H), 5.82-5.88 (m, 2H); ^{13}C NMR (101 MHz, CDCl_3) δ 11.3, 17.9, 24.7, 24.7, 24.8, 28.2, 34.0, 82.8, 105.2, 105.7, 150.0, 154.4, the carbon directly attached to the boron atom was not detected, likely due to quadropolar relaxation.²⁵⁶; **Mixture**: $\nu_{\text{max}}/\text{cm}^{-1}$ (neat) 2978, 2923, 1570; Rt min, % by UV; HRMS exact mass calculated for $[\text{M}+\text{H}]^+$ ($\text{C}_{16}\text{H}_{26}\text{BO}_3$) requires m/z 277.1970, found 277.1965.

4,4,5,5-Tetramethyl-2-(2-methyl-2-phenylcyclopropyl)-1,3,2-dioxaborolane,
236¹⁸³

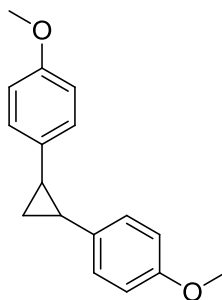


Prepared following the general procedure C (scale: *tert*-butyldimethyl((2-phenylbut-3-yn-2-yl)oxy)silane, 39 mg). Isolated yield: 13 mg, 34% (as a 1:1.4 *cis:trans* mixture), clear oil. Diastereomeric ratio was calculated by comparing ^1H NMR integrals of the

CONFIDENTIAL – PROPERTY OF GSK – DO NOT COPY

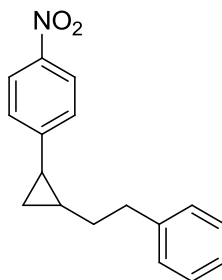
following peaks: *cis* - 0.30 (dd, $J = 9.1, 6.8$ Hz, 1H), *trans* - 0.39 (dd, $J = 9.7, 7.2$ Hz, 1H); **Cis**: ^1H NMR (400 MHz, CDCl_3) δ 0.30 (dd, $J = 9.1, 6.8$ Hz, 1H), 0.85 (s, 6H), 0.91 (dd, $J = 9.1, 3.8$ Hz, 1H), 1.06 (s, 6H), 1.39 (dd, $J = 6.8, 3.8$ Hz, 1H), 1.47 (s, 3H), 7.15-7.40 (m, 5H); ^{13}C NMR (101 MHz, CDCl_3) δ 17.2, 24.3, 24.8, 29.5, 32.7, 82.7, 125.8, 127.2, 129.0, 147.6, the carbon directly attached to the boron atom was not detected, likely due to quadropolar relaxation.²⁵⁶; **Trans**: ^1H NMR (400 MHz, CDCl_3) δ 0.39 (dd, $J = 9.7, 7.2$ Hz, 1H), 1.03 (dd, $J = 7.2, 3.6$ Hz, 1H), 1.21 (dd, $J = 9.7, 3.6$ Hz, 1H), 1.29 (s, 6H), 1.31 (s, 6H), 1.52 (s, 3H), 7.15-7.40 (m, 5H); ^{13}C NMR (101 MHz, CDCl_3) δ 20.2, 22.9, 24.6, 25.1, 26.7, 83.2, 125.5, 127.0, 128.1, 148.1, the carbon directly attached to the boron atom was not detected, likely due to quadropolar relaxation.²⁵⁶; **Mixture**: $\nu_{\text{max}}/\text{cm}^{-1}$ (neat) 2971, 2926; HRMS exact mass calculated for $[\text{M}+\text{H}]^+$ ($\text{C}_{16}\text{H}_{24}\text{BO}_2$) requires m/z 259.1869, found 259.1863.

1,2-Bis(4-methoxyphenyl)cyclopropane, 314²⁶⁴



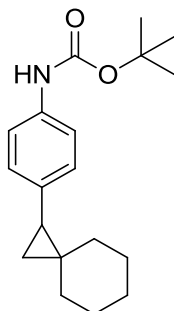
Prepared following the general procedure D (scale: *tert*-butyl((1-(4-methoxyphenyl)prop-2-yn-1-yl)oxy)dimethylsilane, 20 mg) (purified by normal phase on silica 0-20% ethyl acetate:cyclohexane gradient). Isolated yield 10 mg, 54% (as a 1:1 *cis:trans* mixture), clear glass. Diastereomeric ratio was calculated by comparing ^1H NMR integrals of the following peaks: *cis* - 2.38 (dd, $J = 8.8, 6.4$ Hz, 2H), *trans* - 2.08 (t, $J = 7.6$ Hz, 2H); **Mixture**: $\nu_{\text{max}}/\text{cm}^{-1}$ (neat) 1611, 1581; ^1H NMR (400 MHz, $\text{DMSO}-d_6$) δ 1.23 (q, $J = 6.1$ Hz, 1H), 1.34 (t, $J = 7.4$ Hz, 2H), 1.42 (td, $J = 8.7, 5.3$ Hz, 1H), 2.08 (t, $J = 7.6$ Hz, 2H), 2.38 (dd, $J = 8.8, 6.4$ Hz, 2H), 3.74 (s, 6H), 3.82 (s, 6H), 6.65-6.70 (m, 4H), 6.84-6.90 (m, 4H), 6.84-6.90 (m, 4H), 7.06-7.13 (m, 4H); ^{13}C NMR (101 MHz, $\text{DMSO}-d_6$) δ 11.5, 17.3, 23.2, 26.7, 55.1, 55.3, 113.2, 113.9, 126.9, 129.9, 130.6, 134.7, 157.5, 157.8; LCMS (Method A): MH^+ 255, R_t 1.32 & 1.35 min, 87% by UV; HRMS exact mass calculated for $[\text{M}+\text{H}]^+$ ($\text{C}_{17}\text{H}_{19}\text{O}_2$) requires m/z 255.1385, found 255.1379.

1-Nitro-4-(2-phenethylcyclopropyl)benzene, 315



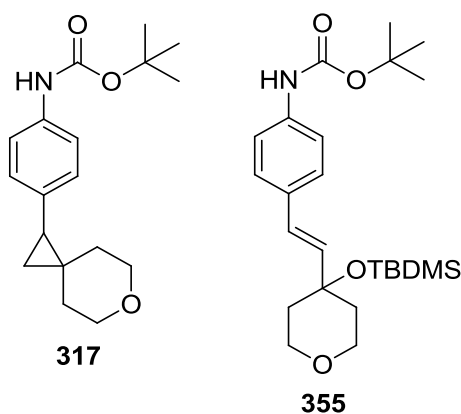
Prepared following the general procedure D (scale: *tert*-butyldimethyl((5-phenylpent-1-yn-3-yl)oxy)silane, 20 mg), (purified by normal phase on silica 0-20% ethyl acetate:cyclohexane gradient). Isolated yield 7.8 mg, 40% (as a 1.6:1 *cis:trans* mixture), clear glass. Diastereomeric ratio was calculated by comparing ^1H NMR integrals of the following peaks: *cis* - 0.83 (q, $J = 5.6$ Hz, 1H), *trans* - 1.04 (dt, $J = 8.6$, 5.0 Hz, 1H); **Cis**: ^1H NMR (400 MHz, CDCl_3) δ 0.83 (q, $J = 5.6$ Hz, 1H), 1.16 (td, $J = 7.8$, 5.4 Hz, 1H), 1.23-1.35 (m, 2H), 1.83 (tq, $J = 7.8$, 6.4 Hz, 1H), 2.24 (td, $J = 8.3$, 6.1 Hz, 1H), 2.48-2.63 (m, 2H), 6.99-7.03 (m 2H), 7.15-7.28 (m, 3H), 7.32 (d, $J = 8.8$ Hz, 2H), 8.15 (d, $J = 8.8$ Hz, 2H); **Trans**: ^1H NMR (400 MHz, CDCl_3) δ 0.96-1.00 (m, 1H), 1.04 (dt, $J = 8.6$, 5.0 Hz, 1H), 1.35-1.49 (m, 2H), 1.70 (dq, $J = 8.5$, 4.5 Hz, 1H), 1.75 (q, $J = 7.3$ Hz, 1H), 2.75-2.85 (m, 2H), 7.07 (d, $J = 8.8$ Hz, 2H), 7.15-7.28 (m, 5H), 8.10 (d, $J = 8.8$ Hz, 2H); **Mixture**: $\nu_{\text{max}}/\text{cm}^{-1}$ (neat) 1598, 1515; ^{13}C NMR (101 MHz, CDCl_3) δ 11.0, 17.8, 20.3, 21.5, 23.8, 25.4, 30.4, 35.5, 35.6, 36.1, 123.1, 123.6, 125.8, 125.8, 125.9, 125.9, 128.3, 128.4, 128.4, 129.3, 141.7*, 141.9*, 145.7*, 146.2*, 148.1*, 152.3*, *Peak not observed in 1D ^{13}C spectrum, coupling detected to this chemical shift in HMBC. The carbon directly attached to the boron atom was not detected, likely due to quadrupolar relaxation.²⁵⁶; LCMS (Method A): MH^+ mass not observed, Rt 1.45 & 1.46 min, 89% by UV; HRMS exact mass calculated for $[\text{M}+\text{H}]^+$ ($\text{C}_{17}\text{H}_{18}\text{NO}_2$) requires m/z 268.1338, found 268.1442.

***Tert*-butyl (4-(spiro[2.5]octan-1-yl)phenyl)carbamate, 316**



Prepared following the general procedure D (scale: *tert*-butyl((1-ethynylcyclohexyl)oxy)dimethylsilane, 100 mg) (purified by reverse phase on C₁₈-silica using a 75-95% 10 mM aqueous ammonium bicarbonate solution:acetonitrile with 0.1% ammonia gradient). Isolated yield: 10 mg, 25%, clear glass. $\nu_{\max}/\text{cm}^{-1}$ (neat) 2926, 1714; ¹H NMR (400 MHz, CDCl₃) δ 0.70 (dd, $J = 8.2, 5.5$ Hz, 1H), 0.79 (t, $J = 5.5$ Hz, 1H), 1.05-1.12 (m, 2H), 1.24-1.33 (m, 2H), 1.38-1.50 (m, 4H), 1.54 (s, 9H), 1.59-1.63 (m, 2H), 1.83 (dd, $J = 8.2, 5.5$ Hz, 1H), 6.40 (br. s., 1H), 7.12 (d, $J = 8.3$ Hz, 2H), 7.26 (d, $J = 8.3$ Hz, 2H); ¹³C NMR (101 MHz, CDCl₃) δ 16.6, 25.0, 25.8, 26.2, 26.5, 28.3, 28.4, 28.8, 30.4, 37.9, 118.1, 129.3, 134.6, 135.7, 152.8; LCMS (Method A): [M-H]⁻ 300, Rt 1.58 min, 71% by UV; HRMS exact mass calculated for [M+H]⁺ (C₁₉H₂₈NO₂) requires m/z 302.2120, found 302.2126.

***Tert*-butyl (4-(6-oxaspiro[2.5]octan-1-yl)phenyl)carbamate, 317 & (*E*)-*tert*-butyl (4-(2-(4-((*tert*-butyldimethylsilyl)oxy)tetrahydro-2*H*-pyran-4-yl)vinyl)phenyl)carbamate, 355**

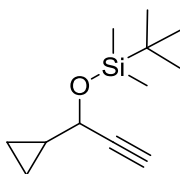


Prepared following the general procedure D (scale: *tert*-butyl((4-ethynyltetrahydro-2*H*-pyran-4-yl)oxy)dimethylsilane, 200 mg) (purified by reverse phase on C₁₈-silica

CONFIDENTIAL – PROPERTY OF GSK – DO NOT COPY

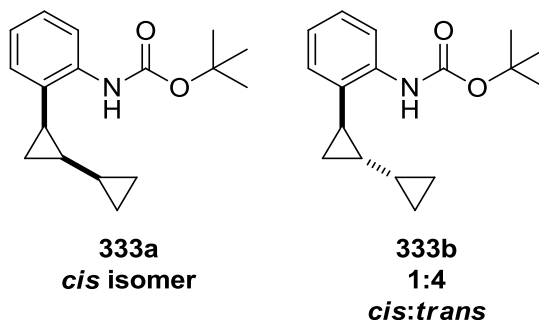
using a 75-95% 10mM aqueous ammonium bicarbonate solution:acetonitrile with 0.1% ammonia gradient). **Product 317**: Isolated yield: 9 mg, 26%, clear glass. $\nu_{\max}/\text{cm}^{-1}$ (neat) 3315, 2974, 1719, 1708; $^1\text{H NMR}$ (400 MHz, CDCl_3) δ 0.83 (dd, $J = 8.6, 5.1$ Hz, 1H), 0.90 (t, $J = 5.4$ Hz, 1H), 1.23 (s, 2H), 1.54 (s, 9H), 1.57-1.68 (m, 2H), 1.95 (dd, $J = 8.3, 6.1$ Hz, 1H), 3.48-3.59 (m, 2H), 3.72-3.86 (m, 2H), 6.44 (br. s., 1H), 7.13 (d, $J = 8.6$ Hz, 2H), 7.28 (d, $J = 8.5$ Hz, 2H); $^{13}\text{C NMR}$ (101 MHz, CDCl_3) δ 16.2, 23.9, 28.4, 30.7, 37.6, 67.2, 67.4, 80.4, 118.3, 129.3, 133.5, 136.2, 152.8; LCMS (Method B): (M-H)⁻ 302, Rt 1.28 min, 96% by UV; HRMS exact mass calculated for [M+H]⁺ ($\text{C}_{18}\text{H}_{26}\text{NO}_3$) requires m/z 304.1913, found 304.1918. **By-product 355**: Isolated yield: 9 mg, 25%, clear glass. $\nu_{\max}/\text{cm}^{-1}$ (neat) 2980, 2923, 2859, 1725, 1590); $^1\text{H NMR}$ (400 MHz, CDCl_3) δ 0.05 (s, 6H), 0.93 (s, 9H), 1.55 (s, 9H), 1.70-1.77 (m, 2H), 1.82-1.92 (m, 2H), 3.79 (dt, $J = 10.9, 3.8$ Hz, 2H), 3.91 (td, $J = 11.0, 2.3$ Hz, 2H), 6.20 (d, $J = 16.4$ Hz, 1H), 6.43 (d, $J = 16.4$ Hz, 1H), 6.51 (br. s., 1H), 7.32-7.38 (m, 4H); $^{13}\text{C NMR}$ (101 MHz, CDCl_3) δ -2.0, 18.4, 26.0, 28.3, 38.4, 63.8, 70.9, 118.6, 127.0, 127.3, 131.7, 134.8, 137.9, 152.6; LCMS (Method B): (M-H)⁻ 432, Rt 1.71 min, 100% by UV; HRMS exact mass calculated for [M+H]⁺ ($\text{C}_{24}\text{H}_{40}\text{NO}_4\text{Si}$) requires m/z 434.2721, found 434.2726.

***Tert*-butyl((1-cyclopropylprop-2-yn-1-yl)oxy)dimethylsilane, 331**

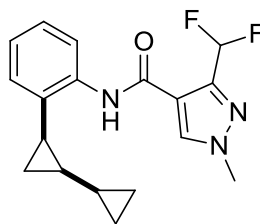


Prepared following the general procedure A (scale: step i) cyclopropanecarbaldehyde, 300 mg; step ii) 1-cyclopropylprop-2-yn-1-ol (portion of crude product from step i), 250 mg). Isolated yield: 269 mg, 44% (from aldehyde), clear oil. $\nu_{\max}/\text{cm}^{-1}$ (neat) 2954, 2926, 2855; $^1\text{H NMR}$ (400 MHz, CDCl_3) δ 0.14 (s, 3H), 0.16 (s, 3H), 0.38-0.55 (m, 4H), 0.93 (s, 9H), 1.15-1.26 (m, 1H), 2.39 (d, $J = 2.0$ Hz, 1H), 4.19 (dd, $J = 5.8, 2.0$ Hz, 1H); $^{13}\text{C NMR}$ (101 MHz, CDCl_3) δ -4.9, -4.5, 1.7, 2.6, 17.7, 18.3, 25.8, 65.2, 71.7, 84.4; HRMS exact mass calculated for [M+H]⁺ ($\text{C}_{12}\text{H}_{23}\text{OSi}$) requires m/z 211.1513, found 211.1510.

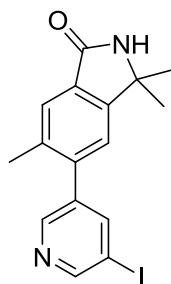
***Tert*-butyl (2-([1,1'-bi(cyclopropan)]-2-yl)phenyl)carbamate, 333**



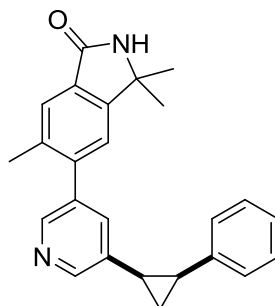
Prepared following the general procedure D (scale: *tert*-butyl((1-cyclopropylprop-2-yn-1-yl)oxy)dimethylsilane, 100 mg) (purified by reverse phase on C₁₈-silica using a 75-95% 10mM aqueous ammonium bicarbonate solution:acetonitrile with 0.1% ammonia gradient). Overall yield 6 mg, 22% (1.6:1 *cis:trans*); Diastereomeric ratio was calculated by comparing ¹H NMR integrals of the following peaks: *cis* - 1.10 (td, *J* = 8.6, 5.1 Hz, 1H), *trans* - 0.51-0.63 (m, 2H); **334a**: Isolated yield: 3 mg, 11%, clear glass; $\nu_{\max}/\text{cm}^{-1}$ (neat) 3432, 2970, 1731, 1587; ¹H NMR (400 MHz, CDCl₃) δ -0.01-0.09 (m, 1H), 0.14-0.21 (m, 1H), 0.21-0.28 (m, 1H), 0.28-0.35 (m, 1H), 0.38-0.47 (m, 1H), 0.76 (q, *J* = 5.6 Hz, 1H), 0.87 (qd, *J* = 8.3, 5.4 Hz, 1H), 1.10 (td, *J* = 8.6, 5.1 Hz, 1H), 1.57 (s, 9H), 1.87 (td, *J* = 8.3, 6.1 Hz, 1H), 6.99 (td, *J* = 7.5, 1.1 Hz, 1H), 7.14 (br. s., 1H), 7.21-7.27 (m, 2H), 8.04 (d, *J* = 8.3 Hz, 1H); ¹³C NMR (101 MHz, CDCl₃) δ 3.7, 4.9, 9.2, 9.6, 17.2, 21.7, 28.4, 80.2, 118.3, 122.3, 127.2, 127.3, 130.1, 138.6, 152.9; LCMS (Method B): [M-H]⁻ 272, Rt 1.44 min, 99% by UV; HRMS exact mass calculated for [M+H]⁺ (C₁₇H₂₄NO₂) requires *m/z* 274.1802, found, 274.1819; **334b**: Isolated yield: 3 mg, 11%, clear glass. $\nu_{\max}/\text{cm}^{-1}$ (neat) 2970, 2922, 2849, 1737; ¹H NMR (400 MHz, CDCl₃) δ 0.20-0.39 (m, 2H), 0.51-0.63 (m, 2H), 0.73-0.93 (m, 4H), 1.55 (br. s., 1H), 1.57 (s, 9H), 6.93-6.98 (m, 1H), 7.07 (br. s., 1H), 7.10 (d, *J* = 7.6 Hz, 1H), 7.17-7.24 (m, 1H), 8.01 (d, *J* = 8.3 Hz, 1H); ¹³C NMR (101 MHz, CDCl₃) δ 3.5, 3.8, 11.2, 13.2, 17.9, 22.7, 28.4, 80.3, 118.3, 122.4, 127.1, 128.4, 130.1, 138.2, 152.8; LCMS (Method B): [M-H]⁻ 272, Rt 1.44 & 1.46 min, 100% by UV; HRMS exact mass calculated for [M+H]⁺ (C₁₇H₂₄NO₂) requires *m/z* 274.1802, found 274.1800.

***N*-(2-([1,1'-Bi(cyclopropan)]-2-yl)phenyl)-3-(difluoromethyl)-1-methyl-1*H*-pyrazole-4-carboxamide, 318²⁶⁵**

To a suspension of 3-(difluoromethyl)-1-methyl-1*H*-pyrazole-4-carboxylic acid (25 mg, 0.15 mmol) in toluene (1 mL) was added dimethyl formamide (10 μ L) and thionyl chloride (214 μ L, 2.93 mmol) and the mixture was heated to 90 °C for 3 hours. The solvent was then removed *in vacuo* and the residue azeotroped with toluene (5 mL) and petroleum ether 40-60 (5 mL) to provide acid chloride (15 mg).²⁶⁶ To a solution of *cis-tert*-butyl (2-([1,1'-bi(cyclopropan)]-2-yl)phenyl)carbamate (20 mg, 0.07 mmol) in DCM (1 mL) was added trifluoroacetic acid (56 μ L, 0.73 mmol). The mixture was then stirred at room temperature for 2 hours. The volatiles were then removed *in vacuo* to yield trifluoroacetic acid ammonium salt (22 mg). Ammonium salt (22 mg, 0.07 mmol) and acid chloride (15 mg, 0.15 mmol) were then dissolved in DCM (1 mL) and triethylamine (51 μ L, 0.34 mmol) was added. The mixture was stirred at room temperature for 1.5 hours. Water (1 mL) was then added and the organic phase separated, dried over a hydrophobic frit and the solvent removed. The residue was then purified by column chromatography on silica using a 0-50% ethyl acetate/cyclohexane gradient. The appropriate fractions were combined and concentrated *in vacuo* to yield the title compound (12 mg, 50%) as a clear glass. $\nu_{\max}/\text{cm}^{-1}$ (neat) 3423, 2999, 2924, 1666; ^1H NMR (400 MHz, CDCl_3) δ 0.02-0.13 (m, 3H), 0.18-0.25 (m, 1H), 0.27-0.34 (m, 1H), 0.82 (q, $J = 5.4$ Hz, 1H), 0.93-1.02 (m, 1H), 1.08 (td, $J = 8.5, 4.8$ Hz, 1H), 1.95-2.02 (m, 1H), 4.00 (s, 3H), 6.93 (t, $J = 54.5$ Hz, 1H), 7.10 (td, $J = 7.5, 1.3$ Hz, 1H), 7.28 (d, $J = 7.5$ Hz, 2H), 8.04 (s, 1H), 8.30 (d, $J = 7.8$ Hz, 1H), 8.49 (br. s, 1H); ^{13}C NMR (101 MHz, CDCl_3) δ 3.6, 4.3, 9.0, 9.4, 17.4, 21.8, 39.6, 111.6 (t, $J = 233.5$ Hz), 117.6, 121.3, 124.1, 126.9, 129.3, 129.8, 135.5, 138.0, 142.6 (t, $J = 28.5$ Hz), 159.3; ^{19}F NMR (376 MHz, CDCl_3) δ -109.94 (dd, $J = 307.3, 53.8$ Hz, 1 F), -107.29 (dd, $J = 307.3, 53.8$ Hz, 1 F); HRMS exact mass calculated for $[\text{M}+\text{H}]^+$ ($\text{C}_{18}\text{H}_{20}\text{F}_2\text{N}_3\text{O}$) requires m/z 332.1569, found 332.1558.

5-(5-Iodopyridin-3-yl)-3,3,6-trimethylisoindolin-1-one, 337

To 5-(5-bromopyridin-3-yl)-3,3,6-trimethylisoindolin-1-one (50 mg, 0.15 mmol), sodium iodide (45.3 mg, 0.30 mmol), copper(I) iodide (1.438 mg, 7.5 μ mol) and *N,N'*-dimethylethylenediamine (1 mg, 0.015 mmol), was added 1,4-dioxane (0.5 mL). The mixture was then stirred at 80 °C for 16 hours. Water (1 mL) was then added to the reaction mixture and the product extracted with DCM (3 mL). The organic layer was then dried over a hydrophobic frit and the solvent removed *in vacuo*. The sample was loaded in DCM and purified by column chromatography on silica using a 0-50% ethyl acetate/cyclohexane gradient. The appropriate fractions were combined and concentrated *in vacuo* to give the title compound (39 mg, 0.10 mmol, 68% yield) as an off white solid. $\nu_{\max}/\text{cm}^{-1}$ (neat) 1696, 2963, 3021, 3173; $^1\text{H NMR}$ (400 MHz, CDCl_3) δ 1.59 (s, 6H), 2.35 (s, 3H), 6.86 (br. s., 1H), 7.22 (s, 1H), 7.76 (s, 1H), 8.04 (t, $J = 2.0$ Hz, 1H), 8.57 (d, $J = 2.0$ Hz, 1H), 8.89 (d, $J = 2.0$ Hz, 1H); $^{13}\text{C NMR}$ (101 MHz, CDCl_3) δ 20.5, 28.0, 58.9, 93.0, 122.2, 125.7, 130.9, 136.0, 138.8, 140.6, 144.4, 148.1, 151.0, 154.7, 169.0; LCMS (Method B): MH^+ 378.9, R_t 1.00 min, 79% by UV; HRMS exact mass calculated for $[\text{M}+\text{H}]^+$ ($\text{C}_{16}\text{H}_{16}\text{IN}_2\text{O}$) requires m/z 379.0307, found 379.0307.

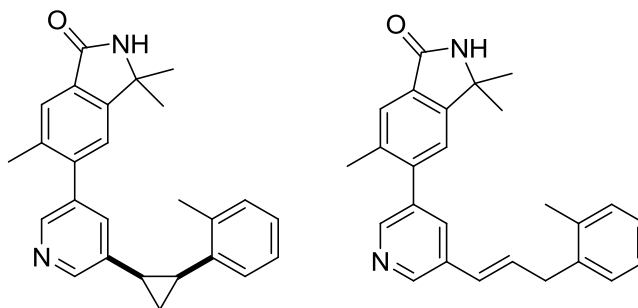
***Cis*-3,3,6-trimethyl-5-(5-(2-phenylcyclopropyl)pyridin-3-yl)isoindolin-1-one, 338**

Prepared following the general procedure E (scale: 4,4,5,5-tetramethyl-2-(2-phenylcyclopropyl)-1,3,2-dioxaborolane, 6.5 mg). Isolated yield: 1.6 mg, 16%, clear

CONFIDENTIAL – PROPERTY OF GSK – DO NOT COPY

oil. $\nu_{\max}/\text{cm}^{-1}$ (neat) 1695; $^1\text{H NMR}$ (400 MHz, CDCl_3) δ 1.49 (app. q, $J = 6.1$ Hz, 1H), 1.53 (s, 3H), 1.55 (s, 3H), 1.62 (td, $J = 8.6, 5.9$ Hz, 1H), 1.99 (s, 3H), 2.56 (td, $J = 8.8, 6.4$ Hz, 1H), 2.69 (td, $J = 9.0, 6.8$ Hz, 1H), 6.05 (s, 1H), 6.75 (s, 1H), 6.87 (s, 1H), 7.04 (dd, $J = 7.3, 0.7$ Hz, 2H), 7.14-7.21 (m, 3H), 7.64 (s, 1H), 8.28 (d, $J = 1.5$ Hz, 1H), 8.52 (d, $J = 1.5$ Hz, 1H); LCMS (Method B): MH^+ 369, Rt 1.08 min, 100% by UV; HRMS exact mass calculated for $[\text{M}+\text{H}]^+$ ($\text{C}_{25}\text{H}_{25}\text{N}_2\text{O}$) requires m/z 369.1967, found 369.1964. Not enough material remained after biological testing to obtain a ^{13}C NMR spectrum.

***Cis*-3,3,6-trimethyl-5-(5-(2-(*o*-tolyl)cyclopropyl)pyridin-3-yl)isoindolin-1-one, 340 and (*E*)-3,3,6-trimethyl-5-(5-(3-(*o*-tolyl)prop-1-en-1-yl)pyridin-3-yl)isoindolin-1-one, 350**

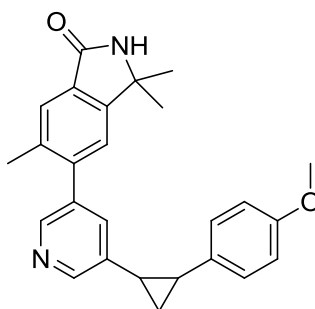


Prepared following the general procedure E (scale: 4,4,5,5-tetramethyl-2-(2-(*o*-tolyl)cyclopropyl)-1,3,2-dioxaborolane, 6.8 mg). **340**: Isolated yield 1.2 mg, 12%, clear oil. $\nu_{\max}/\text{cm}^{-1}$ (neat) 1696, 2964, 3021; $^1\text{H NMR}$ (400 MHz, CDCl_3) δ 1.50 (dt, $J = 9.0, 5.4$ Hz, 1H), 1.60 (s, 6H), 1.61-1.65 (m, 1H), 2.16 (dt, $J = 8.7, 5.3$ Hz, 1H), 2.31 (dt, $J = 8.8, 5.9$ Hz, 1H), 2.36 (s, 3H), 2.39 (s, 3H), 6.14 (s, 1H), 7.11-7.23 (m, 4H), 7.25 (s, 1H), 7.45 (t, $J = 2.0$ Hz, 1H), 7.77 (s, 1H), 8.46 (d, $J = 1.7$ Hz, 1H), 8.57 (d, $J = 2.0$ Hz, 1H); ^{13}C NMR (101 MHz, CDCl_3) δ 16.5, 19.9, 20.5, 23.2, 26.6, 28.1, 58.8, 122.2, 125.6, 125.7, 126.1, 126.6, 129.9, 130.5, 133.8, 133.8, 136.1, 137.0, 137.8, 138.5, 139.0, 142.0, 146.2, 146.2, 150.9, 168.8; LCMS (Method B): MH^+ 383, Rt 1.19 min, 100% by UV; HRMS exact mass calculated for $[\text{M}+\text{H}]^+$ ($\text{C}_{26}\text{H}_{27}\text{N}_2\text{O}$) requires m/z 383.2123, found 383.2119. **350**: Isolated yield 1.5 mg, 15%, clear oil. $\nu_{\max}/\text{cm}^{-1}$ (neat) 1693, 3208 (broad); $^1\text{H NMR}$ (400 MHz, CDCl_3) δ 1.58 (s, 6H), 2.33-2.34 (m, 3H), 2.37 (s, 3H), 3.62 (dd, $J = 6.50, 1.10$ Hz, 2H), 6.10 (s, 1H), 6.42 (dt, $J = 15.8, 1.10$ Hz, 1H), 6.55 (dt, $J = 16.0, 6.51$ Hz, 1H), 7.20-7.22 (m, 5H), 7.71 (s, 1H), 7.76 (s, 1H), 8.43-8.47 (m, 1H), 8.60-8.64 (m, 1H); ^{13}C NMR (101 MHz, CDCl_3) δ 19.4,

CONFIDENTIAL – PROPERTY OF GSK – DO NOT COPY

20.5, 28.1, 37.0, 58.8, 122.2, 125.0* 125.7, 126.3, 126.4, 126.8, 126.9, 129.4, 130.4, 130.6, 130.8* 133.4,* 136.1, 136.4, 137.2, 145.4,* 146.6,* 150.9, 168.8, *Peak not observed in 1D ¹³C spectrum, coupling detected to this chemical shift in HMBC; LCMS (Method B): MH+ 383, Rt 1.22 min, 98% by UV; HRMS exact mass calculated for [M+H]⁺ (C₂₆H₂₇N₂O) requires m/z 383.2123, found 383.2120.

***Cis*-5-(5-(2-(4-methoxyphenyl)cyclopropyl)pyridin-3-yl)-3,3,6-trimethylisoindolin-1-one, 342 & *trans*-5-(5-(2-(4-methoxyphenyl)cyclopropyl)pyridin-3-yl)-3,3,6-trimethylisoindolin-1-one, 343**

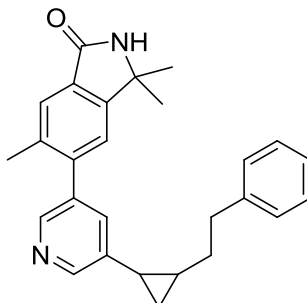


Prepared following the general procedure E (scale: 2-(2-(4-methoxyphenyl)cyclopropyl)-4,4,5,5-tetramethyl-1,3,2-dioxaborolane, 14.5 mg). **319** (*Cis*): Isolated yield 5.3 mg, 25%, clear oil. $\nu_{\max}/\text{cm}^{-1}$ (neat) 1695, 2972, 3211 (broad); ¹H NMR (400 MHz, CDCl₃) δ 1.40 (q, $J = 6.1$ Hz, 1H), 1.53 (s, 3H), 1.54 (s, 3H), 1.58 (td, $J = 8.6, 5.4$ Hz, 1H), 2.01 (s, 3H), 2.49 (td, $J = 8.7, 6.2$ Hz, 1H), 2.62 (td, $J = 8.8, 6.8$ Hz, 1H), 3.75 (s, 3H), 6.21 (s, 1H), 6.70-6.77 (m, 2H), 6.80 (s, 1H), 6.82 (t, $J = 2.0$ Hz, 1H), 6.96 (d, $J = 8.3$ Hz, 2H), 7.65 (s, 1H), 8.28 (d, $J = 2.2$ Hz, 1H), 8.49 (d, $J = 2.2$ Hz, 1H); ¹³C NMR (101 MHz, CDCl₃) δ 11.3, 20.1, 20.7, 24.1, 27.8, 30.8, 55.1, 58.7, 113.6, 119.6, 122.1, 125.3, 130.0, 130.7, 134.5, 135.2, 136.0, 142.4, 146.5, 149.5, 150.6, 158.1, 169.0, 179.3; LCMS (Method B): MH+ 399, Rt 1.08 min, 100% by UV; HRMS exact mass calculated for [M+H]⁺ (C₂₆H₂₇N₂O₂) requires m/z 399.2072, found 399.2074. **320** (*trans*): Isolated yield 2.4 mg, 11%, clear oil. $\nu_{\max}/\text{cm}^{-1}$ (neat) 1695, 2971, 3235 (broad); ¹H NMR (400 MHz, CDCl₃) δ 1.45-1.56 (m, 2H), 1.59 (s, 6H), 2.18 (dt, $J = 8.3, 5.9$ Hz, 1H), 2.25 (dt, $J = 8.7, 5.7$ Hz, 1H), 2.35 (s, 3H), 3.83 (s, 3H), 6.25 (br. s., 1H), 6.89 (d, $J = 8.7$ Hz, 2H), 7.13 (d, $J = 8.7$ Hz, 2H), 7.23 (s, 1H), 7.38 (t, $J = 2.0$ Hz, 1H), 7.76 (s, 1H), 8.44 (d, $J = 2.0$ Hz, 1H), 8.51 (d, $J = 2.0$ Hz, 1H); ¹³C NMR (101 MHz, CDCl₃) δ 17.8, 20.6, 24.7, 27.5, 28.1, 55.4, 58.8, 114.0, 122.2, 125.6, 127.0, 128.4, 128.5, 130.3, 133.3, 133.4, 136.1, 142.3, 146.7, 146.8, 150.9, 158.2,

CONFIDENTIAL – PROPERTY OF GSK – DO NOT COPY

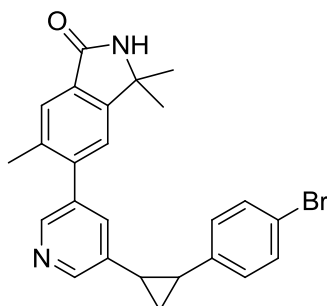
169.0; LCMS (Method B): MH⁺ 399, Rt 1.11 min, 92% by UV; HRMS exact mass calculated for [M+H]⁺ (C₂₆H₂₇N₂O₂) requires m/z 399.2072, found 399.2067.

Cis-3,3,6-trimethyl-5-(5-(2-phenethylcyclopropyl)pyridin-3-yl)isoindolin-1-one, 344 & **trans-3,3,6-trimethyl-5-(5-(2-phenethylcyclopropyl)pyridin-3-yl)isoindolin-1-one, 345**



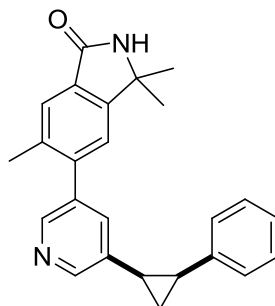
Prepared following the general procedure E (scale: 4,4,5,5-tetramethyl-2-(2-phenethylcyclopropyl)-1,3,2-dioxaborolane, 7.2 mg). **344 (cis)**: Isolated yield 1.6 mg, 15%, clear oil. $\nu_{\max}/\text{cm}^{-1}$ (neat) 1695, 2921, 2973, 3211; ¹H NMR (400 MHz, CDCl₃) δ 0.78 (q, $J = 5.6$ Hz, 1H), 1.14 (td, $J = 8.3, 5.1$ Hz, 1H), 1.27-1.29 (m, 1H), 1.35-1.54 (m, 2H), 1.58 (s, 6H), 2.21 (td, $J = 8.6, 6.1$ Hz, 1H), 2.31 (s, 3H), 2.54-2.69 (m, 2H), 6.15 (s, 1H), 7.01-7.06 (m, 2H), 7.13-7.19 (m, 1H), 7.20-7.26 (m, 3H), 7.44 (t, $J = 2.0$ Hz, 1H), 7.75 (s, 1H), 8.44 (d, $J = 2.0$ Hz, 1H), 8.56 (d, $J = 2.0$ Hz, 1H); ¹³C NMR (101 MHz, CDCl₃) δ 9.9, 18.6, 19.2, 20.5, 28.0, 30.7, 35.5, 58.8, 110.0, 122.2, 125.6, 125.8, 128.3, 128.5, 130.4, 136.1, 136.3, 136.8, 141.8, 142.2, 146.3, 149.2, 150.9, 168.9; LCMS (Method B): MH⁺ 397, Rt 1.22 min, 100% by UV; HRMS exact mass calculated for [M+H]⁺ (C₂₇H₂₉N₂O) requires m/z 397.2280, found 397.2277. **345 (trans)**: Isolated yield 2.5 mg, 24%, clear oil. $\nu_{\max}/\text{cm}^{-1}$ (neat) 1695, 2933, 2973, 3211 (broad); ¹H NMR (400 MHz, CDCl₃) δ 0.92 (dt, $J = 8.6, 5.6$ Hz, 1H), 0.99 (dt, $J = 8.5, 4.9$ Hz, 1H), 1.10-1.19 (m, 1H), 1.59 (s, 6H), 1.68 (dt, $J = 9.0, 4.6$ Hz, 1H), 1.72-1.88 (m, 2H), 2.31 (s, 3H), 2.77-2.84 (m, 2H), 6.29 (br. s, 1H), 7.16-7.22 (m, 5H), 7.23-7.28 (m, 2H), 7.75 (s, 1H), 8.35-8.39 (m, 2H); ¹³C NMR (101 MHz, CDCl₃) δ 16.2, 20.5, 20.8, 23.7, 28.0, 35.6, 36.1, 58.8, 122.2, 125.5, 125.9, 128.3, 128.5, 130.2, 132.8, 136.5,* 136.1, 139.0,* 141.9, 142.5, 146.4, 147.1, 150.8, 169.0, *Peak not observed in ID ¹³C spectrum, coupling detected to this chemical shift in HMBC; LCMS (Method B): MH⁺ 397, Rt 1.24 min, 93% by UV; HRMS exact mass calculated for [M+H]⁺ (C₂₇H₂₉N₂O) requires m/z 397.2280, found 397.2278.

Cis-5-(5-(2-(4-bromophenyl)cyclopropyl)pyridin-3-yl)-3,3,6-trimethylisoindolin-1-one, **346** & *trans*-5-(5-(2-(4-bromophenyl)cyclopropyl)pyridin-3-yl)-3,3,6-trimethylisoindolin-1-one, **347**



Prepared following the general procedure E (scale: 2-(2-(4-bromophenyl)cyclopropyl)-4,4,5,5-tetramethyl-1,3,2-dioxaborolane, 8.5 mg). **346** (*cis*): Isolated yield 3.9 mg, 33%, clear oil. $\nu_{\max}/\text{cm}^{-1}$ (neat) 1693, 2973, 3212 (broad); ^1H NMR (400 MHz, CDCl_3) δ 1.46 (q, $J = 6.1$ Hz, 1H), 1.56 (s, 3H), 1.57 (s, 3H), 1.62 (td, $J = 8.7, 5.9$ Hz, 1H), 2.02 (s, 3H), 2.53-2.64 (m, 2H), 6.30 (s, 1H), 6.82 (s, 1H), 6.87 (t, $J = 1.8$ Hz, 1H), 6.90 (d, $J = 8.3$ Hz, 2H), 7.30 (d, $J = 8.6$ Hz, 2H), 7.67 (s, 1H), 8.25-8.32 (m, 1H), 8.46-8.53 (m, 1H); ^{13}C NMR (101 MHz, CDCl_3) δ 11.0, 20.0, 21.2, 24.1, 28.0, 28.0, 58.8, 120.1, 122.0, 125.4, 130.2, 131.2, 131.2, 133.7, 135.6, 136.0, 136.0, 136.3, 142.1, 146.8, 149.6, 150.7, 169.4*, *Peak not observed in 1D ^{13}C spectrum, coupling detected to this chemical shift in HMBC; LCMS (Method B): MH+ 447, Rt 1.16 min, 92% by UV; HRMS exact mass calculated for $[\text{M}+\text{H}]^+$ ($\text{C}_{25}\text{H}_{24}\text{BrN}_2\text{O}$) requires m/z 447.1072, found 447.1071. **347** (*trans*): Isolated yield 1.8 mg, 15%, clear oil. $\nu_{\max}/\text{cm}^{-1}$ (neat) 1693, 3218 (broad); ^1H NMR (400 MHz, CDCl_3) δ 1.56 (app. t, $J = 7.3$ Hz, 2H), 1.59 (s, 6H), 2.21-2.27 (m, 2H), 2.35 (s, 3H), 6.13 (br. s, 1H), 7.04-7.09 (m, 2H), 7.23 (s, 1H), 7.38 (t, $J = 2.1$ Hz, 1H), 7.43-7.48 (m, 2H), 7.76 (s, 1H), 8.45 (d, $J = 2.2$ Hz, 1H), 8.51 (d, $J = 2.2$ Hz, 1H); ^{13}C NMR (101 MHz, CDCl_3) δ 18.1, 20.5, 25.2, 27.6, 28.1, 58.8, 119.9, 122.3, 125.7, 127.6, 130.5, 131.6, 133.7, 136.1, 136.9, 137.5, 140.4, 140.6, 142.0, 146.5, 150.9, 168.8; LCMS (Method B): MH+ 447, Rt 1.24 min, 100% by UV; HRMS exact mass calculated for $[\text{M}+\text{H}]^+$ ($\text{C}_{25}\text{H}_{24}\text{BrN}_2\text{O}$) requires m/z 447.1072, found 447.1067.

(+)-Cis-3,3,6-trimethyl-5-(5-(2-phenylcyclopropyl)pyridin-3-yl)isoindolin-1-one,
348



Prepared following the general procedure E (scale: 4,4,5,5-tetramethyl-2-(2-phenylcyclopropyl)-1,3,2-dioxaborolane, 1.9 mg). Isolated yield 0.6 mg, 21%, clear oil. $\nu_{\max}/\text{cm}^{-1}$ (neat) 1694, 2975, 3241 (broad); $^1\text{H NMR}$ (400 MHz, CDCl_3) δ 1.49 (q, $J = 6.1$ Hz, 1H), 1.53 (s, 3H), 1.55 (s, 3H), 1.62 (td, $J = 8.6, 5.6$ Hz, 1H), 1.99 (s, 3H), 2.56 (td, $J = 8.7, 6.2$ Hz, 1H), 2.69 (td, $J = 9.0, 6.8$ Hz, 1H), 6.06 (s, 1H), 6.75 (s, 1H), 6.87 (s, 1H), 7.02-7.06 (m, 2H), 7.14-7.21 (m, 3H), 7.64 (s, 1H), 8.28 (d, $J = 1.5$ Hz, 1H), 8.51 (d, $J = 1.5$ Hz, 1H); LCMS (Method A): MH^+ 369, Rt 1.08 min, 92% by UV; HRMS exact mass calculated for $[\text{M}+\text{H}]^+$ ($\text{C}_{25}\text{H}_{25}\text{N}_2\text{O}$) requires m/z 369.1967, found 369.1961. $[\alpha]_{\text{D}}^{25} = +34$ (c 0.5, CHCl_3) Not enough material remained after biological testing to obtain a ^{13}C NMR spectrum.

5.2.4 Supplementary Protocols

Computational modelling

Computational modelling was conducted by the author using Molecular Operating Environment 2016.¹⁰¹ Conformational searches were conducted using the built in conformational search tool using a LowModeMD method with the following parameters: Rejection limit: 100, Iteration limit: 10000, RMS gradient: 0.005, MM iteration limit: 500 RMS limit: 0.25, Energy window: 7. Strain energies were separated by stereo chains and chair conformations were enforced. The energy of the generated conformations were calculated in the AMBER10:EHT force field. The lowest energy conformations are shown in figures. Surfaces were generated with the built in surface tool to give a Van Der Waal's surface.

PI3K Alpha, Beta, Gamma and Delta Assays²⁴⁶

The assay readout exploits the specific and high affinity binding of PIP₃ to an isolated pleckstrin homogy (PH) domain in the generation of a signal. Briefly, the PIP₃ product is detected by displacement of biotinylated PIP₃ from an energy transfer complex consisting of Europium (Eu)-labelled anti-GST monoclonal antibody, a GST-tagged PH domain, biotin-PIP₃ and Streptavidin-APC. Excitation of Eu leads to a transfer of energy to APC and a sensitised fluorescence emission at 665 nm. PIP₃ formed by PI3kinase activity competes for the binding site on the PH domain, resulting in a loss of energy transfer and a decrease in signal.

Assay protocols:

Solid compounds are typically plated with 0.1 µL of 100% DMSO in all wells (except column 6 and 18) of a 384-well, v bottom, low volume Greiner plate. The compounds are serially diluted (4-fold in 100% DMSO) across the plate from column 1 to column 12 and column 13 to column 24, leaving columns 6 and 18 containing only DMSO to yield 11 different concentrations for each test compounds.

The assays are run using specific PI3kinase kits from Millipore (Cat# 33-047).²⁶⁷

The assay kits consist of the following:

CONFIDENTIAL – PROPERTY OF GSK – DO NOT COPY

- 4 x PI3K reaction buffer (contains 200 mM hepes pH7, 600 mM NaCl, 40 mM MgCl₂, <1% cholate (w/v), <1% chaps (w/v), 0.05% sodium azide (w/v))
- PIP₂ (1 mM)
- 3x Biotin PIP₃ (50 μM)
- Detection Mix C (contains 267 mM KF)
- Detection Mix A (contains 60 μg/mL Steptavidin-APC)
- Detection Mix B (contains 36 μg/mL Europium-anti-GST (anti-GST-K) and 90 μg/mL GST-SRP1-PH-domain and 1 mM DTT)
- Stop solution (contains 150 mM EDTA)

3 μL of reaction buffer (contains 1 mM DTT) is manually added to column 18 only for 100% inhibition control (no activity).

3 μL of 2 x enzyme solution is manually added to all wells except column 18. Pre-incubate with compound for 15 min.

3 μL of 2 x substrate solution is manually added to all wells (column 6 represents 0% inhibition control).

The plate is left for 1 h (covered from light). In case of the gamma assay only a 50 min incubation is required.

3 μL of the stop/detection solution is manually added to all wells.

The plate is left for 1 h (covered from light).

The assay is read on a microplate reader and the ratio data is utilised to calculate 11 point curves.

NB. The substrate solution (concentrations) differ with each isoform:

Alpha: 2 x substrate solution containing 500 μM ATP, 16 μM PIP₂ and 0.03 μM 3x biotin-PIP₃

Beta: 2 x substrate solution containing 800 μM ATP, 16 μM PIP₂ and 0.03 μM 3x biotin-PIP₃

Delta: 2 x substrate solution containing 160 μM ATP, 10 μM PIP₂ and 0.03 μM 3x biotin-PIP₃

Gamma: 2 x substrate solution containing 30 μM ATP, 16 μM PIP₂ and 0.03 μM 3x biotin-PIP₃

Analysis Method:

Data processed through the XC₅₀ 4-parameter logistic curve fit algorithm in Activity Base.

CONFIDENTIAL – PROPERTY OF GSK – DO NOT COPY

Normalise to% inhibition between the high and low controls (0% and 100% inhibition respectively).

Primary Module fits: Slope, Min and Max asymptotes varies

Secondary Module fits: (i) Fix Min asymptote, (ii) Fix Max asymptote, (iii) Fix Min and Max asymptotes

Curve Fit AC: pXC_{50} 95% CL ratio > 10

$-20 < \text{Min asymptote} < 20$

$80 < \text{Max asymptote} < 120$

CLND and CAD Kinetic Solubility Assay²⁶⁸

A 5 μL of 10 mM DMSO stock solution is diluted to 100 μL with pH 7.4 phosphate buffered saline, allowed to equilibrate for 1 h at room temperature and then filtered through Millipore Multiscreen HTS-PCF filter plates (MSSL BPC). The filtrate is quantified by suitably calibrated Chemi-Luminescent Nitrogen Detection²⁶⁹ or Charged Aerosol Detection.²⁷⁰ The standard error of this kinetic assay is 30 μM , the upper limit of the solubility is 500 μM when working from 10 mM DMSO stock solution. This is a very rapid method of assessing approximate solubility but is likely to overestimate a compound's true solubility, particularly if that compound is highly crystalline and/or has a high melting point; it also takes no account of the compound's thermodynamic solubility or dissolution rate. This technique can detect solubilities in the range 1 μM -500 μM .

ChromLogD Assay^{44,268,271}

The Chromatographic Hydrophobicity Index (CHI) values are measured using reversed phase HPLC column (50 x 2 mm 3 μM Gemini NX C18, Phenomenex, UK) with fast acetonitrile gradient at starting mobile phase of aqueous ammonium acetate solution adjusted to pH 7.4. The conditions for the gradient elution were initially 0% B, increasing linearly to 100% B over 1.3 min, remaining at 100% B for 0.3 min then decreasing to 0% B over 0.4 min. The flow rate was 0.7 mL/min. CHI values were derived directly from retention time by using a calibration line obtained for standard compounds. The CHI value approximates to the volume% organic concentration when the compound elutes. CHI is linearly transformed into ChromLogD by least-square

CONFIDENTIAL – PROPERTY OF GSK – DO NOT COPY

fitting of experimental CHI values to calculated LogP values for over 20 thousand research compounds using the following formula: $\text{ChromLogD} = 0.0857 \text{ CHI} - 2.00$.

Artificial Membrane Permeability Assay^{268,272}

The donor cell contains 2.5 μL of 10 mM sample solution in pH 7.4 phosphate buffer. To enhance solubility, 0.5% hydroxypropylcyclodextrin (encapsin) is added to the buffer. The artificial membrane is prepared from 1.8% phosphatidylcholine and 1% cholesterol in decane solution. The sample concentration in both the donor and acceptor compartments is determined by LC-UV after 3 h incubation at room temperature. The permeability ($\log P_{\text{app}}$) measuring how fast molecules pass through the black lipid membrane is expressed in nm s^{-1} . The average standard error of the assay is around 30 nm s^{-1} but can be higher in the low permeability range. This assay is different from the commercially available PAMPA assay offered regarding the thickness of the membrane, which in the case of the GSK assay is much thinner and can be considered as phospholipid bi-layer formed in the pores of the filter.

pK_a determination²⁶⁸

Sirius T3 (Sirius Analytical Inc, UK) instrument is used for pK_a determination of compounds. The pK_a determination is based on acid-base titration and the protonation/deprotonation of the molecule is measured either by UV spectroscopy or potentiometrically. The pK_a value is calculated from the pH where the 50% of the protonated and unprotonated form of the molecules are present. The UV-metric method provides pK_a results for samples with chromophores whose UV absorbance changes as a function of pH. It typically requires 5 μL of a 10 mM solution of the samples and the UV absorbance is monitored over 54 pH values in a buffered solution in about 5 min. When the ionization centre is far from the UV chromophore pH-metric method based on potentiometric acid-base titration is used. The pH of each point in the titration curve is calculated using equations that contain pK_a, and the calculated points are fitted to the measured curve by manipulating the pK_a. The pK_a that provides the best fit is taken to be the measured pK_a. When the compound precipitates at some point during the pH titration, a co-solvent method using methanol is applied using various concentration of co-solvent. The pK_a in water is calculated using the Yasuda-Shedlovsky extrapolation method.

HSA and AGP binding assay²⁷³

Chemically bonded Human Serum Albumin (HSA) and Alpha-1-acidglycoprotein (AGP) HPLC stationary phases (Chiral Technologies, France) are used for measuring compounds' binding to plasma proteins, applying linear gradient elution up to 30% iso-propanol. The run time is 6 minutes including the re-equilibration of the stationary phases with the 50 mM pH 7.4 ammonium acetate buffer. The gradient retention times are standardised using a calibration set of mixtures as described in the reference. The average standard error of the assay depends on the binding strength and kinetic of the compounds. It ranges from $\pm 5\%$ in the medium binding range which reduces to 0.1% at binding above 99% with fast kinetics.

References

1. Halpin, D. M. G.; Tashkin, D. P. *COPD*, **2009**, *6*, 211-225.
2. Adeloje, D.; Chua, S.; Lee, C.; Basquill, C.; Papan, A.; Theodoratou, E.; Nair, H.; Gasevic, D.; Sridhar, D.; Campbell, H.; Chan, K. Y.; Sheikh, A.; Rudan, I.; Global Health Epidemiology Reference, G. *J. Glob. Health*, **2015**, *5*, 020415.
3. *WHO Factsheet 310*; 2014, 2014.
4. Decramer, M.; Janssens, W.; Miravittles, M. *Lancet*, **2012**, *379*, 1341-1351.
5. Tashkin, D. P.; Taube, C. *Am. J. Respir. Crit. Care Med.*, **2017**, *196*, 402-404.
6. Lipson, D. A.; Barnacle, H.; Birk, R.; Brealey, N.; Locantore, N.; Lomas, D. A.; Ludwig-Sengpiel, A.; Mohindra, R.; Tabberer, M.; Zhu, C.-Q.; Pascoe, S. J. *Am. J. Respir. Crit. Care Med.*, **2017**, *196*, 438-446.
7. Rhen, T.; Cidlowski, J. A. *New Engl. J. Med.*, **2005**, *353*, 1711-1723.
8. McKeage, K. *Drugs*, **2014**, *74*, 1509-1522.
9. Jarvis, S.; Ind, P. W.; Shiner, R. J. *Age Ageing*, **2007**, *36*, 213-218.
10. Grant, A. C.; Walker, R.; Hamilton, M.; Garrill, K. *J. Aerosol Med. Pulm. Drug Deliv.*, **2015**, *28*, 474-485.
11. Fabbri, L. M.; Piattella, M.; Caramori, G.; Ciaccia, A. *Drugs*, **1996**, 20-28.
12. Bamborough, P.; Drewry, D.; Harper, G.; Smith, G. K.; Schneider, K. *J. Med. Chem.*, **2008**, *51*, 7898-7914.
13. Manning, G.; Whyte, D. B.; Martinez, R.; Hunter, T.; Sudarsanam, S. *Science*, **2002**, *298*, 1912-1916, 1933.
14. Heath, C. M.; Stahl, P. D.; Barbieri, M. A. *Histol. Histopathol.*, **2003**, *18*, 989-98.
15. Sun, Y.; Thapa, N.; Hedman, A. C.; Anderson, R. A. *Bioessays*, **2013**, *35*, 513-522.
16. Williams, R.; Berndt, A.; Miller, S.; Hon, W. C.; Zhang, X. *Biochem. Soc. Trans*, **2009**, *37*, 615-626.
17. Ito, K.; Caramori, G.; Adcock, I. M. *J. Pharmacol. Exp. Ther.*, **2007**, *321*, 1-8.
18. Finan, P. M.; Thomas, M. J. *Biochem. Soc. Trans*, **2004**, *32*, 378-382.
19. Walker, C.; Thomas, M.; Edwards, M. J. *Drug Discov. Today Dis. Mech.*, **2006**, *3*, 63-69.

20. Okkenhaug, K.; Bilancio, A.; Farjot, G.; Priddle, H.; Sancho, S.; Peskett, E.; Pearce, W.; Meek, S. E.; Salpekar, A.; Waterfield, M. D.; Smith, A. J. H.; Vanhaesebroeck, B. *Science*, **2002**, 297, 1031-1034.
21. Hirsch, E.; Katanaev, V. L.; Garlanda, C.; Azzolino, O.; Pirola, L.; Silengo, L.; Sozzani, S.; Mantovani, A.; Altruda, F.; Wymann, M. P. *Science*, **2000**, 287, 1049-1053.
22. Lee, K. S.; Lee, H. K.; Hayflick, J. S.; Lee, Y. C.; Puri, K. D. *FASEB J.*, **2006**, 20, 455-465.
23. To, Y.; Ito, K.; Kizawa, Y.; Failla, M.; Ito, M.; Kusama, T.; Elliott, W. M.; Hogg, J. C.; Adcock, I. M.; Barnes, P. J. *Am. J. Respir. Crit. Care Med.*, **2010**, 182, 897-904.
24. Ali, K.; Bilancio, A.; Thomas, M.; Pearce, W.; Gilfillan, A. M.; Tkaczyk, C.; Kuehn, N.; Gray, A.; Giddings, J.; Peskett, E.; Fox, R.; Bruce, I.; Walker, C.; Sawyer, C.; Okkenhaug, K.; Finan, P.; Vanhaesebroeck, B. *Nature*, **2004**, 431, 1007-1011.
25. Puri, K. D.; Doggett, T. A.; Douangpanya, J.; Hou, Y.; Tino, W. T.; Wilson, T.; Graf, T.; Clayton, E.; Turner, M.; Hayflick, J. S.; Diacovo, T. G. *Blood*, **2004**, 103, 3448-3456.
26. Hoenderdos, K.; Condliffe, A. *Am. J. Respir. Cell Mol. Biol.*, **2013**, 48, 531-539.
27. Quint, J. K.; Wedzicha, J. A. *J. Allergy Clin. Immunol.*, **2007**, 119, 1065-1071.
28. Angulo, I.; Vadas, O.; Garçon, F.; Banham-Hall, E.; Plagnol, V.; Leahy, T. R.; Baxendale, H.; Coulter, T.; Curtis, J.; Wu, C.; Blake-Palmer, K.; Perisic, O.; Smyth, D.; Maes, M.; Fiddler, C.; Juss, J.; Cilliers, D.; Markelj, G.; Chandra, A.; Farmer, G.; Kielkowska, A.; Clark, J.; Kracker, S.; Debré, M.; Picard, C.; Pellier, I.; Jabado, N.; Morris, J. A.; Barcenas-Morales, G.; Fischer, A.; Stephens, L.; Hawkins, P.; Barrett, J. C.; Abinun, M.; Clatworthy, M.; Durandy, A.; Doffinger, R.; Chilvers, E. R.; Cant, A. J.; Kumararatne, D.; Okkenhaug, K.; Williams, R. L.; Condliffe, A.; Nejentsev, S. *Science*, **2013**, 342, 866-871.
29. Coulter, T. I.; Chandra, A.; Bacon, C. M.; Babar, J.; Curtis, J.; Sreaton, N.; Goodlad, J. R.; Farmer, G.; Steele, C. L.; Leahy, T. R.; Doffinger, R.; Baxendale, H.; Bernatoniene, J.; Edgar, J. D. M.; Longhurst, H. J.; Ehl, S.; Speckmann, C.; Grimbacher, B.; Sediva, A.; Milota, T.; Faust, S. N.; Williams, A. P.; Hayman, G.; Kucuk, Z. Y.; Hague, R.; French, P.; Brooker, R.; Forsyth, P.; Herriot, R.; Cancrini, C.; Palma, P.; Ariganello, P.; Conlon, N.; Feighery, C.; Gavin, P. J.; Jones, A.; Imai, K.; Ibrahim, M. A. A.; Markelj, G.; Abinun, M.; Rieux-Laucat, F.; Latour, S.; Pellier, I.; Fischer, A.; Touzot, F.; Casanova, J.-L.; Durandy, A.; Burns, S. O.; Savic, S.; Kumararatne, D. S.; Moshous, D.; Kracker, S.; Vanhaesebroeck, B.; Okkenhaug, K.; Picard, C.; Nejentsev, S.; Condliffe, A. M.; Cant, A. J. *J. Allergy Clin. Immunol.*, **2017**, 139, 597-606.

30. Arcaro, A.; Wymann, M. P. *Biochem. J.*, **1993**, 296 (Pt 2), 297-301.
31. Wipf, P.; Halter, R. J. *Org. Biomol. Chem.*, **2005**, 3, 2053-2061.
32. Liu, Y.; Shreder, K. R.; Gai, W.; Corral, S.; Ferris, D. K.; Rosenblum, J. S. *Chem. Biol.*, **2005**, 12, 99-107.
33. Sadhu, C.; Masinovsky, B.; Dick, K.; Sowell, C. G.; Staunton, D. E. *J. Immunol.*, **2003**, 170, 2647-2654.
34. Furman, R. R.; Sharman, J. P.; Coutre, S. E.; Cheson, B. D.; Pagel, J. M.; Hillmen, P.; Barrientos, J. C.; Zelenetz, A. D.; Kipps, T. J.; Flinn, I.; Ghia, P.; Eradat, H.; Ervin, T.; Lamanna, N.; Coiffier, B.; Pettitt, A. R.; Ma, S.; Stilgenbauer, S.; Cramer, P.; Aiello, M.; Johnson, D. M.; Miller, L. L.; Li, D.; Jahn, T. M.; Dansey, R. D.; Hallek, M.; O'Brien, S. M. *New Engl. J. Med.*, **2014**, 370, 997-1007.
35. Somoza, J. R.; Koditek, D.; Villaseñor, A. G.; Novikov, N.; Wong, M. H.; Liclican, A.; Xing, W.; Lagpacan, L.; Wang, R.; Schultz, B. E.; Papalia, G. A.; Samuel, D.; Lad, L.; McGrath, M. E. *J. Biol. Chem.*, **2015**, 290, 8439-8446.
36. Deng, C.; Lipstein, M. R.; Scotto, L.; Jirau Serrano, X. O.; Mangone, M. A.; Li, S.; Vendome, J.; Hao, Y.; Xu, X.; Deng, S.-X.; Realubit, R. B.; Tatonetti, N. P.; Karan, C.; Lentzsch, S.; Fruman, D. A.; Honig, B.; Landry, D. W.; O'Connor, O. A. *Blood*, **2016**, 129, 88-99.
37. Vakkalanka, S.; Viswanadha, S.; Boise, L. H.; Sportelli, P.; Miskin, H.; Lonial, S. *Blood*, **2012**, 120, 5018-5018.
38. Down, K.; Amour, A.; Baldwin, I. R.; Cooper, A. W. J.; Deakin, A. M.; Felton, L. M.; Guntrip, S. B.; Hardy, C.; Harrison, Z. A.; Jones, K. L.; Jones, P.; Keeling, S. E.; Le, J.; Livia, S.; Lucas, F.; Lunniss, C. J.; Parr, N. J.; Robinson, E.; Rowland, P.; Smith, S.; Thomas, D. A.; Vitulli, G.; Washio, Y.; Hamblin, J. N. *J. Med. Chem.*, **2015**, 58, 7381-7399.
39. Bieth, B.; Burkhart, C.; Christ, A.; De Buck, S.; Kalis, C.; Lindgren, S. Use of Inhibitors of the Activity or Function of PI3K for the Treatment of Primary Sjogren's Syndrome. WO2017118965A1, **2017**.
40. Cooke, N. G.; Fernandes Gomes Dos Santos, P.; Graveleau, N.; Hebach, C.; Hoegenauer, K.; Hollingworth, G.; Smith, A. B.; Soldermann, N.; Stowasser, F.; Strang, R.; Tuffilli, N.; Von Matt, A.; Wolf, R.; Zecri, F. Tetrahydropyrido[4,3-d]pyrimidine Derivatives as PI3K Inhibitors and their Preparation and Use for the Treatment of PI3K-Mediated Diseases. WO2012004299A1, **2012**.
41. Hoegenauer, K.; Soldermann, N.; Zécric, F.; Strang, R. S.; Graveleau, N.; Wolf, R. M.; Cooke, N. G.; Smith, A. B.; Hollingworth, G. J.; Blanz, J.; Gutmann, S.; Rummel, G.; Littlewood-Evans, A.; Burkhart, C. *ACS Med. Chem. Lett.*, **2017**, 8, 975-980.

42. Allen, R. A.; Brookings, D. C.; Powell, M. J.; Delgado, J.; Shuttleworth, L. K.; Merriman, M.; Fahy, I. J.; Tewari, R.; Silva, J. P.; Healy, L. J.; Davies, G. C. G.; Twomey, B.; Cutler, R. M.; Kotian, A.; Crosby, A.; McCluskey, G.; Watt, G. F.; Payne, A. *J. Pharmacol. Exp. Ther.*, **2017**, *361*, 429-440.
43. Cushing, T. D.; Hao, X.; Shin, Y.; Andrews, K.; Brown, M.; Cardozo, M.; Chen, Y.; Duquette, J.; Fisher, B.; Gonzalez-Lopez de Turiso, F.; He, X.; Henne, K. R.; Hu, Y. L.; Hungate, R.; Johnson, M. G.; Kelly, R. C.; Lucas, B.; McCarter, J. D.; McGee, L. R.; Medina, J. C.; San Miguel, T.; Mohn, D.; Pattaropong, V.; Pettus, L. H.; Reichelt, A.; Rzasa, R. M.; Seganish, J.; Tasker, A. S.; Wahl, R. C.; Wannberg, S.; Whittington, D. A.; Whoriskey, J.; Yu, G.; Zalameda, L.; Zhang, D.; Metz, D. P. *J. Med. Chem.* **2015**, *58*, 480-511.
44. Young, R. J.; Green, D. V. S.; Luscombe, C. N.; Hill, A. P. *Drug Discov. Today*, **2011**, *16*, 822-830.
45. Bertrand, S.; Barton, N.; Baldwin, I., unpublished work, GlaxoSmithKline, **2015**
46. Mann, A., Conformational restriction and/or steric hindrance in medicinal chemistry Wermuth CG (Ed.). Academic Press, London, UK (2008). In *The Practice Of Medicinal Chemistry*, Wermuth CG (Ed.). Academic Press, London, UK2008.
47. Mallinson, J.; Collins, I. *Future Med. Chem.* **2012**, *4*, 1409-1438.
48. William, A. D.; Lee, A. C.-H.; Blanchard, S.; Poulsen, A.; Teo, E. L.; Nagaraj, H.; Tan, E.; Chen, D.; Williams, M.; Sun, E. T.; Goh, K. C.; Ong, W. C.; Goh, S. K.; Hart, S.; Jayaraman, R.; Pasha, M. K.; Ethirajulu, K.; Wood, J. M.; Dymock, B. W. *J. Med. Chem.* **2011**, *54*, 4638-4658.
49. Kiss, R.; Sayeski, P. P.; Keserü, G. M. *Expert Opin. Ther. Pat.*, **2010**, *20*, 471-495.
50. Stachel, S. J.; Coburn, C. A.; Sankaranarayanan, S.; Price, E. A.; Pietrak, B. L.; Huang, Q.; Lineberger, J.; Espeseth, A. S.; Jin, L.; Ellis, J.; Holloway, M. K.; Munshi, S.; Allison, T.; Hazuda, D.; Simon, A. J.; Graham, S. L.; Vacca, J. P. *J. Med. Chem.* **2006**, *49*, 6147-6150.
51. Johnson, T. W.; Richardson, P. F.; Bailey, S.; Brooun, A.; Burke, B. J.; Collins, M. R.; Cui, J. J.; Deal, J. G.; Deng, Y. L.; Dinh, D.; Engstrom, L. D.; He, M.; Hoffman, J.; Hoffman, R. L.; Huang, Q.; Kania, R. S.; Kath, J. C.; Lam, H.; Lam, J. L.; Le, P. T.; Lingardo, L.; Liu, W.; McTigue, M.; Palmer, C. L.; Sach, N. W.; Smeal, T.; Smith, G. L.; Stewart, A. E.; Timofeevski, S.; Zhu, H.; Zhu, J.; Zou, H. Y.; Edwards, M. P. *J. Med. Chem.* **2014**, *57*, 4720-4744.
52. Morris, S. W.; Kirstein, M. N.; Valentine, M. B.; Dittmer, K. G.; Shapiro, D. N.; Saltman, D. L.; Look, A. T. *Science*, **1994**, *263*, 1281-4.
53. Wang, Q.; Rager, J. D.; Weinstein, K.; Kardos, P. S.; Dobson, G. L.; Li, J.; Hidalgo, I. J. *Int. J. Pharm.* **2005**, *288*, 349-359.

CONFIDENTIAL – PROPERTY OF GSK – DO NOT COPY

54. McCoull, W.; Abrams, R. D.; Anderson, E.; Blades, K.; Barton, P.; Box, M.; Burgess, J.; Byth, K.; Cao, Q.; Chuaqui, C.; Carbajo, R. J.; Cheung, T.; Code, E.; Ferguson, A. D.; Fillery, S.; Fuller, N. O.; Gangl, E.; Gao, N.; Grist, M.; Hargreaves, D.; Howard, M. R.; Hu, J.; Kemmitt, P. D.; Nelson, J. E.; O'Connell, N.; Prince, D. B.; Raubo, P.; Rawlins, P. B.; Robb, G. R.; Shi, J.; Waring, M. J.; Whittaker, D.; Wylot, M.; Zhu, X. *J. Med. Chem.*, **2017**, *60*, 4386-4402.
55. Baldwin, I.; Cansfield, A.; Barton, N., unpublished work, GlaxoSmithKline, **2014**
56. GVKBiosciencesPrivateLimited. *Hyderabad, India*, **2014**.
57. Convery, M., unpublished work, GlaxoSmithKline, **2014**
58. Perozzo, R.; Folkers, G.; Scapozza, L. *J. Recept. Signal Transduct. Res.*, **2004**, *24*, 1-52.
59. Damian, L. *Methods Mol. Biol.*, **2013**, *1008*, 103-18.
60. Klebe, G. *Nat. Rev. Drug Discov.*, **2015**, *14*, 95.
61. de Mol, N. J.; Dekker, F. J.; Broutin, I.; Fischer, M. J.; Liskamp, R. M. *J. Med. Chem.*, **2005**, *48*, 753-63.
62. Day, Y. S. N.; Baird, C. L.; Rich, R. L.; Myszka, D. G. *Protein Sci.*, **2002**, *11*, 1017-1025.
63. Nguyen, H. H.; Park, J.; Kang, S.; Kim, M. *Sensors*, **2015**, *15*, 10481-10510.
64. Madeira, A.; Ohman, E.; Nilsson, A.; Sjogren, B.; Andren, P. E.; Svenningsson, P. *Nat. Protocols*, **2009**, *4*, 1023-1037.
65. Hahnefeld, C.; Drewianka, S.; Herberg, F. W. *Methods Mol. Med.*, **2004**, *94*, 299-320.
66. Frazee, J. S.; Hammond, M.; Kano, K.; Manns, S.; Nakamura, H.; Thompson, S. K.; Washburn, D. G. Preparation of 1H-Pyrrolo[2,3-b]Pyridines as Inhibitors of Serum and Glucocorticoid-Regulated Kinase 1 (Sgk-1). WO2006/63167, **2006**.
67. Zeng, J.; Chung, C.-W., unpublished work, GlaxoSmithKline, **2017**
68. Hao, M.-H. *J. Chem. Theory Comput.*, **2006**, *2*, 863-872.
69. Sasikala, W. D.; Mukherjee, A. *J. Phys. Chem. B*, **2014**, *118*, 10553-10564.
70. Kuntz, I. D.; Chen, K.; Sharp, K. A.; Kollman, P. A. *PNAS*, **1999**, *96*, 9997-10002.
71. Berges, D. A. 7-Acyl-3-(sulfonic acid and sulfamoyl substituted tetrazolyl thiomethyl)cephalosporins. US4048311, **1977**.

72. Moree, W. J.; van Gent, L. C.; van der Marel, G. A.; Liskamp, R. M. J. *Tetrahedron*, **1993**, *49*, 1133-1150.
73. Sutherland, H.; Shriner, R. L. *J. Am. Chem. Soc.*, **1936**, *58*, 62-63.
74. Derivatives of 7-(2-substituted-2-hydroxyiminoacetamido)-3-(1-substituted tetrazol-5-ylthiomethyl)-3-cephem-4-carboxylic acid. US4066762, **1978**.
75. A cycloalkyl sulfonyl amide compounds and its preparation method and application (by machine translation). CN104211621, **2016**.
76. Fan, Y.-H.; Li, W.; Liu, D.-D.; Bai, M.-X.; Song, H.-R.; Xu, Y.-N.; Lee, S.; Zhou, Z.-P.; Wang, J.; Ding, H.-W. *Eur. J. Med. Chem.*, **2017**, *139*, 95-106.
77. Botyanszki, J.; Dickerson, S. H.; Leivers, M. R.; Li, X.; McFadyen, R. B.; Redman, A. M.; Shotwell, J. B.; Xue, J. Benzimidazole Derivatives as Antiviral Agents and their Preparation. WO2012/174312, **2012**.
78. Leivers, A. L.; Tallant, M.; Shotwell, J. B.; Dickerson, S.; Leivers, M. R.; McDonald, O. B.; Gobel, J.; Creech, K. L.; Strum, S. L.; Mathis, A.; Rogers, S.; Moore, C. B.; Botyanszki, J. *J. Med. Chem.*, **2014**, *57*, 2091-2106.
79. Wang, M.; Gao, M.; Miller, K. D.; Sledge, G. W.; Zheng, Q.-H. *Bioorg. Med. Chem. Lett.*, **2012**, *22*, 1569-1574.
80. Pyridopyrimidine Derivatives As PI3 Kinase Inhibitors. WO2009/39140, **2009**.
81. Kim, J.-G.; Jang, D. O. *Synlett*, **2007**, *2007*, 2501-2504.
82. Surry, D. S.; Buchwald, S. L. *Chemical Science*, **2011**, *2*, 27-50.
83. Wolfe, J. P.; Tomori, H.; Sadighi, J. P.; Yin, J.; Buchwald, S. L. *J. Org. Chem.*, **2000**, *65*, 1158-1174.
84. Ghosez, L. *Angew. Chem. Int. Ed.*, **1972**, *11*, 852-853.
85. Edward, B.; Kazuhiko, S.; Teruaki, M. *Chem. Lett.*, **1975**, *4*, 1163-1166.
86. Carpino, L. A.; El-Faham, A. *J. Am. Chem. Soc.*, **1995**, *117*, 5401-5402.
87. Kunishima, M.; Kawachi, C.; Iwasaki, F.; Terao, K.; Tani, S. *Tetrahedron Lett.*, **1999**, *40*, 5327-5330.
88. El-Faham, A.; Albericio, F. *J. Pept. Sci.*, **2010**, *16*, 6-9.
89. Ogura, H.; Kobayashi, T.; Shimizu, K.; Kawabe, K.; Takeda, K. *Tetrahedron Lett.*, **1979**, *20*, 4745-4746.
90. Belleau, B.; Malek, G. *J. Am. Chem. Soc.*, **1968**, *90*, 1651-1652.

91. Castro, B.; Dormoy, J. R.; Evin, G.; Selve, C. *Tetrahedron Lett.*, **1975**, *16*, 1219-1222.
92. Helferich, B.; Schaefer, W. *Org. Synth.*, **1929**, *9*, 32-3.
93. Ligang, Q.; Zhong, S.; Tamboue, D.; Bowman Mertes, K. *Tetrahedron Lett.*, **1990**, *31*, 6469-6472.
94. Chen, F. M. F.; Benoiton, N. L. *Synthesis*, **1979**, *1979*, 709-710.
95. Wissmann, H.; Kleiner, H.-J. *Angew. Chem. Int. Ed.*, **1980**, *19*, 133-134.
96. Carpino, L. A. *J. Am. Chem. Soc.*, **1993**, *115*, 4397-4398.
97. Coste, J.; Le-Nguyen, D.; Castro, B. *Tetrahedron Lett.*, **1990**, *31*, 205-208.
98. Staab, H. A. *Angew. Chem. Int. Ed.*, **1962**, *1*, 351-367.
99. Komura, K.; Nakano, Y.; Koketsu, M. *Green Chem.*, **2011**, *13*, 828-831.
100. Bürgi, H. B.; Dunitz, J. D.; Lehn, J. M.; Wipff, G. *Tetrahedron*, **1974**, *30*, 1563-1572.
101. *Molecular Operating Environment (MOE)*, 2013.08, Chemical Computing Group ULC, 1010 Sherbooke St. West, Suite #910, Montreal, QC, Canada, H3A 2R7, **2018**.
102. Barbe, G.; Charette, A. B. *J. Am. Chem. Soc.*, **2008**, *130*, 18-19.
103. Pelletier, G.; Bechara, W. S.; Charette, A. B. *J. Am. Chem. Soc.*, **2010**, *132*, 12817-12819.
104. Blank, B. R.; Alayoglu, P.; Engen, W.; Choi, J. K.; Berkman, C. E.; Anderson, M. O. *Chem. Biol. Drug Des.*, **2011**, *77*, 241-247.
105. Zhang, Y.-M.; Fan, X.; Yang, S.-M.; Scannevin, R. H.; Burke, S. L.; Rhodes, K. J.; Jackson, P. F. *Bioorg. Med. Chem. Lett.*, **2008**, *18*, 405 - 408.
106. Zhang, Y.-M.; Xiang, B.; Yang, S.-M.; Rhodes, K.; Scannevin, R.; Jackson, P.; Chakravarty, D.; Fan, X.; Wilson, L. J.; Karnachi, P. Heterocyclic Derived Metalloprotease Inhibitors. US2008/103129, **2008**.
107. Kawashima, Y.; Ota, A.; Morikawa, Y.; Mibu, H. 3-oxo-1,4-benzothiazine derivatives. US5547952, **1996**.
108. Shigeta, Y.; Hirokawa, Y.; Nagai, H.; Nagae, K.; Watanabe, T.; Io, M.; Matsuura, Y.; Kamon, J.; Horikawa, M.; Takeuchi, K. Pyridazinone Derivatives And Use Thereof As P2X7 Receptor Inhibitors. WO2009/57827, **2009**.
109. Gololobov, Y. G.; Zhmurova, I. N.; Kasukhin, L. F. *Tetrahedron*, **1981**, *37*, 437-472.

110. Staudinger, H.; Meyer, J. *Helv. Chim. Acta*, **1919**, *2*, 635-646.
111. Zhang, X.; Zhang, N.; Chen, G.; Turpoff, A.; Ren, H.; Takasugi, J.; Morrill, C.; Zhu, J.; Li, C.; Lennox, W.; Paget, S.; Liu, Y.; Almstead, N.; George Njoroge, F.; Gu, Z.; Komatsu, T.; Clausen, V.; Espiritu, C.; Graci, J.; Colacino, J.; Lahser, F.; Risher, N.; Weetall, M.; Nomeir, A.; Karp, G. M. *Bioorg. Med. Chem. Lett*, **2013**, *23*, 3947-3953.
112. Banka, A. L.; Botyanszki, J.; Dickerson, S. H.; Duan, M.; Leivers, M. R.; Mcfadyen, R. B.; Moore, C. B.; Redman, A. M.; Shotwell, J. B.; Tai, V. Preparation of aminoquinoline derivatives as antiviral agents. 2012037108, 9/13/2011.
113. Hoveyda, A. H.; Zhugralin, A. R. *Nature*, **2007**, *450*, 243-251.
114. Fuerstner, A.; Ackermann, L.; Gabor, B.; Goddard, R.; Lehmann, C. W.; Mynott, R.; Stelzer, F.; Thiel, O. R. *Chem. - Eur. J*, **2001**, *7*, 3236-3253.
115. Grubbs, R. H.; Miller, S. J.; Fu, G. C. *Acc. Chem. Res*, **1995**, *28*, 446-452.
116. Nicola, T.; Brenner, M.; Donsbach, K.; Kreye, P. *Org. Process Res. Dev*, **2005**, *9*, 513-515.
117. Yee, N. K.; Farina, V.; Houpis, I. N.; Haddad, N.; Frutos, R. P.; Gallou, F.; Wang, X. J.; Wei, X.; Simpson, R. D.; Feng, X.; Fuchs, V.; Xu, Y.; Tan, J.; Zhang, L.; Xu, J.; Smith-Keenan, L. L.; Vitous, J.; Ridges, M. D.; Spinelli, E. M.; Johnson, M.; Donsbach, K.; Nicola, T.; Brenner, M.; Winter, E.; Kreye, P.; Samstag, W. *J. Org. Chem*, **2006**, *71*, 7133-7145.
118. Bennett, C. E. *e-EROS Encycl. Reagents Org. Synth*, **2007**.
119. Scholl, M.; Ding, S.; Lee, C. W.; Grubbs, R. H. *Org. Lett*, **1999**, *1*, 953-956.
120. Formentin, P.; Gimeno, N.; Steinke, J. H. G.; Vilar, R. *J. Org. Chem*, **2005**, *70*, 8235-8238.
121. Schmidt, B. *Eur. J. Org. Chem*, **2004**, 1865-1880.
122. Hong, S. H.; Sanders, D. P.; Lee, C. W.; Grubbs, R. H. *J. Am. Chem. Soc*, **2005**, *127*, 17160-17161.
123. Csjernyik, G.; Ell, A. H.; Fadini, L.; Pugin, B.; Bäckvall, J. E. *J. Org. Chem*, **2002**, *67*, 1657-1662.
124. Yamamoto, K.; Biswas, K.; Gaul, C.; Danishefsky, S. J. *Tetrahedron Lett*, **2003**, *44*, 3297-3299.
125. Campbell, M.; Hamblin, J. N.; Bertrand, S.; Down, K.; Harrison, Z.; Talbot, E., unpublished work, GlaxoSmithKline, **2014**

CONFIDENTIAL – PROPERTY OF GSK – DO NOT COPY

126. Kugler-Steigmeier, M. E.; Friederich, U.; Graf, U.; Lutz, W. K.; Maier, P.; Schlatter, C. *Mutat. Res., Fundam. Mol. Mech. Mutagen*, **1989**, *211*, 279-289.
127. Sinsheimer, J. E.; Hooberman, B. H.; Das, S. K.; Brezzell, M. D.; You, Z. *Mutat. Res., Fundam. Mol. Mech. Mutagen*, **1992**, *268*, 255-264.
128. Biscoe, M. R.; Fors, B. P.; Buchwald, S. L. *J. Am. Chem. Soc.*, **2008**, *130*, 6686-6687.
129. Nahm, S.; Weinreb, S. M. *Tetrahedron Lett*, **1981**, *22*, 3815-3818.
130. Okuma, K.; Tanaka, Y.; Kaji, S.; Ohta, H. *J. Org. Chem*, **1983**, *48*, 5133-5134.
131. Appel, R. *Angew. Chem. Int. Ed.*, **1975**, *14*, 801-811.
132. Hamblin, J. N.; Jones, P. S.; Keeling, S. E.; Le, J.; Parr, N. J.; Willacy, R. D. Preparation of polymorphs and salts of 6-(1H-indol-4-yl)-4-(5-{{4-(1-methylethyl)-1-piperazinyl}methyl}-1,3-oxazol-2-yl)-1H-indazole as PI3k inhibitors. 2012055846, 10/25/2011.
133. Hamblin, J. N.; Jones, P. S.; Keeling, S. E.; Le, J.; Mitchell, C. J.; Parr, N. J. Preparation of oxazole-substituted indazole derivatives for use as PI3-kinase inhibitors. 2010125082, 4/28/2010.
134. Waldman, S. A. *Ann. Allergy, Asthma, Immunol*, **2002**, *89*, 7-12.
135. Abad-Zapatero, C. *Expert Opin. Drug Discov.*, **2007**, *2*, 469-488.
136. Hopkins, A. L.; Keserü, G. M.; Leeson, P. D.; Rees, D. C.; Reynolds, C. H. *Nature Reviews Drug Discovery*, **2014**, *13*, 105.
137. Pade, V.; Stavchansky, S. *J. Pharm. Sci*, **1998**, *87*, 1604-1607.
138. Savjani, K. T.; Gajjar, A. K.; Savjani, J. K. *ISRN Pharm*, **2012**, *10*, 195727.
139. Tolman, J. A.; Williams, R. O., III. *Drug Dev. Ind. Pharm*, **2010**, *36*, 1-30.
140. Yang, W., *Improvement in the Bioavailability of Poorly Water-Soluble Drugs via Pulmonary Delivery of Nanoparticles*, PhD Thesis, Univ. of Texas, Austin, **2009**.
141. Forbes, B.; O'Lone, R.; Allen, P. P.; Cahn, A.; Clarke, C.; Collinge, M.; Dailey, L. A.; Donnelly, L. E.; Dybowski, J.; Hassall, D.; Hildebrand, D.; Jones, R.; Kilgour, J.; Klapwijk, J.; Maier, C. C.; McGovern, T.; Nikula, K.; Parry, J. D.; Reed, M. D.; Robinson, I.; Tomlinson, L.; Wolfreys, A. *Adv. Drug Deliv. Rev.*, **2014**, *71*, 15-33.
142. Zhu, C.; Jiang, L.; Chen, T. M.; Hwang, K. K. *Eur. J. Med. Chem*, **2002**, *37*, 399-407.
143. Kell, D. B.; Dobson, P. D.; Oliver, S. G. *Drug Discov. Today*, **2011**, *16*, 704-714.

CONFIDENTIAL – PROPERTY OF GSK – DO NOT COPY

144. Tronde, A.; Norden, B.; Marchner, H.; Wendel, A. K.; Lennernaes, H.; Bengtsson, U. H. *J. Pharm. Sci.*, **2003**, *92*, 1216-1233.
145. Kratochwil, N. A.; Huber, W.; Muller, F.; Kansy, M.; Gerber, P. R. *Biochem. Pharmacol.*, **2002**, *64*, 1355-1374.
146. Yang, F.; Zhang, Y.; Liang, H. *Int. J. Mol. Sci.*, **2014**, *15*, 3580-3595.
147. Waring, M. J. *Expert Opin. Drug Discovery*, **2010**, *5*, 235-248.
148. Blackwell, J.; Wellaway, N.; Bush, J., unpublished work, GlaxoSmithKline, **2015**
149. Talele, T. T. *J. Med. Chem.*, **2016**, *59*, 8712-8756.
150. Taylor, R. D.; MacCoss, M.; Lawson, A. D. G. *J. Med. Chem.*, **2014**, *57*, 5845-5859.
151. Labelle, M.; Belley, M.; Gareau, Y.; Gauthier, J. Y.; Guay, D.; Gordon, R.; Grossman, S. G.; Jones, T. R.; Leblanc, Y.; McAuliffe, M.; McFarlane, C.; Masson, P.; Metters, K. M.; Ouimet, N.; Patrick, D. H.; Piechuta, H.; Rochette, C.; Sawyer, N.; Xiang, Y. B.; Pickett, C. B.; Ford-Hutchinson, A. W.; Zamboni, R. J.; Young, R. N. *Bioorg. Med. Chem. Lett.*, **1995**, *5*, 283-288.
152. Sampson, P. B.; Liu, Y.; Patel, N. K.; Feher, M.; Forrest, B.; Li, S.-W.; Edwards, L.; Laufer, R.; Lang, Y.; Ban, F.; Awrey, D. E.; Mao, G.; Plotnikova, O.; Leung, G.; Hodgson, R.; Mason, J.; Wei, X.; Kiarash, R.; Green, E.; Qiu, W.; Chirgadze, N. Y.; Mak, T. W.; Pan, G.; Pauls, H. W. *J. Med. Chem.*, **2015**, *58*, 130-146.
153. Abe, H.; Kikuchi, S.; Hayakawa, K.; Iida, T.; Nagahashi, N.; Maeda, K.; Sakamoto, J.; Matsumoto, N.; Miura, T.; Matsumura, K.; Seki, N.; Inaba, T.; Kawasaki, H.; Yamaguchi, T.; Kakefuda, R.; Nanayama, T.; Kurachi, H.; Hori, Y.; Yoshida, T.; Kakegawa, J.; Watanabe, Y.; Gilmartin, A. G.; Richter, M. C.; Moss, K. G.; Laquerre, S. G. *ACS Med. Chem. Lett.*, **2011**, *2*, 320-324.
154. Blanksby, S. J.; Ellison, G. B. *Acc. Chem. Res.*, **2003**, *36*, 255-263.
155. Yu, K.-L.; Sin, N.; Civiello, R. L.; Wang, X. A.; Combrink, K. D.; Gulgeze, H. B.; Venables, B. L.; Wright, J. J. K.; Dalterio, R. A.; Zadjura, L.; Marino, A.; Dando, S.; D'Arienzo, C.; Kadow, K. F.; Cianci, C. W.; Li, Z.; Clarke, J.; Genovesi, E. V.; Medina, I.; Lamb, L.; Colonno, R. J.; Yang, Z.; Krystal, M.; Meanwell, N. A. *Bioorg. Med. Chem. Lett.*, **2007**, *17*, 895-901.
156. Simmons, H. E.; Smith, R. D. *J. Am. Chem. Soc.*, **1958**, *80*, 5323-5324.
157. Dauben, W. G.; Berezin, G. H. *J. Am. Chem. Soc.*, **1963**, *85*, 468-472.
158. Denmark, S. E.; O'Connor, S. P. *J. Org. Chem.*, **1997**, *62*, 584-594.

CONFIDENTIAL – PROPERTY OF GSK – DO NOT COPY

159. Charette, A. B.; Molinaro, C.; Brochu, C. *J. Am. Chem. Soc.*, **2001**, *123*, 12168-12175.
160. Paulissen, R.; Hubert, A. J.; Teyssie, P. *Tetrahedron Lett.*, **1972**, *13*, 1465-1466.
161. Corey, E. J.; Chaykovsky, M. *J. Am. Chem. Soc.*, **1962**, *84*, 867-868.
162. Corey, E. J.; Chaykovsky, M. *J. Am. Chem. Soc.*, **1965**, *87*, 1353-1364.
163. Appel, R.; Hartmann, N.; Mayr, H. *J. Am. Chem. Soc.*, **2010**, *132*, 17894-17900.
164. Zhu, C.; Falck, J. R. *Adv. Synth. Catal.*, **2014**, *356*, 2395-2410.
165. Sandford, C.; Aggarwal, V. K. *Chem. Commun.*, **2017**, *53*, 5481-5494.
166. Brown, H. C.; Zweifel, G. *J. Am. Chem. Soc.*, **1959**, *81*, 247-247.
167. Mlynarski, S. N.; Karns, A. S.; Morken, J. P. *J. Am. Chem. Soc.*, **2012**, *134*, 16449-16451.
168. Nave, S.; Sonawane, R. P.; Elford, T. G.; Aggarwal, V. K. *J. Am. Chem. Soc.*, **2010**, *132*, 17096-17098.
169. Cazorla, C.; Métya, E.; Andrioletti, B.; Lemaire, M. *Tetrahedron Lett.*, **2009**, *50*, 3936-3938.
170. Thiebes, C.; Thiebes, C.; Prakash, G. K. S.; Petasis, N. A.; Olah, G. A. *Synlett*, **1998**, *1998*, 141-142.
171. Miyaura, N.; Yamada, K.; Suzuki, A. *Tetrahedron Lett.*, **1979**, *20*, 3437-3440.
172. Suzuki, A. *J. Organomet. Chem.*, **1999**, *576*, 147-168.
173. Miyaura, N.; Suzuki, A. *Chem. Rev.*, **1995**, *95*, 2457-2483.
174. Chan, D. M. T.; Monaco, K. L.; Wang, R.-P.; Winters, M. P. *Tetrahedron Lett.*, **1998**, *39*, 2933-2936.
175. Evans, D. A.; Katz, J. L.; West, T. R. *Tetrahedron Lett.*, **1998**, *39*, 2937-2940.
176. Lam, P. Y. S.; Clark, C. G.; Saubern, S.; Adams, J.; Winters, M. P.; Chan, D. M. T.; Combs, A. *Tetrahedron Lett.*, **1998**, *39*, 2941-2944.
177. Petasis, N. A.; Akritopoulou, I. *Tetrahedron Lett.*, **1993**, *34*, 583-586.
178. Matteson, D. S.; Sadhu, K. M. *J. Am. Chem. Soc.*, **1983**, *105*, 2077-2078.
179. Leonori, D.; Aggarwal, V. K. *Acc. Chem. Res.*, **2014**, *47*, 3174-3183.

180. Thomas, S. P.; French, R. M.; Jheengut, V.; Aggarwal, V. K. *Chem. Rec.*, **2009**, *9*, 24-39.
181. Pietruszka, J.; Witt, A. *J. Chem. Soc., Perkin Trans. I*, **2000**, 4293-4300.
182. Köster, R.; Arora, S.; Binger, P. *Angew. Chem. Int. Ed.*, **1969**, *8*, 205-205.
183. Rubina, M.; Rubin, M.; Gevorgyan, V. *J. Am. Chem. Soc.*, **2003**, *125*, 7198-7199.
184. Liskey, C. W.; Hartwig, J. F. *J. Am. Chem. Soc.*, **2013**, *135*, 3375-3378.
185. Chotana, G. A.; Vanchura II, B. A.; Tse, M. K.; Staples, R. J.; Maleczka, J. R. E.; Smith III, M. R. *Chem. Commun.*, **2009**, 5731-5733.
186. Zhong, C.; Kunii, S.; Kosaka, Y.; Sawamura, M.; Ito, H. *J. Am. Chem. Soc.*, **2010**, *132*, 11440-11442.
187. Benoit, G.; Charette, A. B. *J. Am. Chem. Soc.*, **2017**, *139*, 1364-1367.
188. Murai, M.; Mizuta, C.; Taniguchi, R.; Takai, K. *Org. Lett.*, **2017**, *19*, 6104-6107.
189. Gandon, V.; Szymoniak, J. *Chem. Commun.*, **2002**, 1308-1309.
190. Zheng, B.; Srebnik, M. *Tetrahedron Lett.*, **1994**, *35*, 1145-1148.
191. Zheng, B.; Deloux, L.; Pereira, S.; Skrzypczak-Jankun, E.; Cheesman, B. V.; Sabat, M.; Srebnik, M. *Appl. Organomet. Chem.*, **1996**, *10*, 267-278.
192. Pereira, S.; Srebnik, M. *Organometallics*, **1995**, *14*, 3127-3128.
193. Wang, Y. D.; Kimball, G.; Prashad, A. S.; Wang, Y. *Tetrahedron Lett.*, **2005**, *46*, 8777-8780.
194. Hart, D. W.; Schwartz, J. *J. Am. Chem. Soc.*, **1974**, *96*, 8115-8116.
195. Ragan, J. A.; Nakatsuka, M.; Smith, D. B.; Uehling, D. E.; Schreiber, S. L. *J. Org. Chem.*, **1989**, *54*, 4267-4268.
196. Zhang, D.; Ready, J. M. *J. Am. Chem. Soc.*, **2007**, *129*, 12088-12089.
197. Strom, A. E.; Hartwig, J. F. *J. Org. Chem.*, **2013**, *78*, 8909-8914.
198. Wipf, P.; Kendall, C. *Chem. – Eur. J.*, **2002**, *8*, 1778-1784.
199. Venanzi, L. M.; Lehmann, R.; Keil, R.; Lipshutz, B. H. *Tetrahedron Lett.*, **1992**, *33*, 5857-5860.
200. Maksymowicz, R. M.; Roth, P. M. C.; Fletcher, S. P. *Nat Chem*, **2012**, *4*, 649-654.

CONFIDENTIAL – PROPERTY OF GSK – DO NOT COPY

201. Hart, D. W.; Blackburn, T. F.; Schwartz, J. *J. Am. Chem. Soc.*, **1975**, *97*, 679-680.
202. Wipf, P.; Jahn, H. *Tetrahedron*, **1996**, *52*, 12853-12910.
203. Smith, M. T. *Annu. Rev. Public Health*, **2010**, *31*, 133-148.
204. Kaluszyner, A.; Reuter, S. *J. Am. Chem. Soc.*, **1953**, *75*, 5126-7.
205. Priestley, E. S.; Decicco, C. P. Preparation of lactam acylaminoalkaneboronates as inhibitors of hepatitis C virus NS3 protease. US20030008828A1, **2003**.
206. Buchwald, S. L.; LaMaire, S. J.; Nielsen, R. B.; Watson, B. T.; King, S. M. *Org. Synth.*, **1993**, *71*, 77-82.
207. Wetzel, D. M.; Brauman, J. I. *J. Am. Chem. Soc.*, **1988**, *110*, 8333-8336.
208. Brookhart, M.; Liu, Y. *Organometallics*, **1989**, *8*, 1569-1572.
209. Brookhart, M.; Liu, Y. *J. Am. Chem. Soc.*, **1991**, *113*, 939-944.
210. Brookhart, M.; Kegley, S. E.; Husk, G. R. *Organometallics*, **1984**, *3*, 650-652.
211. Li, C.; Wang, J.; Barton, L. M.; Yu, S.; Tian, M.; Peters, D. S.; Kumar, M.; Yu, A. W.; Johnson, K. A.; Chatterjee, A. K.; Yan, M.; Baran, P. S. *Science*, **2017**, *356*.
212. Houk, K. N.; Rondan, N. G.; Wu, Y.-D.; Metz, J. T.; Paddon-Row, M. N. *Tetrahedron*, **1984**, *40*, 2257-2274.
213. Boyall, D.; Frantz, D. E.; Carreira, E. M. *Org. Lett.*, **2002**, *4*, 2605-2606.
214. Takita, R.; Yakura, K.; Ohshima, T.; Shibasaki, M. *J. Am. Chem. Soc.*, **2005**, *127*, 13760-13761.
215. Kotani, S.; Kukita, K.; Tanaka, K.; Ichibakase, T.; Nakajima, M. *J. Org. Chem.*, **2014**, *79*, 4817-4825.
216. Brinkmeyer, R. S.; Kapoor, V. M. *J. Am. Chem. Soc.*, **1977**, *99*, 8339-8341.
217. Midland, M. M.; McDowell, D. C.; Hatch, R. L.; Tramontano, A. *J. Am. Chem. Soc.*, **1980**, *102*, 867-869.
218. Hortense, E.; Jackson, S.; Knaggs, A., unpublished work, GlaxoSmithKline, **2016**
219. Salkind, J.; Rosenfeld, A. *Chem. Ber.*, **1924**, *57*, 1690.
220. Vo, D. D.; Gautier, F.; Barillé-Nion, S.; Juin, P.; Levoine, N.; Grée, R. *Tetrahedron*, **2014**, *70*, 301-311.

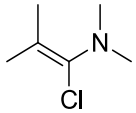
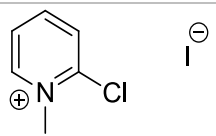
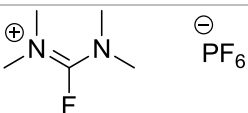
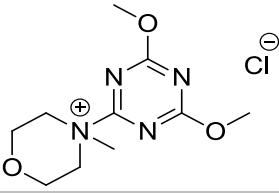
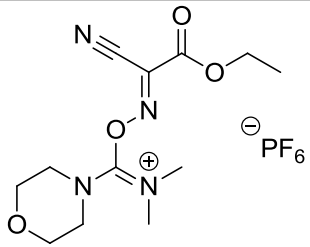
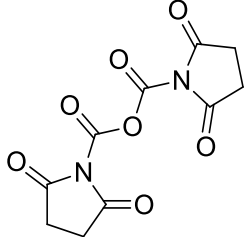
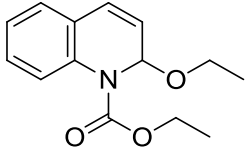
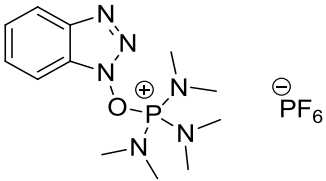
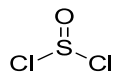
221. Nishimura, T.; Guo, X.-X.; Ohnishi, K.; Hayashi, T. *Adv. Synth. Catal.*, **2007**, *349*, 2669-2672.
222. Boutonnet, F.; Dufour, N.; Straw, T.; Igau, A.; Majoral, J. P. *Organometallics*, **1991**, *10*, 3939-3941.
223. Maraval, A.; Igau, A.; Donnadiou, B.; Majoral, J.-P. *Eur. J. Org. Chem.*, **2003**, *2003*, 385-394.
224. White, J. M.; Tunoori, A. R.; Georg, G. I. *J. Am. Chem. Soc.*, **2000**, *122*, 11995-11996.
225. Schedler, D. J. A.; Li, J.; Ganem, B. *J. Org. Chem.*, **1996**, *61*, 4115-4119.
226. Noble, A.; McCarver, S. J.; Macmillan, D. W. C. *J. Am. Chem. Soc.*, **2015**, *137*, 624-627.
227. Sherman, E. S.; Fuller, P. H.; Kasi, D.; Chemler, S. R. *J. Org. Chem.*, **2007**, *72*, 3896-3905.
228. Zabawa, T. P.; Chemler, S. R. *Org. Lett.*, **2007**, *9*, 2035-2038.
229. Lovering, F.; Bikker, J.; Humblet, C. *J. Med. Chem.*, **2009**, *52*, 6752-6756.
230. Zheng, Y.; Tice, C. M.; Singh, S. B. *Bioorg. Med. Chem. Lett.*, **2014**, *24*, 3673-3682.
231. Johansson, A.; Löfberg, C.; Antonsson, M.; von Unge, S.; Hayes, M. A.; Judkins, R.; Ploj, K.; Benthem, L.; Lindén, D.; Brodin, P.; Wennerberg, M.; Fredenwall, M.; Li, L.; Persson, J.; Bergman, R.; Pettersen, A.; Gennemark, P.; Hogner, A. *J. Med. Chem.*, **2016**, *59*, 2497-2511.
232. Bell, I. M. *J. Med. Chem.*, **2014**, *57*, 7838-7858.
233. Zheng, Y.-J.; Tice, C. M. *Expert Opin. on Drug Discov.*, **2016**, *11*, 831-834.
234. Miyamura, S.; Araki, M.; Suzuki, T.; Yamaguchi, J.; Itami, K. *Angew. Chem. Int. Ed.*, **2015**, *54*, 846-851.
235. Spencer, J. A.; Jamieson, C.; Talbot, E. P. A. *Org. Lett.*, **2017**, *19*, 3891-3894.
236. Ehrenfreund, J.; Tobler, H.; Walter, H. Preparation of heterocyclic ortho-cyclopropyl-carboxanilides and their use as fungicides. WO2003074491A1, **2003**.
237. Walter, H.; Tobler, H.; Gribkov, D.; Corsi, C. *CHIMIA*, **2015**, *69*, 425-434.
238. Zeun, R.; Scalliet, G.; Oostendorp, M. *Pest Manage. Sci.*, **2013**, *69*, 527-534.
239. Kizhner, N. *J. Russ. Phys.-Chem. Soc.*, **1929**, *61*, 781-8.
240. Smith, L. I.; Rogier, E. R. *J. Am. Chem. Soc.*, **1951**, *73*, 3840-3842.

241. de Meijere, A.; Kozhushkov, S. I.; Spath, T. *Org. Synth.*, **2002**, 78, 142-151.
242. Löhr, S.; de Meijere, A. *Synlett*, **2001**, 2001, 0489-0492.
243. Rassadin, V. A.; Sokolov, V. V.; Khlebnikov, A. F.; Ulin, N. V.; Kozhushkov, S. I.; de Meijere, A. *Synthesis*, **2012**, 44, 372-376.
244. Goldfinger, M. B.; Crawford, K. B.; Swager, T. M. *J. Am. Chem. Soc.*, **1997**, 119, 4578-4593.
245. Klapars, A.; Buchwald, S. L. *J. Am. Chem. Soc.*, **2002**, 124, 14844-14845.
246. Rowedder, J.; Thomas, D. A., unpublished work, GlaxoSmithKline,
247. Chawner, S. J.; Cases-Thomas, M. J.; Bull, J. A. *Eur. J. Org. Chem.*, **2017**, 2017, 5015-5024.
248. Kita, Y.; Tamura, O.; Itoh, F.; Yasuda, H.; Miki, T.; Tamura, Y. *Chem. Pharm. Bull.*, **1987**, 35, 562-569.
249. Liverton, N. J.; McComas, C. C.; Habermann, J.; Koch, U.; Narjes, F.; Li, P.; Peng, X.; Soll, R.; Wu, H.; Palani, A.; He, S.; Dai, X.; Liu, H.; Lai, Z.; London, C.; Xiao, D.; Zorn, N.; Nargund, R. Tetracyclic Heterocycle Compounds and Methods of Use Thereof for the Treatment of Viral Diseases. US2014/213571, **2014**.
250. Atkinson, S. J.; Aylott, H. E.; Cooper, A. W. J.; Demont, E. H.; Harrison, L. A.; Hayhow, T. G. C.; Lindon, M. J.; Preston, A. G.; Seal, J. T.; Wall, I. D.; Watson, R. J.; Woolven, J. M. Pyridinone Dicarboxamide For Use As Bromodomain Inhibitors. WO2017/37116, **2017**.
251. Ozaki, F.; Kaneko, T.; Tabata, M.; Takahashi, Y.; Miyazaki, K.; Kamata, J.; Yoshida, I.; Matsukura, M.; Suzuki, H.; Yoshinaga, T.; Ishihara, H.; Katoh, H.; Sawada, K.; Onogi, T.; Kobayashi, K.; Ohkubo, M. Novel piperidine compounds and drugs containing the same. US2003/220368, **2003**.
252. Tetracyclic Heterocycle Compounds And Methods Of Use Thereof For The Treatment Of Viral Diseases. WO2013/33971, **2013**.
253. Kitamura, M.; Hayashi, H.; Yano, M.; Tanaka, T.; Maezaki, N. *Heterocycles*, **2007**, 71, 2669 - 2680.
254. Sajiki, H.; Mori, S.; Ohkubo, T.; Ikawa, T.; Kume, A.; Maegawa, T.; Monguchi, Y. *Chem. Eur. J.*, **2008**, 14, 5109 - 5111.
255. Pietruszka, J.; Schoene, N. *Eur. J. Org. Chem.*, **2004**, 5011 - 5019.
256. Wrackmeyer, B. *Prog. Nucl. Magn. Reson. Spectrosc.*, **1979**, 12, 227-259.
257. Bartoszewicz, A.; Kalek, M.; Stawinski, J. *Tetrahedron*, **2008**, 64, 8843 - 8850.

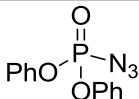
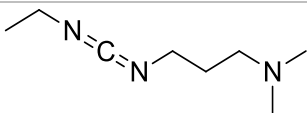
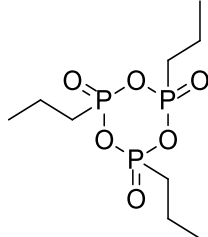
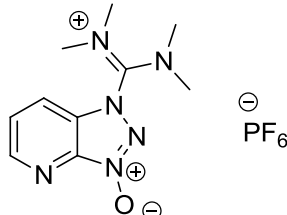
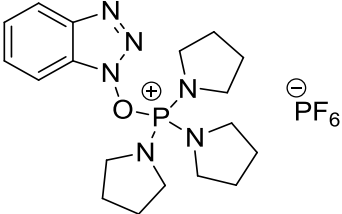
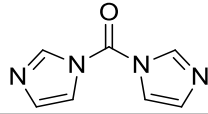
CONFIDENTIAL – PROPERTY OF GSK – DO NOT COPY

258. Linderman, R. J.; Jamois, E. A.; Tennyson, S. D. *J. Org. Chem.*, **1994**, *59*, 957 - 962.
259. Seregin, I. V.; Gevorgyan, V. *J. Am. Chem. Soc.*, **2006**, *128*, 12050 - 12051.
260. Liu, T.; Qiao, J. X.; Poss, M. A.; Yu, J.-Q. *Angew. Chem. Int. Ed.*, **2017**, *56*, 10924 - 10927.
261. Koolman, H. F.; Kantor, S.; Bogdan, A. R.; Wang, Y.; Pan, J. Y.; Djuric, S. W. *Org. Biomol. Chem.*, **2016**, *14*, 6591 - 6595.
262. Sawamura, M.; Ito, H. Manufacturing Method of Organoboron Compound. US2008/262257, **2008**.
263. Pietruszka, J.; Rieche, A. C. M.; Wilhelm, T.; Witt, A. *Adv. Synth. Catal.*, **2003**, *345*, 1273 - 1286.
264. Solorio-Alvarado, C. R.; Wang, Y.; Echavarren, A. M. *J. Am. Chem. Soc.*, **2011**, *133*, 11952-11955.
265. Howe, P. W. A. *Magn. Reson. Chem.*, **2010**, *48*, 837 - 841.
266. Tyagi, S.; Cook, C. D.; DiDonato, D. A.; Key, J. A.; McKillican, B. P.; Eberle, W. J.; Carlin, T. J.; Hunt, D. A.; Marshall, S. J.; Bow, N. L. *J. Org. Chem.*, **2015**, *80*, 11941-11947.
267. http://www.merckmillipore.com/GB/en/product/PI-3-Kinase-3-step-HTRF-Assay,MM_NF-33-047 (Accessed: 19/02/18),
268. Bunally, S.; Reid, I.; Valko, K.; Bardoni, S.; Hill, A. P., unpublished work, GlaxoSmithKline, **2018**
269. Bhattachar, S. N.; Wesley, J. A.; Seadeek, C. *J. Pharm. Biomed. Anal.*, **2006**, *41*, 152-7.
270. Robinson, M. W.; Hill, A. P.; Readshaw, S. A.; Hollerton, J. C.; Upton, R. J.; Lynn, S. M.; Besley, S. C.; Boughtflower, B. J. *Anal. Chem.*, **2017**, *89*, 1772-1777.
271. Valkó, K.; Bevan, C.; Reynolds, D. *Anal. Chem.*, **1997**, *69*, 2022-2029.
272. Kansy, M.; Senner, F.; Gubernator, K. *J. Med. Chem.*, **1998**, *41*, 1007-1010.
273. Valko, K.; Nunhuck, S.; Bevan, C.; Abraham, M. H.; Reynolds, D. P. *J. Pharm. Sci.*, **2003**, *92*, 2236-2248.

Appendix**Structure of amide coupling reagents**

Reagent	Structure
Ghosez ⁸⁴	
Mukaiyama ⁸⁵	
TFFH ⁸⁶	
DMTMM ⁸⁷	
COMU ⁸⁸	
SucOCOOSuc ⁸⁹	
EEDQ ⁹⁰	
BOP ⁹¹	
Thionyl chloride ⁹²	

CONFIDENTIAL – PROPERTY OF GSK – DO NOT COPY

DPPA ⁹³	
EDC ⁹⁴	
T3P ⁹⁵	
HATU ⁹⁶	
PyBOP ⁹⁷	
CDI ⁹⁸	
Mesoporous silica MCM-41 ⁹⁹	

Animal Studies Declaration

All animal studies were ethically reviewed and carried out in accordance with Animals (Scientific Procedures) Act 1986 and the GSK Policy on the Care, Welfare and Treatment of Animals.